Theoretical and experimental analysis of biomass gasification processes using the attainable region theory

By

RALPH FARAI MUVHIIWA

submitted in accordance with the requirements

for the degree of

DOCTOR OF PHILOSOPHY

at the

UNIVERSITY OF SOUTH AFRICA

SUPERVISOR: DR B C SEMPUGA

CO-SUPERVISORS: Prof D HILDEBRANDT

JUNE 2018

Declaration

I the undersigned **Ralph Farai Muvhiiwa (54133084)** hereby declare that the work contained in this dissertation has been produced by me without any collaboration with other students, staff or third parties aside from those acknowledged. I have not engaged in any acts of plagiarism and to the best of my knowledge. I have recognised all information obtained from other authors' work. It is being submitted for the degree of Doctor of Philosophy to the University of South Africa, Pretoria. It has not been submitted before for any degree or examination in any other University.

SIGNATURE: 

DATE: 7 June 2018

Abstract

There are limits on performance of processes and reactions set by material balances and by thermodynamics. The interaction of these theoretical limits and how they influence the behaviour of reactions and equipment is of interest to researchers and designers. This thesis looks at the conversion of biomass to gaseous products under various conditions, including a range of temperatures from ambient to 1500 ^{0}C and in the presence or absence of oxygen.

The limits of performance of the material balance can be represented as an Attainable Region (AR) in composition or extent space; we call this the MB-AR. The MB-AR represents all possible material balances that can be achieved for a given a set of feeds and set of possible products. The dimension of this space depends on the number of independent material balances. The extreme points of the MB-AR are of particular interest as these define the limiting compositions and the edges of the boundary of the MB-AR represent the limiting material balances. The MB-AR does not depend on temperature.

The thermodynamic limits of performance of can be represented as an AR in the space of Gibbs Free Energy (G) and Enthalpy (H); this is called the G-H AR. The G-H AR is always two dimensional, no matter what the dimension of the MB-AR. Extreme points in the G-H AR are also extreme points in the MB-AR are; however not all extreme points in the MB-AR are extreme points in the G-H AR. The extreme points in the MB-AR are transformed by calculating G and H of the points at the condition of interest (reaction temperature and pressure). It is then necessary to find the convex hull in G-H space of this set of transformed points which gives us the boundary of the G-H AR. The extreme points in the G-H AR can be associated with material balances and the extreme point with the minimum G represents the global equilibrium or equivalently the most favoured material balance for the system. The edges of G-H AR are defined by the lines between neighbouring extreme points in the boundary of the G-H AR. These edges represent the limiting material balances in terms of defining the extremes of the G and H of the system.

The G-H AR depends on the feed and products through the MB-AR, but also depends on temperature (and pressure). The set of points which are extreme points of both the MB-AR and the G-H AR changes with temperature. Geometrically, the transformed set of extreme points for the MB-AR moves in the GH space as temperature is changed and they move at different rates. Hence when finding the convex hull in the G-H space of the transformed extreme points of the MB-AR, G-H points become either boundary (extreme) points or move into the convex hull at different temperatures. Thus, the material balance which corresponds to the global minimum in G may change with temperature, as do the material balances which are associated with the edges of the G-H AR.

Experiments are performed on biomass anaerobically at ambient temperature using microbes as the catalyst, and the products of this process are called biogas. The experiments were performed in a nitrogen plasma system on biomass at higher temperatures (400 ^{0}C to 1000 ^{0}C) also in the absence of oxygen, and this process would typically be referred to as pyrolysis. Oxygen was added to the plasma system and operated at temperatures between 700 ^{0}C and 900 ^{0}C, and this would typically be referred to as gasification. Thus, it was able to change the MB-AR by presence or absence of oxygen. By changing operating temperatures, the G-H AR is effectively changed with either the same or different MB-AR's.

The experiments show that in all cases, the product tends towards minimum G. Although this might not be surprising at the higher temperatures, minimizing G is not thought to be the driving force in microbial systems. An important insight from this is that if one were to try and make hydrogen only in a biological system, the system would need to have organisms that make hydrogen only. This is because the material balance that produces hydrogen has a lower change in G than the material balance that make methane. Thus, if there was a consortium of organisms and some of them could make methane, the methane producing organisms would dominate as they have the higher Gibbs Free Energy driving force.

If the boundary of the G-H AR around the minimum G is fairly flat, or if many of the extreme points of the MB-AR lie close to the minimum G in the boundary of the G-H AR, then there are many material balances that will give the same G and H. Thus,

there are a range of compositions with similar G and H and how one approaches the minimum G will determine the chemical composition of the product. This has important implications for the design, scale up and operation of equipment if a particular product is desired rather process efficiency.

The low temperature anaerobic route to gasifying waste, using microbes as catalysts, has a very simple G-H AR, and the preferred products are CH_4 and CO_2, known as biogas. These units should be relatively stable to operate as none of the other products have G's that are as negative as that of the biogas. Although not part of this thesis, small-scale anaerobic digesters were installed in communities and these do run easily and stably with fairly little intervention from the operator which seems to support our conclusion.

We however could ask, why then have simple technologies, such an anaerobic digestion, not been widely adopted in Africa? To this end we worked with communities and spoke to people about their knowledge about the technology, their concerns and their possible interest in using new approaches to supply energy for cooking and lighting. We found that people were not aware of the technology but would be very interested in adopting a technology that supplied energy cheaply. To our surprise however, their major concern was around hygiene and safety, in that if the gas was made from "poo" how could the gas be clean and would cooking with it not contaminate the food and make people sick? This in hindsight is a very reasonable concern, although it had never occurred to us that this would be a perception. Engineers will have to work with social scientists and psychologist, amongst others, to address the concerns and needs of communities in order for sustainable technologies to be successfully adopted by communities.

In summary, this thesis presents a tool for analysing biomass conversion to gaseous products in general, whether microbial or thermal. This tool gives insight into what is achievable, what the major factors are that affect the favoured product and how this can be manipulated to improve efficiency from an overall material and energy point of view.

Dedications

This work is dedicated to all my family members.

Acknowledgements

Firstly, I would like to thank Prof Diane Hildebrandt and Dr Baraka Sempuga for their supervision, encouragement, invaluable support and diligent guidance. This work would not have succeeded without their supervision.

Prof David Glasser, Dr Xiaojun Lu, Dr James Fox, Dr Yali Yao, Dr Xinying Liu, Niel Stacey and Dr Tonderayi Matambo are also greatly acknowledged for their advice, contribution and unqualified encouragement. It was always a privilege to be guided by you during the research meetings every week. Special thanks to Jaco Van de Walt and Anthony from NECSA for the help during the commissioning and maintenance of the plasma gasifier which yielded the experimental results in this research project. Mrs Pippa Lange (late) and Mrs Ruby Mushonga are acknowledged for their contribution in improving my English writing skills.

My colleagues Mr Velinjani Mthethwa, Miss Saneliswa Magagula and Mr Maphala Llane, are acknowledged for the stimulating discussions, timely advice, and critical suggestions which helped to enhance the quality of this work.

I also want to thank my family and friends for their moral support during the course of this work. To my brother and sister, I want to thank you for encouraging and being excited with me as I have worked again to complete this Doctoral degree. To my mother and father, I want to say thank you for loving and continuing to believe in me and for the foresight to plan for me to be able to finish this degree. Kimberly my wife, your unconditional love kept me going.

I also would like to acknowledge the funding from the Institute for the Development of African Sustainability (IDEAS) formerly Materials and Process Synthesis (MaPS), University of South Africa and the South African Nuclear Energy Corporation SOC Limited (NECSA) for the sustainable laboratory facilities.

Above all, I would like to thank the Lord for his guidance and mercy on all the activities carried out during the making of this doctoral research project.

Table of Contents

List of Figures

List of Tables

List of Abbreviations

AD	Anaerobic Digestion
AR	Attainable Region
BTE	Biomass-To-Energy
CGC	Cold Gas Efficiency
COP21	21st Conference of Parties, (Paris 2015)
DC	Direct Current
ER	Equivalent Ratio
Ex	Exergy
FT	Fischer-Tropsch
G	Gibbs Free Energy
GC	Gas Chromatography
G-H	Gibbs Free Energy - Enthalpy
H	Enthalpy
LHV	Lower Heating Value
MBL	Material Balance Limited
MGE	Mechanical Gas Efficiency
P	Pressure
S	Entropy
SABIA	Southern Africa Biogas Industry Association
SBR	Steam to Biomass Ration
SDG	Sustainable Development Goals
SR	Stoichiometric Ratio
T	Temperature
W	Work
We	Work supplied from electricity
WGS	Water Gas Shift
∆G	Change in Gibbs Free Energy
∆H	Change in Enthalpy
∆Ex	Change in Exergy

Definition of terms

Attainable Region = Set of all possible outcomes, for a defined system under consideration.

Biogas = Gas containing mainly a mixture of methane and carbon dioxide from Anaerobic Digestion (AD) process.

Biomass = Organic matter from plants and animals that has stored energy within it.

ESKOM = South Africa National Power Supply Company

Exergy = Energy that is available to be used by a system

Gaussian Elimination = An algorithm for solving systems of linear equations.

HCOALGEN = A model that uses the proximate, ultimate, sulfur analysis to calculate the enthalpy of coal.

Plasma = A form of matter created by adding enough energy to a gas to ionise it.

Syngas = A fuel gas containing mainly of hydrogen and carbon monoxide.

Chapter 1: Introduction and Background

1.1. Background and Motivation

When countries who participated in the Paris Climate Change Conference (COP21) in November 2015 announced their action plans for reducing greenhouse gas emissions, two issues dominated the discussion. One of the major targets they identified was that countries should keep the rise in temperature caused by industrial emissions to a minimum (at less than 2 ^{0}C (3.6 ˚F) higher than those pertaining to pre-industrial times). Any increase in temperature beyond that point would be dangerous and cause irreversible climate change. However, many of the country representatives argued that a more stringent cap of 1.5 ^{0}C, though ambitious, would be even more efficacious. Another key issue discussed exhaustively at the conference was that countries should reduce the greenhouse gas emitted by human activities to a level that can be absorbed naturally by trees, soil and oceans (COP21).

The question arising out of COP21, and which this researcher strives to work towards, is how these goals can be achieved.

In order to cut down on harmful emissions while continuing to use industrial technology, engineers and researchers have been investigating ways to design more efficient manufacturing processes that are less harmful to the environment, and to improve efficiency of already existing systems.

Some of the most ground-breaking results of the research in designing more sustainable processes, to date, have been found in the field of energy and fuel

production from biomass. Lately, this source of energy has become an increasingly promising option because not only is it sustainable, but it carries with it several environmental benefits (Hassan et al., 2009; Heberlein and Murphy (2008)). In addition, biomass is expected to remain by far, the single most important primary source of renewable energy for decades to come IEA (2008). It is imperative that engineers design more efficient biomass-to-energy processes that are can meet society's need for electricity and fuel.

In the research in this thesis, the writer had two primary aims: to consider the use of biomass materials that have been conventionally treated as landfill waste or simply burned during the combustion process, in Anaerobic Digestion (AD), pyrolysis and gasification processes and to optimise these processes using theoretical and experimental methods.

Already, different biomass conversion processes have been successfully applied to generate energy (Somayeh et al., 2016; Gonawala (2014)). However, according to David (2015) technologies for biomass conversion are still in the developmental stage and therefore cannot be currently considered as reliable options for small and medium-scale applications. The researcher's aim is to remedy that deficiency by providing a more detailed analysis of the biomass conversion processes. Key to this is to understand through comparison, how these different processes work and how they relate to each other. This is achieved by using theoretical techniques based on material balances and thermodynamics as well experimental findings. The information obtained above will help to design processes that are more efficient in mass, heat and workflows.

1.2. The Challenge

Global growth of energy demand is not balanced with its availability and this demand will continue to increase, especially in the developing world (Vashal and Vistal, 2016). Furthermore, greenhouse gas emissions in the form of methane (CH_4) from biomass waste materials (animal and vegetable) that are landfilled (even when sealed) continue to be a significant concern (Dovetail Partners INC.,2010). Landfills are reported to contribute to approximately 20 % of the CH_4 emissions globally (EPA (2016); Naidoo (2017)) with all the emissions coming from degraded biomass. This calls for a need to reduce these emissions by harnessing the chemical potential in waste biomass and converting it to a useful energy source. According to (EPA., 2016) about 8% of the CH_4 emissions come from manure management hence trying to harness this material and use it for energy production will help reduce these emissions. Methane is about 24 times a larger contributor than carbon dioxide. While it is best to avoid emitting both greenhouse gases, the author aim is to harness the methane that can be potentially emitted from biomass and combust the gas to make energy and produce carbon dioxide which is 24 time less harmful when the same amount is emitted into the atmosphere. Thus, a sustainable strategy is to understand and improve waste biomass to energy processes with the aim of generating energy and reducing biomass landfill disposal, thus minimising the environmental impact.

According to (IEA., 2008) the quality of data on biomass production rates, storage and composition is often very poor, which hampers decision-making and future projections. Another drawback is that conventional pyrolysis/ gasification methods are generally unsuitable for harvesting energy directly from biomass because of the lower reaction temperature (a maximum average temperature of 800 ^{0}C) (Hlina et al., 2014) and

dilution by oxidation agents (Lombardi et al., 2012). To achieve equilibrium or high conversion of carbon (C) in biomass in addition to a low tar content, a high operating temperature (>800 ^{0}C) in the reactor is recommended (Ngubevana et al., 2010; Mathieu P and Dubuisson R., 2002). In conventional pyrolysis/ gasification, the energy content of the product gas depends on the amount of oxygen (O_2) added. The O_2 is used in combustion and this supplies heat to the process causing the reactor bulk temperatures to reach around 400 ^{0}C - 850 ^{0}C (Rajasekhar et al., 2015; Wang et al., 2009; Mountouris et al., 2006). A fuel, either in the form of reactant (biomass) or in product (syngas), is usually combusted in order to achieve the required reaction temperatures. However, the combustion process commensurately increases the carbon dioxide (CO_2) production, which in turn compromises the caloric value of the syngas (Lemmens et al., 2007). Another problem encountered in the existing processes is the formation and handling of tars in gasifiers. Much research has been devoted to finding the solution because the presence of tars hinders the efficient operation of high-temperature convectional pyrolysis/ gasification processes (Brage., 1997).

An emerging biomass conversion process is the use of a high-temperature gasification process, namely plasma gasification, to produce energy from non-food biomass. The new system can reportedly use bio-based waste, woody biomass, energy crops, agricultural and animal waste, and some kinds of municipal wastes as feedstock (Dovetail Partners INC., 2010). While the decomposition of waste and dangerous materials in thermal plasmas has been intensively studied in the last decade and industrial scale systems for treatment of various types of waste have been installed, plasma gasification of biomass is a relatively recent application (Hrabovsky., 2011).

Numerous technologies and approaches exist for plasma treatment of wastes as summarised by (Heberlein and Murphy, 2008), but there is still a pressing need for research that can advance sustainability in this field, especially when converting biomass.

Although plasma pyrolysis/ gasification has been studied recently, the research still lacks a detailed analysis of biomass applications to different designs (Danthurebandara et al., 2015). However, according to (Dovetail Partners INC., 2010), performance data for plasma gasification plants, many of which are pilot operations, are often treated as proprietary and no information is readily available on industrial plasma pyrolysis facilities of waste (Bosmans et al., 2013). The experimental data available on performance of plasma gasifiers, especially on industrial scale, is hence very limited (Zhang et al., 2012; Fabry et al., 2013). Thus, information regarding the quantity of the products from plasma gasification and the nature of any problems that might have been encountered is difficult to obtain. This hinders the understanding and application of the plasma gasification technology. Therefore, if this technology is to be developed further, there is a need for researchers to carry out both qualitative and quantitative work that can provide vital information that will help researchers to make advances.

Plasma systems use different gases including argon, air and nitrogen as ionising gases. Researchers have mostly used argon, steam and air as plasma gases because of reasons pertaining to cost and the ease of forming a plasma gas. Hrabovsky., 2009 used an argon/steam plasma in various situations. The argon plasma requires a high current to achieve high voltages (Hrabovsky., 2009; Hrabovsky., 2011; Hlina., 2014). Because the argon plasma requires high currents to get to high voltages, this results

in an increase in power input into the process. High currents however result in lower electrode lifespan due to electrode erosion. In this thesis, a continuous nitrogen plasma system is used as it is thought to achieve high voltages at lower currents compared to other ionising gases.

In terms of reducing volume of waste biomass, combustion and incineration of biomass results in production of CO_2 with minimum recovery of energy. The incineration technology that is currently used to treat municipal waste results in the emission of pollutant species such as NO_x, SO_x, HCl, harmful organic compounds, and heavy metals (Zhang et al., 2012). If the same process is to be used for biomass, energy and exergy losses are very large and the quantity of pollutants produced is very high when compared to a plasma system. Hence, the plasma system is a focus of this research.

On another note, traditional biomass has been used in the form of firewood and animal dung to provide energy for cooking, heating and lighting mostly in third world countries, such as in Africa, Asia and Latin America, especially in rural areas where access to affordable, modern energy services is limited (IEA., 2008). However, a cause for concern is that most of these biomass materials are not used efficiently, resulting in poor energy utilisation and, at the same time, leading to health issues for the users. For example, direct burning of firewood may cause respiratory infections in the long run. It is, therefore, prudent to support the idea of using the biomass efficiently with the adoption of processes such as biogas production and perhaps high temperature pyrolysis or gasification that are better designed for efficient production of useful energy.

Biological methods for converting biomass to gas have not been considered in most scenarios for future energy production because of their perceived low rate of valuable gas production (Somayeh et al., 2016). Biogas production is a sustainable biological process that utilises waste materials to produce a gas of high calorific value that can be used as a more convenient form of energy. In this process, bacteria are used to convert biomass material to gases, mainly CH_4 and CO_2, under anaerobic conditions at ambient temperatures. Although this is a slow process, biogas technology can be used to harness CH_4 produced from biomass that would otherwise be left to pollute the atmosphere when left to degrade naturally. Thus, this research also gives emphasis on understanding the thermodynamics of AD. In particular, it will be shown that the products at minimum Gibbs Free Energy (minimum G) drives the preferred product distribution and that genetic modifications to microorganisms to change the preferred product distribution will be an attempt to work against thermodynamics.

To conclude, given the high price of conventionally sourced energy and the extent of greenhouse pollution caused by underutilised biomass waste, it is possible that we can turn to the biodigestion and plasma pyrolysis and/or gasification to convert the waste to energy, providing a sustainable technology. These offer a more viable solution to both harnessing energy and reducing carbon emissions. Owing to the current concern across the world regarding the need for energy and the reduction of greenhouse gas emissions, the demand for the use of biomass and waste for energy is increasing by 1.4 % per year (IEA., 2008). Hence, there is need for the development of innovative and economical technologies with high efficiencies to guarantee sustainable energy production from biomass directly (Somayeh et al., 2016).

1.3. The Approach

To start with, the main aims of converting biomass are to generate heat when biomass is combusted; produce a product such as synthesis gas, biogas; and produce liquid fuels that can be used as a more useful energy carrier. In this way, the emissions associated with biomass degrading in the environment will be minimised. These objectives and/ or products are achieved by using processes such as AD -biogas production, pyrolysis, incineration, combustion and gasification. Although these processes are all used to convert biomass, most researchers see them as separate processes without any fundamental relationship and for this reason they are named differently. Biomass conversion in general can be looked at as a universal set in which biogas production (AD), pyrolysis, combustion and gasification are individual subsets as illustrated in Figure 1.1.

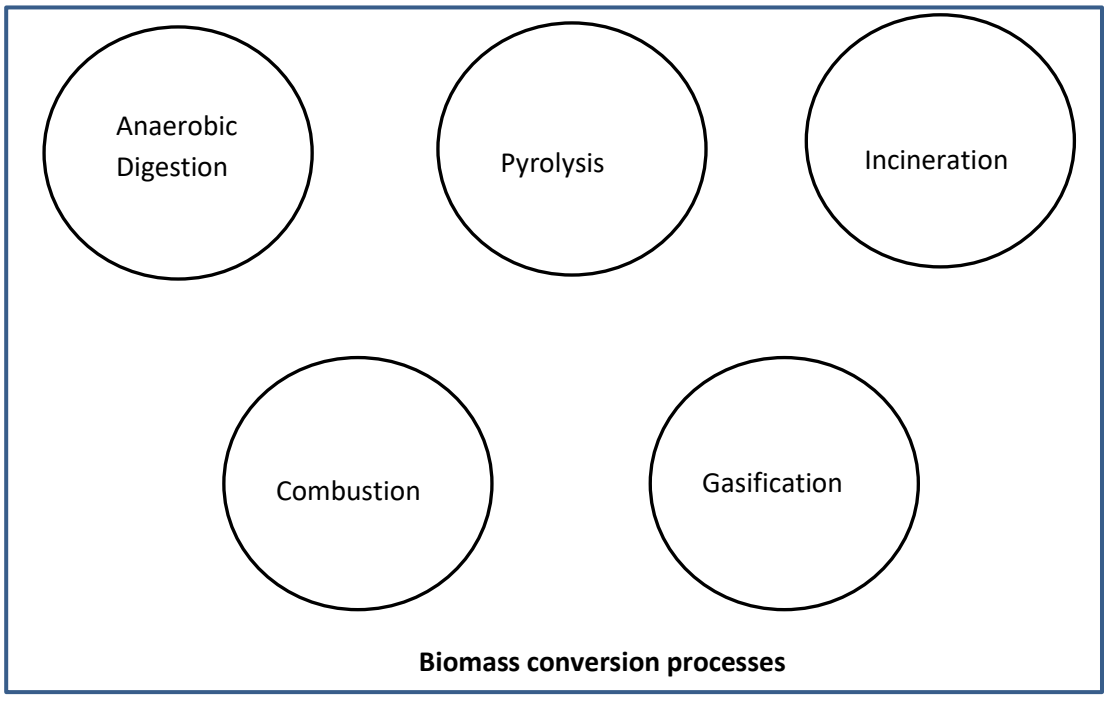

Figure 1.1: Universal set showing biomass conversion processes.

Two factors define each subset namely: i) the temperature at which it operates and ii) the supply or lack of oxygen at either extreme (zero to complete combustion). However, before we can show how these processes are related, it is important to define the five processes for biomass conversion shown in Figure 1.1.

- **Anaerobic Digestion (AD)** – A simple biological process, which usually occurs at temperatures below 70 ^{0}C and can be used to produce CH_4 and CO_2 (biogas) from biomass material with the aid of bacteria under anaerobic conditions. This means that the process only occurs when there is no O_2 present in the system. Biogas production typically occurs in the presence of large quantities of (H_2O) (up to 90 %) in relation to the solid biomass being converted.
- **Combustion** – The process of burning which involves the breakdown of biomass materials in the presence of sufficient or excess O_2 to form mainly CO_2 and H_2O. This process is exothermic and hence generates heat and light in the form of a flame.
- **Incineration** –This process is similar to combustion where organic materials contained in waste materials are burnt with the aim of reducing its volume. The waste can be reduced up to 96 % by volume thus reducing waste that is sent to landfills. Energy recovery is typically not the primary purpose of the incineration process.
- **Gasification** –The process involves the conversion of various carbonaceous feedstock into clean syngas, through a reaction with controlled amounts of oxygen, air or steam.
- **Pyrolysis** –Involves an irreversible change in the chemical composition of biomass at an elevated temperature in an inert environment. No H_2O or O_2 is added to the process and this means that the pyrolysis reactions are mainly

endothermic. Hence, heat needs to be added to the process and this is typically done via external heat transfer. Pyrolysis is usually the first step in the gasification and combustion processes and is usually carried out at temperatures around 500 ^{0}C or even higher in some cases. Pyrolysis usually produces condensate liquid which may be in the form of pyrolysis oil (bio-oil) or tar.

The above processes are mainly governed or controlled either by a supply of oxygen or by the temperature at which heat is supplied.

- Firstly, if we classify processes as to whether there is a supply/ presence of O_2, the five processes are confined to two groups. The one class is where the systems have zero supply of O_2 (pyrolysis and AD) and the other where a certain amount of oxygen is supplied, such as gasification, combustion and incineration.
- The second classification of these processes is the temperature at which heat is supplied/ rejected to the process. Heat transfer in AD processes occurs at low temperature whereas the other processes occur at high temperatures.

These two classifications are shown diagrammatically in Figure 1.2a for oxygen and Figure 1.2b for temperature.

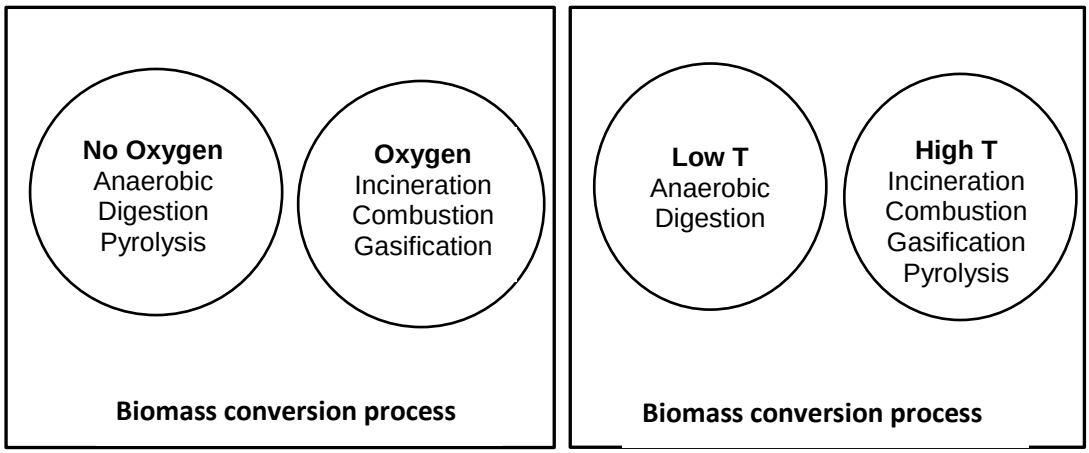

Figure 1.2: Subsets of biomass conversion process based on **a)** oxygen supply **b)** process temperature.

The biomass conversion processes can now be related depending on the amounts O_2 supplied or the operating temperatures. These two variables, however, classify and relate these processes differently where we look at the combinations of variables, namely:

- High Temperature, Supply Oxygen
- High Temperature, No Oxygen
- Low Temperature, Supply Oxygen,
- High Temperature, No Oxygen.

The four cases can be diagrammatically represented as shown in Figure 1.3, which shows three important unions namely A, B and C.

There are three regions where the sets intersect. These three unions denoted A, B and C narrows down the number of subsets for analysis.

- If Union A is considered where all three processes, gasification, combustion and incineration, require Oxygen and High Temperatures, it is important to note that the incineration and combustion processes are similar in that biomass is burnt in excess O_2 to reduce volume. These two differ from gasification in the quantity of O_2 supplied. In simple terms, when a limited/ controlled amount of oxygen is supplied to biomass and sufficient heat is provided through the partial combustion of biomass, this results in gasification. When excess oxygen is supplied in the gasification processes, the biomass is combusted or incinerated. This therefore gives the basis for choosing gasification as an umbrella term to represent the processes where high temperature and oxygen are both factors when converting biomass to products.

- Union B, corresponding to High Temperature and No Oxygen, contains pyrolysis.
- Union C, corresponding to Low Temperature and No Oxygen, contains AD.

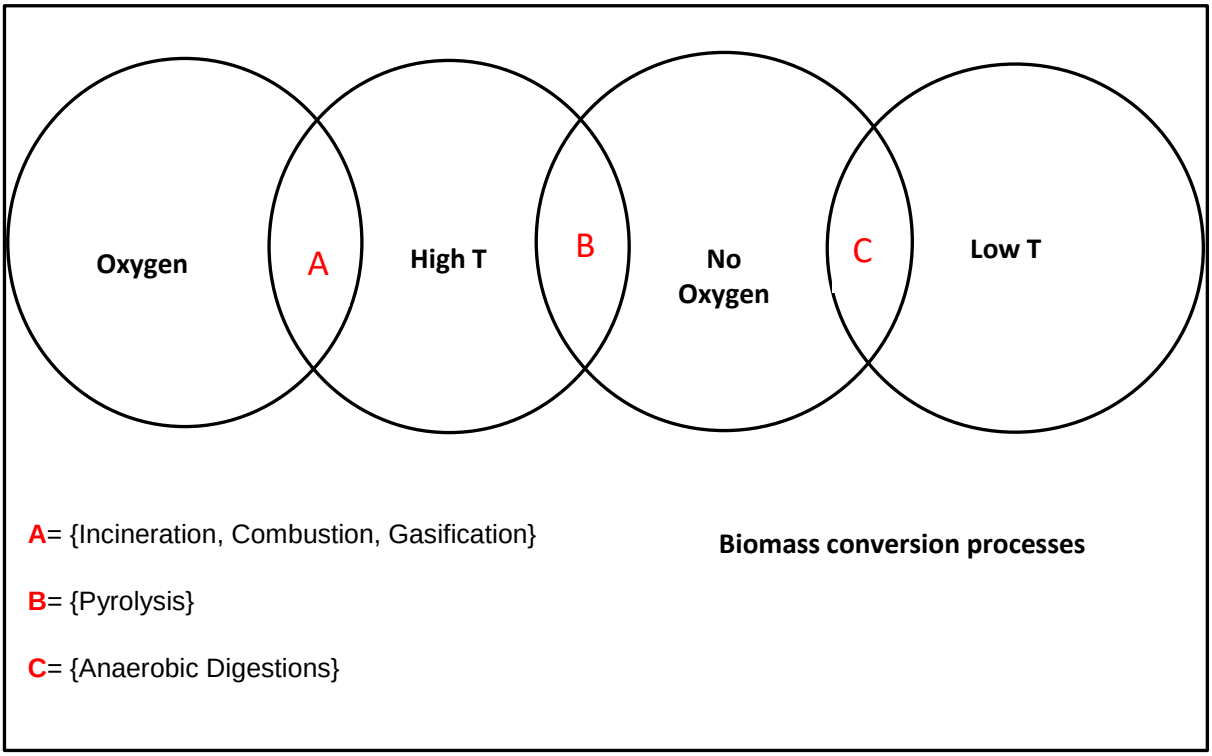

Figure 1.3: Universal set showing biomass conversion processes unions.

However, both pyrolysis and AD occur in the absence of Oxygen in common. Similarly, pyrolysis and gasification (including combustion and incineration), all occur at High Temperature.

The simple use of grouping processes in sets forms the basis for the investigation of three processes namely, AD, Pyrolysis and Gasification in this thesis. These processes are related by the amount of oxygen supplied as well as temperature and a simplified illustration of their relationship is shown in Figure 1.4. These three processes are investigated using the three main process syntheses tools, namely

material, energy and work balances or requirements when oxygen and temperature are varied.

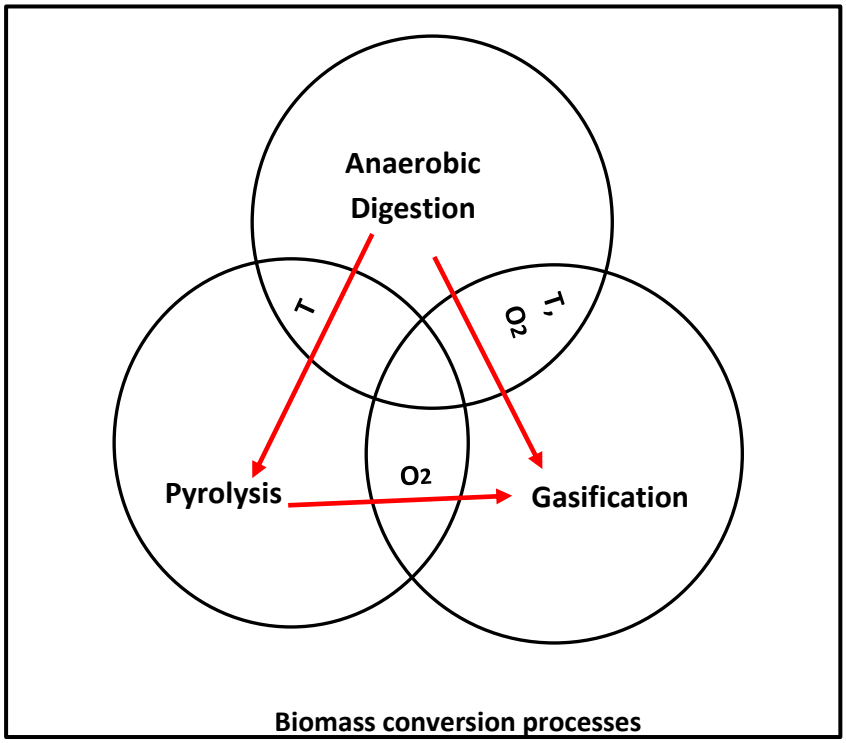

Figure 1.4: Universal set showing relationship of AD, gasification and pyrolysis.

The results of these analyses are represented by finding the appropriate Attainable Regions.

1.4. The Attainable Region (AR)

It is often hard to choose the best type of reactor to use for a particular chemical process. In order to determine the optimum reactor system, one needs to know what reactors to use, as well as the best way to connect these reactors together in a flow sheet. The AR method is a technique that helps to build and optimise a flow sheet for a reaction system.

The AR is defined as the set of all possible outcomes, for the system under consideration, which can be achieved using the fundamental processes operating within the system that satisfies all constraints placed on the system.

Glasser et al. (1987) showed how this region could be determined for reaction and mixing using a geometrical approach. The initial work found the AR in a two-dimensional concentration space for steady flow reactors.

The approach has been extended and used for different applications and has proved to be a successful tool in chemical engineering design. Ming et al., 2013 showed an application of the AR theory to batch reactors. AR analysis has also been used in comminution processes to reduce grinding times and energy requirements in order to achieve a specific particle size distribution (Chimwani et al., 2014; Danha et al 2015).

The AR has also been extended to processes rather than only reactors (Patel., 2007). Patel specified the feed and the set of possible product species. From this the set of independent material balances were then determined and the AR found in the space of extents of reaction. This region represents the set of all possible outputs from all possible processes and can be useful in identifying desired processes and synthesising these (Fox et al., 2013; Sempuga et al., 2010). This AR is referred to as the Material Balance Limited AR (MBL-AR).

The AR can also be found in the space of Enthalpy (H) versus Gibbs Free Energy (G) (Sempuga et al., 2010) and is called the G-H AR. The space remains two dimensional, irrespective of the number of feed or product species considered (and hence the

number of independent material balance that described the system) and the number of fundamental processes incorporated into the analysis. The G-H AR defines the set heat and work required for all possible processes. In this thesis, the technique developed by Sempuga of determining a G-H AR using a G-H plot is applied to biomass gasification processes (Sempuga et al., 2010).

Figure 1.5 shows how the G-H AR is used to illustrate the approach for the methanol synthesis from syngas (Okonye., et al 2012) with the simultaneous Water Gas Shift (WGS) reaction. He postulated that the preferred reactions were those that decreased G the most, and that the reaction pathway would tend to follow the boundary of the G-H space, and in particular the steepest boundary, in this case from the feed (represented by the origin in Figure 1.5) towards point a and then terminating at point b.

The AR has been applied to coal gasification where researchers have looked at the effect of feed composition and choice of reaction conditions (T and P) on the product (Ngubevana et al., 2011). He concluded that the use of graphical methods to asses and predict gasification is viable and definitely the most economical way of investigating gasification processes. In this regard, the technique of using the AR with G-H plots is applied for biomass gasification processes in the study.

Conventionally, researchers have also used the Ellingham diagrams, such as that shown in Figure 1.6, to show the relationship between G and temperature for a particular reaction. This however does not provide any easy analysis on the heat requirements for a specific process. When using process synthesis to design a

process, one is interested in both the heat and work requirements of a process. One is particularly interested in how far the process is away from adiabatic conditions (that is the heat requirements for the process) and where the minimum G occurs. One would prefer to work at adiabatic conditions because there is neither heat added nor rejected by the process thereby reducing overall process costs. Systems also tend to go where G is minimum as this gives the maximum driving force for a process to occur. If the G is recovered as work, then the process will be reversible. However, if there is no work recovery, then this leads to irreversibility in the process. The points for both adiabatic operation as well as minimum G can be determined from the 2-dimestion G-H AR of a process similar to the one shown in Figure 1.5. In reality, due to process conditions and equipment, it may be difficult to achieve either adiabatic or closer to reversible operation. However, it is important then to understand the implications on the work and heats flows to the process when operating at other points in the region.

The Ellingham diagram shown in Figure 1.6 does not show the energy requirements at the equilibrium compositions at different operating temperatures. The AR in Figure 1.5 effectively shows how the composition changes at the point of minimum G (such as point b) with temperature.

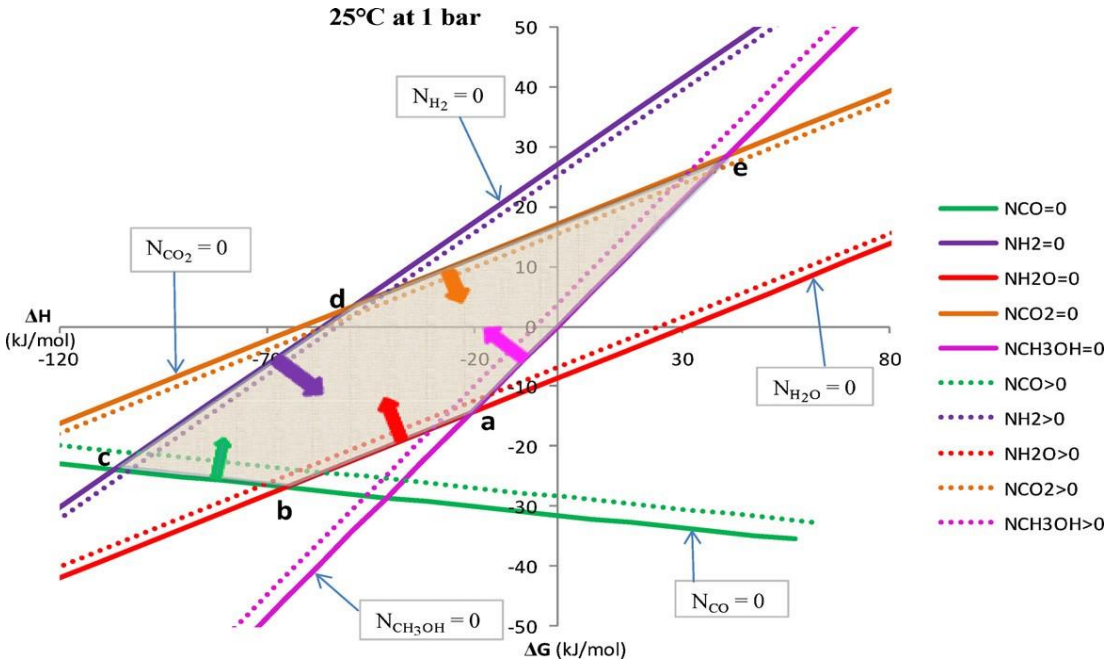

Figure 1.5: G-H AR for a chemical process showing A R for two reactions, methanol synthesis and WGS at 25 ^{0}C and 1 bar, using a feed of 1 mole CO_2, 1 mole H_2 and 0.5 moles H_2O, (Okonye et al., 2012).

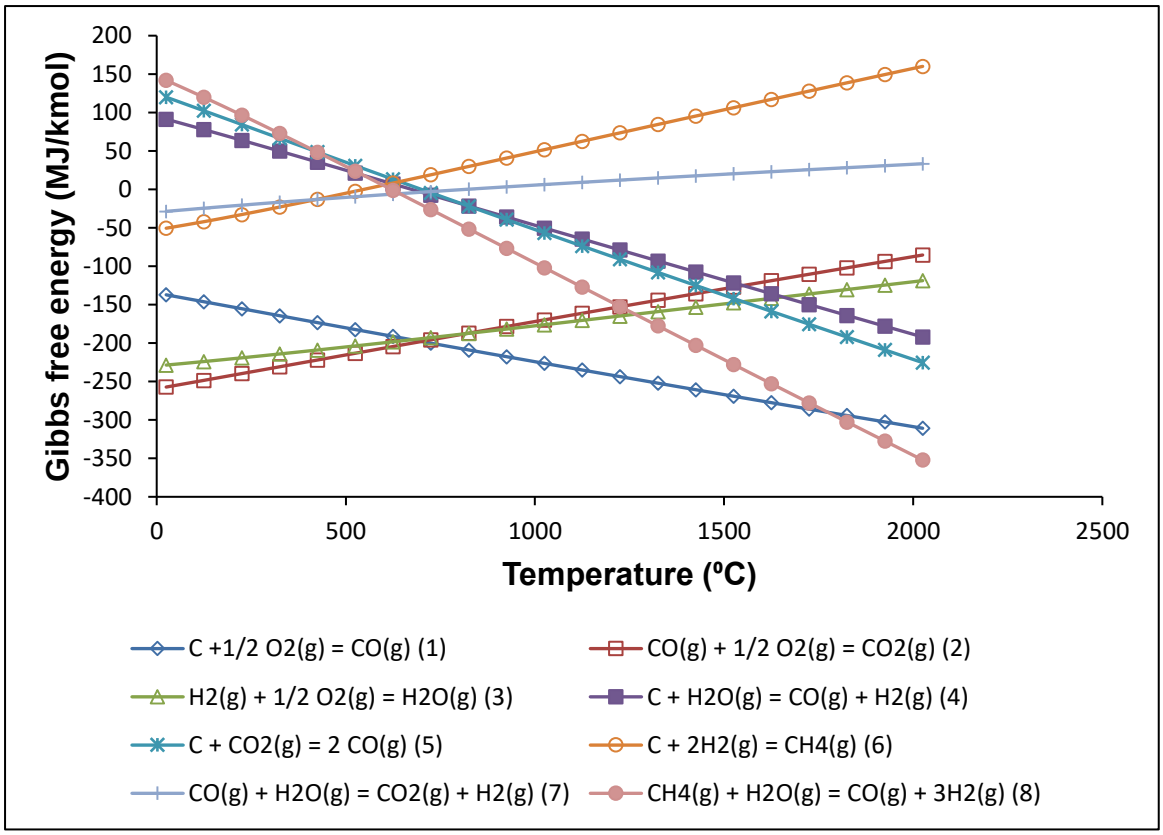

Figure 1.6: Ellingham diagram of possible reactions in the gasification process, Van der Walt and Jansen (2015).

The application of both the MBL-AR and as well as the G-H AR to biomass gasification processes is at the heart of this thesis. Particularly, interest is in what can be achieved by gasifiying a biomass feed at different temperatures, heat inputs and oxygen concentrations.

The two regions found most useful in this work are:

- **The MBL-AR:** This is the set of all possible material balances for a given feed and defined possible species in the products. The AR lies in the space that describes the material balances for the process. The axes for this space could be, for example, extents of the independent reactions or some other variable(s) that defines and tracks the composition of the product. This region represents all possible products (outputs) for all possible steady state processes for a given feed.
- **The G-H AR:** This is the set of all possible heat (H) and work (G) requirements for a given feed and defined possible species in the product. The AR lies in the G-H space. The axes of the two-dimensional space are H and G that the AR represents the set of all possible heat and work flows for all processes the use the given feed.

The experimentally measured data for AD and a plasma system for pyrolysis and gasification are compared to the theoretically calculated AR in this thesis.

For the theoretical calculations, a feed of glucose is assumed to be a surrogate of biomass. This is because it is the closest compound to various composition of elements biomass that we have the G values available to enable us to do work

analysis. For experimental analysis, wood pellets are used for pyrolysis and gasification processes while glucose, cow dung and dog faeces are analysed for AD.

1.5. AD, pyrolysis and gasification

Biomass can be converted into different products depending on its composition, the quantity and quality of heat supplied as well as whether an oxidation media is also added to the process. The main products of AD are CH_4 and CO_2 while the principal products of plasma pyrolysis/ gasification is a low to medium calorific value gas composed of mainly CO and H_2. These main products may also be coupled with a mixture of other gases in small quantities including CH_4, CO_2 as well as light hydrocarbons like ethane and propane and heavier hydrocarbons like tars (Somayeh et al., 2016). Solid products in the form of carbon/ biochar can also be formed.

The main products that are usually present when biomass is converted using various process conditions are described by the global gasification material balance reaction in Eq. (1.1) (Mountouris et al., 2006). It shows the possible molar products and the relative amount of reagent required to break down a given biomass. The relative molar amounts of product and reagents depend on the respective composition of each biomass material.

$$CHxOy + \boldsymbol{w}H_2O + \boldsymbol{m}O2 + 3.76\boldsymbol{m}N_2 \rightarrow \boldsymbol{a}H_2 + \boldsymbol{b}CO + \boldsymbol{c}CO_2 + \boldsymbol{d}H_2O + \boldsymbol{e}CH_4 + \boldsymbol{f}N_2 + \boldsymbol{g}C \quad \textbf{(1.1)}$$

The quality of product formed is affected by composition of the feedstock material, gasifying agent (H_2O or O_2), reactor design, the presence of catalyst, reactor operating

conditions and the typical lower heating value of the feed which ranges from 4-13 MJ/Nm^3 (Parthasarathy and Narayanan, 2014). However, thermodynamics, and in particular reaction equilibrium, drives the process towards the material balance that minimizes the G of the product.

Figure 1.7 shows how the products at equilibrium changes with temperatures between ~25 ^{0}C to ~2500 ^{0}C and when O_2 is introduced for biomass gasification. The theoretical data obtained from Aspen in Figure 1.7a shows pyrolysis of biomass in the form of dry wood. The results show that wood of mass ratio (C=0.511, H=0.064, O=0.425) is decomposed into mainly syngas at temperatures above 900 ^{0}C. Solid carbon is also present when no gasification agent was added to the process. Figure 1.7b shows a drastic decrease in the quantity of C when O_2 was added to the gasification process (Hrabovsky., 2011). This shows that there is potential to achieve high, clean gas in biomass conversion processes if the operation can be done at these high temperatures.

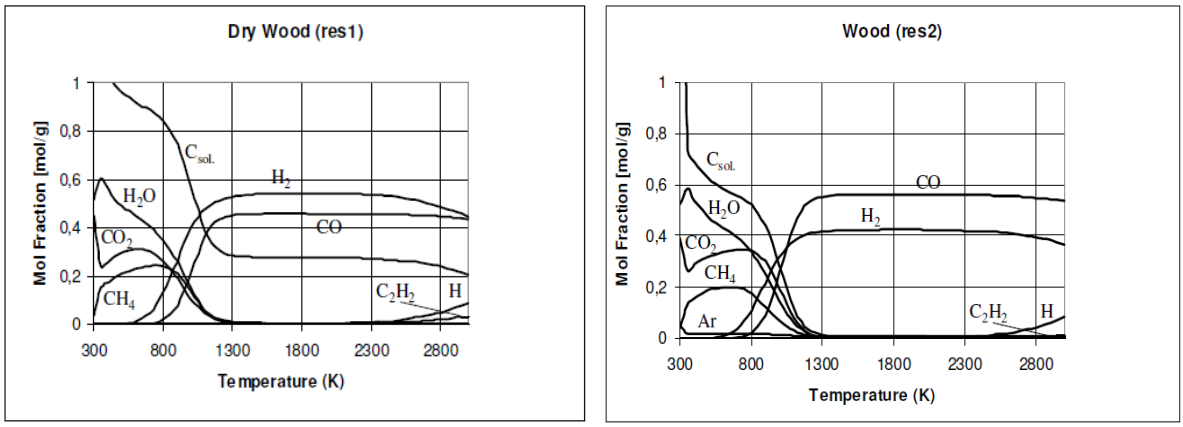

Figure 1.7 (a): Changes in product gas composition at equilibrium with temperature. **(b)** Effect of adding a gasification agent to gas product on gasification of wood (Hrabovsky., 2011; Van Oost., et al., 2008).

At relatively lower temperatures (i.e. below ~700 ^{0}C), C and O_2 prefer to exist as CO_2 and C char, i.e. the char conversion is lower (Hrabovsky., 2011). At high temperatures,

if there is an excess of C, the CO_2 breaks down to form CO. Moreover, O_2 prefers to react with C (to form CO and CO_2) rather than with H_2 to form H_2O (so H_2 content increases at higher temperatures). Methane and other hydrocarbons tend to decompose at temperatures above ~700 ^{0}C; this can also imply a significant decrease in the tar content at temperature higher than 1000 ^{0}C.

The analysis in Figure 1.7 concentrates mostly on analysing results of high temperature processes (Hrabovsky., 2011). Most researchers are more comfortable in accepting that thermodynamics drives the products that can be obtained during gasification and pyrolysis processes. However, it can be seen in Figure 1.7 that at lower temperatures around 25 ^{0}C, CH_4; CO_2, H_2O and C are dominant at equilibrium. CH_4 and CO_2 are experimentally found to be products of AD and it can be observed that these are the thermodynamically favoured products at 25 ^{0}C. However, biologists typically look to change the ratio of CO_2 to CH_4 or improve the yield of H_2 by changing the microbial population or the conditions in the digester. Hence, there appears to be a belief that these determine the product distribution rather than thermodynamics.

The research in this thesis investigates the relationship between the low and high temperature processes to try to contribute further into understanding the relationship between these processes. Specifically, the researcher aims to find out what drives the range of products that can be formed from biomass from low to high temperatures, placing emphasis on low temperature systems (AD). This is interesting because AD is a biological process and is catalysed/ facilitated by a group of bacteria while pyrolysis/ gasification is known to be governed by kinetics and thermodynamics.

AD takes place at low temperature in the absence of oxygen. One of the main concerns when designing such a process is the stability of the process in order to ensure the viability of the microorganism. This differs from pyrolysis and gasification processes where much time is spent in designing the reactor system and in particular the heat transfer systems in the process. There are various pyrolysis and gasification reactors currently used but this research places emphasis only on plasma gasification. Plasma pyrolysis/ gasification allows us to add heat at effectively a single temperature. This allows us to compare the theoretical approach used to the experimental results, which helps us gain a better understanding of the relationship between the material, energy and work balances and the product composition from the process.

1.6. Plasma pyrolysis/ gasification

Recognising the limitations of many waste treatment and energy generation processes in terms of environmental, energy efficiency and health and safety concerns, the use of plasma systems has currently become a technology of interest to help solve the issues of waste utilization. Plasma pyrolysis/ gasification is a technology used to convert carbon-containing materials to syngas at high temperatures (Rajasekhar et al., 2015). Plasma technologies have been used in various industries to treat radioactive and medical wastes (Rutberg., 2002; IAEA., 2006). However, it has received increasing attention over the last decades (Somayeh et.al., 2016) for other uses including conversion of biomass.

Plasma is often referred to as the fourth state of matter as it is distinct from solid, liquid and gaseous states (Gonawala., 2014; Higman and Van der Burgt, 2007). Plasma is formed when atoms, typically in a gas, are ionised. An electrical current under high voltage is fed through two electrodes and ionises the gas between the electrodes,

thereby generating a plasma arc (Patel and Chauhan, (212). Gas is ionised as it passes between the electrodes, forming a plasma, and this becomes both thermally and electrically conductive. The most frequently used plasma gas is air while nitrogen, carbon dioxide, steam and argon are also sometimes used (Heberlein and Murphy, 2008). Copper, tungsten and various alloys can be used as electrodes in plasma systems. When the plasma gas is ionised, it illuminates, and this forms what is called a plasma torch.

Plasma torches can operate at very high temperatures (up to 100 000 ^{0}C at the arc) and can process all kinds of waste: municipal solid, toxic, medical, biohazard, industrial and nuclear waste at atmospheric pressure (Hlina et al., 2014; Arena., 2011; Chung et al., 2012; Edbertho Leal-Quir´os., 2004; Galeno et al., 2011; Lemmens et al., 2007). These high temperatures at the arc helps to achieve high bulk temperatures that cannot be reached by convectional gasification processes where the energy is mainly provided by oxygen through the combustion process. At temperatures more than 5 000 ^{0}C, no ash is produced because all the organic molecules disintegrate and only the product, which is a mixture of H_2 and CO, remains at high temperature (Edbertho Leal-Quir'os., 2004). This may not be entirely true as ashes are mainly inorganic matter. Ashes may be burnt in the gaseous phase but will still agglomerate with other inorganic materials, such as metals, present. However, a plasma system can achieve the highest reduction in volume size of organic waste materials hence can also be used specifically to reduce volumes of biomass sent to landfills.

The plasma gasification process is deemed the future method for treating solid waste materials (Spyridon and Evangelos, 2013). Plasma gasification exploits the

thermochemical properties of plasma. Heat is converted to kinetic energy of the particles and this is used for decomposing biomass. In addition, the presence of charged and excited species renders the plasma environment highly reactive, which can catalyse homogeneous and heterogeneous chemical reactions. Several chemical reactions occur during the gasification process at the plasma arc, which is the central component of the system. Electrical energy is converted to plasma energy and is stored in the syngas as chemical energy. The composition of the product syngas is not strongly influenced by the plasma gas composition. Less energy is consumed when heating plasma reactors to reaction temperature compared to conventional systems (Hrabovsky., 2011). This means that lower plasma flow rates can carry sufficient energy for the process. The reaction temperature in a plasma gasifier can be reached between seconds to 30 minutes in comparison to the waste processing mechanisms like incineration which may require up to 36 hrs to reach reaction phase (Vishal and Vastal, 2016; Ganawala., 2014). Plasma is a medium with the highest energy content resulting in a more efficient process producing syngas with minimum contamination/ dilution (Andrijsevic and Gero, 2007).

Plasma gasification is different from incineration in the sense that the latter is focused on reduction of waste to smaller volumes of ash in the presence of excess O_2. Usually, the main driver of this process is the volume reduction of the waste material, rather than energy recovery or production of valuable gaseous products. With incineration, the products are CO_2 and the ash. On the other hand, with plasma systems, there is an advantage in producing syngas rather than CO_2.

For this research, a plasma gasifier was chosen instead of conventional gasifiers because of its ability to convert biomass materials at higher temperatures, thus yielding a high concentration of syngas. Although the author used a small-scale plasma system for the experimental work, Ganawala claims that plasma gasifiers are as efficient at large scale as small-scale systems (Ganawala., 2014). Thus, the experimental results achieved in the lab reactor should be applicable to large scales systems. Another advantage of a plasma gasifier over other convectional gasifiers, such as downdraft and updraft gasifiers is that the plasma system can typically handle a wider range of feeds and sizes. Operating parameters can be varied over a wider range. Plasma gasification also has the ability to use both electrical and combustion energy simultaneously, so that one can vary the energy input from only electrical energy to a combination of electrical and chemical energy (added via oxygen).

A report from the Secretary of the Energy Advisory Board Panel on Technological Alternatives to Incineration (2000), questions the reliability of the plasma torch technology. It points out that the water-cooled copper torch must be replaced periodically due to erosion of the plasma arc to prevent burn-through at the attachment point of the arc and a subsequent steam explosion due to rapid heating of the released cooling water. On the other hand, (Heberlein and Murphy, 2008) argued that this could be avoided by using a radio-frequency induction plasma reactor. The erosion of electrodes and degradation of plasma torch performance reportedly needs to be addressed through periodic inspections and maintenance (Heberlein and Murphy, 2008; Tendler et al., 2005).

Although plasma gasification has great promise of producing high quality syngas and is flexible with feedstock, this technology has not been applied extensively, especially on municipal biomass waste. This is because large-scale plasma gasification facilities are expensive, and it takes the right combination of tipping fees, electric power rates, and other higher-value products to pay for the facility (Recovered Energy, Inc. 2010; USST., 2010). In addition, to date, lack of public domain data on economics and operability, means that plasma gasification of biomass feed stocks has been overlooked (NNFCC., 2009). Currently thermal plasma reactors range from 1 t/day-30 t/day (Li et al., 2016).

Given all these advantages and problems associated with plasma systems, this thesis investigates the use of a new design for plasma gasification, which uses pure nitrogen as a plasma ionising gas. This is perceived to use less current but at the same time achieves high voltages in the systems. It is thought that this will help reduce the erosion of electrodes, reduce energy supplied to the process, hence reducing overall costs. The researcher also wishes to provide much more detailed information, often not provided by other researchers on plasma systems. This includes heat and work requirements for the reaction process as well as the product distribution.

1.7. Thesis Outline

The aim of this research is to show that the use of mass, energy and work balances can be used to analyse biomass conversion to gas processes. It is shown that there is an underlying relationship between AD, pyrolysis and gasification processes. This was achieved through both theoretically and experimental analysis. The issue of knowing what drives processes to achieve certain products at both low and high

temperature was considered important. This has been discussed in the various chapters of this thesis. However, it is important to note that individual chapters were further analysed for other parameters to try to understand and demonstrate the common relationship between the three processes studied.

Chapter 1 gives the researcher's motivation of why the investigation undertaken can contribute to the understanding of process that convert biomass to gas. It also provides the background of biomass conversion technologies and outlines the scope of the work undertaken. It provides technical information and relationship on AD, pyrolysis and gasification; defines what the AR means and ultimately explains the principles of plasma technology. Chapter 1 describes the approach the researcher chose to carry out the theoretical and experimental analysis of the biomass gasification process carried out for both low and high temperatures.

Chapter 2 shows the results on the theoretical analysis for the low-temperature AD (often referred to as biogas production) and pyrolysis processes. It reports details of the gases produced for the temperature range 25 ^{0}C to 100 ^{0}C when water is in liquid state and shows the changes in the AR for biogas production conditions. Chapter 2 also offers the theoretical results for AR theory for high temperature pyrolysis and gasification processes. It shows how the composition of the product gas changes when the temperature is raised from 100 ^{0}C to 1500 ^{0}C. Chapter 2 has been published and referenced as:

> **Ralph Farai Muvhiiwa*.,** Xiaojun Lu., Diane Hildebrandt., David Glasser., Tonderayi Matambo., 2018. **Applying thermodynamics to**

digestion/gasification processes: The Attainable Region approach. *Journal of Thermal Analysis and Calorimetry,* Vol. 131(1), pp. 25-36.

Chapter 2 Addendum introduces the generalised approach to determine the MBL - AR and G-H AR and applies this to biomass conversion processes. The effect of the amount of O_2 added as well as temperature on the thermodynamically favoured product is investigated. It also shows how the AR changes when oxygen is added to the process at a particular temperature.

Chapter 3 shows a comparison of experimental and theoretical (AR) for low temperature gasification, specifically for biogas production at 30 ^{0}C. The results show the relationship between the operating points that bacteria operate and the thermodynamic limits of performance. Chapter 3 has been presented at a conference under

Muvhiiwa R*., Hildebrandt D., Matambo T., Glasser D., 2015.**Theoretical and experimental analysis on biogas production**. PSE2015/ESCAPE25. Poster Presentation # 302, Copenhagen, Denmark, 31 May - 4 June 2015.

Chapter 4 provides an analysis of the results obtained from the experimental work using a plasma gasifier. It also records the different products obtained when wood pellets, which were used as the biomass substrate, are subject to pyrolysis in a continuous nitrogen plasma reactor. Additionally, it provides the results of changing the operating temperature for the feed. The chapter also makes a comparison between the experimental results and the AR in material balance space. A work and exergy

analysis is introduced in this chapter based on the experimental results obtained. Chapter 4 has been published and is referenced as:

> **Ralph Farai Muvhiiwa*.,** Baraka Sempuga., Diane Hildebrandt., Jaco Van Der Walt., 2018 **Study of the effects of temperature on syngas composition from pyrolysis of wood pellets using a nitrogen plasma torch reactor.** *Journal of Analytical and Applied Pyrolysis*, Vol 130, pp. 159-168.

Chapter 5 presents further work on optimisation of the results described in the preceding chapter. It includes the outcome of the researcher adding a gasification agent (O_2) into the plasma gasifier for the biomass material studied to see how the product gas changes with temperature. It further shows a heat and work analysis on the system. A relationship of the experimental and theoretical analysis is also discussed in this chapter.

Chapter 6 looks at the study from an engineering and social perspective rather than from a scientific point of view. It shows a different issue to the scope of this thesis but provides an application of a real system for biogas production that has been discussed. The researcher attributes that to be a leader in science one should be able to go from theory into practice. It looks at how a community in the study responds to use of biogas for energy. This was investigated based on a 10 m^3 biodigester implemented as a community project in Muldersdrift, South Africa. This chapter involves the impacts and challenges of biogas implementation towards building a sustainable society with a motive to utilise available waste and reduce emissions. Chapter 6 has been published and referenced as:

Muvhiiwa R*., Hildebrandt D., Matambo T., Chimwani C., Ngubevana L., 2017. **The impact and challenges of sustainable biogas implementation: moving towards a bio-based economy.** *Energy, Sustainability and Society*, **7**:20 https://doi.org/10.1186/s13705-017-0122-3.

Chapter 7 summarises the main findings of the work done and the contribution to knowledge in this crucial field of utilising biomass sustainably. It also makes recommendations for how this research could be applied in industry and carried forward.

It was decided to include the chapters that have already been published as they appear in the journals with minimum changes. The nomenclature and abbreviations used in the rest of the thesis may thus differ from that that is used in the published work.

References

1. Andrijaevi M., Gero M., (2007). Renewable Energy: A Solution for Croatia. http://www.amcham.hr/_dwnls/committee/mislav_andrijasevic.ppt#1.
2. Arena U., Zaccariello L., Mastellone M.L., 2010. Fluidized bed gasification of waste derived fuels. Waste Management, Vol. 30, pp. 1212–1219.
3. Arena U., 2011. Process and technological aspects of municipal solid waste gasification. Journal of Waste management, Vol. 27, pp. 625–639.
4. Bosmans A., Vanderreydt I., Geysen D., Helsen L., 2013. The crucial role of Waste to-Energy technologies in enhanced landfill mining: a technology review. Journal Cleaner Production, Vol. 55, pp. 10–23.
5. Chimwani N., Mulenga F., Hildebrandt D., Glasser D., Bwalya M., 2014. Scale-up of batch grinding data for simulation of industrial milling of platinum group minerals ore. Minerals Engineering, Vol. 63, pp. 100–109.
6. Chung J., Youngchul B., Moohyun C., Soon-Mo H., 2012. Thermal Plasma Gasification of Municipal Solid Waste (MSW), INTECH Open Science.
7. COP21/CMP11., 2015. United Nations Conference on Climate Change, Nov 30 to Dec 12 2015. Paris. http://www.cop21.gouv.fr/en/more-details-about-the-agreement/
8. Danha G., Hildebrandt D., Glasser D., Bhondayi C., 2015. A laboratory scale application of the attainable region technique on a platinum ore. Powder Technology, Vol. 274, pp. 14–19.
9. Danthurebandara M., Steven Van P., Ive V., Karel Van A., 2015. Environmental and economic performance of plasma gasification in Enhanced Landfill Mining. Waste Management, Vol. 45, pp. 458–467.

10. David E., 2015. Steam reforming of biomass tar using iron-based catalysts. Chemical Engineering Transactions, Vol. 43.
11. Dovetail Partners, INC., 2010. Plasma Gasification: An examination of the Health, Safety, and Environmental Records of Established Facilities Prepared for the City of Palisade, Minnesota June 7.
12. Edbertho L., 2004. Plasma Processing of Municipal Solid Waste. Brazilian Journal of Physics, Vol. 34(4B).
13. Environmental protection Agency (EPA), USA., 2016.
14. Fabry F., Christophe R., Vandad J. R., Laurent F., 2013. Waste Gasification by Thermal Plasma: A Review. Waste and Biomass Valorization, Vol. 4 (3), pp. 421–439.
15. Fox J., Hildebrandt D., Glasser D., Patel., 2013. A graphical approach to process synthesis and its application to steam reforming. AIChE Journal, Vol. 59(10), pp. 3714–3729.
16. Galeno G., M. Minutillo M., Perna A., 2011. From waste to electricity through integrated plasma gasification/fuel cell (IPGFC) system. International Journal of Hydrogen Energy, Vol. 36(9).
17. Glasser D., Hildebrandt D., Crowe C. A., 1987. A geometric approach to steady flow reactors: the attainable region and optimization in concentration space. Industrial Engineering Chemical Resource, Vol. 26, pp. 1803–1810.
18. Gonawala K., Ankita P., Mehali M., 2014. Plasma Gasification of Municipal Solid Waste: A Review. International Journal of Engineering Sciences & Research Technology, Vol. 3(1).
19. Hassan E. M., Yu F., Ingram L., Steele P., 2009. The potential use of whole-tree biomass for bio-oil fuels. Energy Source, Vol. 31, pp. 1829–39.

20. Hlina M., Hrabovsky M., Kavka T., Konrad M., 2014. Production of high quality syngas from argon/water plasma gasification of biomass and waste. Waste Management, Vol. 34, pp. 63–66.
21. Heberlein J., Murphy A. B., 2008. Topical Review: Thermal plasma waste treatment Journal of Physics D. Applied Physics, Vol. 41(5), pp. 1–19.
22. Hrabovsky M., Hlina M., Kavka T., Konrad M., Chumak O., Maslani A., 2009. Thermal plasma gasification of biomass for fuel gas production. High Temperature Material Processes: An International Quarterly of High-Technology Plasma Processes, Vol. 13(3-4), pp. 299–313.
23. Hrabovsky M., 2011. Thermal Plasma Gasification of Biomass. Institute of Plasma Physics ASCR Czech Republic. Progress in Biomass and Bioenergy Production. Chapter 3 of a book edited by Syed Shaid Shaukat, ISBN 978-953-307-491-7, NC-SA 3.0 liscence www.intechopen.com
24. IEA, World Energy Outlook., 2008. International Energy Agency: Paris.
25. Lemmens., Elslander H., Vanderreydt I., Peys K., Diels L., Oosterlinck M., Joos M., 2007. Assessment of plasma gasification of high caloric waste streams. Waste Management, Vol. 27, pp. 1562–1569.
26. Li J., Liu K., Yan S., Li Y., Han D., 2016. Application of thermal plasma technology for the treatment of solid wastes in China: an overview. Waste Management, Vol. 58, pp. 260–269.
27. Lombardi L., Carnevale E., Corti A., 2012. Analysis of energy recovery potential using innovative technologies of waste gasification. Waste Management, Vol. 32, pp. 640–652.
28. Mathieu P., Dubuisson R., 2002. Performance analysis of a biomass gasifier. Energy Conversion Management, Vol. 43, pp. 1291–9.

29. Ming D., Glasser D. Hildebrandt D., 2013. Application of attainable region theory to batch reactors. Chemical Engineering Science, Vol. 99, pp. 203–214.
30. Mountouris A., Voutsas E., Tassios D., 2006. Solid waste plasma gasification: equilibrium model development and exergy analysis. Energy Conversion Management, Vol. 47, pp. 1723–37.
31. Naidoov R., 2017. Improving landfilling: correct practices and useful technologies. Landfills, News, Waste [Accessed 22 Feb 2017]. http://www.infrastructurene.ws/2017/02/22/improving-landfilling-correct-practices-and-useful-technologies/#
32. Ngubevana L., Hildebrandt D., Glasser D., 2011. Introducing novel graphical techniques to assess gasification. Energy Conversion and Management, Vol. 52, pp. 547–563.
33. NNFCC project 09/008., 2009. Review of Technologies for Gasification of Biomass and Wastes, Final report. A project funded by DECC, project managed by NNFCC and conducted by E4Tech June.
34. Okonye L. U., Hildebrandt D., Glasser D., Patel B., 2012. Attainable regions for a reactor: Application of G-H plot. Chemical Engineering Research and Design, Vol. 90, pp. 1590–1609.
35. Patel B., 2007. Fundamental targets for the synthesis and evaluation of chemical processes. Doctoral thesis, University of the Witwatersrand, Johannesburg, South Africa.
36. Patel M. L., Chauhan J. S., 2012. Plasma Gasification: A Sustainable Solution for the Municipal Solid Waste. International Journal of Environmental Sciences, Vol. 3(1).

37. Parthasarathy P., Narayanan K.S., 2014. Hydrogen production from steam gasification of biomass: influence of process parameters on hydrogen yield-a review. Renewable Energy, Vol. 66, pp. 570–579.
38. Rajasekhar M., Venkat Rao N., Chinna Rao G., Priyadarshini G., Jeevan Kumar N., 2015. Energy Generation from Municipal Solid Waste by Innovative Technologies – Plasma Gasification. Procedia Materials Science, Vol. 10, pp. 513–518.
39. Recovered Energy, Inc., 2010. The Recovered Energy System. (http://www.recoveredenergy.com/faq.html).
40. Rutberg P. G., Bratsev A. N., Safronov A. A., Surov A. V., Schegolev V. V., 2002. The technology and execution of plasma chemical disinfection of hazardous medical waste. IEEE Trans. Plasma Science, Vol. 30, pp. 1445–1448.
41. Rutberg P. G., Bratsev A. N., Ufimtsev A. A., 2004. Plasmochemical technologies for processing of hydrocarbonic raw material with syngas production. Journal of High Temp. Material Processes, Vol. 8, pp. 433–446.
42. Sempuga B. C., Hausberger B., Patel B., Hildebrandt D., Glasser D., 2010. Classification of Chemical Processes: A Graphical Approach to Process Synthesis to Improve Reactive Process Work Efficiency, Industrial and Engineering Chemistry Research, Vol. 49:17, pp.8227–8237.
43. Somayeh F., Mohsen A. M., Johann F. G., 2016. A critical review on biomass gasification, co-gasification, and their environmental assessments. Biofuel Research Journal, Vol. 12, pp. 483–495.
44. Spyridon A., Evangelos K., 2013. Efficiency Evaluation of RDF Plasma Gasification Process. Energy and Environment Research, Vol. 3(1).

45. Tellus Institute., 2008. Assessment of Materials Management Options for the Massachusetts Solid Waste Master Plan Review. Final Report Contract EQE193, Boston MA.
46. Tendler M., Rutberg P., van Oost G., 2005. Plasma Based Waste Treatment and Energy Production. Plasma Physics and Controlled Fusion, Vol. 47(5), pp. A219–A230. (http://www.iop.org/EJ/abstract/0741-3335/47/5A/016)
47. U.S. Science & Technology (USST)., 2010. Plasma Gasification: Frequently Asked Questions. (http://www.usstcorp.com/faq.html) [Accessed 16 Apr 2016].
48. Van der Walt I. J., Jansen A. A. (2015). Plasma Biomass Gasifier, Revision 1, R1. DOC No: AC-EURO4-DES-12001.
49. Vishal S., Vatsal N., 2016. Gasification – A Process for Energy Recovery and Disposal of Municipal Solid Waste. American Journal of Modern Energy, Vol. 2(6), pp. 38–42.
50. Zhang Q., Dor L., Fenigshtein D., Yang W., Blasiak W., 2012. Gasification of Municipal Solid Waste in the Plasma Gasification Melting Process. Applied Energy, Vol. 90(1), pp. 106–112.

Chapter 2: Applying Thermodynamics to Digestion/Gasification Processes: The Attainable Region Approach

This chapter has been published in the Journal of Thermal Analysis and Calorimetry cited as **Muvhiiwa, R.F**., Lu, X., Hildebrandt, D., Glasser D, Matambo T. *J Thermal of Analysis and Calorimetry* (2018). Vol 131(1). pp. 25-36. https://doi.org/10.1007/s10973-016-6063-9

This is completely my work, I did all the theoretical calculations and processing of data as well as writing the paper, the other authors are my supervisors.

Abstract

The research shows theoretical calculations on the thermodynamics of Anaerobic Digestion (AD) and pyrolysis processes where glucose is used as a surrogate for biomass. The change in Enthalpy (ΔH) and Gibbs Free Energy (ΔG) are used to obtain the Attainable Region (AR) that shows the overall thermodynamic limits for AD and pyrolysis gasification from 1 mole of glucose. Gibbs Free Energy and Enthalpy (G-H) plots were constructed for the temperature range 25 ^{0}C – 1500 ^{0}C. The results show the effect of temperature on the AR for the processes when water is both in liquid and gas states using 25 ^{0}C, 1 bar as reference state. The AR results show that the production of CO, H_2, CH_4 and CO_2 are feasible at all temperatures studied. The minimum Gibbs Free Energy (minimum G) becomes more negative from -418.68 kJ mol^{-1} at 25 ^{0}C to -3024.34 kJ mol^{-1} at 1500 ^{0}C while the process shifts from exothermic (-141.90 kJ mol^{-1}) to endothermic (1161.80 kJ mol^{-1}) for the respective temperatures studied. Methane and carbon dioxide are favoured products (minimum G) for temperatures up to about 600 ^{0}C and this therefore includes AD. The process is exothermic below 500 ^{0}C thus AD requires heat removal. As the temperature

continues to increase, hydrogen production becomes more favourable than methane production. The production of gas is endothermic above 500 ^{0}C and it needs a supply of heat that could be done either by combustion or by electricity (plasma gasification). The calculations show that glucose conversion at temperatures around 700 ^{0}C favours the production of carbon dioxide and hydrogen at minimum G. Generally, the results show that the gas from high temperature pyrolysis/ gasification (> ~800 ^{0}C) typically carries the energy mainly in syngas components CO and H_2, whereas at low temperature processes (< 500 ^{0}C) the energy is carried in CH_4. The overall analysis for the temperature range (25 ^{0}C - 1500 ^{0}C) also suggests a close relationship between biogas production/digestion and gasification as biogas production can be referred to as a form of low temperature gasification.

2.1. Introduction

There is still need for research towards sustainability particularly in the gasification field Heberlein and Murphy (2008). The theory of gasification has been studied but there still exist opportunities to optimise the process. Also, the robustness of life cycle assessment on gasification technologies is still limited as there is need to have a base analysis on simulations and actual pilot results (Evangelisti et al., 2015). Plis et al., 2016 has used thermogravimetric analysis to investigate the combustion characteristics of both raw and torrefied biomasses up to a temperature of 866 ^{0}C. Thermogravimetric analysis and mass spectrometry are useful techniques to investigate the kinetics and combustion of biomass materials Mardziarz and Wilk, (2013). Experimental gasification results have shown that product gas yield and composition is affected by temperature (Raheem et al., 2015; Portofino et al., 2013;

Pacioni et al., 2016). Simulations on biomass materials have been carried out using different software such as Aspen and have provided theoretical predictions in the gasification field (Lombardi et al., 2012; Hrabovsky et al., 2009; Leal-Quiros (2004)). However, there is also need to provide a simple fundamental technique that uses thermodynamic laws and gives an overall graphical picture of the process.

Thermodynamics is very important to all processes as it tells us the limits on what is achievable. It shows the feasible outputs from a given feedstock based on material, energy and work (G) constraints. Thermodynamics is also an important tool in obtaining ARs for all processes and this helps to design efficient systems. Significant research has been carried out in order to find how the thermodynamic AR theory can provide vital optimisation information to researchers and an application of this theory will be used to study AD, pyrolysis and gasification in this research. The AR method is a technique from chemical reaction engineering that helps to build and optimize a flow sheet for a reaction system (Glasser et al., 1987). The AR is defined as the set of all possible outcomes for the system under consideration that can be achieved; using the fundamental processes operating within the system and that satisfies all constraints placed on the system (Glasser et al., 1987). Thermodynamics is also an important tool in obtaining ARs for processes and these can be used to help design efficient systems. The AR can show the overall region where fundamental processes of reaction, mixing, heat and mass transfer can take a system (Glasser et al., 1987). In this research, the AR is the set of all possible output concentrations of products that can be obtained in a steady state AD, pyrolysis or gasification system with a given biomass feed represented by glucose.

The technique developed by Sempuga of showing an AR using a G-H plot is applied in this chapter to biomass conversion processes (Sempuga et al., 2010). This technique has been used by Okonye for methanol synthesis from syngas simultaneous with the Water Gas Shift (WGS) reaction (Okonye et al., 2012). The theory of the AR has also been applied to batch reactors (Ming et al., 2013). The two later referenced researchers have shown that this approach can work on chemical processes while other researchers have also shown that this analysis can be used in comminution processes to reduce grinding times and energy requirements to achieve a specific result (Chimwani et al., 2014; Danha et al., 2014). It is also necessary to note the difference in the product spectrum as the temperature changes as well as the amount of heat and work requirements to achieve specific gas products in the region. The AR technique is used to show the possible region for digestion/gasification of glucose, a surrogate for biomass for temperatures 25 ^{0}C – 1500 ^{0}C. This is achieved graphically using G-H AR and locating the global minimum G.

The reason for using glucose as a surrogate for biomass is twofold. First of all, there is no such thing as a single form of biomass. There are large differences between material from different plants and sources. Secondly, even if one chooses a single source, the required thermodynamic data to do the calculations is not readily available. Under these circumstances and to make progress in developing the tools that are needed to do the analysis, glucose, where all the required information was available, was chosen as something that was reckoned to be a reasonable surrogate for biomass. Glucose does not contain sulphur or nitrogen while biomass does. However, most biomass materials usually have very low sulphur and nitrogen content and produce very small quantities of respective oxides Mardziarz and Wilk (2013); Nanda

et al., 2016; Vassilev et al., 2010; Morrin et al., 2014; Sulc et al., 2012). The oxides of sulphur and nitrogen in the product are also assumed to be very small compared to the C, H and O products in the gasification processes. This is further affirmed by some researchers (Sulc et al., 2012) who showed that fluctuating moisture and nitrogen contents in feedstock have lower impact on composition of the resulting syngas on the two-stage gasification process. What is intended is then to do experiments with different biomass materials and compare the results with these predictions. The researcher will follow this with experiments on a well-known biomass such as wood pellets/ cow dung and using the experimental results to derive the required thermodynamic properties of the wood pellets that explain the results. If all works out as planned, this approach could then be used on other forms of biomass.

2.2. Theoretical Procedure

2.2.1. Assumptions

Biomass in this case represented by glucose is used for this analysis. Principally all C, H and O from glucose ($C_6H_{12}O_6$) is converted to gases mainly CO, CO_2, H_2O, CH_4 and H_2 via (low temperature) biological AD and (high temperature) plasma gasification processes. The reason why glucose is used in this theoretical analysis is because there is thermodynamic data of G available for this compound. Glucose is the closest compound to the different biomass materials examined that we have thermodynamic data that we can use for minimum G calculations to achieve the ARs. All calculations were made at a pressure of 1 bar.

2.2.2. Low and High temperature gasification, ARs

There are three independent material balances that relate to the conversion of the feed material (1 mole glucose) to the possible products and are shown in Eqs. (2.1), (2.2) and (2.3). These material balance equations apply to both low temperature digestion/gasification (biogas production) and high temperature gasification (e.g. plasma technology) processes. However, it was assumed that all the glucose converts to gas. Hence, formation of carbon was not included in the analysis due to the complexity of the calculation (degrees of freedom).

$C_6H_{12}O_{6(s)} \dot{\Rightarrow} 3CO_{2(g)} + 3CH_{4(g)}$, ε_1, ΔH^0 = -141.90 kJ mol^{-1}, ΔG^0 = -418.68 kJ mol^{-1} **(2.1)**

$C_6H_{12}O_{6(s)} + 6H_2O_{(l)} \dot{\Rightarrow} 12H_{2(g)} + 6CO_{2(g)}$, ε_2, ΔH^0 = 616.11 kJ mol^{-1}, ΔG^0= -27.42 kJ mol^{-1} **(2.2)**

$CO_{(g)} + H_2O_{(l)} \dot{\Rightarrow} H_{2(g)} + CO_{2(g)}$, ε_3, ΔH^0 -41.15 kJ mol^{-1}, ΔG^0 = -20.02 kJ mol^{-1} **(2.3)**

2.2.3. Stoichiometric material balance

Eq. (2.4) shows the overall material balance with all stoichiometric coefficients of the species considered in this study. In the equation ***b, c, d, e*** and ***f*** are amounts of CO_2, CH_4, H_2O, H_2 and CO respectively produced per mole of glucose consumed (***a***= 1)

$$aC_6H_{12}O_6 + bCO_2 + cCH_4 + dH_2O + eH_2 + fCO = 0 \quad \textbf{(2.4)}$$

It is thus assumed that one mole of $C_6H_{12}O_6$ is converted to products. The overall values of G and H for of CH_4, CO, CO_2, H_2O and H_2 are plotted showing the regions

where all the product species are ≥ 0. Table 2.1 shows the extents for the material balances shown in Eqs. (2.1), (2.2) and (2.3). It helps to find the degree of conversion of the species involved in this study. In this calculation water is considered to be in excess and so can be formed or used up. The extents of reactions in Eqs. (2.1), (2.2) and (2.3) are given by ε_1, ε_2 and ε_3 respectively.

Table 2.1: Stoichiometric material balance analysis.

Component	Moles in	Change	Moles out
Methane (g)	N_o,CH_4	$+3\varepsilon_1$	$N_o,CH_4 + 3\varepsilon_1 \geq 0$
Water (g)	N_o,H_2O	$-6\boldsymbol{\varepsilon_2} - \boldsymbol{\varepsilon_3}$	$N_o,H_2O - 6\boldsymbol{\varepsilon_2} - \boldsymbol{\varepsilon_3} \geq 0$
Carbon dioxide (g)	N_o,CO_2	$+ 3\varepsilon_1 + 6\varepsilon_2 + \varepsilon_3$	$N_o,CO_2 + 6\varepsilon_2 + 3\varepsilon_1 + \varepsilon_3 \geq 0$
Hydrogen (g)	N_o,H_2	$+ 12\varepsilon_2 + \varepsilon_3$	$N_o,H_2 + 12\boldsymbol{\varepsilon_2} + \varepsilon_3 \geq 0$
Glucose (s)	$N_o,C_6H_{12}O_6$	$-\boldsymbol{\varepsilon_1} - \boldsymbol{\varepsilon_2}$	$N_o,C_6H_{12}O_6 - \boldsymbol{\varepsilon_2} - \boldsymbol{\varepsilon_1} \geq 0$
Carbon Monoxide(g)	N_o,CO	$-\varepsilon_3$	$N_o,CO - \varepsilon_3 \geq 0$

Where $N_o, C_6H_{12}O_6 = 1$ mole, $N_o, CH_4 = 0$, $N_o,CO_2 = 0$, $N_o,H_2 = 0$, $N_o, CO = 0$, $N_o,H_2O = 10$ moles (excess) and that it is assumed that all the glucose is consumed to give Eq. (2.5)

$$\varepsilon_1 + \varepsilon_2 = 1, \qquad \textbf{(2.5)}$$

2.2.4. Transforming the Extents to a G-H AR using Hess's law

Eqs. (2.1), (2.2) and (2.3) were used to construct the G-H AR plot, using a stoichiometric feed of one mole of glucose, and where ε_1 ε_2 and ε_3 are the extents of material balance given by Eqs. (2.1), (2.2) and (2.3) respectively. The G-H AR shows the regions where heat is either added or removed in the AR. The H and G for the material balance were calculated using Eqs. (2.6 – 2.9).

ΔH^0(reaction) =$\sum \Delta H^0$(products) -$\sum \Delta H^0$ (reactants). **(2.6)**

ΔG^0(reaction) = $\sum \Delta G^0$(products) -$\sum \Delta G^0$ (reactants). **(2.7)**

Different extents were used together with the H and G both at standard temperature and pressure (25 ^{0}C, 1 bar) to calculate the values for ΔH and ΔG for the combined process. Using Hess's law which states that heat evolved or absorbed in a chemical process is the same whether the process takes place in one or several steps, the ΔH and ΔG for the combined process on each substance were obtained. Therefore, in this case:

$$\Delta H = \varepsilon_1 \Delta H_1 + \varepsilon_2 \Delta H_2 + \varepsilon_3 \Delta H_3 \quad \textbf{(2.8)}$$

and

$$\Delta G = \varepsilon_1 \Delta G_1 + \varepsilon_2 \Delta G_2 + \varepsilon_3 \Delta G_3 \quad \textbf{(2.9)}$$

Where (ΔH_1, ΔG_1, ΔH_3) and (ΔH_2, ΔG_2, ΔG_3) are the Enthalpy and Gibbs Free Energy at standard conditions for the material balances shown in Eqs. (2.1), (2.2) and (2.3) respectively. The Enthalpy equations used for the G-H AR for the different species using various extent values are shown below. The equivalent equations shown below for ΔH are used for the calculation of the ΔG from the respective component material balance equations (2.10a-2.10e).

- $\Delta \mathbf{H}_{H_2} = (1- \varepsilon_2)\Delta H_1 + \varepsilon_2 \Delta H_2 + (N_{o,}H_2 - 12\varepsilon_2)\Delta H_3$, where $N_{o,}H_2 = 0$ **(2.10.a)**
- $\Delta \mathbf{H}_{CO} = \varepsilon_1 \Delta H_1 + (1- \varepsilon_2)\Delta H_2 + (-N_{o,}CO)\Delta H_3$, where $N_{o,}CO = 0$, $\varepsilon_3 = 0$ **(2.10.b)**
- $\Delta \mathbf{H}_{CO_2} = \varepsilon_1 \Delta H_1 + (1- \varepsilon_1)\Delta H_2 + (3\varepsilon_1 - 6 + N_{o,}CO_2)\Delta H_3$, where $N_{o,}CO_2 = 0$ **(2.10.c)**
- $\Delta \mathbf{H}_{CH_4} = \varepsilon_1 \Delta H_1 + (1- \varepsilon_1)\Delta H_2 + \varepsilon_3 \Delta H_3$, where $\varepsilon_1 = 0$ **(2.10.d)**
- $\Delta \mathbf{H}_{H_2O} = (1- \varepsilon_2)\Delta H_1 + \varepsilon_2 \Delta H_2 + (N_{o,}H_2O - 6\varepsilon_2)\Delta H_3$, where $N_{o,}H_2O = 10$ **(2.10.e)**

It should be clearly noted at this point that the assumption in these calculations is that all product species are pure components. The consequence of this is that there are no mixing effects. This is probably a good assumption for the H but not so good for G. The effect of this is that minimum G will not be at the corners of the AR obtained but a bit removed from them. However, it is believed for the purposes of what the authors are trying to show that this assumption will not significantly affect the overall conclusions.

2.2.5. Changes in Temperature on G-H AR plot

The investigation also involves the effect of temperature on the AR. Considering ideal gas behaviour the ΔH for each component in the material balances with respect to changes in temperature at a constant pressure can be determined by the simplified Eq. (2.11). Pressure changes do not have a significant effect on the G and H for the liquid water over the temperatures studied. In this analysis the feed glucose and products are all considered to be at the reactor temperature (T).

NB: The AR were plotted considering that the inlet and outlet temperature are both at the same temperature T. This means that the feed material to the process has to be

raised to the reactor temperature. Also, the products were assumed to be coming out at the same temperature as that of the reactor temperature.

$$\Delta H^0 = \Delta Ho^0 + R\int_{T_o}^{T} \frac{\Delta Cp^0}{R} dT \quad \textbf{(2.11)}$$

where ΔH^0 and ΔHo^0 are heats of formation at temperature T and reference temperature T_o respectively with the heat capacity term given by Eq. (2.12):

$$\frac{\Delta Cp^0}{R} = A + BT + CT^2 + DT^{-2} \quad \textbf{(2.12)}$$

Where A, B, C and D are heat transfer coefficients.

Integrating Eq. (2.11) gives Eq. (2.13)

$$\int_{T.}^{T} \frac{\Delta Cp^0}{R} dT = \Delta A*T_o*(\tau - 1) + \frac{\Delta B}{2}*T_o^2*(\tau^2 - 1) + \frac{\Delta C}{3}*T_o^3*(\tau^3 - 1) + \frac{\Delta D}{T_o}*(\frac{\tau - 1}{\tau}) \quad \textbf{(2.13)}$$

Where $\tau = \frac{T}{T_o}$

Substituting Eq. (2.13) in Eq. (2.11) gives the heat of reaction at temperature T as shown in Eq. (2.14).

$$\Delta H^0 = \Delta H_o^0 + R*[\Delta A*T_o*(\tau - 1) + \frac{\Delta B}{2}*T_o^2*(\tau^2 - 1) + \frac{\Delta C}{3}*T_o^3*(\tau^3 - 1) + \frac{\Delta D}{T_o}*(\frac{\tau - 1}{\tau})] \quad \textbf{(3.14)}$$

and ΔG can be obtained for any temperature T using Eq. (2.15). ΔG and ΔH for different temperatures are derived as shown by (Smith et al., 2001).

$$\Delta G^{0}_{T} = \Delta H^{0}_{o} - \frac{T}{T_o}(\Delta H^{0}_{o} - \Delta G^{0}_{o}) + R\int_{T.}^{T}\frac{\Delta Cp^{0}}{R}dT - RT\int_{T.}^{T}\frac{\Delta Cp^{0}}{R}\frac{dT}{T} \quad \textbf{(2.15)}$$

Where:

$$\int_{T.}^{T}\frac{\Delta Cp^{0}}{R}dT = \Delta A^{*} T_o^{*}(\tau - 1) + \frac{\Delta B}{2}^{*} T_o^{2} *(\tau^{2} - 1) + \frac{\Delta C}{3}^{*} T_o^{3} *(\tau^{3} - 1) + \frac{\Delta D}{To}*(\frac{\tau - 1}{\tau}) \quad \textbf{(2.16)}$$

And

$$\int_{T.}^{T}\frac{\Delta Cp^{0}}{R}\frac{dT}{T} = \Delta A^{*}\ln\tau + [\Delta B T_o + (\Delta C T_o^{2} + \frac{\Delta D}{\tau^{2} T_o^{2}})(\frac{\tau+1}{2})] *(\tau-1) \quad \textbf{(2.17)}$$

2.3. Results and Discussion

2.3.1. Attainable Region

Figure 2.1 shows the G-H AR space as a result of combining the ΔH and ΔG limits of each separate species. The solid line for each species shows the places in the G-H space where a particular species is zero. The dashed line that is close to each solid line is there to indicate the direction in which each species is formed, that is extents are positive. In quadrant A (ΔH> 0 and ΔG > 0), the process requires both heat and work addition. In quadrant B (ΔG > 0 and ΔH < 0), the process is exothermic, but requires work addition. Therefore, it is not feasible to operate in quadrant A and B as they both require work addition. In quadrant C and D, work is also lost, as ΔG < 0. Quadrant D requires a supply of heat energy to the process while the processes in quadrant C requires heat removal. The relative size of the G-H AR shows how wide the range of possible combinations of mass balances that may be possible to give different products from the respective feed. It is important to note that the G must be less than zero for the overall reaction to be thermodynamically feasible when mixing is excluded.

The G-H AR gives an insight of the thermodynamic limits on what is possible. To be more specific, the AR is bounded at the top by the need for G to be non-positive and then anti-clockwise by successively CO_2, H_2, CO and CH_4 equals zero as shown in Figure 2.1. The minimum of the shaded area then lies at point x where H_2 and CO equals zero. Clearly, if mixing of the gases was considered, these species would not be zero but some smaller number as the slopes of these lines are quite large.

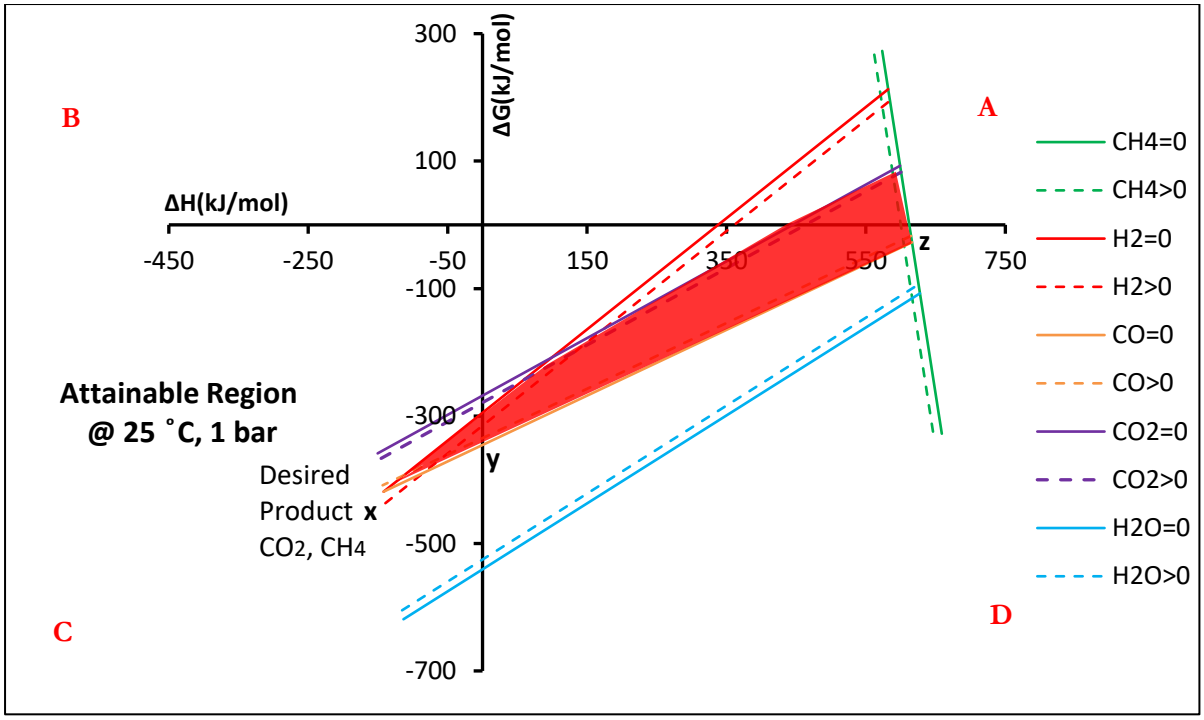

Figure 2.1: G-H diagram showing AR at 25 ^{0}C, 1 bar using a feed of 1 mole glucose.

The material balance at any chosen point on the AR can be obtained using the values of ε_1, ε_2 and ε_3 and the stochiometric material balances. This is done from the G-H AR, by selecting a point in the shaded region. Obtain the H and G of the process at that point, and use the values, together with the H and G of the three reactions at standard state conditions, to get two equations with three variables from which one can solve for, ε_1, ε_2 and ε_3 as shown in Eq. (2.8) and (2.9). The third equation to complete the

calculation is given by Eq. (2.5). Solve for the three variables and obtain a material balance equation for the species present using Table 2.1. The material balance for points shown by x, y and z are given by Eq. (2.18.a - 2.18.c).

x: $\boldsymbol{C_6H_{12}O_{6(s)} \Rightarrow 3CO_{2(g)} + 3CH_{4(g)}}$, ΔH = -141.9 kJ mol^{-1}, ΔG = -418.68 kJ mol^{-1}

(2.18.a)

y: $C_6H_{12}O_{6(s)} + 1.12H_2O_{9(l)} \dot{\Rightarrow} 2.24H_{2(g)} + 3.56CO_{2(g)} + 2.44CH_{4(g)}$, ΔH = 0 kJ mol^{-1}, ΔG = -345 kJ mol^{-1}. **(2.18.b)**

z: $C_6H_{12}O_{6(g)} + 6H_2O_{9(l)} \dot{\Rightarrow} 12\ H_{2(g)} + 6CO_{2(g)}$ ΔH = 616 kJ mol^{-1}, ΔG = -27 kJ mol^{-1}.

(2.18.c)

The equation representing minimum G at 25 ^{0}C, 1 bar is shown by point **x** in Figure 2.1 and is given as Eq. (2.18.a).

2.3.2. Effects of changing Temperature on G-H AR, 50 ^{0}C - 1500 ^{0}C.

Changes in temperature affect both H and G. Using the assumptions that the reactions are reversible and considering ideal conditions Eqs. (2.11) and (2.15) were used to calculate the changes in the AR for temperature variations at constant pressure. The results obtained from different temperatures at constant pressure of 1 bar and liquid water are shown in Figure 2.2 and Figure 2.3.

As temperature increases, the minimum G for the process becomes more negative while the Enthalpy becomes more positive as shown in Figure 2.1, Figure 2.3 and material balance Eq. (2.18a) and Eq. (2.20). The process becomes more favourable

from a Gibbs Free Energy perspective and more endothermic which results in the need to add more heat energy to the system.

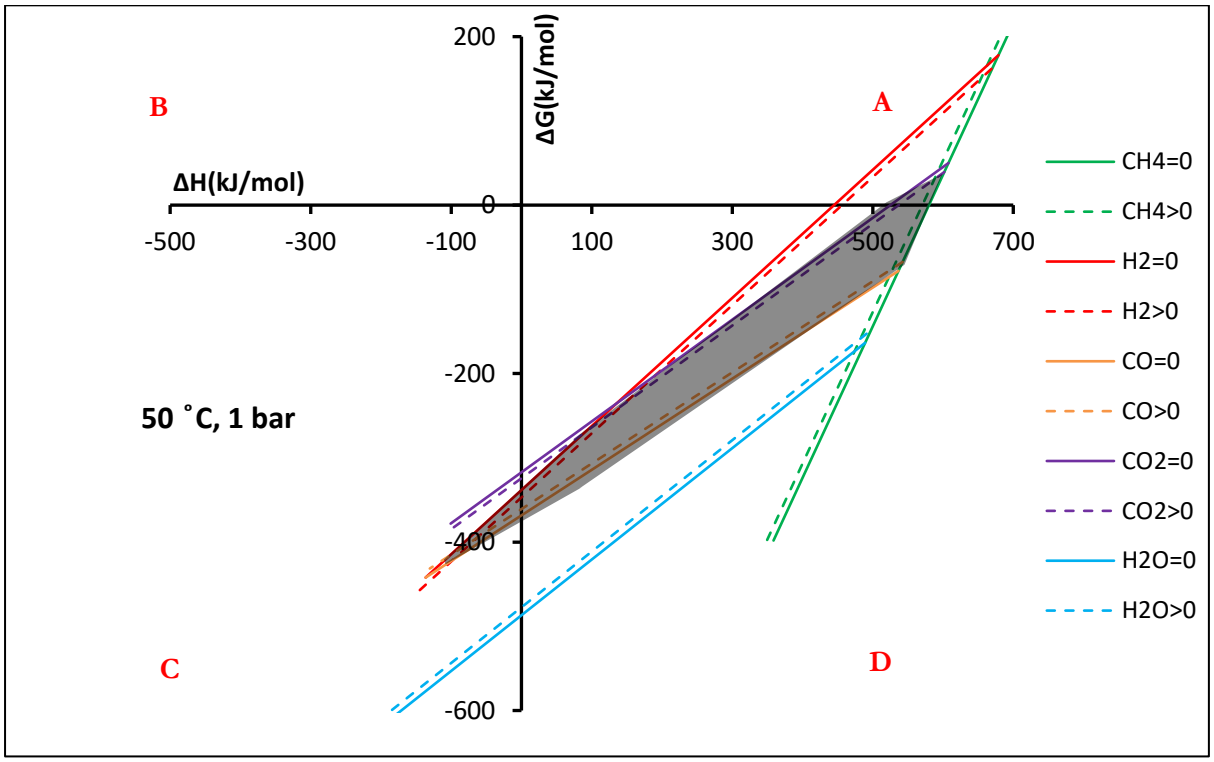

Figure 2.2: G-H diagram showing AR at 50 ^{0}C, 1 bar using a feed of 1 mole glucose.

The AR shows that it is thermodynamically feasible to make CO_2, H_2, CH_4 and CO at 25 ^{0}C, 50 ^{0}C and 98 ^{0}C, 1 bar. The main products of biogas production are CO_2 and CH_4. Different bacteria could work anywhere inside the region to produce biogas from biomass. Hence, for these low temperatures where water is in liquid state, biogas production can be referred to as low temperature gasification. It is assumed that the reaction will proceed to happen where ΔG is most negative (minimum G) in the AR because the system is more stable at this state. Hence, reaction will happen at the point where G is close to -431.41 kJ mol^{-1} in Figure 2.2.

The respective material balances at minimum G for the desired products at 50^{0}C and 98 ^{0}C is given by Eq. (2.19) and (2.20)

$C_6H_{12}O_{6(s)} \Rightarrow 3CO_{2(g)} + 3CH_{4(g)}$, ΔH = -136.35 kJ mol^{-1}, ΔG = -431.41 kJ mol^{-1}.

(2.19)

$C_6H_{12}O_{6(s)} \Rightarrow 3CO_{2(g)} + 3CH_{4(g)}$, ΔH = -125.04 kJ mol^{-1}, ΔG = -456.53 kJ mol^{-1}.

(2.20)

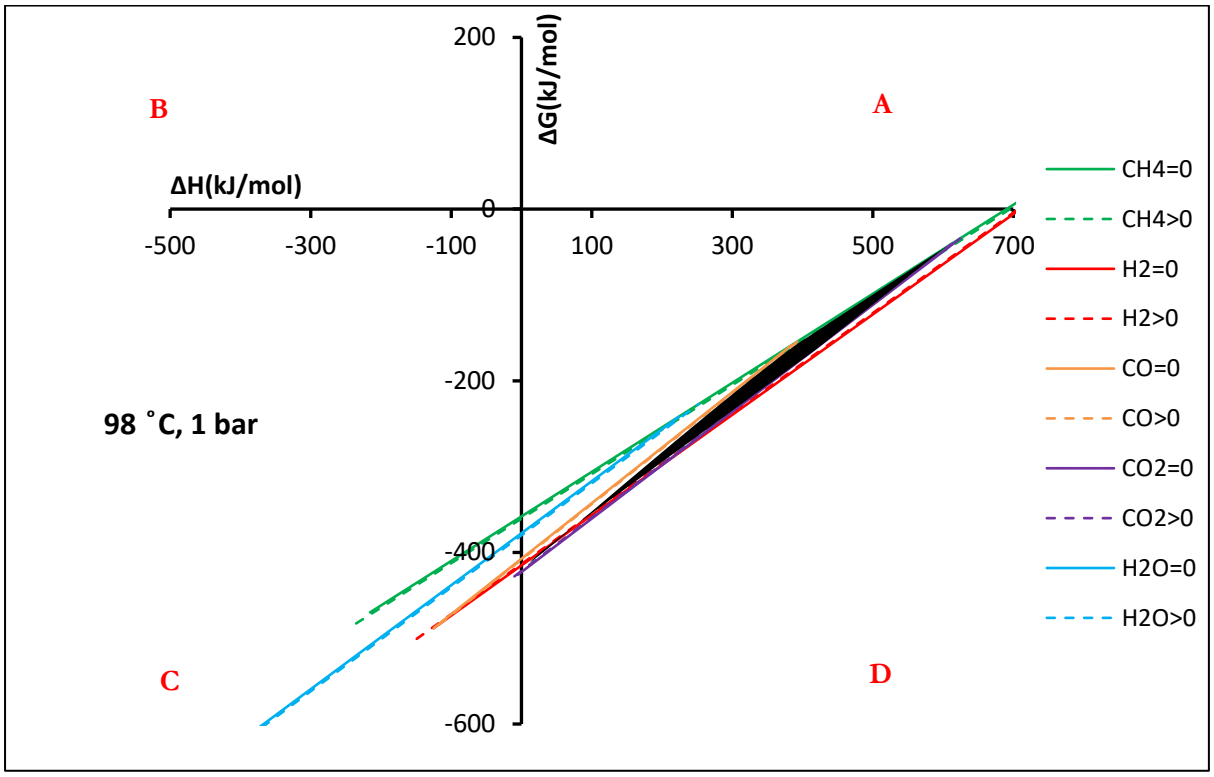

Figure 2.3: G-H diagram showing AR at 98 ^{0}C, 1 bar using a feed of 1 mole glucose.

As temperature increases from 25 ^{0}C - 101 ^{0}C as shown in Figure 2.1-2.4, the AR shows that CO_2 and CH_4 are still favourable products at minimum G. However, the increase in temperature also shows that production of H_2 becomes more favourable to methane. This has resulted in a more negative G (-456 kJ mol^{-1}) at 98 ^{0}C. At 25 ^{0}C, part of the AR lies in the region where G is positive, and this small region is not feasible. However, there is a significant change in the AR for a change in temperature from 25 ^{0}C to 98 ^{0}C as shown in Figure 2.1 and Figure 2.2. At temperatures above 98 ^{0}C, the

whole AR lies in the space where G is negative. This means that all processes at 98 ^{0}C are feasible from a G constraint and will release energy equal to the work that can be performed as a result of the chemical reactions occurring.

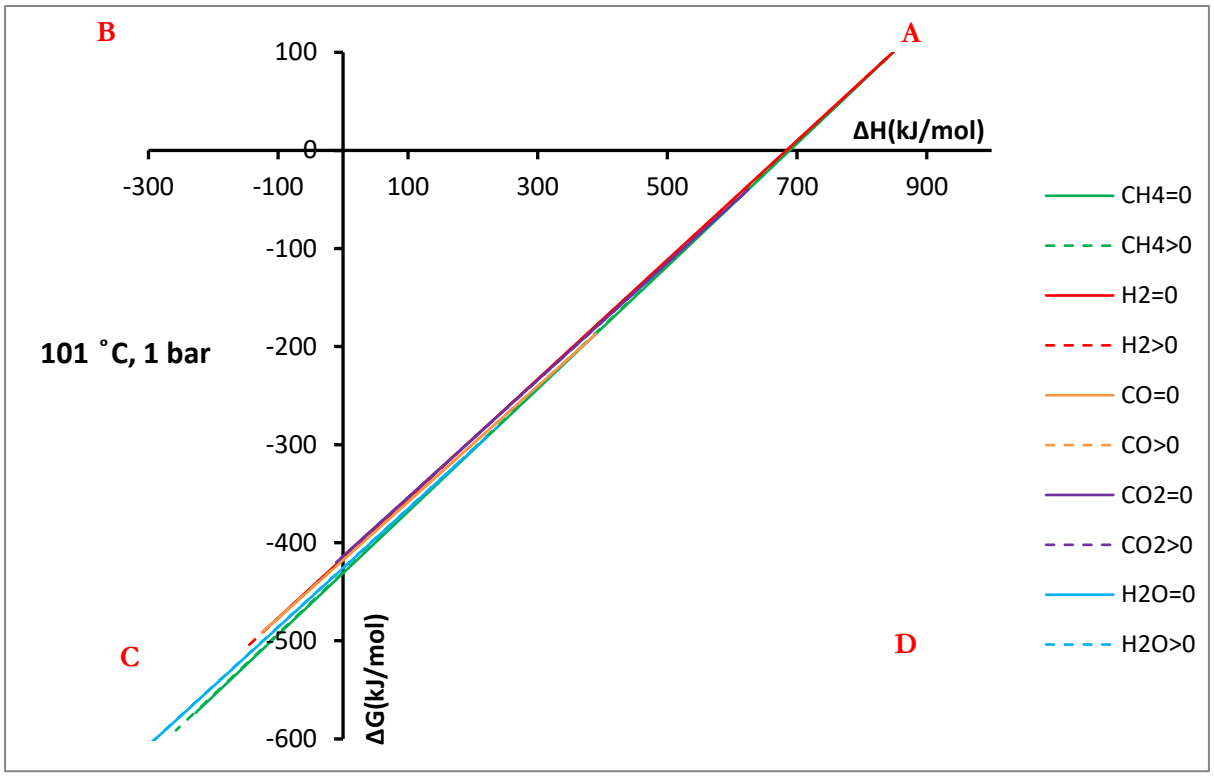

Figure 2.4: G-H diagram showing AR at 101 ^{0}C, 1 bar using a feed of 1 mole glucose.

The results presented in Figure 2.4 - 2.10 show an analysis of higher temperature glucose gasification at a set of arbitrarily chosen temperatures covering the range 101 ^{0}C - 1500 ^{0}C. For temperatures above 100 ^{0}C, water will be in gaseous phase. At 101 ^{0}C, CH_4 and CO_2 are still the ideal products at minimum G. In the AR, the reaction occurring on the zero-methane line is probably the Water Gas Shift (WGS) reaction shown in Eq. (2.3). At 98 ^{0}C and 101 ^{0}C, the results show a small region for the AR. This may be due to the phase change taking place when liquid water is changing to

gaseous phase at 100 ^{0}C and around 1 bar. The material balance at minimum G for the desired products at 101 ^{0}C is given by Eq. (2.21)

$C_6H_{12}O_{6(s)} \Rightarrow 3CO_{2(g)} + 3CH_{4(g)}$, ΔH = -124.31 kJ mol^{-1}, ΔG = -491.26 kJ mol^{-1} **(2.21)**

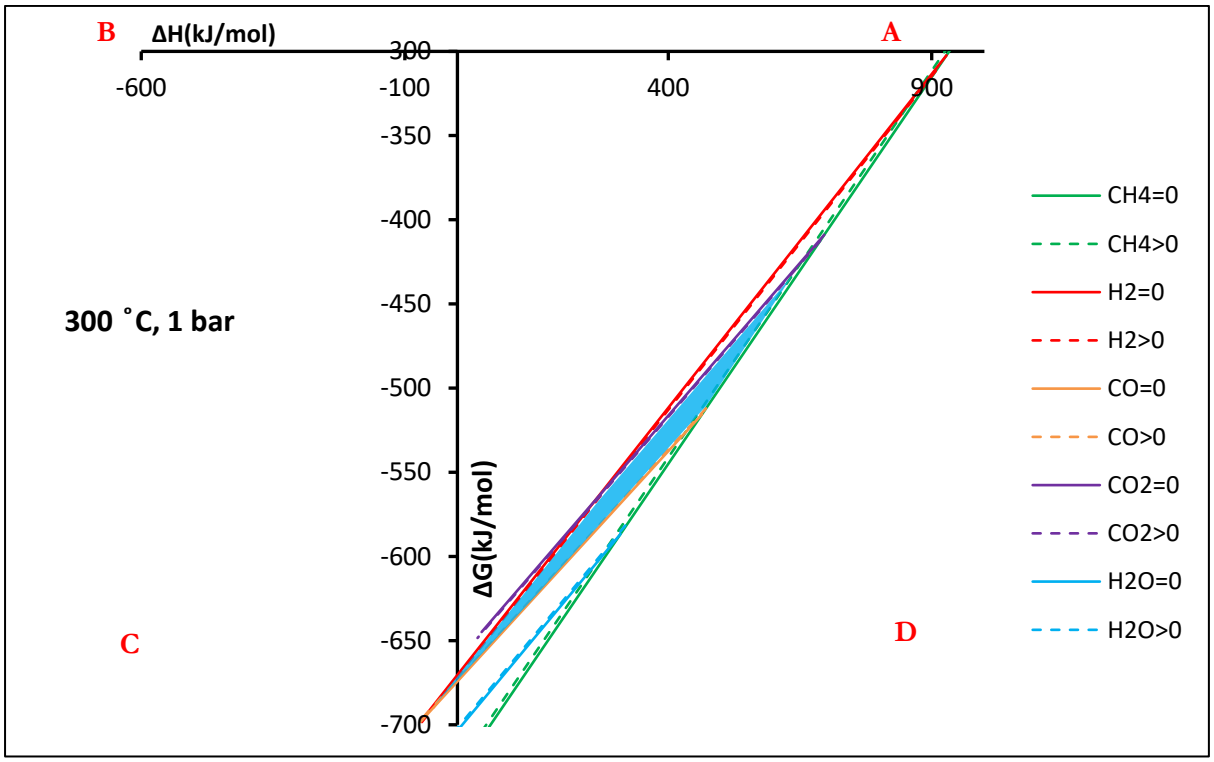

Figure 2.5: G-H diagram showing AR at 300 ^{0}C, 1 bar using a feed of 1 mole glucose.

Figure 2.5 shows that CH_4 and CO_2 are the desired products at minimum G and the material balance at 300 ^{0}C is given by Eq. (2.22).

$C_6H_{12}O_{6(s)} \Rightarrow 3CO_{2(g)} + 3CH_{4(g)}$, ΔH = -70.14 kJ mol^{-1}, ΔG = -698.20 kJ mol^{-1}. **(2.22)**

Figure 2.6 shows that the AR moves towards the more negative G as temperature is increased. As temperature is increased to about 500 ^{0}C, CH_4 and CO_2 are still produced at minimum G, but one can see the production of CO becomes increasingly

more favourable. The material balance for the desired products at minimum G shown in Figure 2.6 at 500 ^{0}C is given by Eq. (2.23) and the system is exothermic.

$C_6H_{12}O_{6(s)} \Rightarrow 3CO_{2(g)} + 3CH_{4(g)}$, ΔH = -6.6 kJ mol^{-1}, ΔG = -927.34 kJ mol^{-1}. **(2.23)**

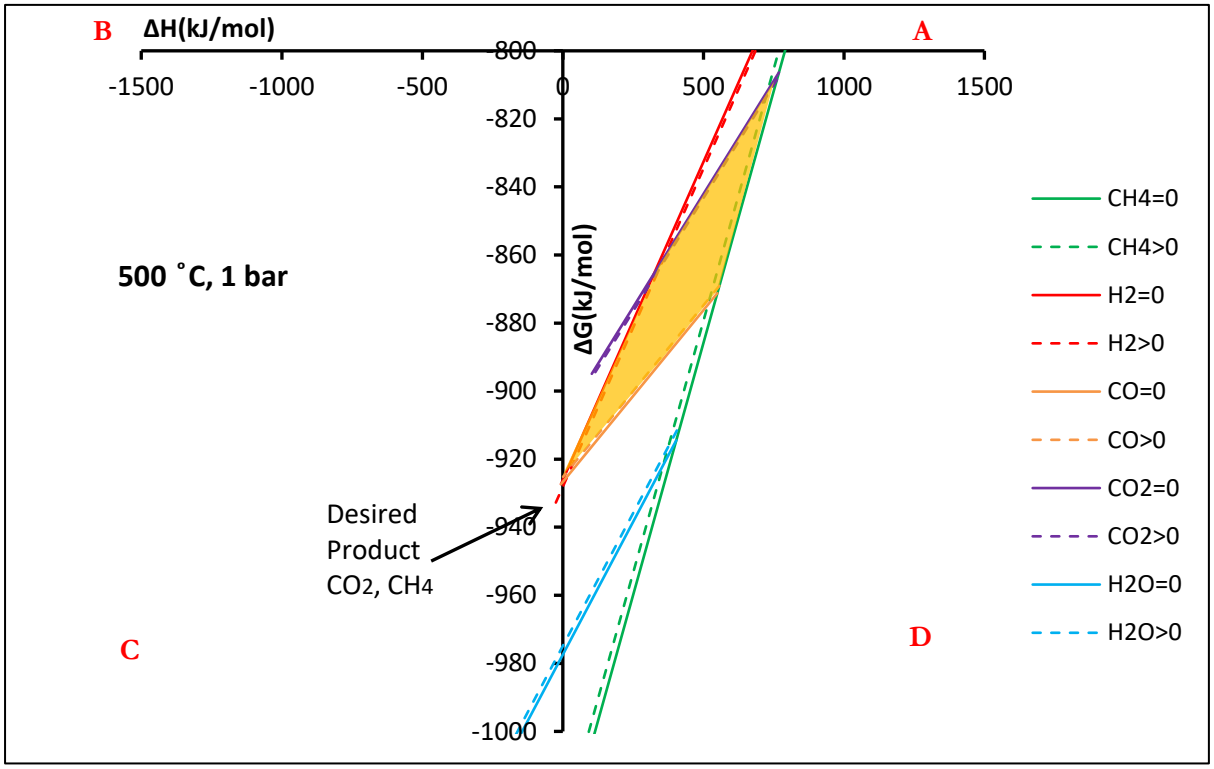

Figure 2.6: G-H diagram showing AR at 500 ^{0}C, 1 bar using a feed of 1 mole glucose.

Figure 2.7 shows the AR at 700 ^{0}C. It shows that CH_4 and CO are zero at minimum G. Gasification at temperatures around 700 ^{0}C favours production of H_2 and CO_2 at minimum G. At about 700 ^{0}C AR lies in the endothermic region. Eq. (2.24) shows the material balance for the desired products at minimum G for the temperature 700 ^{0}C.

$C_6H_{12}O_{6(s)} + 6H_2O_{(g)} \Rightarrow 6CO_{2(g)} + 12H_{2(g)}$, ΔH = 637.11 kJ mol^{-1}, ΔG = -1249.21 kJ mol^{-1} **(2.24)**

As temperature continues to increase, H_2 production becomes more favourable relative to CH_4 production. This suggests that if one wants to concentrate on CH_4 production for combustion purposes, then operation at intermediate temperatures as compared to producing syngas at higher temperatures should be done. For temperatures above about 766 ^{0}C (not shown) at minimum G, the production of syngas i.e. CO and H_2 becomes more dominant.

Comparing Figure 2.6 and Figure 2.8 producing the gas products from high temperature gasification (> 900 ^{0}C) is more endothermic when producing syngas components CO and H_2 than when producing CH_4 and CO_2 hydrocarbons at the low temperature gasification process (< 500 ^{0}C). This means the energy content of the syngas is/ should be greater than that of the low temperature gases. The material balance for the desired products at minimum G for 900 ^{0}C is given by Eq. (2.25).

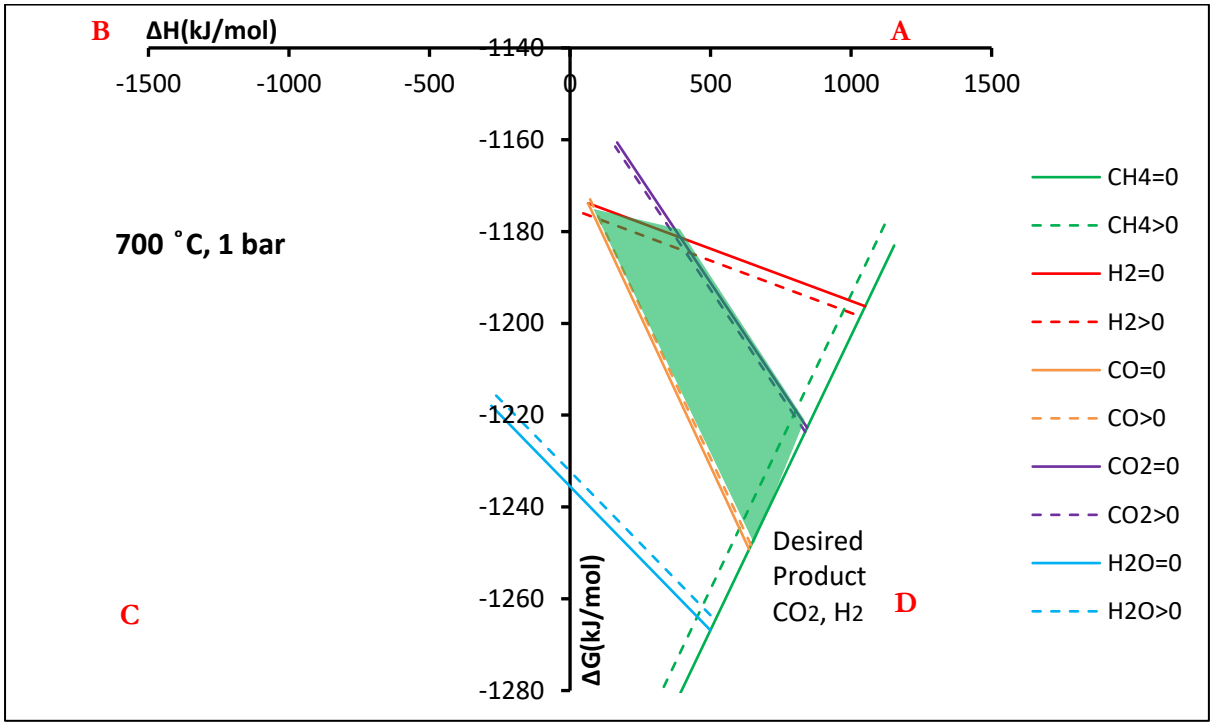

Figure 2.7: G-H diagram showing AR at 700 ^{0}C, 1 bar using a feed of 1 mole glucose.

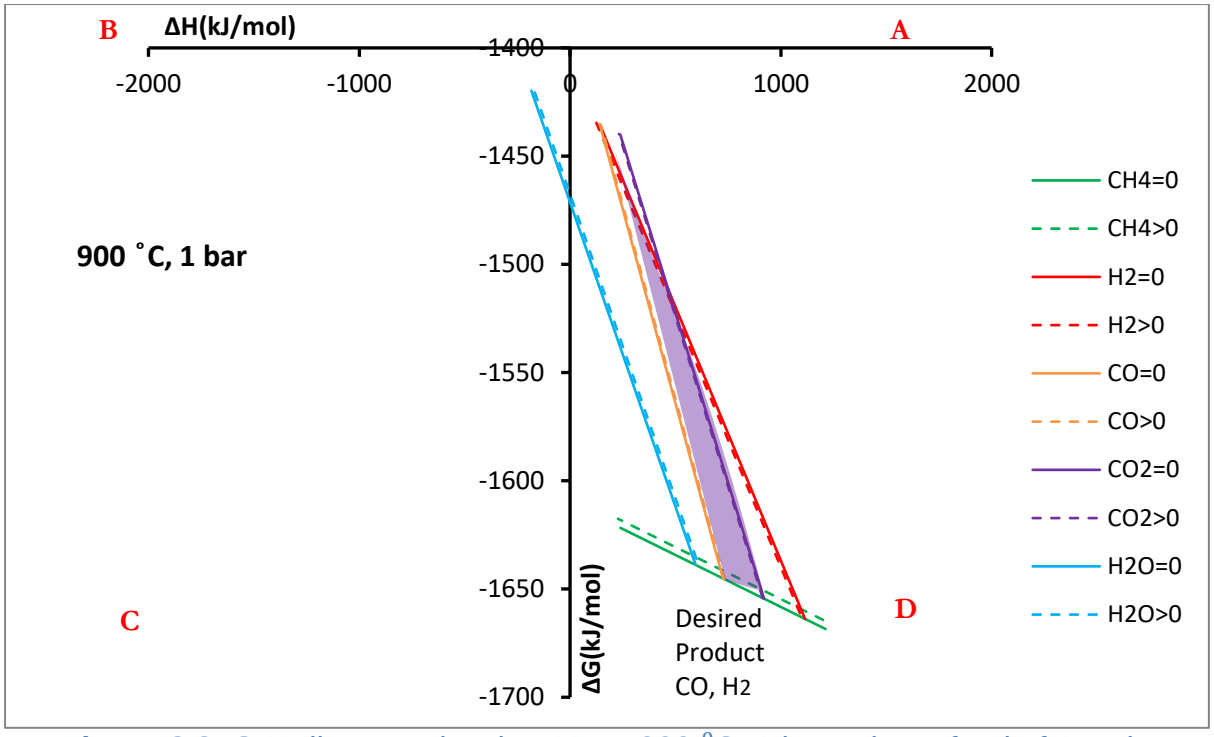

Figure 2.8: G-H diagram showing AR at 900 ^{0}C, 1 bar using a feed of 1 mole glucose.

$C_6H_{12}O_{6(s)} \Rightarrow 6CO_{(g)} + 6H_{2(g)}$, ΔH = 920.20 kJ mol^{-1}, ΔG = -1654.44 kJ mol^{-1}. . **(2.25)**

Figure 2.8 - 2.10 shows how the AR changes when temperature is increased from 900 ^{0}C to 1500^{0}C. H_2 and CO are still the thermodynamically observed main products at minimum G even when the temperature is increased to 1500 ^{0}C. The respective material balances showing the changes in G and H for the desired products at 1100 ^{0}C and 1500 ^{0}C are given by Eq. (2.26) and (2.27).

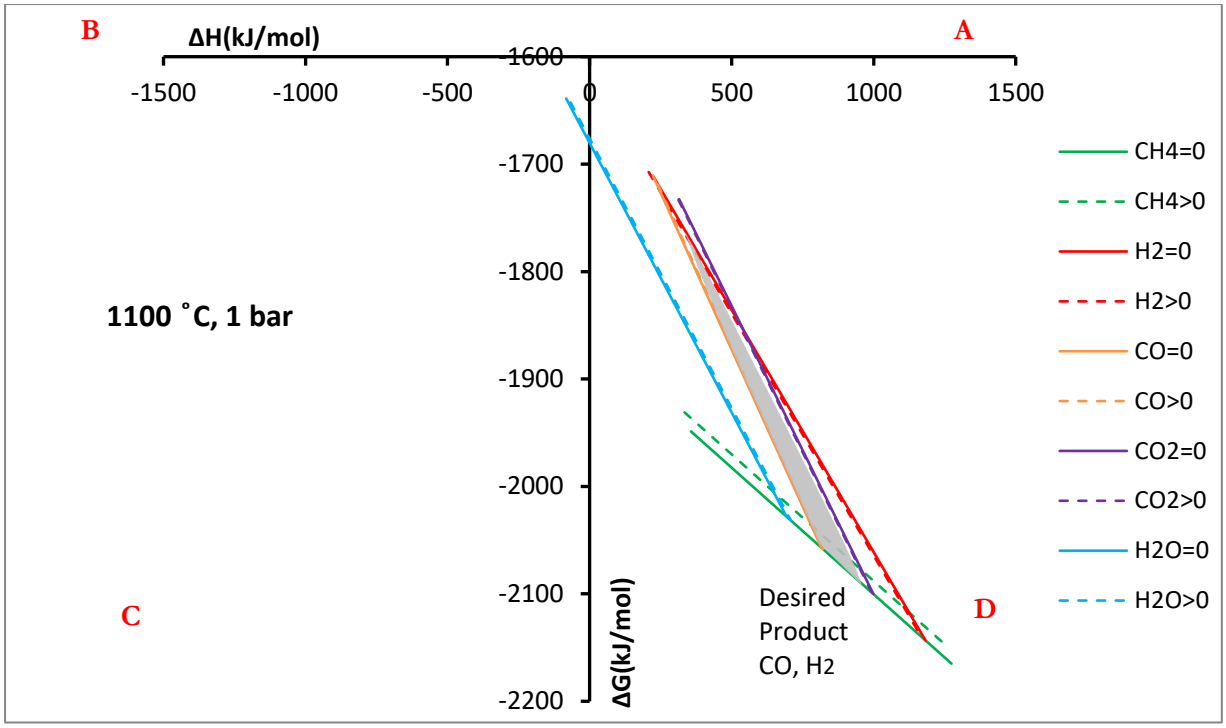

Figure 2.9: G-H diagram showing AR at 1100 ^{0}C, 1 bar using a feed of 1 mole glucose.

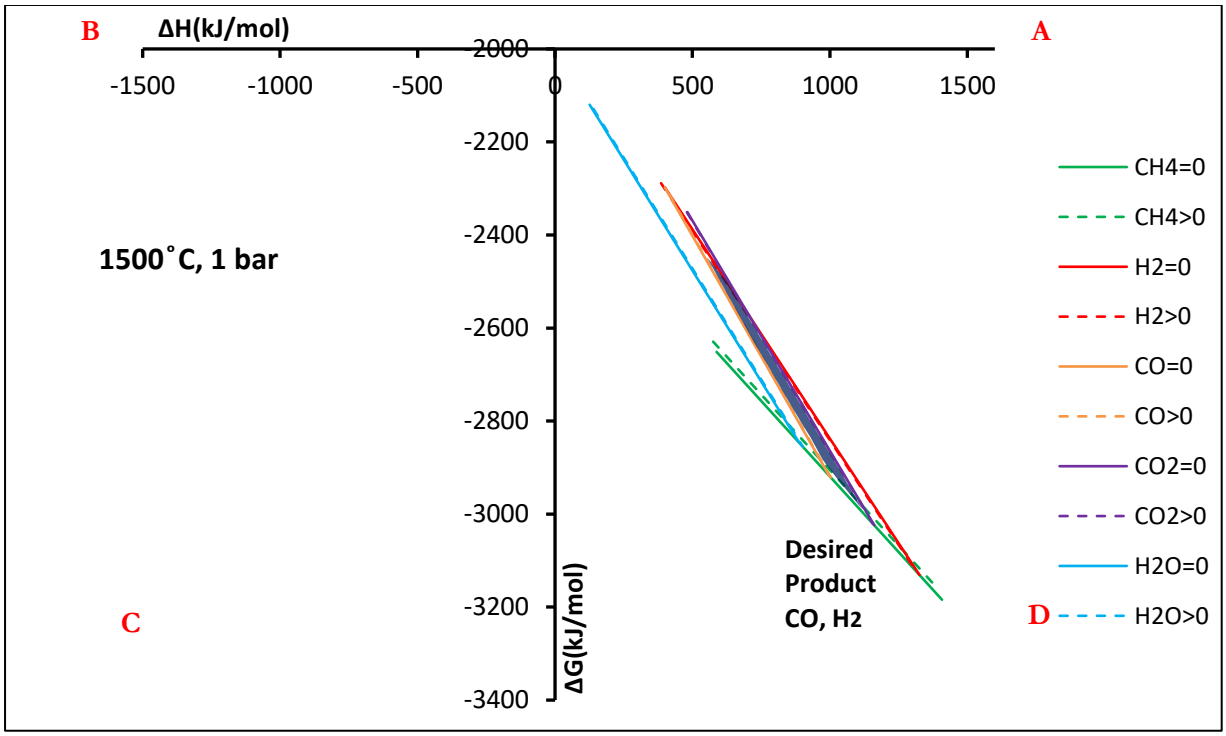

Figure 2.10: G-H diagram showing AR at 1500 ^{0}C, 1 bar using a feed of 1 mole glucose.

$C_6H_{12}O_{6(s)} \Rightarrow 6CO_{(g)} + 6H_{2(g)}$, ΔH = 998.83 kJ mol^{-1}, ΔG = -2100.09 kJ mol^{-1}. **(2.26)**

$C_6H_{12}O_{6(s)} \Rightarrow 6CO_{(g)} + 6H_{2(g)}$, ΔH = 1161.80 kJ mol^{-1}, ΔG = -3024.34 kJ mol^{-1}. **(2.27)**

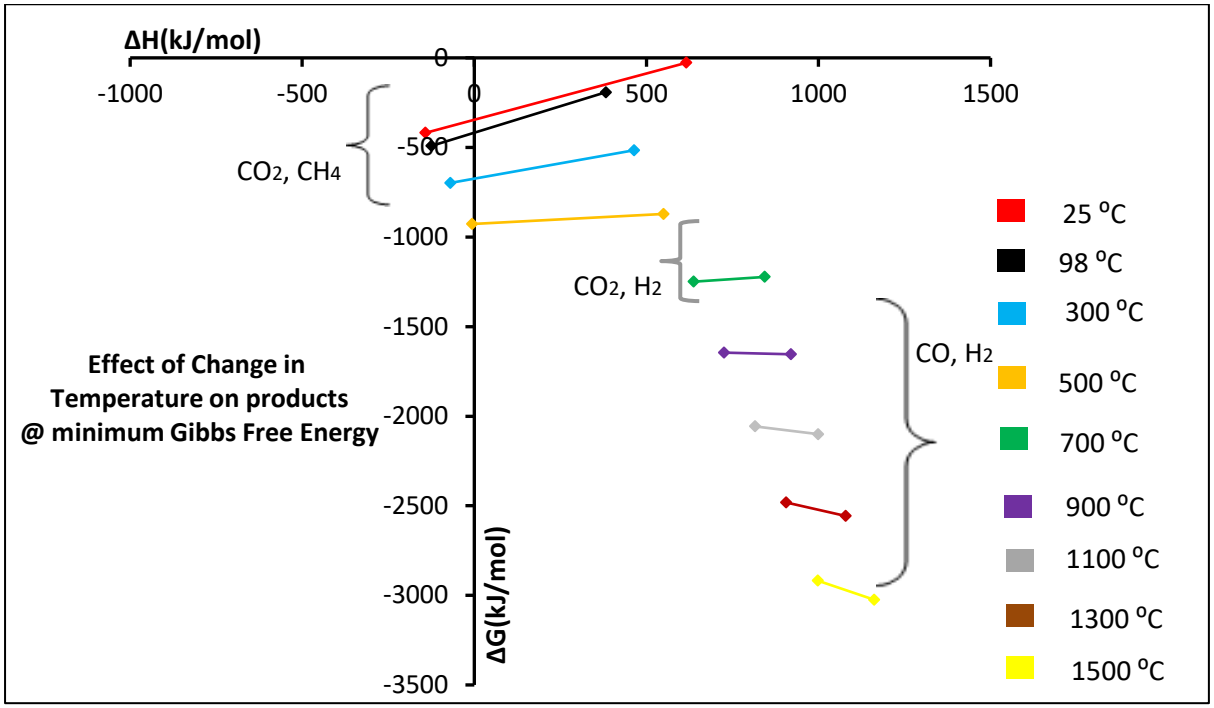

Figure 2.11: G-H diagram showing gas product spectrum in the AR at for the temperature range 25 ^{0}C -1500 ^{0}C, 1 bar using a feed of 1 mole glucose.

Figure 2.11 is a G-H AR plot to try to put all the previous results on a single graph to try and visualise the overall trend. Here, the lowest line of the G-H AR for each temperature is plotted (putting in all of each AR makes the plot too cluttered). The products over each temperature range are shown in Figure 2.11. It also shows that the minimum G becomes more negative as temperature is increased from 25 ^{0}C to 1500 ^{0}C using 1 mole of glucose. This means that the process becomes more spontaneous as temperature is increased. It also shows that the enthalpy becomes more positive (more endothermic) as temperature is increased for this temperature range. All G-H ARs above 1500 ^{0}C show that H_2 and CO gases are favoured at minimum G (not shown). These high temperatures are usually achieved by using plasma systems. Figure 2.1 to Figure 2.10 show that the minimum G shifts from point

x to **y** and to **z** (on Figure 2.1) as temperature is increased, favouring the production of CH_4, CO and H_2 respectively.

The result of this thermodynamic calculation is also important as it shows the reasons why plasma technology could be a sustainable option for high temperature biomass pyrolysis/ gasification. The results and analysis of this work are also meant to show a relationship between biogas production and gasification using glucose as a substrate. It also shows how the product gas spectrum changes from 25 ^{0}C to 1500 ^{0}C, all at 1 bar. Gasification using convectional gasifiers usually takes place around 800^{0}C because they rely on the combustion process for energy to reach high temperatures (Wang et al., 2009). Therefore, oxidation is a key element in sustaining the gasification reaction in these systems. However, the calculation shows that a favourable syngas concentration can still be obtained at higher temperatures without the addition of oxygen. This calls the need for a gasifier that can reach and withstand very high gasification temperatures (around 1000 ^{0}C -1500 ^{0}C). The plasma gasifier is probably the only gasification reactor that can currently reach these higher temperatures because of its ability to use a supply of energy from both combustion and electricity.

2.4. Summary

A thermodynamic AR for AD/pyrolysis-gasification of biomass waste material surrogate (glucose) was obtained using G-H AR for the temperature range 25 ^{0}C - 1500^{0}C. Thermodynamic data for glucose was used for the calculations to resemble the biomass waste material and give an estimated analysis of biomass digestion/gasification. The results show that all the processes for glucose conversion are feasible from a G point of view. The results from the AR show the behaviour of material, energy and work (G) balances occurring in AD, pyrolysis and gasification

processes. The thermodynamic AR shows that CH_4 and CO_2 are favoured products at minimum G for temperatures up to about 600 ^{0}C and the process needs to reject heat. This, therefore, includes AD as a form of low temperature gasification.

At around 700 ^{0}C CO_2 and H_2 are the favoured products at minimum G. CO and H_2 are preferred products from 800 ^{0}C to 1500 ^{0}C and the process is endothermic. The higher the temperature, (irrespective of the products) the more endothermic the process becomes and the more irreversible. Although the products shown by the G-H ARs are thermodynamically feasible, they may not be technologically feasible. Hence, a comparison of the thermodynamic and experimental data is needed to give reasonable conclusions and possible optimisation techniques.

References

1. Agnieszka P., Michalina K. M., Marcin K., Grzegorz Ł., 2016. Furniture wood waste as a potential renewable energy source. A thermogravimetric and kinetic analysis. Journal of Thermal Analysis Calorimetry, Vol. 125, pp.1357–1371.
2. Aneta M., Małgorzata W., 2013. Thermal characteristics of the combustion process of biomass and sewage sludge. Journal of Thermal Analysis Calorimetry, Vol. 114, pp. 519–529.
3. Chimwani N., Mulenga F., Hildebrandt D., Glasser D., Bwalya M., 2014. Scale-up of batch grinding data for simulation of industrial milling of platinum group minerals ore. Minerals Engineering, Vol. 63, pp. 100–109.
4. Danha G., Hildebrandt D., Glasser D., Bhondayi C., 2014. A laboratory scale application of the attainable region technique on a platinum ore. Powder Technology, Vol. 274, pp. 14–19.
5. Edbertho L., 2004. Plasma Processing of Municipal Solid Waste. Brazilian Journal of Physics, Vol. 34(4B).
6. Glasser D., Hildebrandt D., Crowe C., 1987. A. A geometric approach to steady flow reactors: The Attainable Region and optimization in concentration space. Industrial and Engineering Chemistry Research, Vol. 26, pp.1803–1810.
7. Heberlein J., Murphy A., 2008. Thermal Plasma Waste Treatment. Journal of Physics D: Applied Physics. Vol. 41, pp.1–19.
8. Hrabovsky M., Hlina M., Kavka T., Konrad M., Chumak O., Maslani A., 2009. Thermal plasma gasification of biomass for fuel gas production. High Temperature Material Processes: An International Quarterly of High-Technology Plasma Processes, Vol. 13(3-4), pp. 299–313.

9. Lidia L., Ennio C., Andrea C., 2012. Analysis of energy recovery potential using innovative technologies of waste gasification. Waste Management, Vol. 32, pp. 640–652.
10. Ming D., Glasser D., Hildebrandt D., 2013. Application of attainable region theory to batch reactors. Chemical Engineering Science, Vol. 99, pp. 203–214.
11. Morrin S., Lettieri P., Chapman C., Taylor R., 2014. Fluid bed gasification – Plasma converter process generating energy from solid waste: Experimental assessment of sulphur species. Waste Management, Vol. 34, pp.28–35.
12. Okonye L. U., Hildebrandt D., Glasser D., Patel B., 2012. Attainable Regions for a reactor: Application of G-H plot. Chemical Engineering Research and Design, Vol. 90, pp.1590–1609.
13. Portofino S., Donatelli A., Iovanne P., Innella C., Civita R., Martino M., Matera D.A., Russo A., Cornacchia G., Galvano S., 2013. Steam gasification of waste tyre: influence of process temperature on yield and product composition. Waste Manage, Vol. 33, pp. 672–678.
14. Raheem A., Sivasangar S., Azlina W.A.K.G.W., Yap Y.H.T., Danquah M.K., Harun R., 2015. Thermogravimetric study of Chlorella vulgaris for syngas production. Algal Research, Vol.12, pp. 52–59.
15. Sara E., Carla T., Roland C., Paola L., Richard T., Chris C., 2015. Integrated gasification and plasma cleaning for waste treatment: A life cycle perspective. Waste Management, Vol. 43, pp. 485–496.
16. Sempuga B. C., Hausberger B., Patel B., Hildebrandt D., Glasser D., 2010. Classification of Chemical Processes: A Graphical Approach to Process Synthesis to Improve Reactive Process Work Efficiency, Industrial and Engineering Chemistry Research, Vol. 49:17, pp.8227–8237.

17. Smith J. M., Michael A., Hendrick V., 2001. Introduction to Chemical Engineering Thermodynamics, Vol 6, pp. 127–657.
18. Sonil N., Ajay K., Dalai B., Iskender G. C., Janusz A., Kozinski., 2016. Valorization of horse manure through catalytic supercritical water gasification. Waste Management, Vol. 52, pp. 147–158.
19. Sulc J., Jirˇi Š., Miroslav R., Jan P., Karel S., Jirˇi S., Jirˇi V., Siarhei S., Petr B., 2012. Biomass waste gasification – Can be the two-stage process suitable for tar reduction and power generation? Waste Management, Vol. 32, pp. 692–700.
20. Tatiana R. P., Diniara S., Michele D. D., Maria F. R., Regina de Fátima P., Muniz M., Humberto J. J., 2016. Bio-syngas production from agro-industrial biomass residues by steam gasification. Waste Management, Vol 58, pp. 221–229.
21. Vassilev S. V., Baxter D., Andersen L. K., Vassileva, C. G., 2010. An overview of the chemical composition of biomass. Fuels, Vol 89, pp. 913–933.
22. Wang L., Yu-Huan D., Heng T., Tong-Zhang W., 2009. A biomass gasification system for synthesis gas from the new method. Natural Science, Vol 1(3), pp. 195–203.

Addendum Chapter 2

2.1A. Introduction

In addition to Chapter 2, a method has been used in this addendum to improve the G-H (Attainable Region (AR) by including additional elements (carbon and oxygen) that can be formed to cover the more possible processes or reactions that convert glucose (surrogate for biomass) to products. The advantage of the method described in this work is that it is possible to analyse higher dimension systems. Gaussian elimination is used to obtain the independent material balances that describes the relationship between the reactants and products in this process. The requirement that the number of moles for all the species in the system being either zero or positive is solved using linear programming. The vertices of this space, the Material Balance Limited (MBL) AR, are used to calculate the vertices of the G-H AR.

In order to obtain the AR for the gasification system, it is important to define possible products of the process. One mole of glucose is used as the basis for this analysis; while the amount of oxygen fed to the process is varied. The possible products/reactants are defined as carbon monoxide, hydrogen, water, methane, carbon dioxide and carbon. Therefore, for this case, eight compounds are involved in the process and the AR will determine which of the latter species are feeds or products. This AR will be able to describe all three processes i.e. Anaerobic Digestion (AD), pyrolysis and gasification where for the first two processes, the oxygen feed is zero. Combustion process can also be analysed when excess oxygen is provided to the system.

2.2A. Theoretical procedure for gasification AR

There are eight species considered in this analysis, namely $C_6H_{12}O_6$, O_2, CO, CO_2, H_2O, H_2, CH_4 and C.

To start with, three common atoms (C, H and O) are present in the eight species involved in this analysis. The compounds, together with the number of atoms in each species are arranged in matrix form as shown in Table 2.1A. Gaussian elimination is carried out in order to obtain the independent material balances as shown in Table 2.2A. The overall material balance is given by Eq. (2.1A)

$$1C_6H_{12}O_6 + N^o{}_{O2} + aCO + bH_2 + cCH_4 + dCO_2 + eH_2O + fC = 0 \qquad \textbf{(2.1A)}$$

Usually nitrogen does not take part in the reaction and is used to help calculate the composition of other gases formed.

Table 2.1A: Matrix form of the compounds and atoms present in gasification process

C	H	O	Compounds
6	12	6	$C_6H_{12}O_6$
0	0	2	O_2
1	0	1	CO
0	2	0	H_2
1	0	2	CO_2
1	4	0	CH_4
0	2	1	H_2O
1	0	0	C

Table 2.2A: Gaussian elimination to get independent balances

C	H	O	Material balances
0	1	0	$1/12(C_6H_{12}O_6 - 6C) - 1/2\,(CO - C)$
0	0	0	$\boldsymbol{O_2 - 2\,(CO - C)}$
0	0	1	$CO - C$
0	0	0	$\boldsymbol{H_2 - 2(1/12(C_6H_{12}O_6 - 6C)) + (CO - C)}$
0	0	0	$\boldsymbol{CO_2 - C - 2\,(CO - C)}$
0	0	0	$\boldsymbol{CH_4 - C - 4(1/12(C_6H_{12}O_6 - 6C)) + 2\,(CO - C)}$
0	0	0	$\boldsymbol{H_2O - 2\,(1/12(C_6H_{12}O_6 - 6C))}$
1	0	0	C

Five independent material balances are obtained after Gaussian elimination and are given by Eq. (2.2A-2.6A) below.

$$2C + O_2 = 2CO \qquad \boldsymbol{\varepsilon_1} \qquad \textbf{(2.2A)}$$

$$C_6H_{12}O_6 \Rightarrow 6CO + 6H_2 \qquad \boldsymbol{\varepsilon_2} \qquad \textbf{(2.3A)}$$

$$2CO \Rightarrow CO_2 + C \qquad \boldsymbol{\varepsilon_3} \qquad \textbf{(2.4A)}$$

$$C_6H_{12}O_6 + 3C \Rightarrow 6CO + 3CH_4 \qquad \boldsymbol{\varepsilon_4} \qquad \textbf{(2.5A)}$$

$$C_6H_{12}O_6 \Rightarrow 6H_2O + 6C \qquad \boldsymbol{\varepsilon_5} \qquad \textbf{(2.6A)}$$

Table 2.4: Relationship between extents of reaction and number of moles of species

Compounds	Moles out
$C_6H_{12}O_6$	$\varepsilon_2 + \varepsilon_4 + \varepsilon_5 \leq \mathbf{1}$
O_2	$\varepsilon_1 \leq \mathbf{N^{o}O_2}$
CO	$\varepsilon_1 + 3\varepsilon_2 - \varepsilon_3 + 3\varepsilon_4 \geq 0$
H_2	$\varepsilon_2 \geq 0$
CO_2	$\varepsilon_3 \geq 0$
CH_4	$\varepsilon_4 \geq 0$
H_2O	$\varepsilon_5 \geq 0$
C	$-2\varepsilon_1 + \varepsilon_3 - 3\varepsilon_4 + 6\varepsilon_5 \geq 0$

NB: 1 mole of glucose is fed together with $N^{o}o_2$ moles of oxygen

The set of linear inequalities in Table 2.4 are solved using Matlab script in MuPAD to find the Material Balance (MB) AR. The extents of reaction which define the vertices were determined and are given in Appendix A2. These vertices were used together with Hess's law (Eq. (2.7A) and Eq. (2.8A) in a similar way to Chapter 2 to find the respective ΔH and ΔG for the vertices.

$$\Delta H = \varepsilon_1 \Delta H_1 + \varepsilon_2 \Delta H_2 + \varepsilon_3 \Delta H_3 \quad \textbf{(2.7A)}$$

and

$$\Delta G = \varepsilon_1 \Delta G_1 + \varepsilon_2 \Delta G_2 + \varepsilon_3 \Delta G_3 \quad \textbf{(2.8A)}$$

The vertices were plotted in the G-H space and the convex hull of these vertices was found in order to give the G-H AR. The calculation was repeated for:

- Varying amounts of oxygen N^{o}_{O2} (0.000001, 0.5, 5, and 10 moles)
- Varying temperatures from 25 ^{0}C to 400 ^{0}C, 900 ^{0}C and 1500 ^{0}C for specific oxygen flow rates.

Thermodynamically, 6 moles of oxygen are required to combust 1 mole of glucose as shown in Eq. (2.9A). Hence there is excess oxygen fed to the system when N^{o}_{O2}=10.

$$C_6H_{12}O_6 + 6O_2 \Rightarrow 6CO_2 + 6H_2O \quad \textbf{(2.9A)}$$

Equivalent Ratio (ER) is an important parameter in gasification processes and is defined as the ratio of O_2 fed to the stoichiometric amount required for complete combustion), (Gungor., 2009) mentions that all processes for biomass gasification have ERs that vary between 0.1 and 0.3 while to (Vineet et al., 2016) suggests an

optimum gasification ER of 0.2–0.3. This expresses how much oxygen is fed relative to the Stoichiometric Ratio (SR) required for combustion and is given by Eq. (2.10A).

$$\text{Equivalence Ratio (ER)} = \frac{\text{Actual moles of oxygen gas fed to the process}}{\text{Moles of Oxygen required for complete combustion}} \quad \textbf{(2.10A)}$$

ER when 0.00001 moles of oxygen is fed equals zero while ER of 1.67 is attributed to when 10 moles of oxygen are fed. 10 moles of oxygen is considered an extreme case where excess oxygen is fed in gasification processes. This is usually not used in practical application but was applied to show the extent to which the G-H space and products would change at these conditions.

2.3A. Results and discussion for G-H AR for gasification processes

All the vertices of the material balance space are shown in the G-H AR. However, only the vertices that define the boundary of the convex hull of the points in the G-H space have the reaction description shown in the figures below.

2.3.1A. N^{o}_{O2}= 0.000001 and varying temperature

The thermodynamic G-H ARs obtained when 0.000001 moles of oxygen are fed together with 1 mole of glucose during gasification at temperatures 25 ^{0}C, 400, ^{0}C, 900 ^{0}C and 1500 ^{0}C and are shown in Figure 2.1A-2.4A respectively. Very small amounts of oxygen were supplied in this case to try and relate this situation to processes where no oxygen was added (AD and pyrolysis).

The results in Figure 2.1A shows that at 25 ^{0}C the thermodynamically favourable product (corresponding to minimum G) is carbon and water. When carbon was not considered as a species in the analysis, as shown in Chapter 2, the thermodynamically favourable product is CH_4 and CO_2. The addition of carbon as a possible product, has changed the desired product away from CH_4 to C.

One might postulate how this relates to AD, why is carbon not found as a product in typical AD processes. It could also be postulated that microorganisms cannot pass solids, such as carbon, across cell membranes and thus microorganisms produce CH_4 and CO_2, which decreases the G of the system, but which does not reach the global minimum. Nevertheless, while the production of C and H_2O lies at minimum G, the production of CH_4 and CO_2 is not thermodynamically far from the minimum G in the AR. The two material balances shown by point 5 and point 7 are given by Eq. (2.11A) and Eq. (2.12A) respectively.

$C_6H_{12}O_{6(s)} \Rightarrow 6C_{(s)} + 6H_2O_{(g)}$, ΔH = -188 kJ mol^{-1}, ΔG = -455 kJ mol^{-1}. **(2.11A)**

$C_6H_{12}O_{6(s)} \Rightarrow 3CO_{2(g)} + 3CH_{4(g)}$, ΔH = -142 kJ mol^{-1}, ΔG = -419 kJ mol^{-1}. **(2.12A)**

Another interesting point of interest is point 9 which lies at ΔH= 0 kJ/mol and ΔG. is negative. The reaction occurring at point 9 is adiabatic and this means that no heat is added or removed from the system to achieve products. Four products namely CO, CH_4, H_2O and C can be formed, and the material balance is given by Eq. (2.13A).

$C_6H_{12}O_{6(s)} \Rightarrow 2CO_{(g)} + CH_{4(g)} + 3C_{(s)} + 4H_2O_{(g)}$, ΔH = -0.8 kJ mol^{-1}, ΔG = -323 kJ mol^{-1}. **(2.13A)**

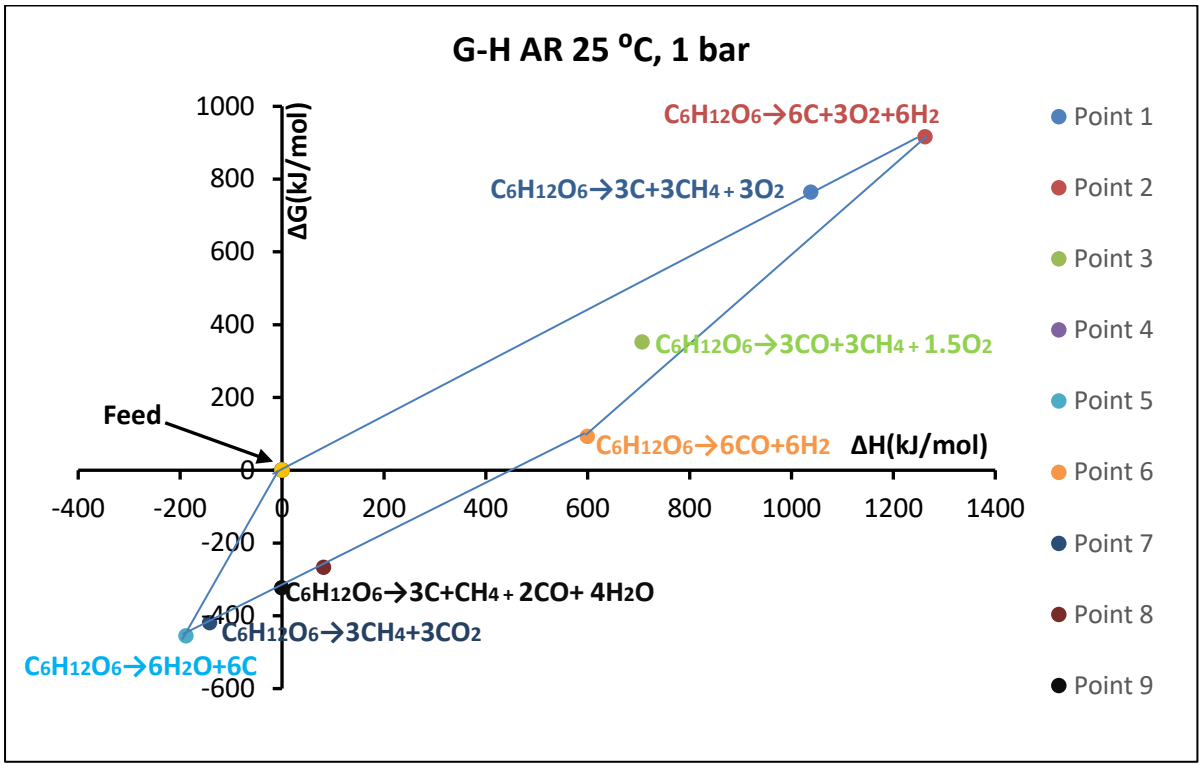

Figure 2.1A: G-H AR obtained when 1 mole of glucose is fed together with 0.000001 moles of oxygen at 25 ^{0}C.

Figure 2.1A also show that a large part of the AR lies in the area where ΔG is greater than zero. In this part of the region, work has to be supplied in order to achieve the material balance processes in this part of the AR. It shows that production of either oxygen or syngas (CO and H_2) is not favourable at 25 ^{0}C. As temperature is increased as shown by Figure 2.2A-2.4A, the production of CO and H_2 becomes more thermodynamically favourable and at 900 ^{0}C becomes more favourable than the product of C and H_2O.

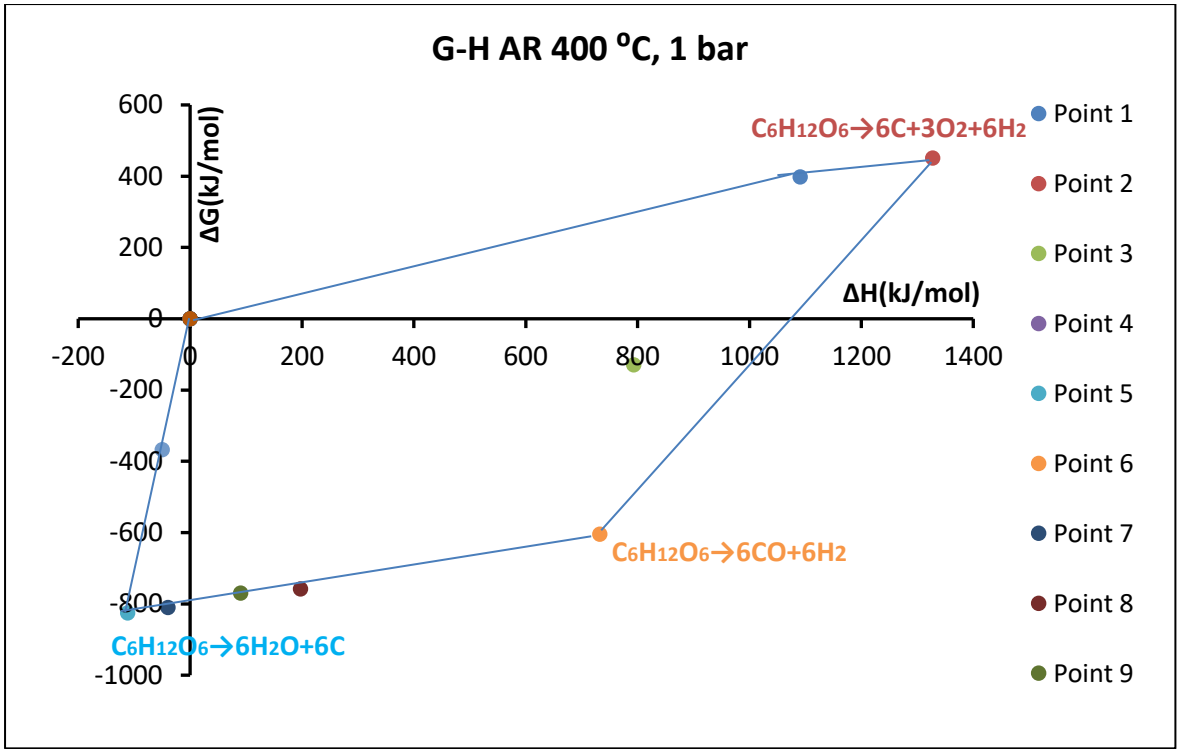

Figure 2.2A: G-H AR obtained when 1 mole of glucose is fed together with 0.000001 moles of oxygen at 400 ^{0}C.

It is also important to note that the whole AR becomes endothermic at temperatures starting from around 900 ^{0}C. Also, all the process in the AR have potential to produce work at this temperature as the AR lies below the G =0 axis. As temperature is increased to 1500 ^{0}C, the minimum G becomes more negative and the AR shifts to the right to become more endothermic. However, the products at minimum G remain to be CO and H_2 even at higher temperatures (Figure 2.3A). Comparing Figure 2.2A and Figure 2.3A it is interesting to note that the global minimum G changes as temperature is increased from 400 ^{0}C to 900 ^{0}C for the same O_2 flow rate. The material balance that makes C and H_2O (point 5) lies closer to adiabatic conditions while that which produces CH_4 and CO_2 (point 7) becomes endothermic. This shows us how thermodynamics influences the products at the global minimum G. This is affirmed by Figure 2.3A that shows distinct syngas production at 1500 ^{0}C.

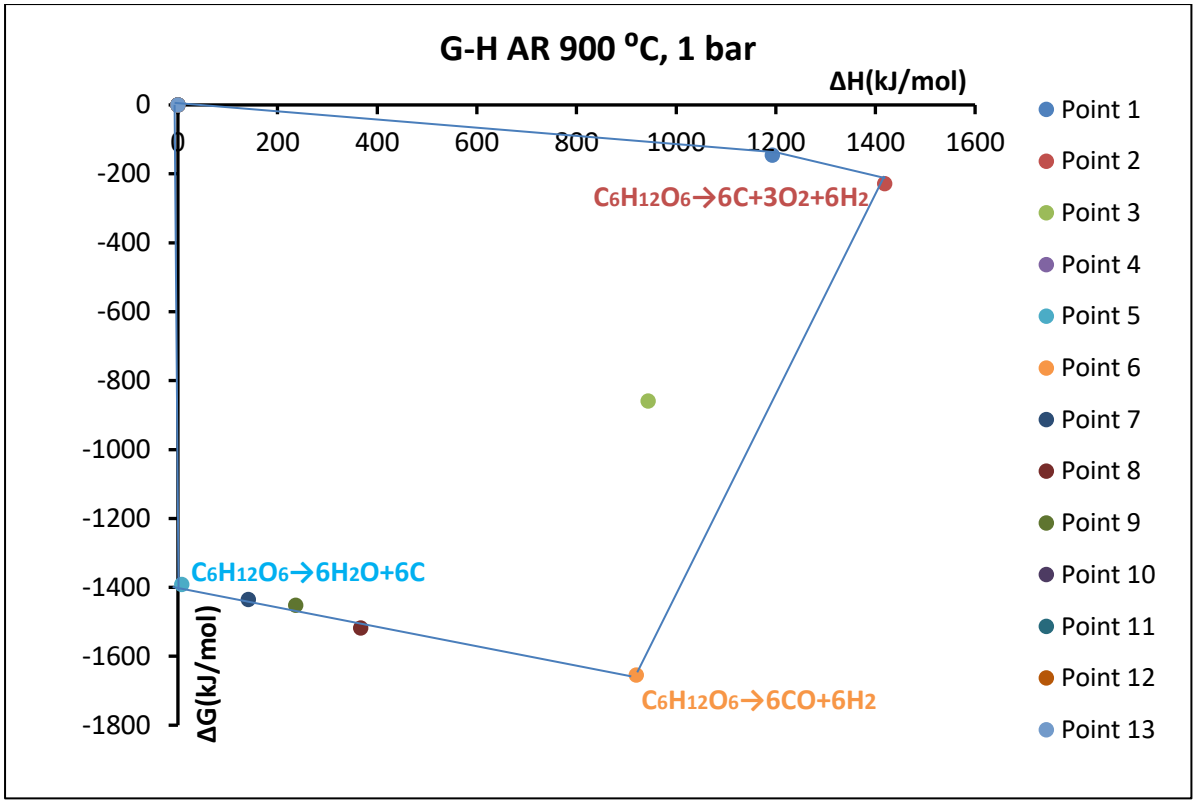

Figure 2.3A: G-H AR obtained when 1 mole of glucose is fed together with 0.000001 moles of oxygen at 900 ^{0}C.

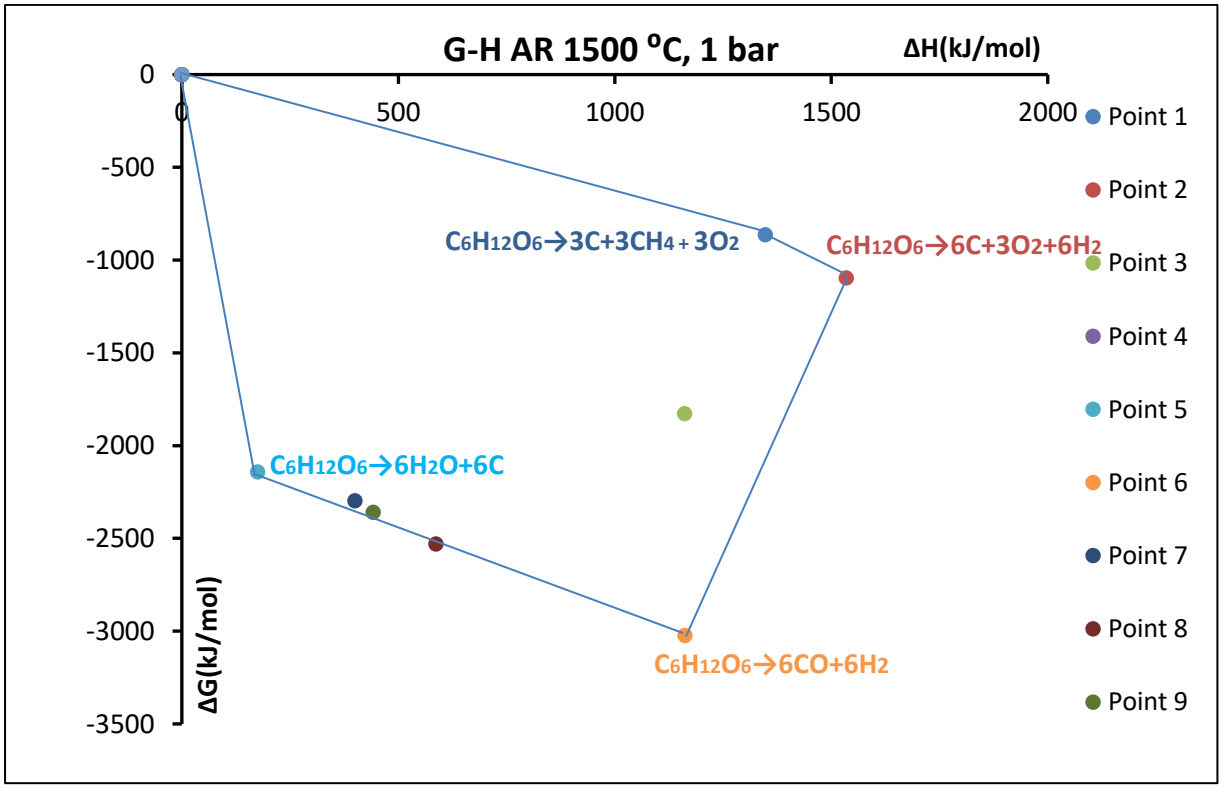

Figure 2.4A: G-H AR obtained when 1 mole of glucose is fed together with 0.000001 moles of oxygen at 1500 ^{0}C.

2.3.2A. N^{o}_{O2} = 0.5 moles of Oxygen and varying temperature

When the moles of oxygen fed together with 1 mole of glucose are increased to 0.5 moles (ER= 0.083), the products at minimum G begin to include CO_2 as a product. It is interesting to note that on this example, a small portion of the AR still lies in the exothermic region even at 1500 ^{0}C despite the whole region lying in the negative G region (Figure 2.5A to Figure 2.8A). The minimum G becomes more negative as temperature is increased but still lies in the endothermic region. This can be attributed to combustion taking place which is an exothermic reaction and produces CO_2 and H_2O as products.

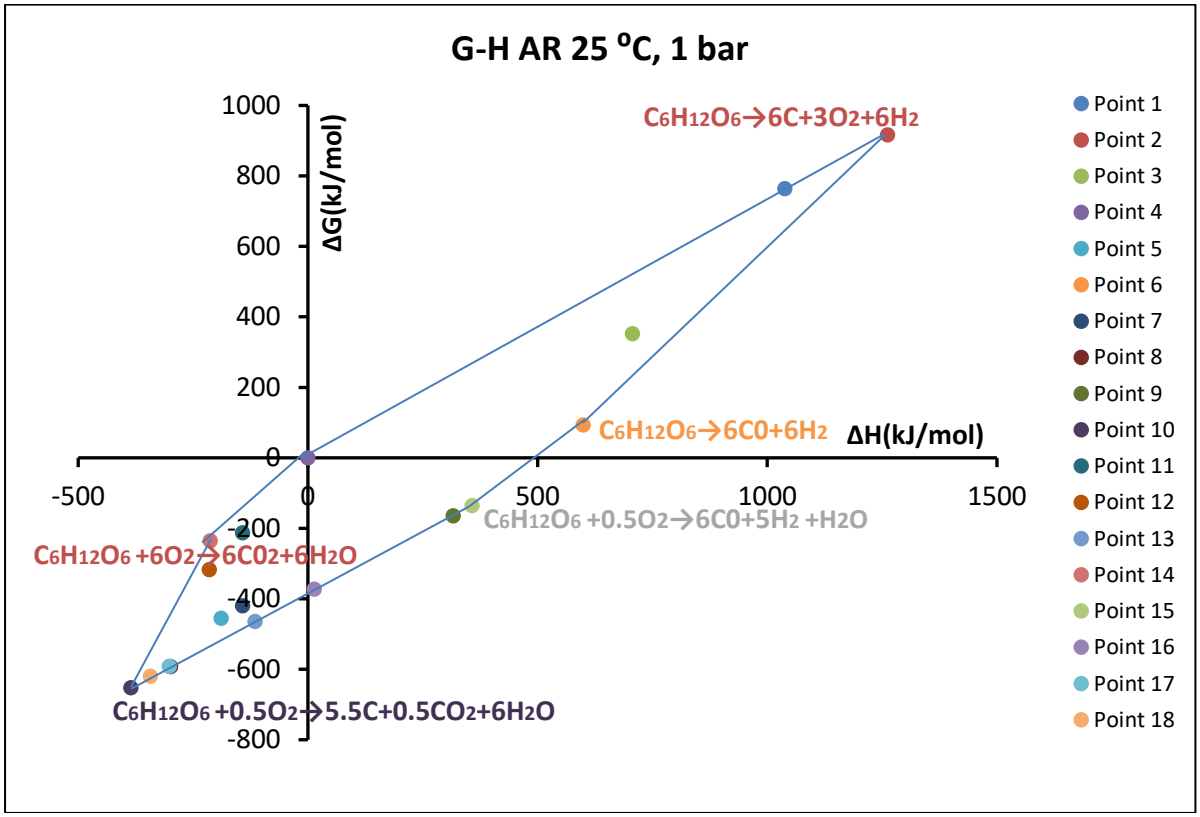

Figure 2.5A: G-H AR obtained when 1 mole of glucose is fed together with 0.5 moles of oxygen at 25 ^{0}C.

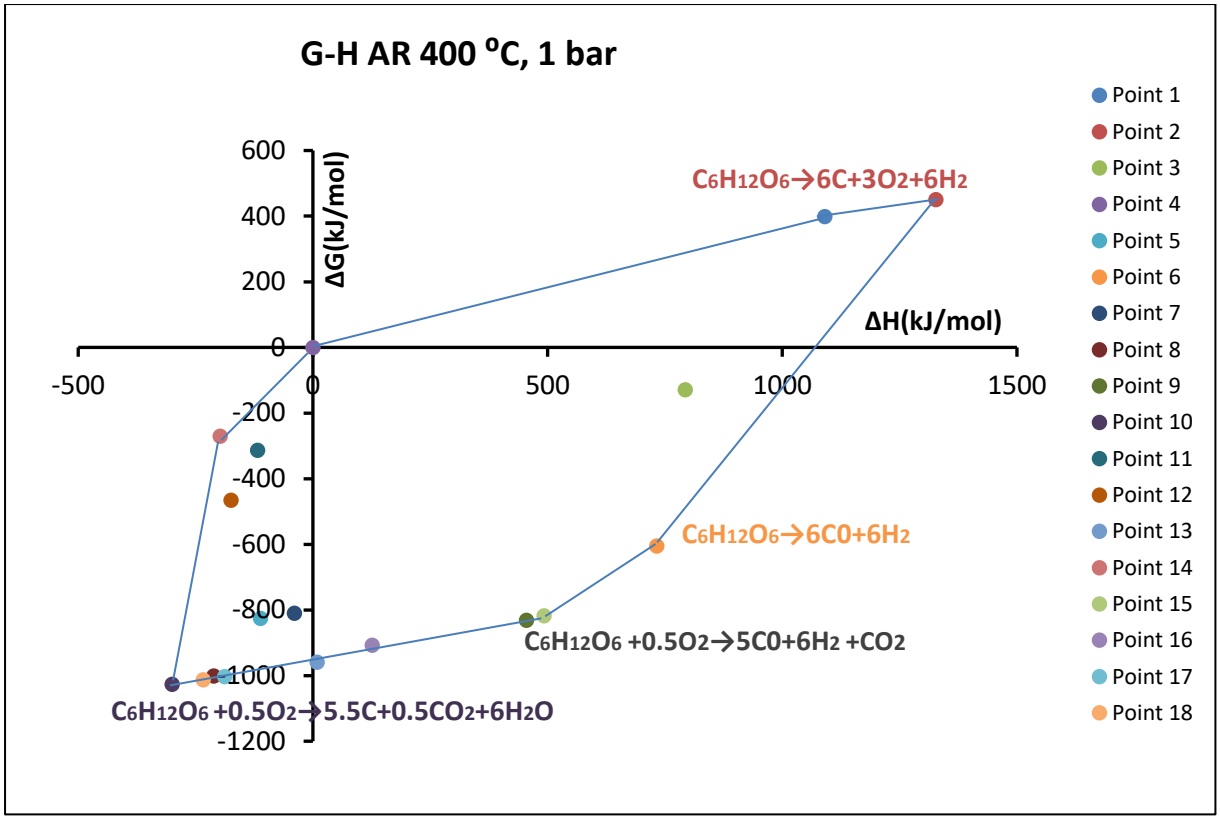

Figure 2.6A: G-H AR obtained when 1 mole of glucose is fed together with 0.5 moles of oxygen at 400 ^{0}C.

If one looks at Figure 2.7A, the analysis at 900 ^{0}C, it can be seen that two material balances are very close to each other at minimum G, i.e. one that produces syngas and H_2O and the other syngas and CO_2. As these two points are so close, one could expect that the G of mixing effects would become important leading to a gas composition at equilibrium that contains CO, H_2, CO_2 and H_2O. Even at higher temperature as shown in Figure 2.8A that the same material balance still exists (point 9 and point 15). At this condition it would be difficult to determine which one of the two material balances is favoured or how and at what proportions each one will have if both of them are favoured. Hence, the thermodynamic AR would not give us much information if one wants to make syngas only unlike in the case for pyrolysis. However, the material balance will have a greater effect on the products of gasification. This is shown in Section 2.3.3A and Section 2.3.4.A that as more O_2 is added into the

process, the system will choose to react the O_2 with some H_2 and CO to make H_2O and CO_2.

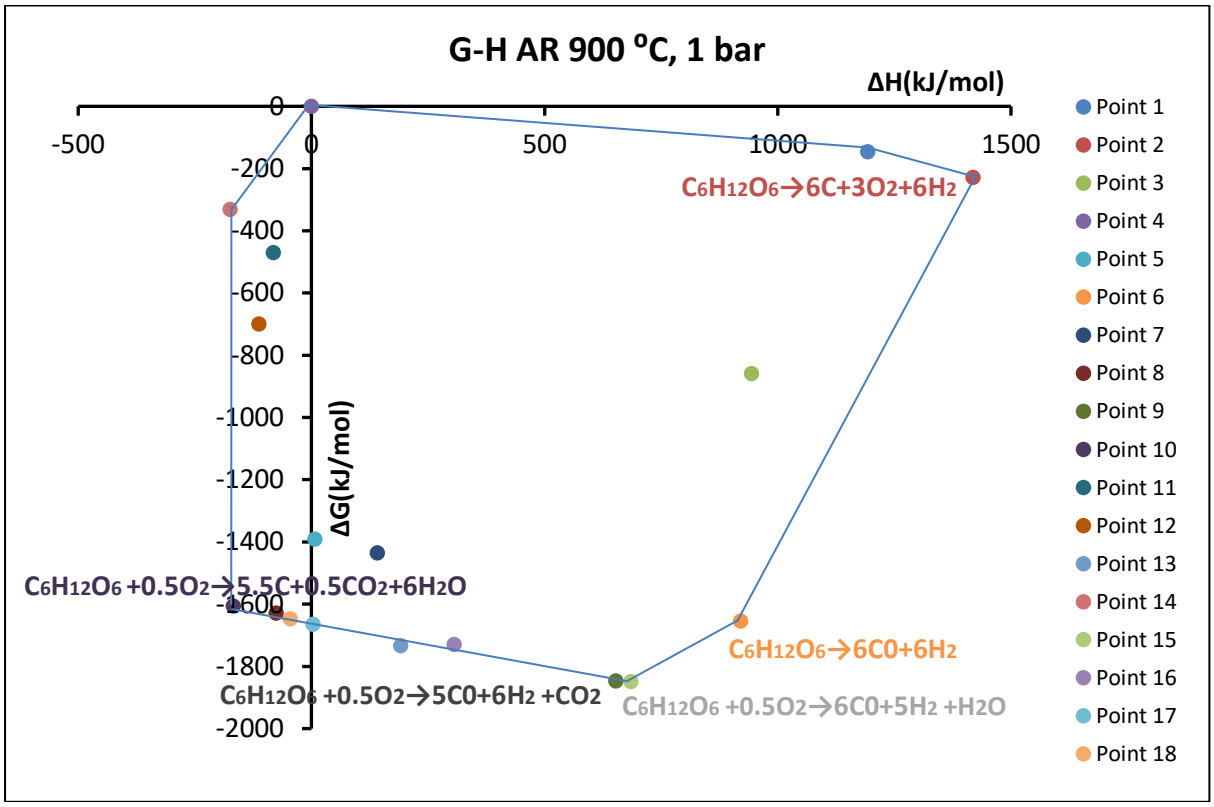

Figure 2.7A: G-H AR obtained when 1 mole of glucose is fed together with 0.5 moles of oxygen at 900 ^{0}C.

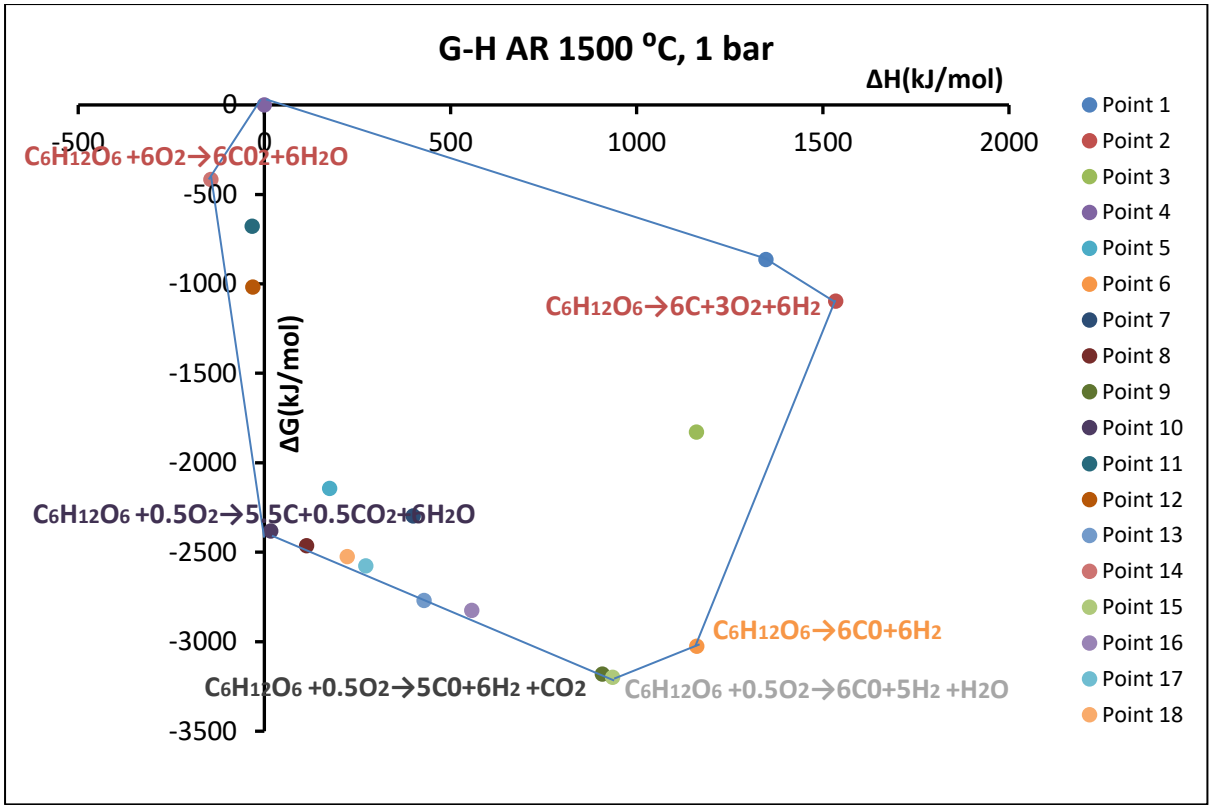

Figure 2.8A: G-H AR obtained when 1 mole of glucose is fed together with 0.5 moles of oxygen at 1500 ^{0}C.

2.3.3A. N^o_{O2} = 5 moles of Oxygen and varying temperature

Figure 2.9A- Figure 2.12A shows the AR when 5 moles of oxygen were added to the process. As previously observed in the latter analysis, the change in G for the whole AR becomes negative as temperature is increased. In addition, the minimum G becomes more negative. However, it is important to note that even when temperature is increased to 1500 ^{0}C, the minimum G remains in the exothermic region. It shows that when more oxygen is added to the process, the combustion reaction, which is exothermic, dominates. This is interesting as this can be easily understood from a 2-dimenssional G-H AR plot. At this point the production of CO_2 and H_2O is favoured instead of syngas.

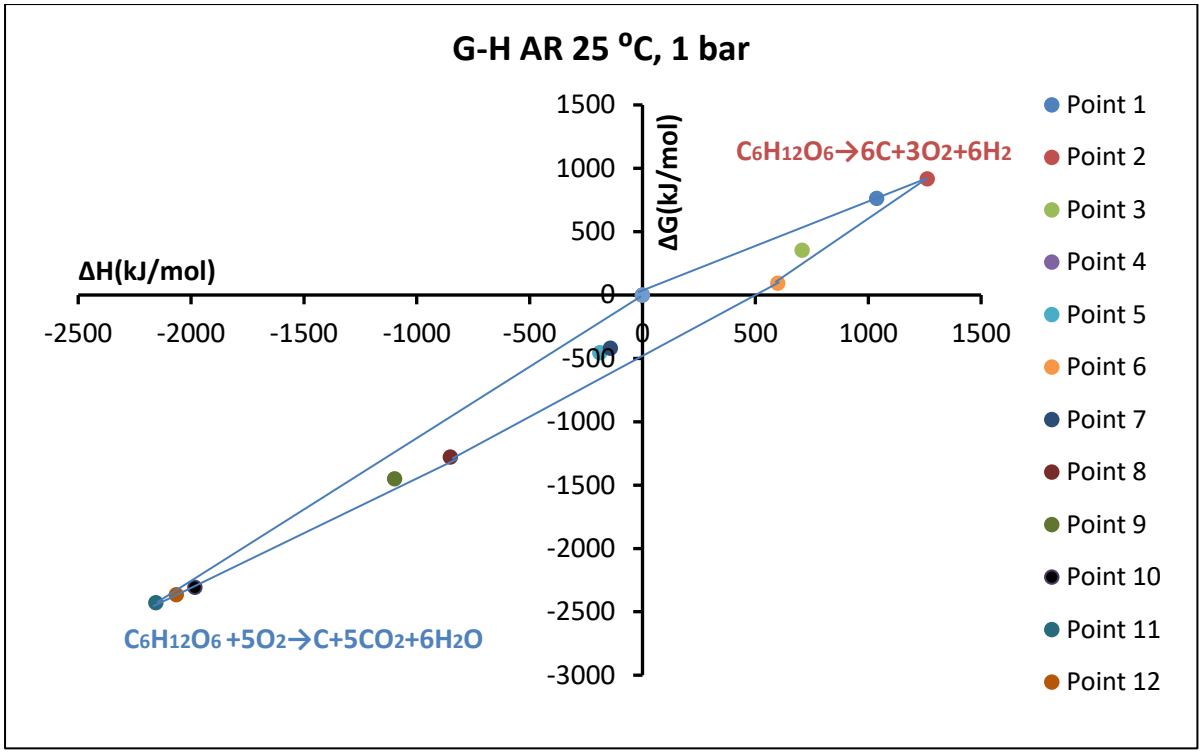

Figure 2.9A: G-H AR obtained when 1 mole of glucose is fed together with 5 moles of oxygen at 25 ^{0}C.

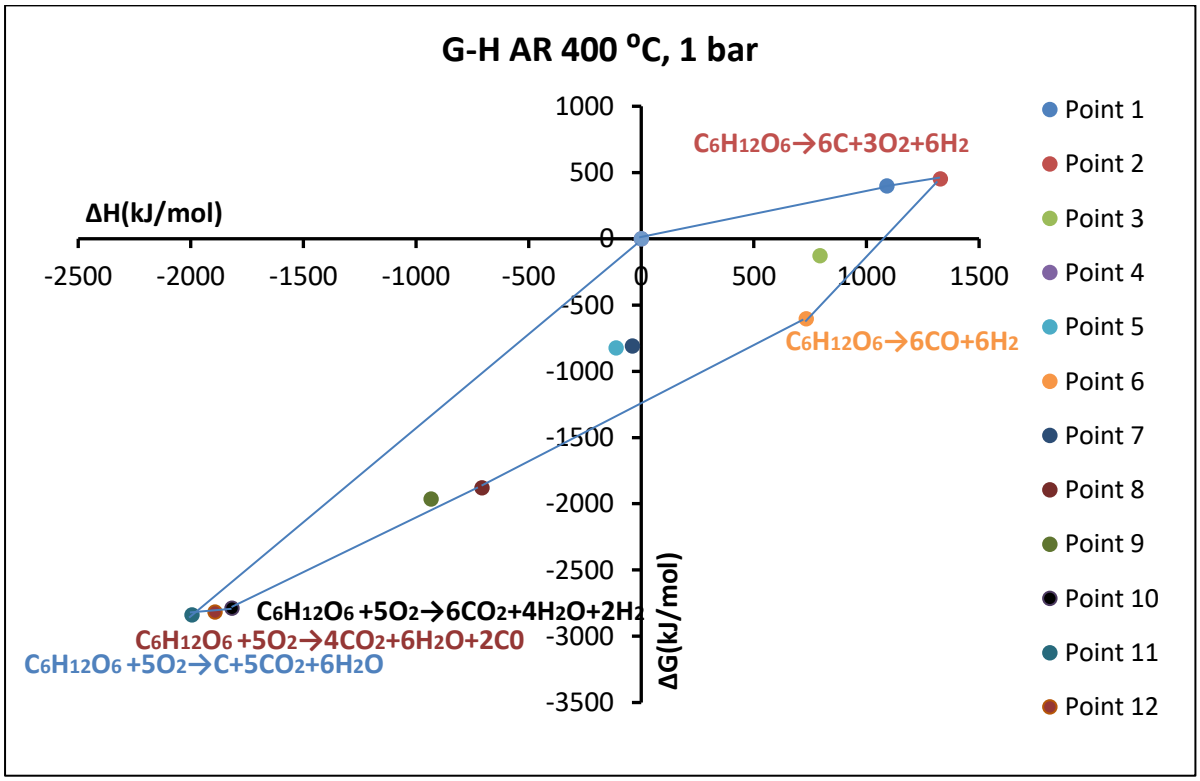

Figure 2.10A: G-H AR obtained when 1 mole of glucose is fed together with 5 moles of oxygen at 400 ^{0}C.

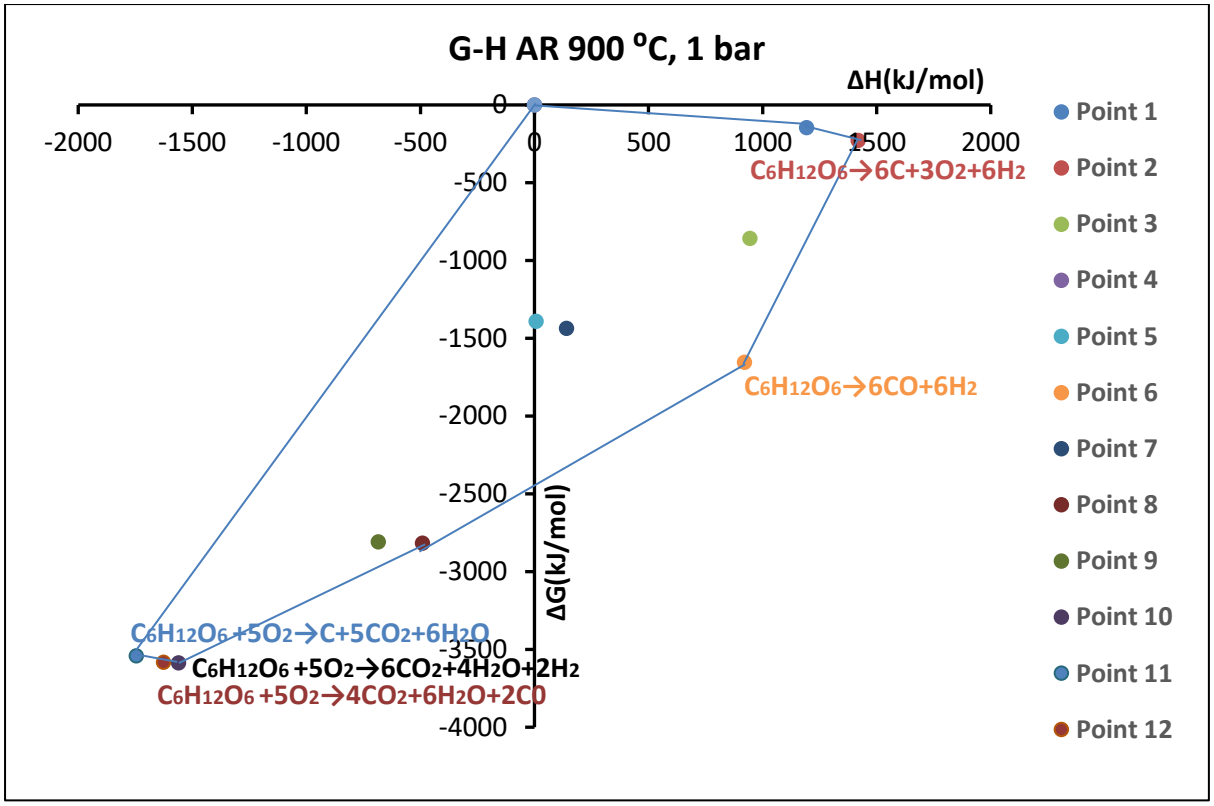

Figure 2.11A: G-H AR obtained when 1 mole of glucose is fed together with 5 moles of oxygen at 900 ^{0}C.

Again, the system when 5 moles of O_2 are added, there are three points at the bottom (minimum G) that are close to each other one might expect the gasifier output to depend on details such as flow, how behaviour approaches equilibrium. Considering that the ER was 0.83 when 5 moles of O_2 was fed, this may suggest that the products may not be at the optimum ER. Thus, with nearly SR oxygen it is not quite clear whether the product will have H_2, CO, H_2O, CO_2 or unburnt C or it is likely to be a mixture of all five which includes more of combustion product. Perhaps C is favoured at lower temperature and at higher temperatures it can be expected that the other gases would be present. In this situation where a number of products are predicted, kinetics may play a major role and/or a catalyst can help favour on group of products at the expense of another.

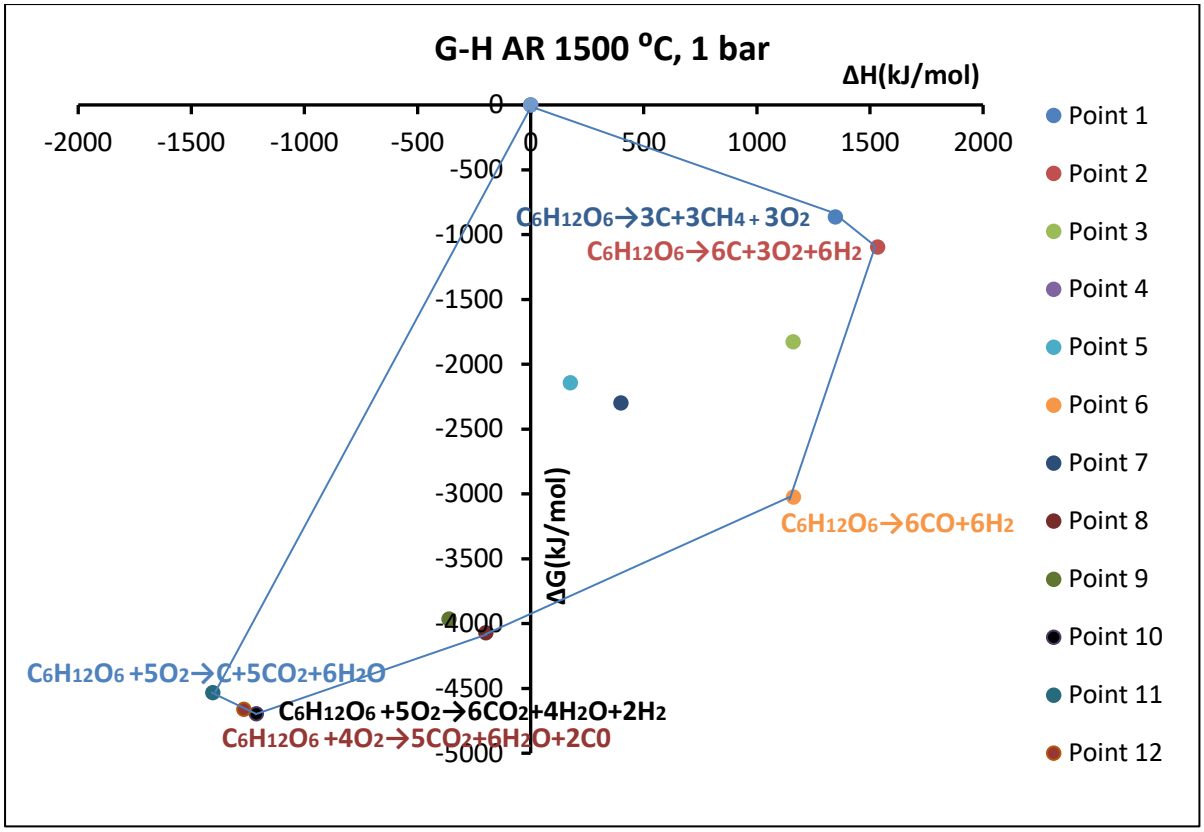

Figure 2.12A: G-H AR obtained when 1 mole of glucose is fed together with 5 moles of oxygen at 1500 ^{0}C.

2.3.4A. N^o_{O2} = 10 moles of Oxygen and varying temperature

A high ER of 1.67 and SR of 10 is used for this analysis when 10 moles of oxygen are fed to 1 mole of glucose. It is observed from Figure 2.1A, Figure 2.5A, Figure 2.9A and Figure 2.13A that the AR at 25 ^{0}C becomes smaller as the amount of oxygen fed is increased. Also, from Figure 2.13A to Figure 2.16A, the production of carbon dioxide and water (combustion) becomes dominant at minimum G for all temperatures studied. All processes above an ER of 1.67 would show a continuous to increase in the AR on the G-H space with a more exothermic combustion process at minimum G. This is as a result of 10 moles of O_2 being supplied to 1 mole of glucose which is an excess amount. The AR for all temperatures falls in the exothermic region where the large magnitudes of the minimum G becomes more negative with increase in temperature.

It is also quite clear from Figure 2.13A to Figure 2.16A that thermodynamics plays a vital role in product distribution in combustion processes

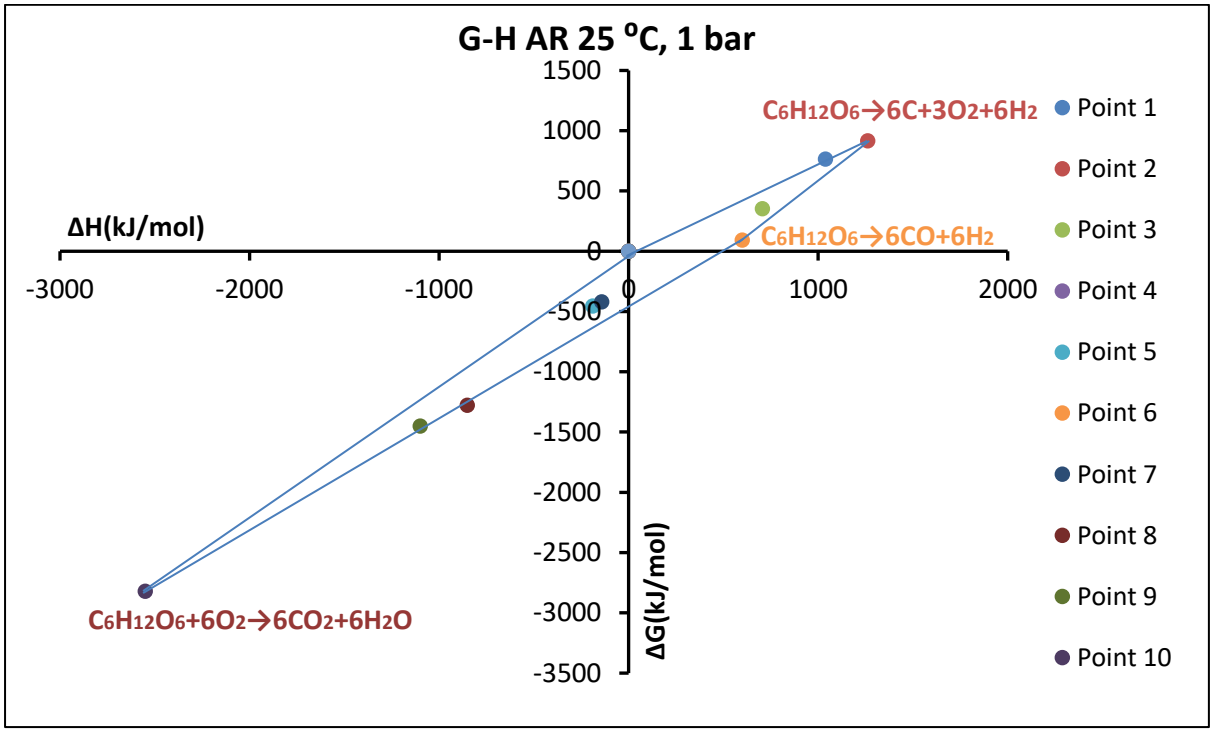

Figure 2.13A: G-H AR obtained when 1 mole of glucose is fed together with 10 moles of oxygen at 25 ^{0}C.

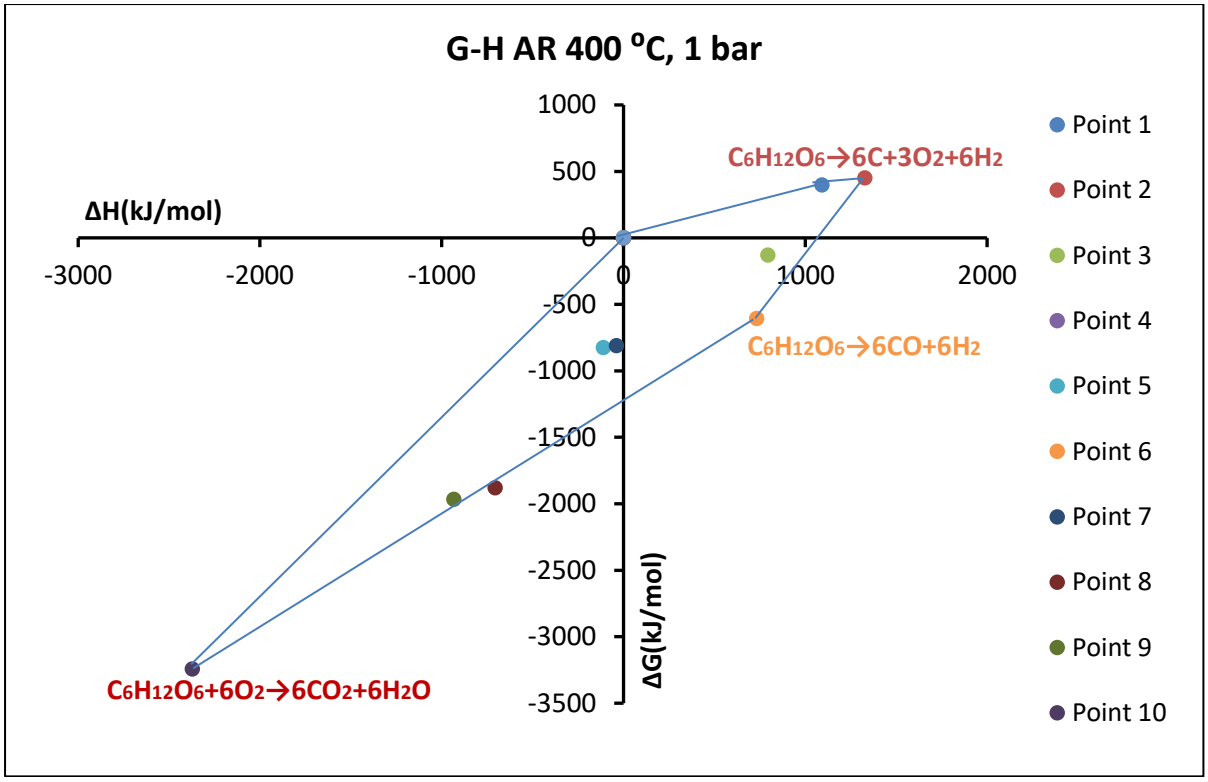

Figure 2.14A: G-H AR obtained when 1 mole of glucose is fed together with 10 moles of oxygen at 400 ^{0}C.

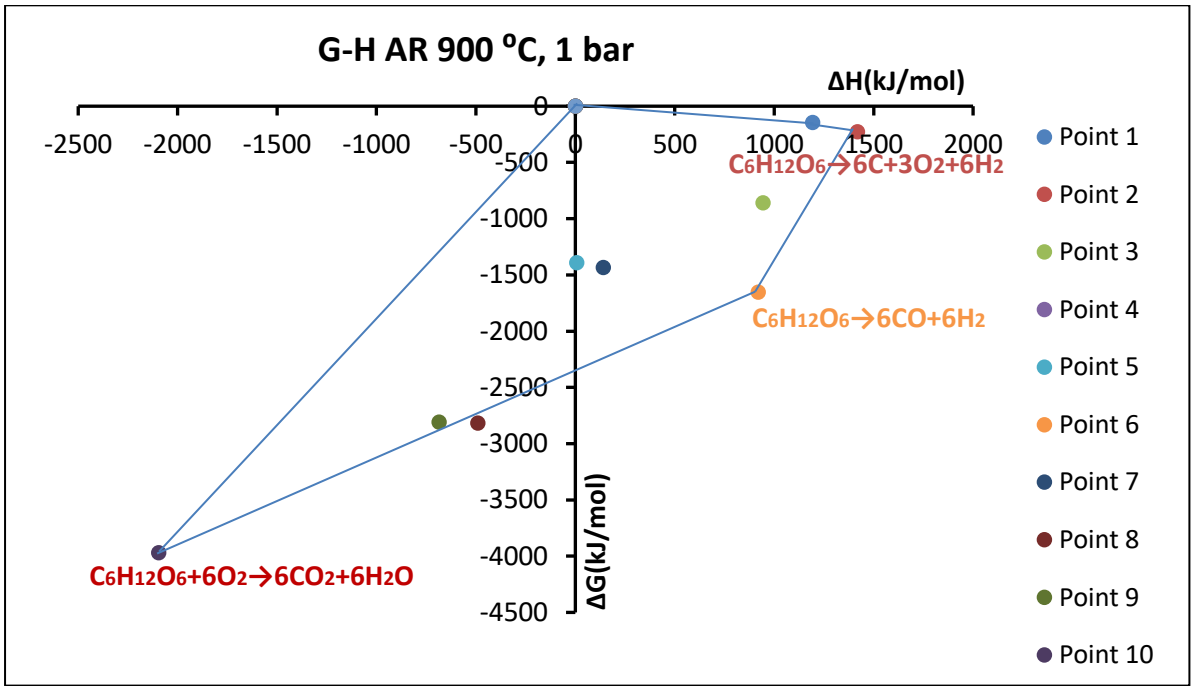

Figure 2.15A: G-H AR obtained when 1 mole of glucose is fed together with 10 moles of oxygen at 900 ^{0}C.

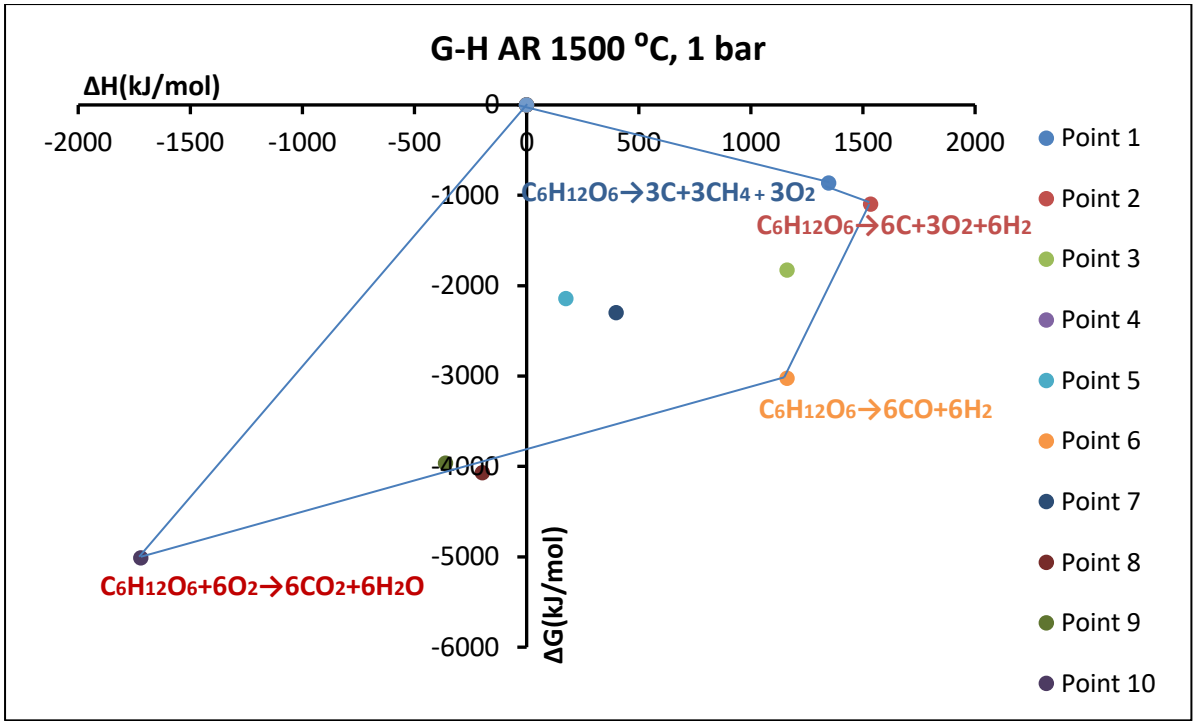

Figure 2.16A: G-H AR obtained when 1 mole of glucose is fed together with 10 moles of oxygen at 1500 ^{0}C.

2.4A. Summary

We have looked at varying both the amount of oxygen as well as the temperature in order to see how G-H AR changes as how the thermodynamically favoured product (corresponding to minimum G) changes. The analysis has looked at the conditions where products of AD, pyrolysis, gasification and combustion can be considered. Temperature controls the range of products that can be formed from solid C, CH_4 and CO_2 gases at low temperatures to H_2 and CO at higher temperatures. It is interesting to note that at 25 ^{0}C, C and H_2O are the preferred products at minimum G when very little amounts (~no O_2) are added to the system. This suggests that scientists need to look at mechanisms that can make carbon from glucose at low temperatures. The production of biogas, which comprise of CH_4 and CO_2 is not very far from the minimum G point. On the other hand, the amount of O_2 added to the system has a strong

influence on the amount of CO_2 that is formed at minimum G despite the changes in temperature.

References

1. Gungor A., 2009 Simulation of The Effects of The Equivalence Ratio on Hydrogen Production in Fluidized Bed Biomass Gasifiers .13th International Research/Expert Conference Trends in the Development of Machinery and Associated Technology TMT 2009, Hammamet, Tunisia, 16–21 October 2009.
2. Vineet S S., Ming Z., Peter C., Joseph Y., Xia Z., Mohammad Z M., Nilay S., Edward J. A., Paul S. F., 2016. An overview of advances in biomass gasification. Energy Environmental. Science, Vol. 9, pp. 2939–2977.

Chapter 3: Theoretical and Experimental Analysis of Biomass Gasification at Low Temperatures (Biogas Production at 30 ^{0}C)

The results of this chapter have been presented at the PSE2015/ESCAPE25 conference, Copenhagen, Denmark on 31 May - 4 June 2015 under the reference: **Muvhiiwa R*.,** Hildebrandt D., Matambo T., Glasser D., Theoretical and Experimental Analysis on Biogas Production, poster #302.

This is completely my work, I did all the simulations and processing of data as well as writing the paper. My supervisors assisted with the analysis of data.

Abstract

The research presents an analysis of experimental data for the different gaseous products of an Anaerobic Digestion (AD) process at a temperature of 30 ^{0}C based on the thermodynamic Attainable Region (AR) obtained. The AR approach is presented; which in itself is an interesting tool for defining the limits of a given process of interest. The Enthalpy (ΔH) and Gibbs Free Energy (ΔG) are used to obtain the AR showing the thermodynamic limits for AD for biogas production from 1 mole of glucose. The glucose was used as a surrogate for the different biomass materials used and in this case cow dung and dog faeces. Thermodynamic results have shown that at minimum G CO_2 and CH_4 are produced at temperatures around 30 ^{0}C. Experimental data using cow dung, glucose and dog faeces (as biomass feed) at 30 ^{0}C lies close to the region were the G is minimum on the G-H AR plot. This suggests that a consortium of anaerobic bacteria operates so as to minimise G under AD provided optimum temperatures for the biological process are met. This is an important observation as it shows that the bacterial action is governed by the limits of thermodynamic laws.

3.1. Introduction

The work presented finds the AR obtained from the G-H plot for the conversion of a biomass feed (in this case assumed to be one mole of glucose) into different gaseous products namely CO, H_2, CH_4 and CO_2. It also shows the comparison of experimental findings of AD using cow dung, glucose and dog faeces to the feasible AR obtained from thermodynamics. Thermodynamics suggests that systems and processes are feasible if ΔG is less than zero (Li et al., 2000) and operation is most favourable when ΔG is most negative (minimum G). Operating at minimum G maximises irreversibility. In chemical engineering, the bigger the ΔG, the bigger the driving force. However, although hard to ascertain, this may also mean a faster reaction and ΔG could be proportional to the speed of the reaction. Conversely, this could also mean that given enough time, time to infinity, predicted products will be formed.

The scope of this work is to compare the theoretical calculations to experimental findings obtained from biogas production. This then is an application of the AR theory to biological processes as well as biomass processes. This work is closely related to the theoretical data presented in the research by (Muvhiiwa et al., 2015) but in this case, a G-H region is plotted at 30 ^{0}C and is compared to experimental findings. The calculations are intended to show how bacterial activity relates to thermodynamic limits from an H and G point of view. This work is only carried out based on an assumed optimum operation conditions for methanogen bacteria in order to try and give a better and estimated analysis.

Biogas production is an anaerobic process meaning that the process is favourable in the absence of oxygen. The biomass materials (in this case are cow dung and dog

faeces) which constitute mainly of C, H and O elements. This means CH_4 and CO_2 gases are formed only from the elements present in the biomass material. The breakdown of elements to form gases in AD is similar to a pyrolysis process where biomass is converted into gases by heating in the absence of oxygen. Unlike in the controlled oxygen gasification process, no oxygen or other elements are added to AD and pyrolysis to help break down the biomass besides bacteria and heat respectively. This allows one to compare how the products of biomass conversion to gases change from low temperatures to high temperatures using the same feed and make a relationship between AD, pyrolysis and gasification as all forms of gasification process.

3.1.1. Low temperature gasification, Anaerobic Digestion

A thermodynamic analysis of low temperature AD was investigated to obtain an AR using G-H plots. The objective was to find the thermodynamic region where all reactions are possible for the biological process on where the bacterial consortium actually operates. This was investigated for the temperature at 30 ^{0}C and 1 bar pressure. These conditions have been chosen because microorganisms that produce biogas generally operate under these conditions in liquid water.

As shown in the latter Chapter 2 that the minimum values of G become more negative as temperature is increased from 25 ^{0}C -100 ^{0}C, suggesting that the process operates better at higher temperatures. However, this does not mean that actual biogas production increases with temperature since it is the anaerobic bacteria that is important and how the bacteria will adapt to the operating temperature. Although water is in liquid/gas state around 70 ^{0}C - 100 ^{0}C, theoretically, biogas can be formed around this temperature. However, in practice, there is no feasibility of biogas production

around these temperatures since it is the anaerobic consortium that is important and how it will adapt to these temperatures. Therefore, in the case of biogas production, the optimum temperature of 30 ^{0}C, without any other factors, was considered.

Biogas production is a slow biological conversion of biomass material at low temperatures under anaerobic conditions. In general, most anaerobic bacteria in the thermophilic group have a maximum growth rate at temperatures around 70 ^{0}C - 75 ^{0}C (Zindler et al., 1984). The process to produce biogas is catalysed by a special group of bacteria called methanogens. Most isolated methanogens have temperature optima around 25 ^{0}C, and upper temperature limits at 30-40 ^{0}C (Nozhevnikova et al., 2001). According to (Uniwersytet Wroclawski., 2017), a website providing data on methanogens, many of the methanogens that feed on CO_2 and H_2 can operate in temperatures ranging from 20 - 40 ^{0}C with optimum temperature averaging to about 30 ^{0}C. A specific methanogen called *Methanobacterium lacus sp. nov.* was studied by (Guillaume et al., 2012) and was found to grow at a temperature range of 14 – 40 ^{0}C (optimum 30 ^{0}C) and at pH 5.0 – 8.6 (optimum pH 6.5) while biogas guideline data from (Werner et al., 1989) shows the suitable digestion temperature of between 20 ^{0}C and 35 ^{0}C. This bacterium uses H_2 and CO_2 for catabolic growth to produce CH_4. The results by (Muvhiiwa et al., 2016) show that, for AD of cow dung and dog faeces, the final composition of CH_4 produced on a nitrogen free basis was similar at temperatures of 20 ^{0}C, 25 ^{0}C and 30 ^{0}C studied. Although the same composition was obtained for the temperatures studied, the gas production rate might be different and also that the composition of the product gas might be set by the material balance. Hence, temperature may not have much effect in the product gas concentration in this small temperature range. Nevertheless, a temperature of 30 ^{0}C was chosen for experimental

purposes as this would ideally provide us with better results for comparison with thermodynamic data from AR. Feed substrates of cow dung and dog faeces were used for the experiment. Cow dung is readily available in farms and carries the methanogen bacteria that help to produce biogas. If one wishes to compare other biological experimental results to the AR theorem, it would also be advisable to try and carry out the experimental work at the optimum conditions. These may include, temperature, pressure etcetera for maximum production rate for the bacterial activity to enable better contrasts.

3.2. Experimental set up for the processes.

3.2.1. Low temperature gasification-AD

The experimental procedure and other results obtained from (Muvhiiwa et al., 2016) at 30 ^{0}C were used for this study and were compared with the thermodynamic AR plot to explore any correlations. This is because biogas production is a biological process, therefore relies on bacteria to convert solid feed to gaseous product. The mesophilic range, 20 ^{0}C – 40 ^{0}C is considered to produce the highest CH_4 composition hence a temperature of 30 ^{0}C was chosen to try and give us a good comparison with the theoretical plots. It is also assumed that the methanogen bacteria in our substrate is similar to the group of methanogens that work at optimum temperatures around 30 ^{0}C hence would help give relatively close data that would allow us for better analysis.

Feed of 25 g cow dung, 25 g dog faeces and 20 g dog faeces + 5 g cow dung were investigated for biogas production at 30 ^{0}C. The amount of feed substrate that was added to the flask was 10 % of the total solid contents. To relate this feed material to

the G-H ARs, all the feed was assumed to be glucose hence thermodynamic data for glucose was used for the theoretical analysis. Distilled water (250 ml) was added to all flasks. Nitrogen was used to purge air out of the flasks to create an anaerobic condition. The total volume of the solution amounted to about 55 % of the 500 ml flask to accommodate for gas production. Gas composition was investigated for the flask at 30 ^{0}C in water baths. The experiments were carried out for 190 days and the gas was analysed using a Gas Chromatography (GC) with CH_4, CO_2 and H_2 gases considered for analysis. The results used for this analysis were obtained at day 82 because the gas composition was constant after this period. Batch processes were run, and gas was collected with a gas syringe through a rubber seal. The CH_4 gas composition was calculated on a nitrogen free basis as shown in Eq. (3.1)

$$\text{Methane composition} = \frac{\textbf{molar amount of } \mathbf{CH_4}}{(\textbf{molar amount } \mathbf{CH_4} + \textbf{molar amount } \mathbf{CO_2} + \textbf{molar amount } \mathbf{H_2}} \qquad \textbf{(3.1)}$$

The concentrations of other gases were calculated in a similar way as in Eq. (3.1). Figure 3.1 show the laboratory flask set up for the biogas experiment.

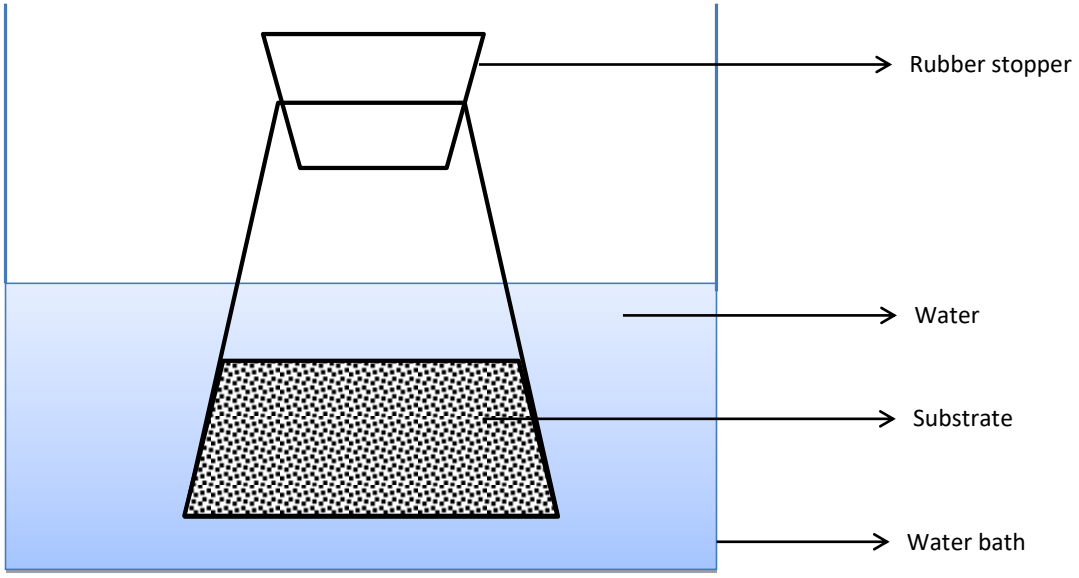

Figure 3.1: Experimental set up for low temperature gasification (AD) at 30 ^{0}C.

3.3. Results and Discussion

3.3.1. AR for anaerobic digestion at 25^{0}C and 1 bar

Figure 3.2 illustrates the AR at 25 ^{0}C, 1 bar when 1 mole of glucose is used as feed material and is obtained using the methods shown Section 2.1 of Chapter 2. The region of interest is where we either add or remove heat without adding work and is shown by the shaded region. It is important to note that the G must be less than zero for the overall reaction to be thermodynamically feasible when mixing is excluded. The main products of biogas production are CO_2, H_2 and CH_4. The AR show that it is thermodynamically feasible to make CO_2, H_2, CH_4 and CO at 25 ^{0}C, 1 bar and different bacteria could work anywhere within the region but not outside the region. However, experimental research has shown that most bacteria do not favour the production of CO at these low temperatures (Danielas et al., 1977). This suggests that biological processes that produce biogas may lie on the zero CO line. It might also be assumed that the reaction will proceed to where ΔG is most negative (minimum G) in the AR because the system is likely to be more stable at this state.

From Figure 3.2 the minimum G i.e. point x, H_2 and CO are zero with CH_4 and CO_2 as the only expected products. This corresponds to Eq. (3.2) and is where the maximum amount of CH_4 can be made of which an equal amount of CO_2 is produced.

$$C_6H_{12}O_{6(s)} \Rightarrow 3CO_{2(g)} + 3CH_{4(g)},\ \Delta H = -141.9\ kJ\ mol^{-1},\ \Delta G = -418.68\ kJ\ mol^{-1} \quad \textbf{(3.2)}$$

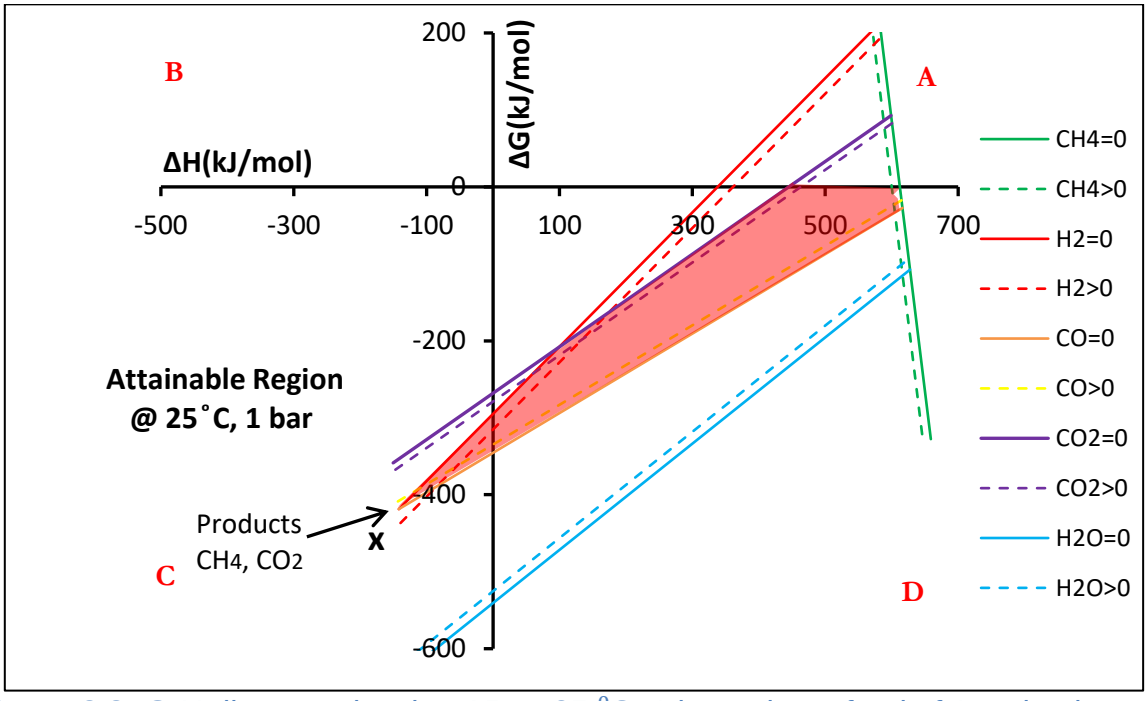

Figure 3.2: G-H diagram showing AR at 25 ^{0}C, 1 bar using a feed of 1 mole glucose. The shaded region in red is the AR.

3.3.2. AR at 30 ^{0}C.

Eqs. (2.11) and (2.15) in Section 2.2.3 of Chapter 2 were used to find how the AR changes with temperature at constant pressure. The resulting AR obtained for the change in temperature from 25 ^{0}C to 30 ^{0}C at constant pressure of 1 bar is shown in Figure 2.3. The AR for the temperature studied in Figure 2.3 show that the products formed at minimum G are quite distinct from the other products in the system. Hence,

mixing was not considered. The material balance at minimum G at 30 ^{0}C is shown by Eq. (3.3).

$$C_6H_{12}O_{6(s)} \Rightarrow 3CO_{2(g)} + 3CH_{4(g)},\ \Delta H = -140.81\ \text{kJ mol}^{-1},\ \Delta G = -423.33\ \text{kJ mol}^{1} \quad \textbf{(3.3)}$$

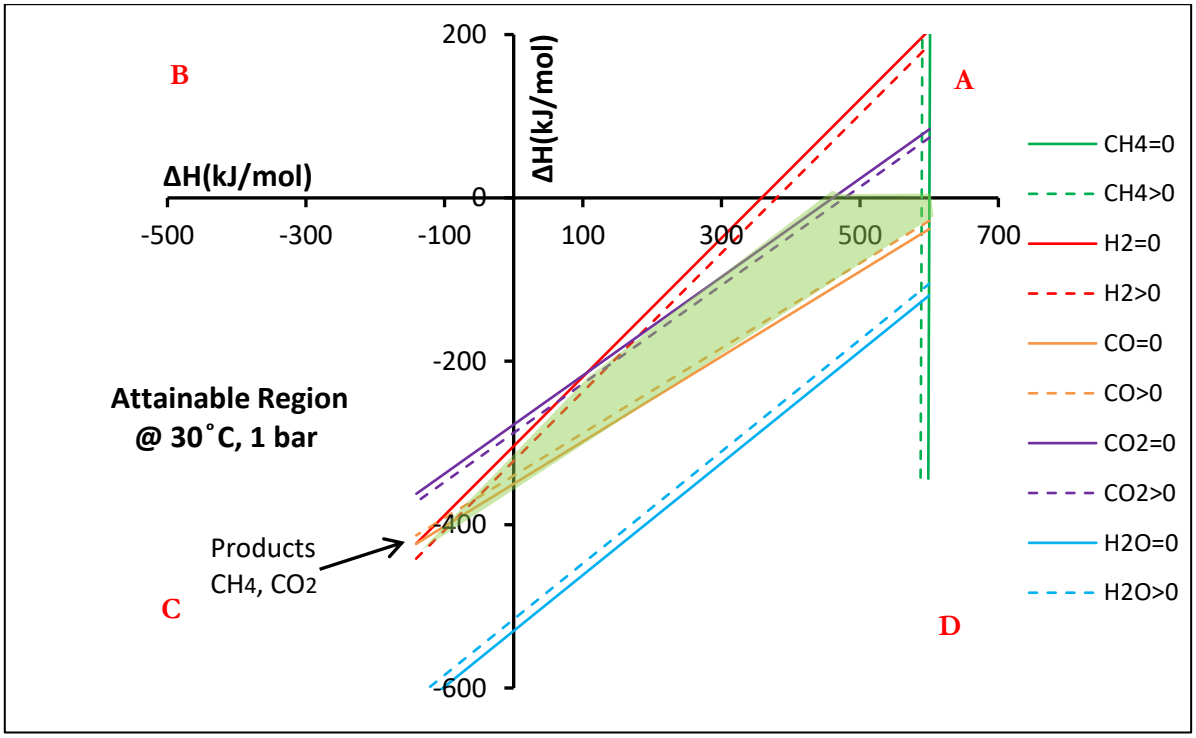

Figure 3.3: G-H diagram showing AR at 30 ^{0}C, 1 bar using a feed of 1 mole glucose. The shaded region in red is the AR.

3.3.3. Experimental vs theoretical results at 30 ^{0}C.

In theory, it is possible to make biogas in the temperature range 25 ^{0}C to 100 ^{0}C. However, there is no feasibility of biogas production at 100 ^{0}C or near this temperature as it is difficult to imagine how a boiling digester would operate and considering that bacteria may be denatured at these temperatures. Hyperthermophilic AD occurs around 70 ^{0}C where the bacteria have maximum growth. Also, it should be noted that biogas can be produced at temperatures below 25 ^{0}C but in this analysis an optimum temperature of 30 ^{0}C was considered for analysis.

Table 3.1 shows experimental data that was plotted on the thermodynamic AR. The experimental method and other results were obtained from AD of cow dung and dog faeces at 30 ^{0}C over a period of 82 days (Muvhiiwa., et al 2016). Figure 3.4 typically shows the diagram for AD of cow dung and dog faeces from which data used to compare with the AR results was obtained. This plot was similar to the other two substrates. CH_4, CO_2 and H_2 gases were produced in significant quantities during this experiment. No CO was observed in the GC analysis.

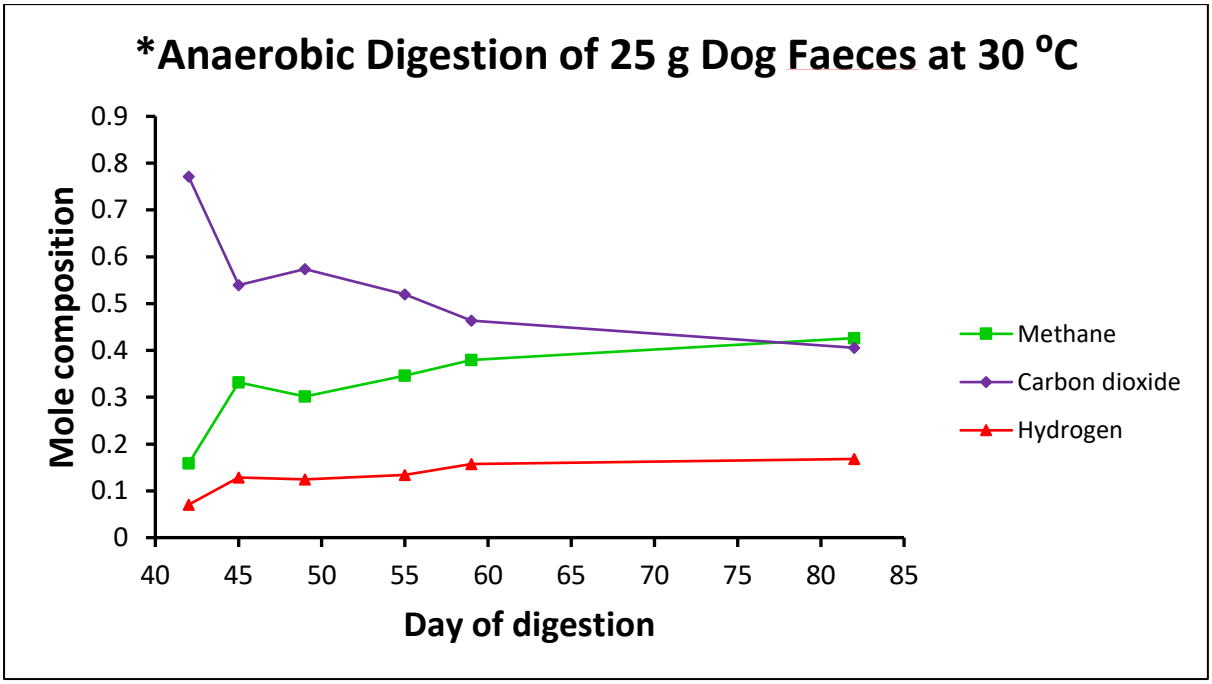

*Figure 3.4: Graph showing changes in gas composition in the sample containing dog faeces and cow dung at 30 ^{0}C.

The results in Table 3.1 show the concentration of CH_4, CO_2 and H_2 in the biogas produced after a period of about 82 days. The highlighted results were carried out by the researcher while the other results are from published data by Muvhiiwa et al., 2016. The results in Table 3.1 for AD of glucose shows a 1:1 ratio of CO_2 and CH_4 and were obtained from experiments carried out by Kalyuzhnyi and Davlyatshina (1997). The

glucose results gave a carbon balance of 80 % suggesting that the balance of 20 % went on to form cells as alluded by the authors.

The results with the asterisk (*) in Table 3.1 are the same results shown in Figure 3.4. It is important to note that the concentrations at the end of the experiment were considered but not the intermediate processes. Also, this was on a nitrogen free basis.

Table 3.1: Experimental results on AD at 30 ^{0}C.

Substrate	Molar Concentration			ΔH (kJ/mol)	ΔG (kJ/mol)
	[Carbon dioxide]	[Methane]	[Hydrogen]		
***25 g Dog faeces**	**0.4056**	**0.4263**	**0.1680**	**-137.6**	**-393.3**
25 g Cow dung	0.4058	0.4247	0.1695	-114.3	-395.3
30g Cow dung	0.4884	0.5091	0.0025	-117.45	-398.6
20 g Dog faeces + 5 g Cow dung	0.4319	0.4050	0.1632	-177.5	-462.3
10.9 mg Glucose @ 35 ^{0}C	0.4940	0.4980	0	118.43	396.84

This experiment was carried out for 199 hours at a pH of 7 and temperature of 35 ^{0}C. The concentrations were normalised to give results for 1 mole of glucose feed and the material balances were used to calculate the ΔH and ΔG for the respective substrates. The process for normalising the experimental data to AR conditions and obtaining the G and H for the experimental work is shown in Eq. (3.4) and Eq. (3.5). Considering the experiment where 25 g of dog faeces digested (glucose as surrogate in the calculation), the mole balance becomes:

$$0.138C_6H_{12}O_{6(s)} \Rightarrow 0.405CO_{2(g)} + 0.426CH_{4(g)} + 0.168H_{2(g)} \quad \textbf{(3.4)}$$

And normalised to 1 mole to fit on the thermodynamic G-H plot as shown in Eq. (3.5).

$$C_6H_{12}O_{6(s)} \Rightarrow 2.934CO_{2(g)} + 3.087CH_{4(g)} + 1.217H_{2(g)}$$ ΔH = -137.65 kJ mol^{-1}, ΔG = -393.3 kJ mol^{1} **(3.5)**

The values of ΔG and ΔH in Eq. (3.5) were plotted on the AR to give a point and the same analysis was done for the other substrates, assuming they were glucose. All the substrates used were not characterised. Although protein and lipids are present in cow dung and dog faeces, it was assumed that the composition of these is low compared to the composition of the carbohydrates. Another major assumption was also to consider the overall material balance for producing H_2, CH_4 and CO_2 and not consider intermediate steps.

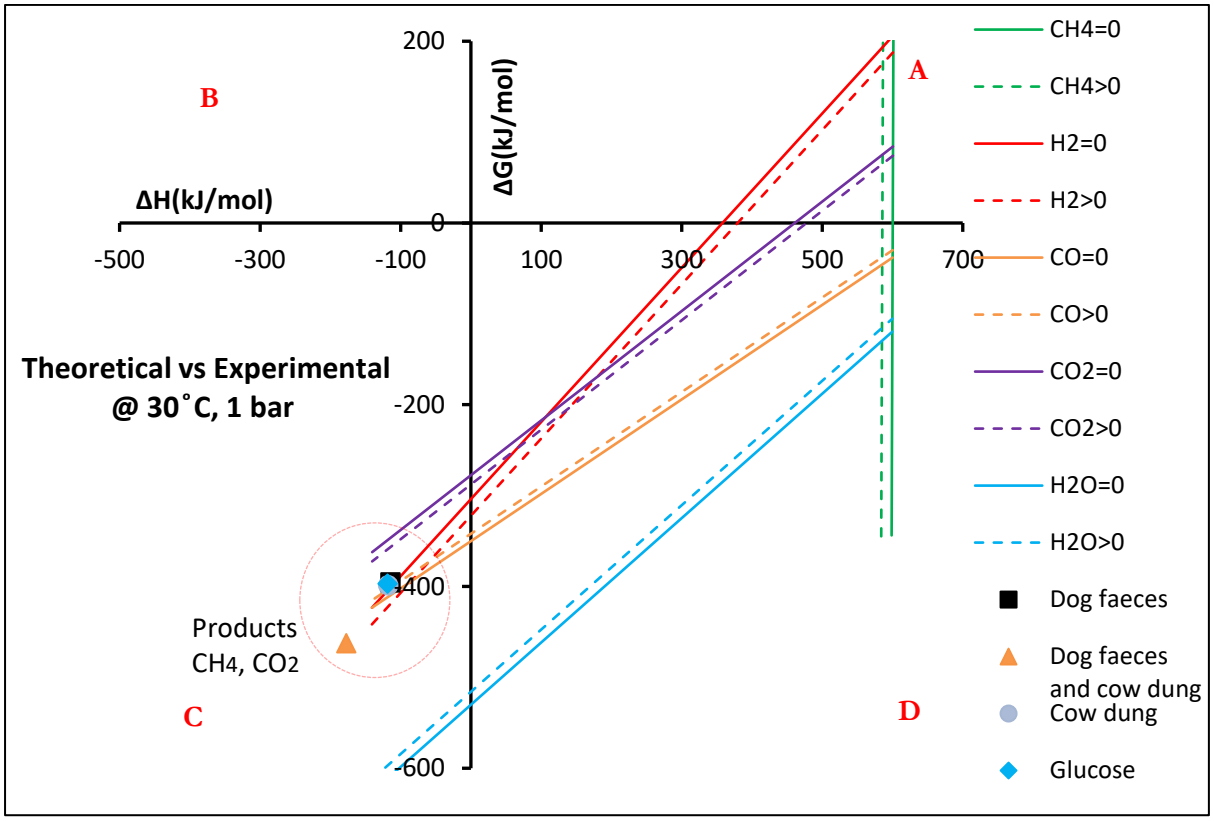

Figure 3.5: G-H diagram showing comparison of theoretical and experimental work.

Figure 3.5 shows the relationship of the experimental data and theoretical calculation on the thermodynamic AR at 30 ^{0}C. Some of the experimental plots in Figure 3.5 lie on top of each other (cow dung and glucose) as the heat and work requirements were similar therefore there are four points instead of the two that are visible. These experimental results are compared to the theoretical data in Figure 3.5, assuming the experimental substrates (cow dung and dog faeces) had the same structure and thermodynamic properties as that of glucose. The assumption is also because the first stage of the AD process (hydrolysis) converts the main elements of biomass into simple sugars; ($C_6H_{12}O_6$) one of which is glucose. Also, we have thermodynamic data of G for glucose, with no data for the biomass material used. The results show that experimental data lie towards the region that minimise G at 30 ^{0}C. This, therefore, suggests that the bacteria operate so as to minimise G in the AD process.

Biogas production is a biological process. Hence, the process is dependent on bacteria. If one wants to obtain a greater concentration of a specific product like H_2 or CO, specific bacteria that produce H_2 or CO only, must be chosen so as not to compete with the methanogen bacteria. Furthermore, it would need a lot of heat from the environment. Also, some of the gases produced may dissolve in the liquid water depending on their solubility at 30 ^{0}C although in very small quantities. This is difficult to analyse in the biological system. Therefore, the overall concentrations recorded at the end of the experiment were used without considering solubility. This is because it was assumed that the small amount of water used (250ml) was saturated at the initial production stages. Considering that the solubilities for CO_2, CH_4 and H_2 at 30 ^{0}C (101.325 kPa) expressed as a mole fraction are $5.41 \times 10^{-4}, 52.346 \times 10^{-4}$

and 1.377×10^{-5}, Gevantman (2003) respectively and that the process was run for a long time, the quantities of gases dissolved may be neglected in favour of the amount produced.

It is hypothesised that in a system with a consortium of bacteria, the bacteria that can get the system to the minimum G and release the most work will typically grow more cells and dominate eventually. This may not be a single species but could be a set of bacteria where each can benefit from the products of the previous one. The results also suggest that the drivers in biology are to minimise G and if one has a consortium of bacteria and leave things to develop, the set that minimise G dominates. This result is very important to consider when designing digesters for anaerobic processes. If some consortia of bacteria are present in the digester, the specific set of bacteria that can, in the end, minimise G may tend to dominate. In this case, the methanogen bacteria that produce CH_4 will usually dominate those that produce H_2. Other bacteria may still be present in the digester but the set that can get to minimum G have the most available free energy to work with and will tend to dominate.

While the actual result from the AR shows that there will only be CH_4 and CO_2, we can see that the experimental results also show production of a significant amount of H_2. However, the presence of the H_2 hardly affects the position of the minimum on the diagram and this suggests that the effect of mixing could play a reasonable part in determining the final composition. It is probably not worth pursuing this point further at this stage considering the absence of the correct G and H for the feed substrate.

3.4. Summary

The work has investigated the relationship between thermodynamics and a biological process (AD). The results show the AR of AD for biogas production on the G-H AR. The results suggest that it is both thermodynamically and experimentally feasible to make CO_2 and CH_4 within the temperature range 30 ^{0}C. CO_2 and CH_4 are produced at minimum G at 30 ^{0}C and their production is driven by thermodynamics. The experimental findings at 30 ^{0}C lie towards the minimum of G, which suggests that a consortium of bacteria tends to operate to minimise the G under anaerobic conditions. Comparing this thermodynamic result to experimental data is an important finding because it shows that the activity of living organisms is also driven and limited by thermodynamics. This suggests that in a consortium of bacteria, the bacteria with the greatest driving force will achieve the products at the global minimum G. This also means that the graphical technique (G-H AR plot) used in this study is an important process synthesis tool and can be used in the design of other biological process systems.

References

1. Daniels L., Fuchs G., Thauer R. K., Zeikus J G., 1977. Carbon monoxide oxidation by methanogenic bacteria. Journal of bacteriology, Vol. 132(1), pp. 118–126.
2. Gevantman L. H., 2003. Solubility of selected gases in water. CRC Handbook of Chemistry and Physics. Elsevier Science B.V., Amsterdam pp. 82–83.
3. Guillaume B., Keith J., Annie G., Jonathan C., Vincent T., Anne-Catherine L., Gerard F., 2012. Methanobacterium lacus sp. nov, isolated from the profundal sediment of a freshwater meromictic lake. International Journal of Systematic and Evolutionary Microbiology, Vol. 62, pp. 1625–1629.
4. Kalyuzhnyi S V., Davlyatshina M. A., 1997. Batch anaerobic digestion of glucose and its mathematical modelling. I. Kinetic investigations. Bioresource Technology, Vol 59. Pp. 73–80.
5. Li M., Hu S., Li Y., Shen J., 2000. A hierarchical optimization method for reaction path synthesis. Industrial & Engineering Chemistry Research, Vol. 39(11), pp. 4315–4319.
6. Muvhiiwa R. F., Chafa P., Chitsiga T., Chikowore N., Matambo T., Low M., 2016. Effects of temperature and pH on biogas production from cow dung and dog faeces. Africa Insight Special Issue: Renewable Energy Transition under Climate Change and Green Economy in Africa: Science-policy and risk-opportunities interface, Vol. 45(4), pp. 167–181.
7. Muvhiiwa R., Hildebrandt D, Matambo T, Sheridan C., Glasser D., 2015. A Thermodynamic Approach Towards Defining the Limits of Biogas Production, American Institute of Chemical Engineers AIChE Journal, Vol. 61(12), pp. 4270–4276.

8. Nozhevnikova A. N., Simankova M. V., Parshina S. N., Kotsyurbenko O. R., 2001. Temperature characteristics of methanogenic archaea and acetogenic bacteria isolated from cold environments. Water Science Technology, Vol. 44(8), pp. 41–8.
9. Uniwersytet Wroclawski., 2017 http://metanogen.biotech.uni.wroc.pl/ [Accessed 03 Feb 2017].
10. Werner U., Stoehr U., Hees N., 1989. Biogas plants in animal husbandry. German Appropriate Technology Exchange (GATE) and German Agency for Technical Cooperation (GTZ) GmbH.
11. Zinder S H., Anguish T., Cardwell S C., 1984. Effects of Temperature on Methanogenesis in a Thermophilic (58^0C) Anaerobic Digestor, Applied Environmental Microbiology, Vol. 47(4): pp. 808–813.

Chapter 4: Study of the effects of temperature on syngas composition from pyrolysis gasification of wood pellets using a nitrogen plasma torch reactor.

The results of this chapter have been published in the Journal of Journal of Analytical and Applied Pyrolysis and is cited as: **Ralph Farai Muvhiiwa*.,** Baraka Sempuga., Diane Hildebrandt., Jaco Van Der Walt., 2018. **Study of the effects of temperature on syngas composition from pyrolysis of wood pellets using a nitrogen plasma torch reactor.** *Journal of Analytical and Applied Pyrolysis*, Vol. 130, pp. 159-168.

This is completely my work, I did all the experimental work and theoretical calculations. My supervisors provided guidance in the writing of the paper.

Abstract

This work shows work flows supported by experimental work to analyse the efficiency of a plasma system in biomass conversion processes. The most common set of problems encountered when using biomass-to-energy (BTE) processes relate to tar formation and product gas composition. However, using plasma technology to convert biomass provides a solution because it unlocks more energy than can be achieved by other BTE systems by using a heat supply derived from electricity. The research presented in this paper focuses on the conversion of biomass to chemical energy (in gaseous form) with the aid of the electrical energy supplied by a water-cooled nitrogen plasma torch. The authors conducted a series of experiments in a pyrolysis gasification set up in which wood pellets were converted to syngas in a small-scale laboratory nitrogen plasma torch reactor with a maximum power supply of 15 kW. The efficiency of the process was measured in terms of the carbon conversion to all product gases which changed from 43 % to 77 %, at temperatures ranging from 400 ^{0}C to

1000 ^{0}C respectively. The combined CO and H_2 mole composition in the product gas (without N_2 and H_2O) was 86 % at 1:1 ratio for all temperatures studied. Syngas yield increased with increase in temperature. The overall biomass conversion obtained increased from 46 % to 82 % for the temperatures 400 ^{0}C to 1000 ^{0}C respectively, with the balance comprising carbon-rich solid residue and liquid. The work flow shows that a plasma system can get to high temperatures, but work is also degraded in the overall process. Exergy analysis shows that the work lost by the overall process decreases with increase in process temperature.

4.1. Introduction

Plasma technology makes it possible to decompose biomass through pyrolysis in order to produce high quality syngas which is a blend of CO and H_2 gases (Argon et al., 2016). In this process, the plasma supplies all the energy needed for pyrolysis resulting in no energy from combustion required for the decomposition of the biomass material. Syngas is produced from the C, H and O elements that are present only in the biomass material, without the need to add any oxidising media (Fabry et al., 2013). Because no extra oxygen is added to the process, the product gas perhaps contains less CO_2, and this results in high calorific value of the syngas produced. According to a model by (Schuster et al., 2001), the O_2 content of biomass has a considerable influence on the chemical efficiency of the biomass conversion system. However, the authors attribute temperature as the strongest effect on chemical efficiency.

Another notable difference between the use of plasma and conventional pyrolysis processes is that the gas produced by the latter is usually contaminated with tars and has therefore to be cleaned before being sent on for downstream processing. Also,

tars are abrasive and increase the maintenance cost of conventional systems. Plasma reactors, on the other hand, can make the gas cleaning process unnecessary as the high temperatures and high heating rate they can achieve are not reliant on a combustion process but produce clean syngas with a high calorific value (Fabry et al., 2013; Je Lueng Shie et al., 2010). The biomass plasma process is also more efficient than the combustion method of BTE because it helps to convert the chemical potential in the solid feed to syngas. This reduces the chemical potential that remains in the solid chars after pyrolysis which in turn results in a higher chemical energy output in the syngas (Fabry et al., 2013).

In the pyrolysis process, thermal decomposition, reforming, water gas shift (WGS) reactions, recombination of radicals and dehydrations can occur as functions of the residence time, temperature and pressure profile (Mohan et al., 2006). For instance, syngas can be used for power generation via a turbine, and as feedstock to produce synthetic liquid fuels in the Fischer-Tropsch (FT) process.

The advantage of using a plasma reactor is that the plasma torch is an independent and direct heat source. This allows the controlling of the reactor temperature independent of fluctuations in the feed quality and also the use of possible different reactants (Lemmens et al., 2007). This is different from the case in some conventional processes where the reactor is designed for a certain feed where the calorific value of the feed materials is required for the heat source (Van Oost., et al., 2009). The analysis made by Lapuerta et al., 2008 and his team indicated that the influence of the reaction temperature on the gasification characteristics was not as significant as that of the biomass/air ratio for conventional biomass processes.

The possible feed rate is determined by the plasma power available for biomass pyrolysis. Conversely, this power requirement is affected by the amount of moisture in the biomass material. Usually, plasma systems for biomass conversion processes are operated at temperatures higher than 900 ^{0}C in order to produce syngas with a low CH_4 content. In addition, high pyrolysis temperatures are required for thermodynamic and kinetic reasons (Fabry et al., 2013). Hence, there is little scope for use of catalysts in gasifiers (Higman and Van der Burgt., 2008; Han and Kim., 2008).

The energy efficiency of biomass gasification processes varies from 75–80 %, depending on the composition and heat capacity of the raw material (Edbertho Leal-Quir´os., 2004). Some researchers have carried out some modelling and simulations using Gibbs Energy minimization to compare the energy efficiency of the plasma process to the conventional air gasification process (Janajreh et al., 2013). The authors recorded that the average plasma efficiency was 42 % compared to 72 % for the conventional method for converting biomass, oil shale, tire and coal to syngas (Janajreh et al., 2013). This was due to the high energy supplied to the plasma system when air or steam are used as plasma gas. In addition, a model by Schuster et al., 2001 shows that a net electric efficiency of about 20% can be achieved in a plasma system. According to Fabry (2013) and his colleagues, gasification by thermochemical decomposition of biomass material produces syngas in which one can recover up to 80 % of the chemical energy contained in the organic matter initially treated. (Hrabovsky., 2011) showed that a gas composition containing a high concentration of CO and H_2 can be achieved at temperatures above 900 ^{0}C with an argon plasma. At even higher temperatures, the composition of CO and H_2 obtained from plasma

gasification of dry wood biomass remains fairly constant at 0.42 and 0.55 respectively (Hrabovsky., 2011). The increase in temperature favours the Boudouard reaction. Hence, it increases the CO/CO_2 ratio which raises the heating value of syngas (Lemmens et al., 2007). It has also been shown through Aspen simulations that a high Equivalence Ratio (ER) reduces H_2 production while a high Steam-to-Biomass Ratio (SBR) increases H_2 production (Favas et al., 2017) The latter authors have further shown that the Lower Heating Value (LHV) of the product gas decrease with increase in ER and SBR but increases with temperature. Another simulation in Aspen shows that temperature increases production of CO and H_2, while increasing ER decreases both the syngas production as well as the Cold Gas Efficiency (CGE) (Ramzan et al., 2011). (Hlina et al., 2014) carried out experiments on wood pellets using a water-argon DC plasma arc and obtained a LHV of 157.4 kWh/kg for syngas from a feed of wood pellets with LHV of 145.1 kWh/kg. The latter authors also attributed the overall low energy efficient of the plasma system to the electricity energy requirement (100-110 kW) despite having obtained a syngas composition of 90 % by volume. The results by (Je-Lueng Shie et al., 2008) shows that the overall syngas yield increased with temperature on plasma pyrolysis of sunflower oil cake and that CO and H_2 have equal volume fractions of ~49 % at 600 ^{0}C. Research has shown that the amount of product gas during pyrolysis can reach up to 80 % of the feed mass Huang and Tang (2007). The syngas produced can reach up to 94 % by volume of the total gas produced from plasma pyrolysis of rice straw biomass using nitrogen as a carrier gas in a batch process (Je Lueng Shie et al., 2010). A maximum C and O_2 conversion of 79 % and 72 % was obtained respectively from pyrolysis of wood and rice husks using an argon/hydrogen plasma system (Zhao et al., 2001).

According to (Hrabovsky., 2011), all C and H atoms from biomass material can be converted into syngas, provided the biomass is heated to a sufficiently high temperature. (Higman and Van der Burgt, 2008) reported that the temperature ranges at which all volatile matter of any biomass material is converted to synthesis gas are around 800–900 ^{0}C. At temperatures higher than 800 ^{0}C, soot formation begins to compete with oxidation processes. Gasification at higher temperatures also prevents the production of higher hydrocarbons (Hrabovsky et al., 2009). However, standard gasification technologies operate the reactor in the 400–850 ^{0}C range (Mountouris et al., 2006). These low temperatures cannot break down all the biomass materials. Hence the product at low temperatures constitute of tars that are difficult to remove and also other contaminants that must be further cleaned. The char residue is up to 15% of the weight of the feed material and must be disposed of in a landfill (Mountouris et al., 2006). Tar form when a reaction occurs between a heated carbon source and a limited amount of oxygen (Hraboskvy., 2011). However, when a plasma pyrolysis system is used, the extreme temperature of the plasma tail-flame which gets in direct contact with the feed materials inside the reactor also prevents tars and other long chain carbon compounds from forming.

This explains the investigation into the results of increasing process temperature that forms the basis of this research paper. The prerequisite for the experiments was to use a plasma reactor to reach higher temperatures (above 800 ^{0}C) at which equilibrium is reached (Ngubevana et al., 2010) and compare the results with that of lower temperatures. The work presents experimental results obtained from a small-scale nitrogen plasma reactor with a power range of 1.8 to 15 kW and a water-cooled plasma torch. Electricity was used to supply energy to the process. Wood pellets were

converted via pyrolysis in a nitrogen plasma reactor at temperatures 400 ^{0}C, 600 ^{0}C, 800 ^{0}C and 1000 ^{0}C and the yields of gaseous, liquid and char products for each temperature were compared. Most of the research that is available in this field has been carried out on steam/argon plasmas (Agon et al., 2016; Hlina et al., 2014; Van Oost., et al., 2009). Steam contains hydrogen and oxygen that may also take part in the reaction to make syngas while argon is chemically inert. However, in this study, a pure nitrogen plasma in a continuous system was used. This was due to its higher enthalpy as it can achieve a higher temperature compared to an argon/steam plasma for the same current input. For this reason, a lower current setting can be used to reach the desired power input. Various researchers have expressed the opinion that at a lower current, electrode erosion is minimised due to a lower current density on the arc attachment points, which extends the lifespan of the electrodes (Szente et al., 1992; Mikimasa and Masatoyo, 1998). For this reason, also, a nitrogen plasma was chosen for this study. According to a critical review by (Gomeza et al., 2009), economic and socio-political drivers are encouraging the adoption of using plasma conversion processes as compared to alternative waste treatment/disposal options.

4.2. Process materials and experimental method

4.2.1. The plasma reactor system

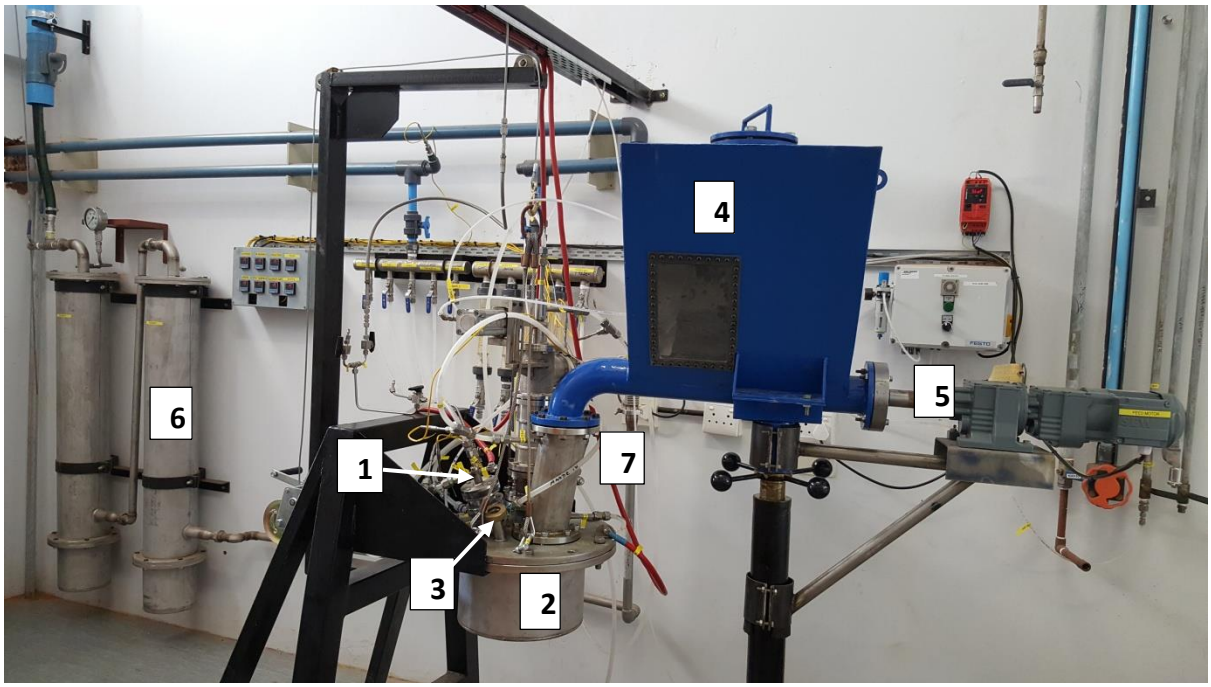

Figure 4.1: View of the laboratory plasma reactor system used for the experiments.

The plasma system shown in Figure 4.1 constitutes a water-cooled, DC, non-transfer arc, thermal plasma torch **(1)** with copper electrodes mounted on top of a reactor chamber **(2).** The reactor chamber volume is ~1.63 L and is made of a 25 mm thick ceramic wall. Silica sand fills the 40 mm thick gap between the side of the ceramic wall and the outside steel casing to reduce heat loses. The top part of the reactor chamber is covered with a ceramic crucible lid 25 mm thick with holes to accommodate only the plasma torch, feed inlet and product outlet sections, a view port **(3)** and a type R thermocouple. A feed hopper **(4)** with a nominal capacity of 96.4 L and fitted with a variable speed screw conveyer **(5)** transports the feed into the plasma reactor. In addition to this, a 15-kW max DC power supply (Jeenel Technology Services), double annulus solid-liquid quench heat exchanger and two Gortex blow-back gas filters **(6)**

forms part of the system. The torch, comprising a copper anode and cathode, is water-cooled and is positioned on the top flange of the reactor chamber. Water is also used to cool the quench probe and the feed inlet pipe **(7)** leading to the reactor chamber. These cooling circuits are used to measure heat losses of the system. The plasma torch power was varied by changing the current setting as well as the nitrogen flow rate. A high nitrogen mass flow rate (1.5 to 2.1 kg/h) at 4 bars was used as plasma gas and ensured good mixing in relation to the small reactor volume. The nitrogen plasma was used to elevate the reactor temperature to the desired value and due to the small reactor chamber size, it was assumed that the reactor temperature was uniform. The current was varied between 80 and 140 amperes (A) to give plasma power between 11 kW-13 kW and the system was operated at a slightly negative pressure (-5 kPa) to that of atmospheric pressure. Argon gas was used to start the plasma and the plasma gas was gradually changed to nitrogen before feeding commenced. A simplified process flow sheet of the plasma system used in this study is shown in Figure 4.2.

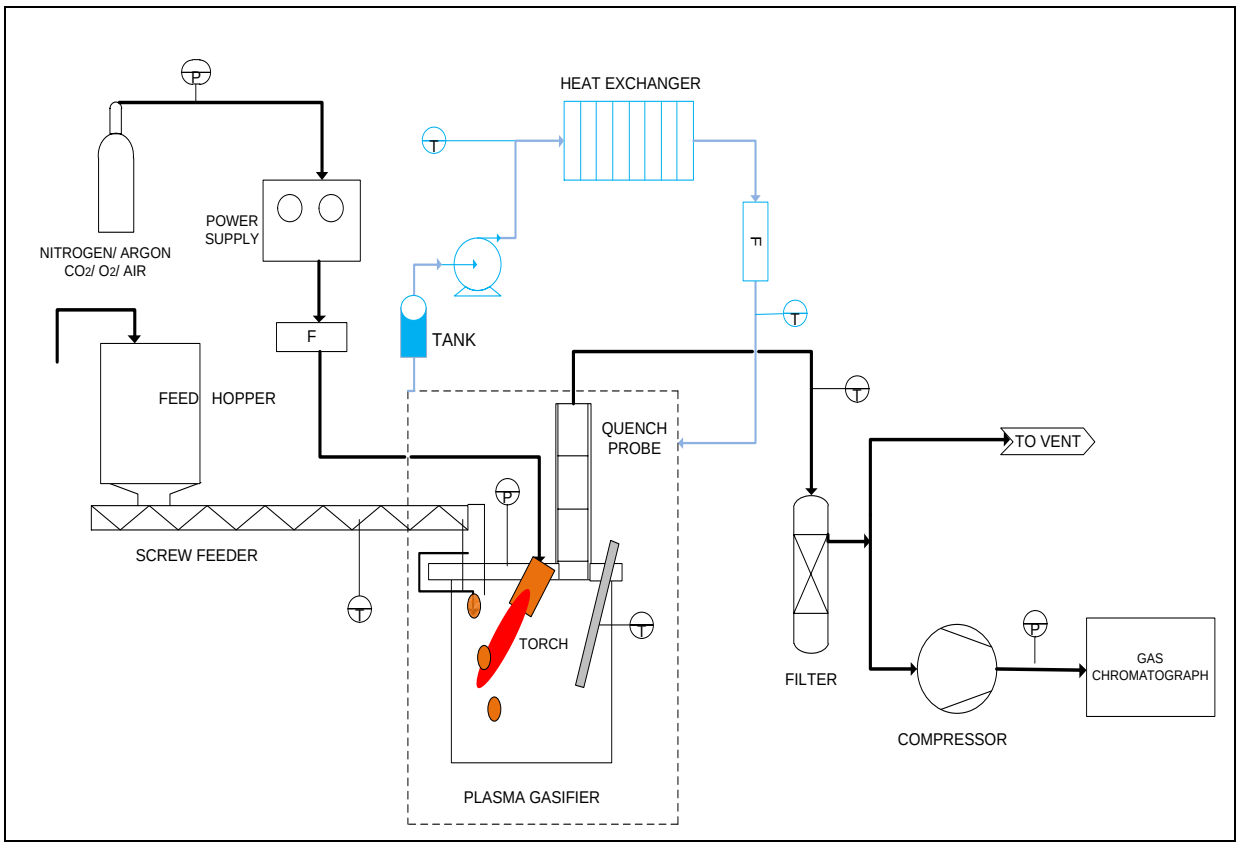

Figure 4.2: Simplified process flow sheet for the laboratory plasma system used for pyrolysis of wood pellets.

4.2.2. Process parameters and procedure

Two experiments were conducted for each temperature studied and the results were compared. The reactor was gradually heated to the desired temperature. The temperature inside the reactor was left to rise to about 50 ^{0}C above the desired temperature before feeding began. Wood pellets were fed into the plasma reactor 10 minutes for the reactor temperature to stabilise and for a representative start sample to be taken. Since the feed materials is transferred at a relatively slow, calibrated, continuous manner into the reactor, the reactor temperature could be kept constant with small corrections throughout the experiment. The feed section is designed to make sure that the feed material falls from a distance of about 0.45 m under gravity

directly to the plasma tail flame in the hot reactor chamber where the reaction occurs. A type R thermocouple is placed in the space between the plasma flame and reactor wall and measures the mean reactor temperature while the water-cooling loops are monitored by K-type thermocouples. The electrical current and nitrogen gas flow to the plasma torch were kept constant for each experimental run.

The product gas outlet is situated at the top part of the reactor where gas passes in a double annulus (8 mm thickness) cylindrical quench probe (0.32 m in length) and the gas is cooled from both sides by water to below 60 ^{0}C. The fast cooling process inhibits the formation of NOx compounds. This is because dioxins and furans need sufficient oxygen and time for them to form and plasma conversion systems does not provide this environment for their formation Vishal and Vastal (2016). The gas then flows through two particle filter bags made of goretex cloth (1 m in length and ~0.25 m diameter each) before the pipe splits, one going to the vent and the other is connected to a diaphragm compressor for sampling.

An online Agilent 7890B Gas Chromatography (GC) was used to take samples every 10 minutes for gas analysis and five gas samples were collected per experiment. The total duration of the whole experiment after pre-heating was 1 hr. The GC consists of two Thermal Conductivity Detectors (TCD) and one Flame Ionisation Detector (FID) that are calibrated to measure the relative concentrations of CO, H_2, CO_2, CH_4, N_2 and hydrocarbons. After each experimental run, the reactor chamber was left to cool down, flushed with nitrogen, opened for inspection and residues were collected for material balance. The solid residues were collected from the reactor, quench, piping and filter bag were subject to ultimate analysis. A vacuum system was used to collect the solid

residues from the respective units of the plasma system. This was done to try and remove as much solid as possible from the system to try and reduce error measurements of residue between experiments. The solid residues that were collected constitute of both carbon and ash and were not separated. Condensed liquids were only found in the filtering units. This was collected at the bottom chamber of the filter trap and weighed for mass balance analysis. However, the measurement of the liquid mass was not accurate because some moisture was still trapped in the filter bag.

4.2.3. The treated material

Wood pellets, consisting of materials with uniform diameter of 6 mm and varying lengths between 5 mm and 30 mm were fed into the plasma reactor. The differences in the particle length resulted in slight fluctuations in the feed rate using the screw feeder.

A constant mass of 4 kg was loaded into the feed hopper and the residual balance was weighed at the end of the experiment. A fairly uniform motor speed for the feed was maintained during each run. The average feed rate was calculated by weight difference of the feed material before and after the experiment. A constant current setting, plasma gas flow rate and wood pellet feed rate was applied throughout each experiment in order to maintain uniformity. However, the feed rate was varied slightly above and below the actual set rate for a specific temperature. This was done to try and keep the varying temperatures constant. The temperatures were maintained within the error of +/- 20 ^{0}C. More so, the feed rate together with nitrogen flow rate

was changed for each of the temperatures (400 ^{0}C, 600 ^{0}C, 800 ^{0}C and 1000 ^{0}C) studied. Hence analysis was done based on a material balance.

Table 4.1: Calorific value, proximate and ultimate analysis of wood pellets on weight basis, values in brackets are from literature, (Renew., 2004).

Proximate analysis			**Ultimate analysis**	**Calorific value**
(As received)			(dry basis)	kWh/(kg)
Volatile matter	71.59	C	47.7 (48.4)	
Ash	2.44	H	6.04 (6.1)	
Moisture	6	O	43.84 (45.3)	5.18
Fixed carbon	25.95	N	0.234 (0.21)	
-	-	S	Not Det	

The calorific value, ultimate and proximate analysis of the feed is given in Table 4.1. A simple material balance using nitrogen as internal standard has been conducted as shown in Figure 4.3. The nitrogen coming into the reactor is used as plasma carrier gas for the torch. The molecular formula ($C_4H_{6.08}O_{2.75}N_{0.02}$) of the biomass in Figure 4.3 was obtained from the results of the dry ultimate analysis. The calorific value in Table 4.1 was obtained using a model in Aspen called HCOALGEN which is the General Coal Enthalpy Model in the Aspen Physical Property System (Aspen Plus V8.6; Doherty et al., 2013; Zheyu et al., 2012; Fajri et al., 2016). Generally, this method is used for calculating the enthalpy values for biomass and ash and is obtained from coal studies. The wood pellets were classified as non-conventional components and the ultimate and proximate analyses were used for computing the enthalpy of formation. The calorific value (~18 648 kJ/kg) for the wood pellets was obtained by combusting the wood pellets Eq. (4.1), using the estimated molecular formula ($C_4H_6O_3$) and enthalpy (-5 177.8 kJ/kg obtained from Aspen). This was because only

C, H and O atoms were considered during combustion. This was similar to the heating value obtained by (Renew., 2004) for wood that had a similar ultimate analysis.

$$C_4H_6O_3(s) + 4O_2(g) \Rightarrow + 4CO_2(g) + 3H_2O(g), \quad \text{-1903.5 kJ/mol} \qquad \textbf{(4.1)}$$

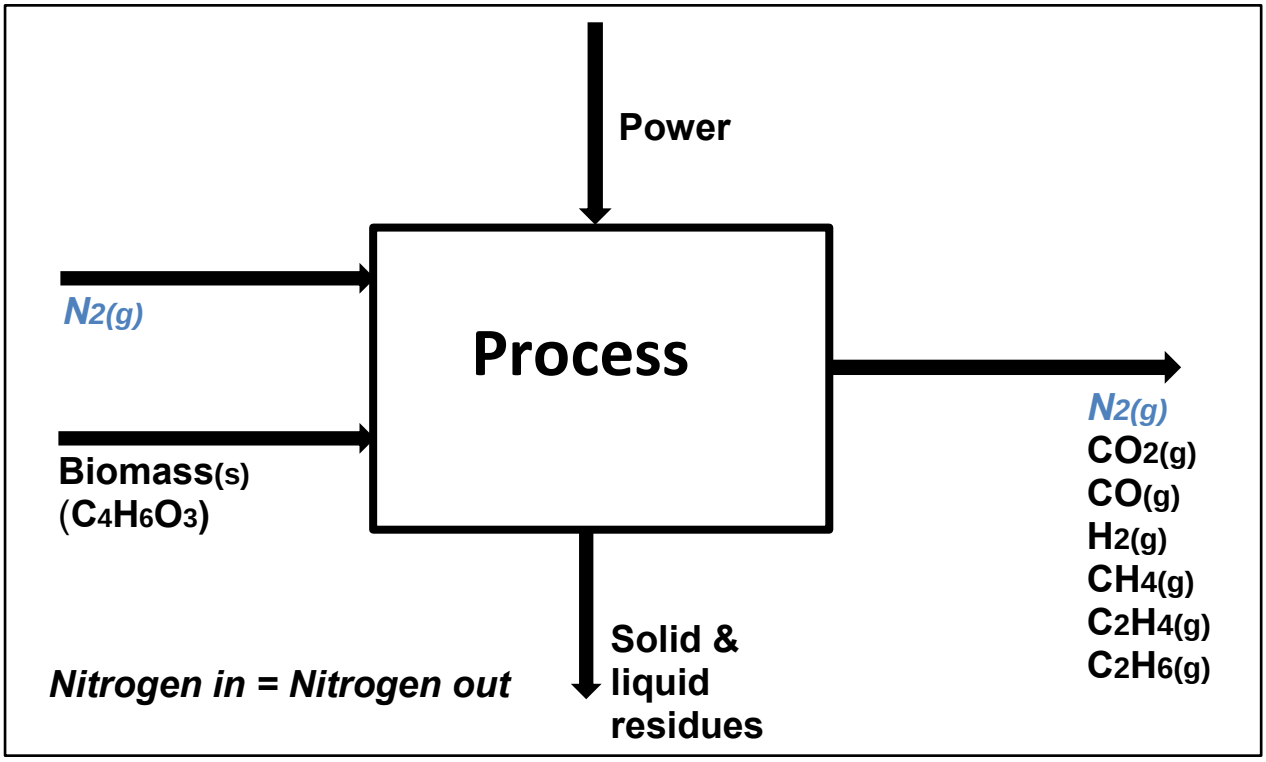

Figure 4.3: Schematic of the process showing a general material balance.

4.3. Results and Discussion

The results show the variations in composition of the product gas stream with temperature. It is assumed that the nitrogen gas supplied to the plasma torch does not take part in the reaction. Hence, nitrogen is used for the calculation of the material balance. Slight variations in gas composition shown in the results obtained may be attributed to inconsistent reactor operating conditions; i.e. slight deviations from the intended temperature as well inconsistent wood pellet feed rate supplied to the reactor by the screw feeding system. This, however, did not have a significant influence on

the results because the five sets of analysis were obtained for each temperature setting and are fairly uniform.

The relative concentrations of CO, H_2, CO_2, CH_4, N_2, C_2H_4 and C_2H_6 were analysed. The molar concentration of the gases observed in the analysis in relation to the calibration gases gave a total mole composition of 0.92, 0.97, 0.98, and 0.94 for pyrolysis at temperatures 400 ^{0}C, 600 ^{0}C, 800 ^{0}C and 1000 ^{0}C respectively. Despite the results not including analysis of water and other small quantities of hydrocarbons produced, the material balance was accurate to between 90 % and 97 % for the temperatures studied. This included the mass of gas produced, solid (biochar) and liquid (water and oils) residues and this was compared to the original mass of wood pellets fed into the process. It is assumed that the balance constitutes other compounds or elements that the measuring method could not account for and this constitutes of lost materials. In the analysis of results, the term product gas refers to all the gases produced from the process while syngas refers to H_2 and CO only in the product gas.

4.3.1. Changes in gas concentration with temperature

Figure 4.4 up to Figure 4.7 shows changes in product gas composition for plasma pyrolysis of wood pellets. For the experiment at 400 ^{0}C, the analysis includes plots of gas composition with nitrogen, Figure 4.4a and without nitrogen, Figure 4.4b. The rest of the temperatures were normalised for nitrogen meaning the plots show composition of the gases excluding that of nitrogen gas. Nitrogen is assumed not to take part in the reactions because of the fast quenching mechanism. Therefore, nitrogen is used as an internal standard. Nitrogen feed flow rate and composition in the product gas is

used to calculate the molar amounts of all other gases produced. The analysis aims to achieve the material balance close to the one in Eq. (4.2) via the pyrolysis process with minimal amounts of other products.

$$\boldsymbol{x}C_4H_6O_3(s) \Rightarrow \boldsymbol{y}H_2(g) + \boldsymbol{z}CO(g) + \boldsymbol{w}C(s) \qquad \textbf{(4.2)}$$

The material balance shows that there is need to add some oxygen to balance the carbon atoms in the feed. However, it is vital to find out how much C is converted to CO using the O_2 already present in the feed when subject to a nitrogen plasma system.

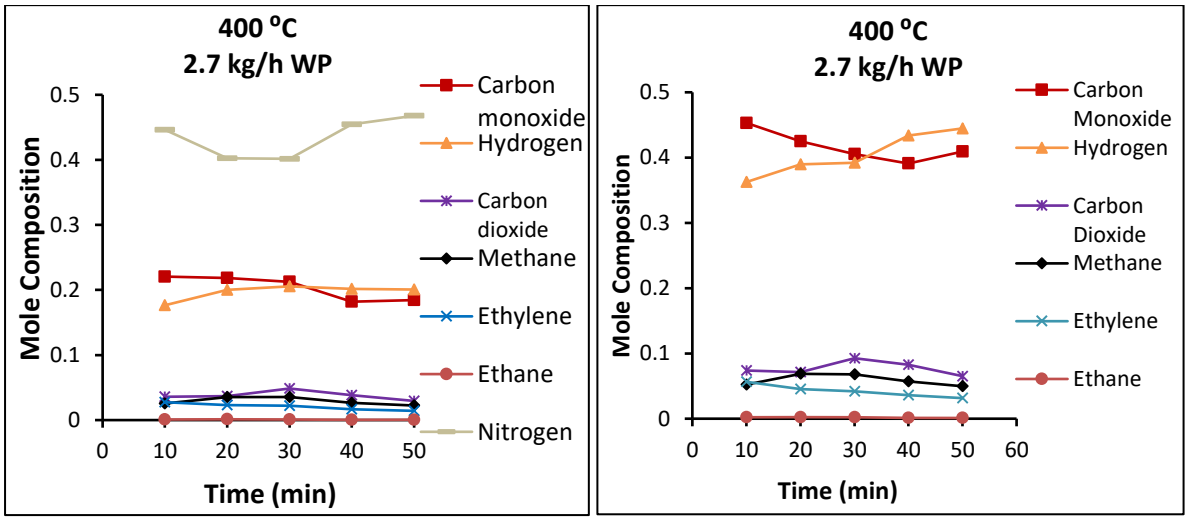

Figure 4.4: Changes in product gas molar composition with time detected in plasma outlet stream at 400 ^{0}C for a feed rate of 2.7 kg/h wood pellets; a) with nitrogen gas composition, b) without nitrogen composition.

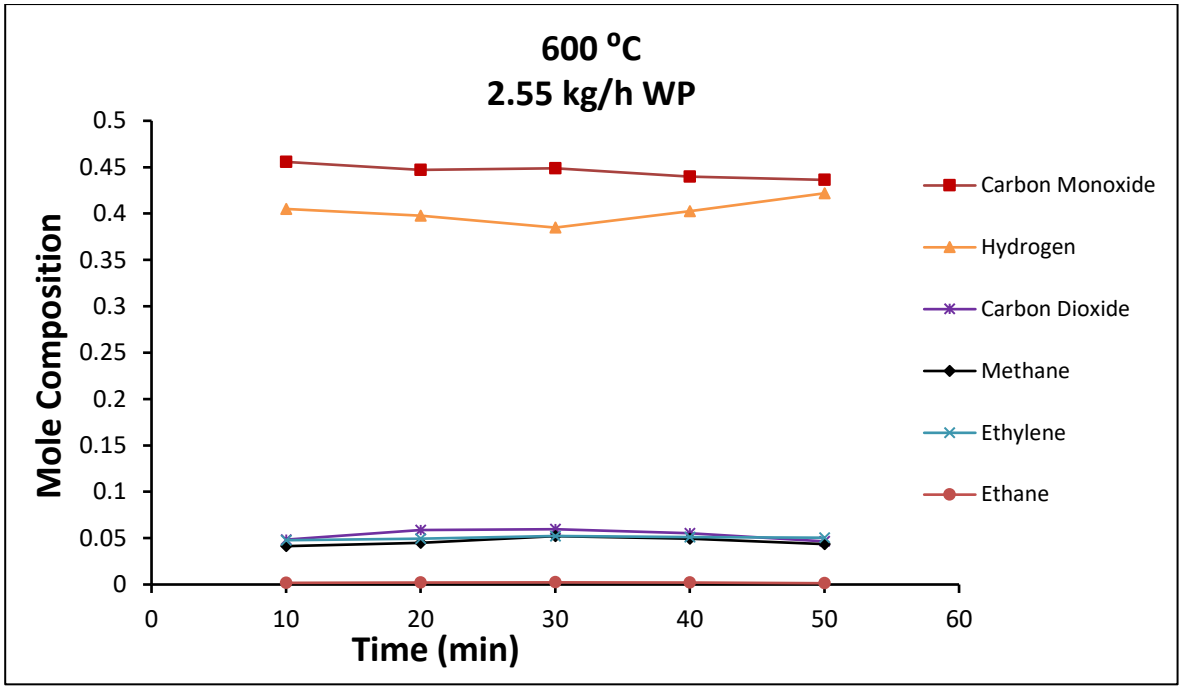

Figure 4.5: Changes in product gas composition with time detected in plasma outlet stream at 600 ^{0}C for a feed rate of 2.55 kg/h wood pellets.

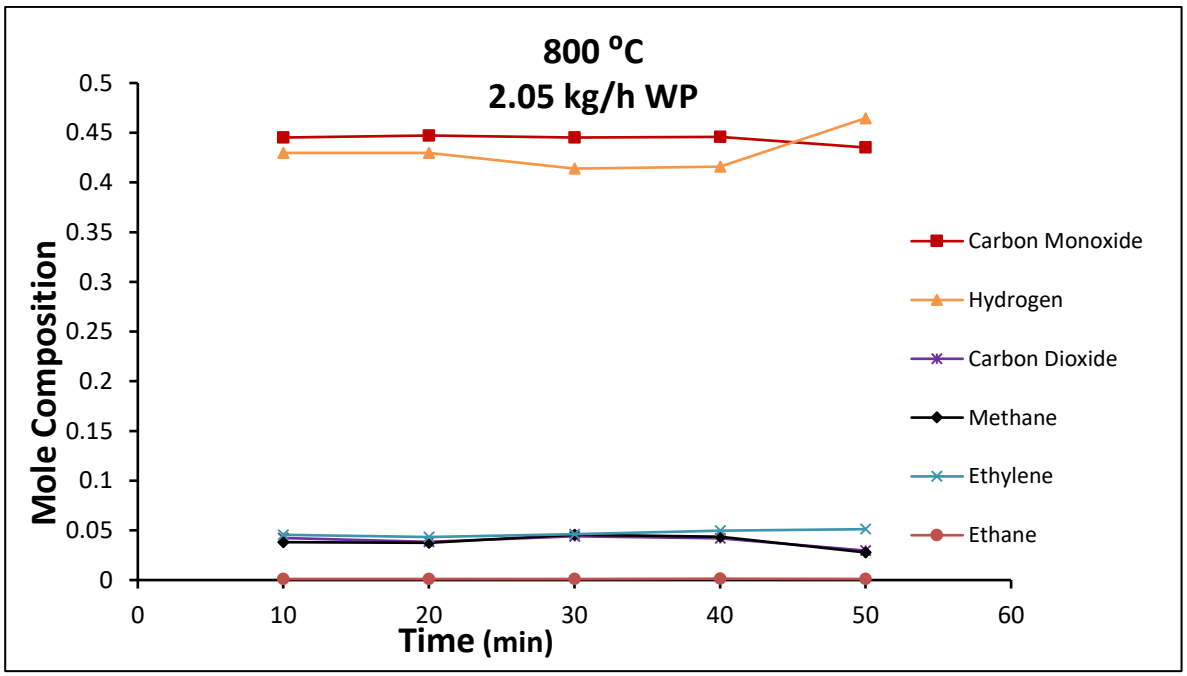

Figure 4.6: Changes in product gas composition with time detected in plasma outlet stream at 800 ^{0}C for a feed rate of 2.05 kg/h wood pellets.

The time to reach a steady state is influenced by nitrogen concentration. Figure 4, Figure 5, Figure 6 and Figure 7 shows that the average steady state is reached after 10 minutes when the nitrogen flow rate was kept constant for each experimental run.

This is owed to the big volume of the filters in relation to the product gas volume. Gas sampling was done after the two filter chambers that are shown in Figure 4.2.

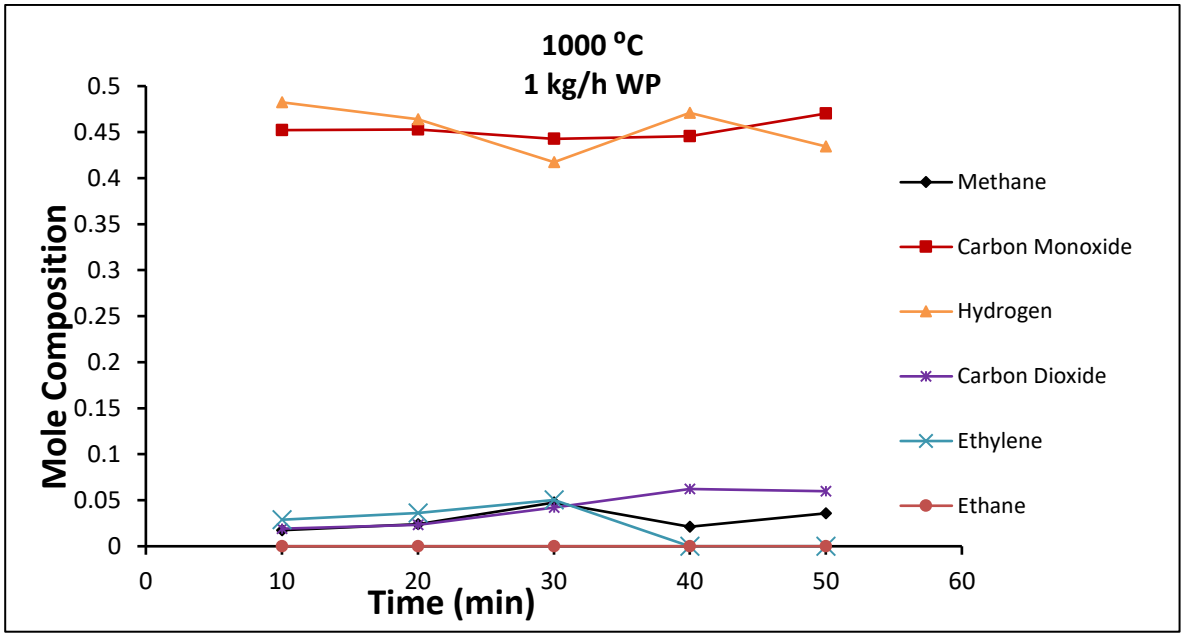

Figure 4.7: Changes in product gas composition with time detected in plasma outlet stream at 1000 ^{0}C for a feed rate of 1 kg/h wood pellets.

There was no ethane produced for the pyrolysis process at 1000 ^{0}C. The results in Figure 4.8 show a plot of the gas composition with temperature. In Figure 4.8, syngas which constitutes a high composition of carbon monoxide and hydrogen in a molar ratio of CO: H_2 of ~1:1 amounted up to 85 mole % of the total gas produced. The results are similar to the study on pyrolysis of sunflower cake using a plasma gasifier by Je-Lueng Shie et al., 2008 who showed that an equal volume fraction of CO and H_2 was obtained at 600 ^{0}C. An average mole composition of 0.425 for H_2 and CO individual content was measured during experiments for the temperatures 400 ^{0}C, 600 ^{0}C, 800 ^{0}C and 1000 ^{0}C investigated. Very low amounts of CH_4, C_2H_6 and C_2H_4 were detected. The mole composition of CO_2 and CH_4 was found to decrease from an average of 0.07 at 400 ^{0}C to 0.04 and 0.03 at 1000 ^{0}C respectively. For the latter

temperatures, the average C_2H_6 and C_2H_4 mole composition was 0.05 and zero respectively.

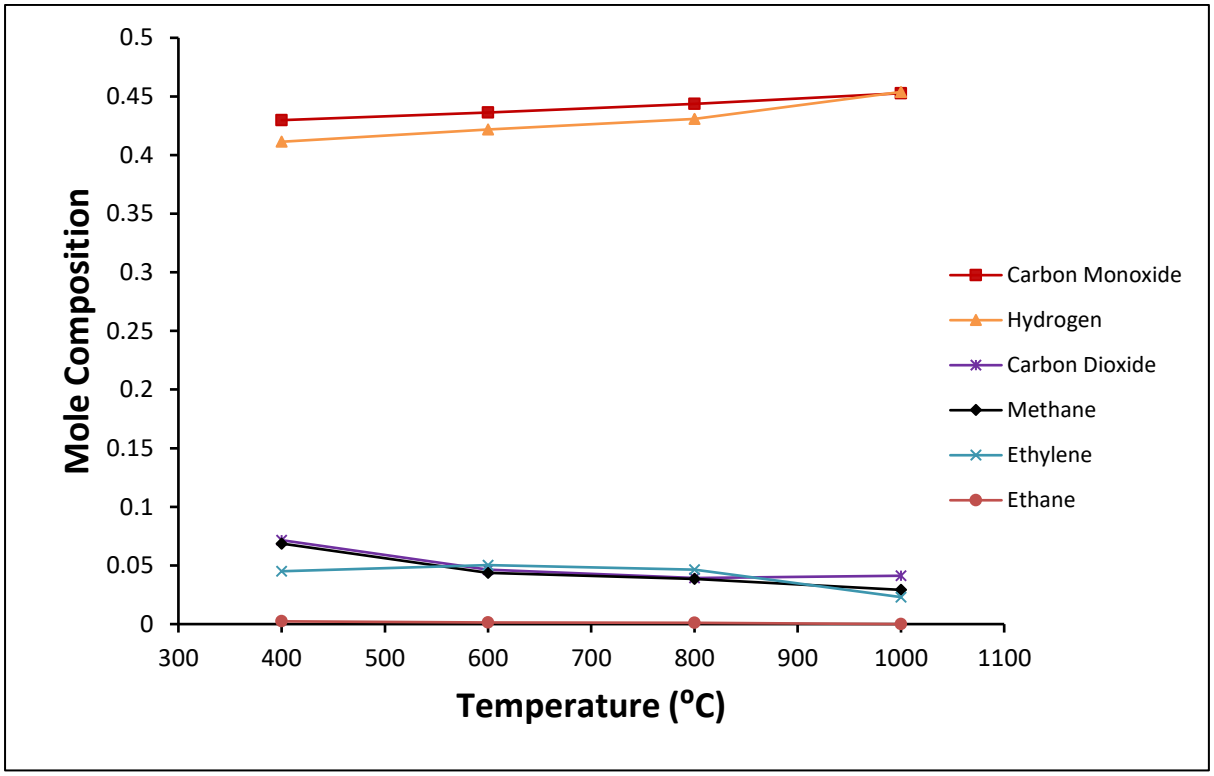

Figure 4.8: Change in the mole concentration of the product gas with temperature.

4.3.2. Biomass conversion

The focus in analysis for the efficiency of converting wood pellets into product gas was centred on a mass basis. In this analysis, syngas is defined to comprise of CO and H_2 gases only.

The biomass conversion is determined using the product yields. H_2 yield is defined by the ratio of the mass of H atoms in the total gas produced per the mass of H atoms introduced in the feed, Eq. (4.3). Carbon yield is the ratio of the mass of C atoms in the gas produced per the mass of the C atoms injected in the feed, (Eq. (4.4)).

However, the yields do not account for the H_2O in the gaseous phase because it could not be analysed by the method used. These ratios are given by the formulas below:

$$\text{H yield} = \frac{\text{H atoms in the product gas}}{\text{H atoms in feed}}, \qquad \text{C yield} = \frac{\text{C atoms in the in product gas}}{\text{C atoms in feed}} \quad \textbf{(4.3; 4.4)}$$

$$\text{O yield} = \frac{\text{O atoms in the product gas}}{\text{O atoms in feed}}, \qquad \text{Gas yield} = \frac{\text{Total gas produced}}{\text{Biomass feed}} \quad \textbf{(4.5; 4.6)}$$

The carbon yield increases from 43 % at 400 ^{0}C to 77 % at 1000 ^{0}C while the hydrogen yield increases from 54 % to 93 % for the respective temperatures as shown in Figure 4.9. The ratio of oxygen atoms in the product gas to the oxygen atoms in the feed gives the overall oxygen yield, Eq. (4.5) which increased from 34 % to 86% for the temperature range 400-1000 ^{0}C. The overall gas yield increased from 30 % at 400 ^{0}C to 82 % at 1000 ^{0}C and is defined in Eq. (4.6). The balance of atoms from the conversion analysis went to form condensate liquid, tars or remained in the solid residues. The conversion at 800 ^{0}C largely resembles the conversion at 1000 ^{0}C. Thus, a further increase in temperature will not have a significant change in the gas composition. This is because the gas composition is dependent on the C, H and O elements present in the feed and also equilibrium state.

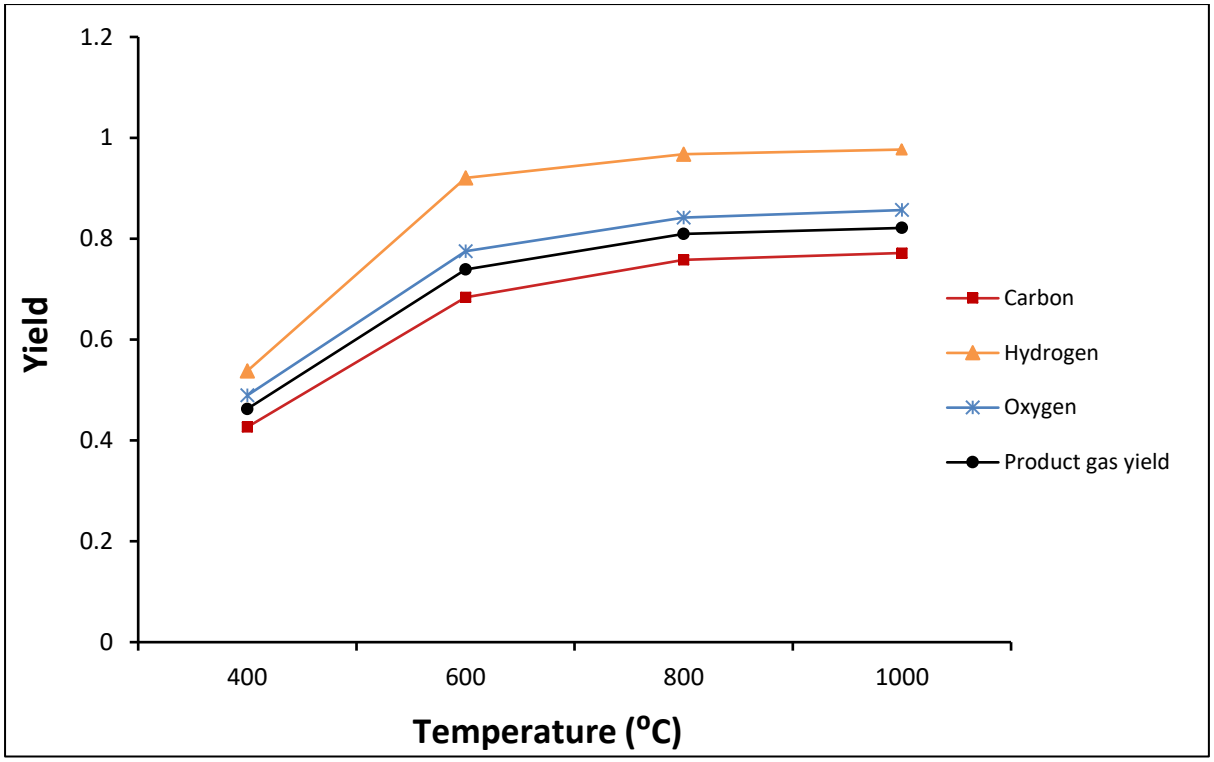

Figure 4.9: Carbon, hydrogen, oxygen and biomass yield to product gases (CO, H_2, CH_4, CO_2, C_2H_4 and C_2H_6).

4.3.3. Carbon (C) and hydrogen (H) efficiency

In biomass conversion processes, the H and C efficiency is an important factor because it provides vital information from a material balance and potential energy perspective. Hydrogen efficiency is defined by the ratio of the mass of H atoms in the hydrogen fraction of total gas produced to the total mass of H atoms introduced in the feed, Eq. (4.7). For the carbon efficiency, it is the ratio of the mass of C atoms in the CO fraction of total gas produced to the mass of the total C atoms in feed substrate, Eq. (4.8). (Argon et al., 2016). The C and H efficiency increases from 27 % - 54 % and 34 % - 62 % for temperatures 400 ^{0}C to 1000 ^{0}C respectively.

$$\text{H efficiency} = \frac{\text{H atoms in the H2 product}}{\text{H atoms in feed}}, \quad \text{C efficiency} = \frac{\text{C atoms in the in CO product}}{\text{C atoms in feed}} \qquad \textbf{(4.7; 4.8)}$$

The syngas yield is defined as the ratio of biomass that went to produce syngas to the total biomass in feed, Eq. (4.9).

$$\text{Syngas yield} = \frac{\text{Biomass to syngas product}}{\text{Biomass feed}}, \quad \textbf{(4.9)}$$

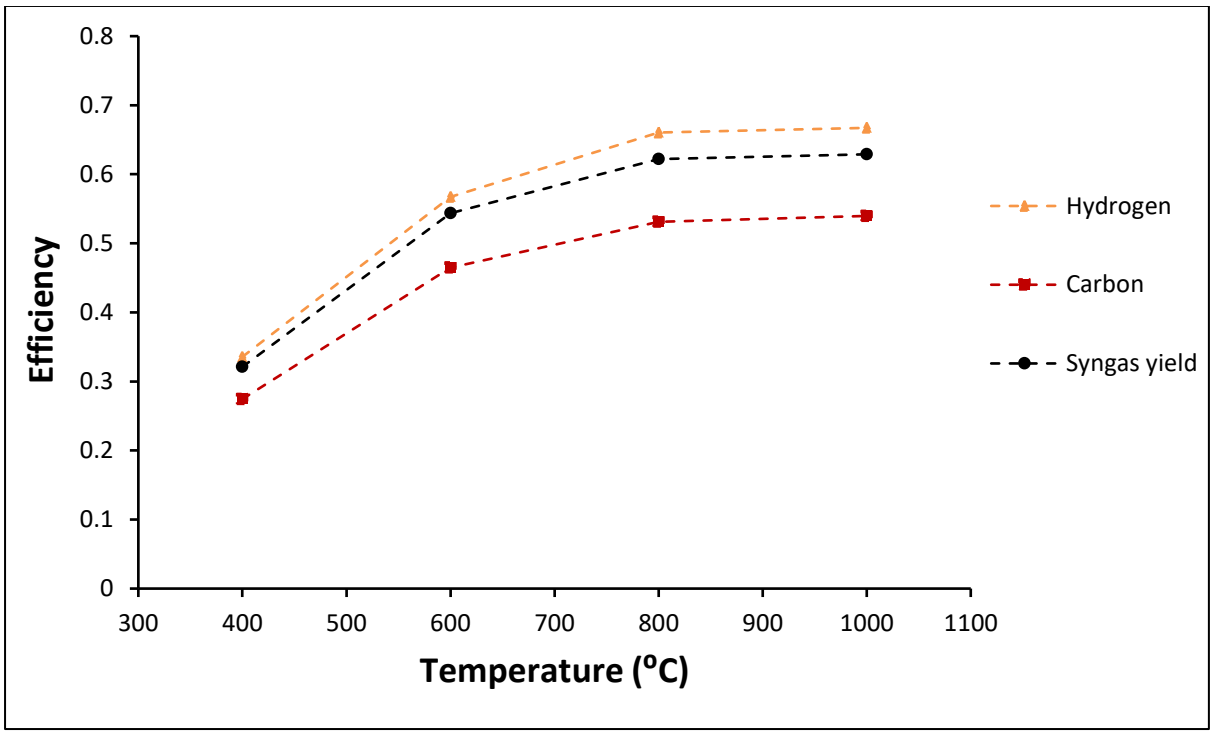

Figure 4.10: H and C efficiency; and syngas yield.

The results in Figure 4.10 show that conversion of carbon, hydrogen and syngas increased with an increase in temperature from 400 ^{0}C to 1000 ^{0}C. The overall syngas yield for the pyrolysis of wood pellets increased with increase in reactor temperature. The results also show that there is an increase of syngas yield from 33 % to 66 % when the temperature is increased from 400 ^{0}C to 1000 ^{0}C respectively. The balance from the syngas yield, which is 31 % and 23 % at the respective temperatures' is accounted for by the CH_4, CO_2, C, H_2O and other short chain hydrocarbons produced. After the pyrolysis processes, the remaining solid residues in the reactor decreased

from 29 % to 14 % at 400 ^{0}C and 1000 ^{0}C respectively of the initial feed. Also, some brown (oily) liquid was formed and this decreased from about 7.5 % of the feed mass for temperatures 400 ^{0}C and 600 ^{0}C to ~0 % at 800 ^{0}C and 1000 ^{0}C. Very small quantities of tars were observed (not quantified) in the process pipelines. The amount of tars observed decreased as temperature for the pyrolysis experiments was increased from 400 ^{0}C to 800 ^{0}C. No tars were observed at 1000 ^{0}C.

4.3.4. Material balance

The analysis for pyrolysis of wood pellets is given by the material balance shown by Table 4.2. The material balances in this analysis are given in moles per hour. The analysis was done per mole of wood pellets fed for all temperatures as shown by Eq. (4.10). The lost mass includes the water vapour that was not analysed, tars produced, small particles remaining on the walls of the pipelines as well as other hydrocarbons formed. In Table 4.2, the lost mass at 400 ^{0}C and 600 ^{0}C includes liquid residues amounting to ~120 g/hr and ~200 g/hr respectively that were measured.

$$C_4H_6O_3(s) \Rightarrow \boldsymbol{a}H_2(g) + \boldsymbol{b}CO(g) + \boldsymbol{c}CO_2(g) + \boldsymbol{d}CH_4(g) + \boldsymbol{e}C_2H_4(g) + \boldsymbol{f}C_2H_6(g) + \boldsymbol{g}(solid) + \boldsymbol{f}(liquid) \quad \textbf{(4.10)}$$

Table 4.2 shows that the amount of syngas produced per mole of wood pellets increases with increase in pyrolysis temperature. The amount of solid residues decreases with an increase in temperature. The large amounts of hydrogen and oxygen moles in the lost mass at 400 ^{0}C and 600 ^{0}C suggest that it constitute mainly of the lost water vapour. At 800 ^{0}C and 1000 ^{0}C the lost mass has small amounts of hydrogen and carbon but a higher amount of oxygen. This may be due to the error

when the molecular formula for the wood pellets ($C_4H_6O_{3(s)}$) was calculated in which the 2.75 moles of oxygen was rounded off to 3 moles.

Table 4.2: Material balance for the pyrolysis process.

T (^{0}C)	(10^{-3} moles/hr)											
	Gas products per mole of $C_4H_6O_{3(s)}$						Solid residue			Lost material		
	H_2	CO	CO_2	CH_4	C_2H_4	C_2H_6	C	H	O	C	H	O
400	1007	1098	184	177	116	7	2140	1107	627	155	1665	907
600	1680	1840	236	208	216	8	1156	520	166	112	376	522
800	1980	2124	199	208	228	4	935	258	90	70	14	388
1000	2053	2086	204	183	265	0	958	178	100	39	78	406

4.3.5. Pyrolysis energy efficiency

Table 4.3 gives a summary for the conversion of wood pellets to syngas. It shows that there is a slight increase in the concentration of syngas as temperature increases. It also shows a slight decrease in the concentration of CH_4, CO_2 and C_2H_6 as temperature is increased. Although there is a slight change in the gas concentration as temperature is increased, the overall biomass conversion shows a significant increase with the same effect. It also shows that as temperature is increased, production of higher hydrocarbons (including C_2H_6) are limited.

Table 4.3: Summary of plasma pyrolysis of wood pellets at different temperatures with energy efficiencies.

	Reactor bulk Temperature (^{0}C)	400	600	800	1000
Input	Current(A)	120	130	131	140
	Voltage(V)	92	93	93	90
	Power(kW)	11.04	12.09	12.18	12.60
	Feed rate(kg/hr)	2.70	2.55	2.05	1.00
	LHV (kWh/kg) Wood pellets	5.18			
Output	[CO] mole	0.429	0.436	0.443	0.452
	[H_2] mole	0.411	0.422	0.431	0.454
	[CO_2] mole	0.071	0.046	0.039	0.041
	[CH_4] mole	0.069	0.044	0.039	0.029
	[C_2H_4] mole	0.045	0.050	0.047	0.023
	[C_2H_6] mole	0.002	0.001	0.001	0
	Solid and liquid residues (kg)	0.9	0.72	0.26	0.14
	Biomass conversion %	46	74	81	82
	LHV (kWh/kg) product gas	2.3	3.8	4.3	4
	Mechanical Gas Efficiency (MGE)	0.44	0.73	0.84	0.77
	Cold Gas Efficiency (CGE)	0.25	0.38	0.39	0.22

The Mechanical Gas Efficiency (MGE) is the ratio between the calorific value of the produced syngas to the calorific value in the wood pellets and is given by Eq. (4.11) (Argon et al., 2016). The net calorific value is the Lower Heating Value (LHV) of a fuel, which is the amount of heat released by combusting a specified amount of it. This assumes latent heat of vaporization of water in the reaction products is not recovered meaning water component of the combustion process is in vapour state at the end of combustion. Table 4.2 shows that the respective MGE increases with the increase in process temperature and typically, the product gas carries about 84 % of the heating value in the feed wood pellets at 800 ^{0}C.

$$MGE = \frac{\text{LHV of product gas}}{\text{LHV wood pellets}} \times 100, \quad \textbf{(4.11)}$$

The energy efficiency of the plasma pyrolysis process studied is reduced by the heat losses at the torch, quench section where the gas is cooled from the respective reactor temperatures to below 60 ^{0}C and losses on the reactor walls to the environment. Although the process produces high quality syngas, the process demands a high heat energy supply from electricity. Subsequently, due to heat losses, the overall efficiency is low and is measured by the Cold Gas Efficiency (CGE) given by Eq. (4.12).

$$MGE = \frac{\text{Chemical energy content in product gas}}{\text{Chemical energy content in wood pellets + electric power supplied}} \times 100 \quad \textbf{(4.12)}$$

The CGE is the ratio between the chemical energy content in the syngas to the sum of the chemical energy in the wood pellets and the electric power supplied by the plasma torch to the process (Argon et al., 2016). However, it must also be noted that not all the energy supplied by the electricity goes into making syngas from wood pellets. Part of the energy supplied is lost by cooling the plasma system and synthesis gas. It also does not account for the energy contained in the remaining biochar or pyrolysis liquid produced and the lost mass. It must be noted that the plasma pyrolysis system used in this study was not designed for energy efficiency. This is reflected in the large heat losses in the plasma torch and the reactor chamber. The results show that the CGE for the temperatures studied are low and are shown in Table 4.3. Despite the decrease in feed rate as temperature increases, CGE increased up to 39 % at 800 ^{0}C. The CGE decreased for the temperature 1000 ^{0}C and this might be due to the reduced biomass feed rate in comparison to increase in heat losses as temperature is increased. In a fairly larger system used by Hrabovsky (2011), the overall energy

efficiency (LHV_{syngas}/ Power supplied) was 0.2 at lower wood saw dust feed rate (6.9 kg/hr) but increased up to 2.3 when feed rate was increased to 47.2 kg/hr. This tells us that small plasma systems are not energy efficient and the efficiency increases with the increase in amount of biomass processed. However, the heat that is lost in the quench section when the gas is cooled from 1000 ^{0}C to around 60 ^{0}C can be recovered and can be used for other purposes. If the system can be redesigned in a process synthesis approach, the heat can be fed back into the system at the expense of extra equipment. This can help improve the CGE of the process.

4.3.6. Heat and work analysis

Figure 4.11 shows the theoretical equilibrium calculation that is compared to the experimental findings from pyrolysis of wood pellets. The measured residual solids and liquids were regarded as carbon and water respectively. Although the experiments were carried out using different nitrogen flow rates at the different temperatures, this does not significantly affect equilibrium. A thermodynamically based simulation of this experimental set up in Aspen Plus using a Gibbs reactor showed that nitrogen flow does not affect equilibrium (shown in Appendix A3). The results show that the pyrolysis process is material balance limited because the products at 1000 ^{0}C show that the amount of syngas produced is dependent on the mass of wood pellets that is fed into the plasma. The experimental results show a trend that is slightly similar to the equilibrium calculation. However, differences may be due to the lost masses that were not accounted for as well as the fact that the solid residues were regarded as carbon in this plot. The atomic balances are shown in Table 4.2. The theoretical plot shows carbon that is formed while in the experimental analysis, the carbon constitutes of carbon formed as well as the unreacted carbon.

Another possible explanation for this is that there might be hot and cold spots within the plasma reactor which create multiple equilibrium spots. In addition, the wood pellets pass directly through the plasma torch flame, which is at a higher temperature as compared to the bulk temperature measured by the thermocouple (shown in Figure 2). This results in the formation of CO and H_2 at the hot spots, which becomes irreversible during the pyrolysis process. Subsequently, the CO and H_2 cannot go back to wood pellets and otherwise form other gases. The material balances in Figure 4.11 were used to carry out the work analysis for the two heat and work cases discussed.

Figure 4.12a and 4.12b shows Gibbs Free energy and Enthalpy lines where each species is zero, to give the shaded region which is termed the thermodynamic AR for pyrolysis of glucose (surrogate for wood pellets) at 400 ^{0}C and 900 ^{0}C. The AR shows the thermodynamically expected products at 400 ^{0}C which are CO_2 and CH_4 while H_2 and CO are anticipated at 900 ^{0}C all at minimum G. This equilibrium prediction is also similar to the one shown in Figure 4.11 where the theoretical equilibrium obtained using a Gibbs reactor in Aspen was compared to the experimental results. The experimental results are in accordance to the AR prediction at 900 ^{0}C but not at 400 ^{0}C.

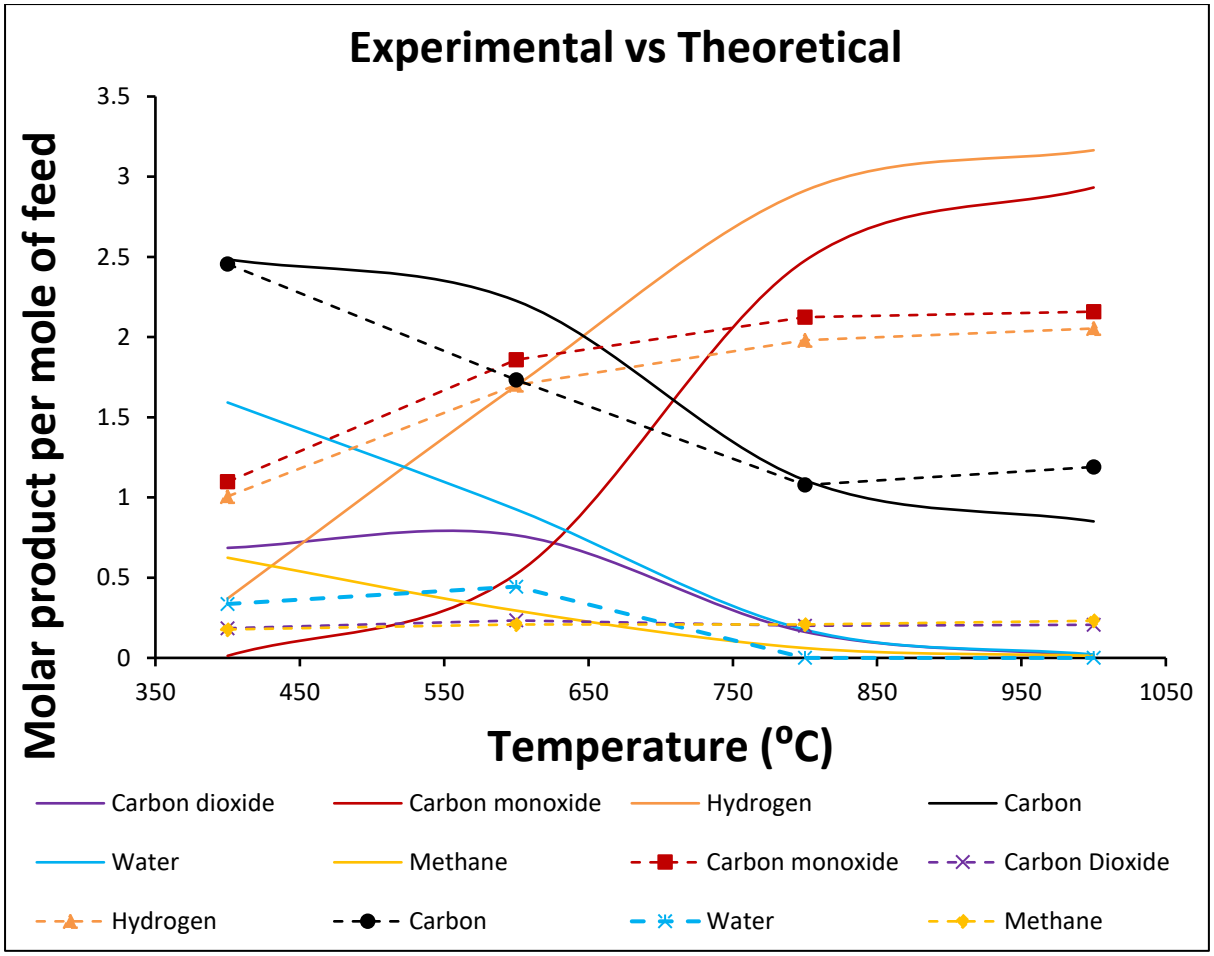

Figure 4.11: Comparison of equilibrium predictions from Aspen simulations (solid line) with experimental data (broken line) from pyrolysis of wood pellets at various temperatures.

The experimental results at 400 ^{0}C shows production of H_2 and CO instead of the predicted equilibrium calculations, which shows CO_2 and CH_4. This may be because carbon was not included in the G-H AR analysis Figure 4.12A while in the real experiment carbon was formed. However, the improved AR in Figure 2.2A where carbon was included still predicts other products of C and H_2O which are not similar to the ones obtained experimentally at 400 ^{0}C. Again, the explanation for this is the assumption that there might be hot and cold spots within the plasma reactor which create multiple equilibrium spots despite the bulk temperature being at 400 C. The AR in Figure 4.12b and Figure 2.3A show similar products to the interpolated experimental

products obtained during pyrolysis at 900 ^{0}C as shown in Figure 11. This shows that temperature has great influence on equilibrium.

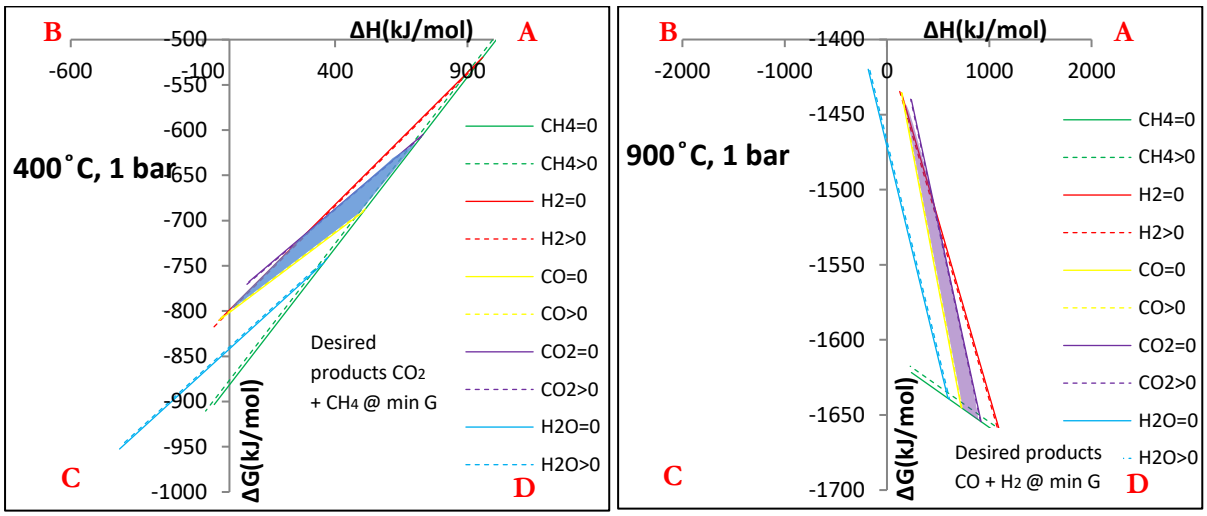

Figure 4.12: AR for pyrolysis of glucose (surrogate for wood pellets) at a) 400 ^{0}C and b) 900 ^{0}C showing expected products at minimum G (Muvhiiwa et al., 2018).

It should be noted that the AR in Figure 4.12 assumes that the feed at 25 ^{0}C and products are all at the reactor temperature. Hence, the calculation for the G and H for the process is at the reactor temperature and this scenario is discussed further in Case 2 below.

Figure 4.13 and Figure 4.14 shows work analysis for the pyrolysis of wood pellets using a nitrogen plasma reactor. The analysis looks at the efficiency of the work that is used to make products rather than the work analysis of the plasma system. The analysis for both cases was subject to the following assumptions

- Gibbs free energy and enthalpy for cellulose ($C_6H_{10}O_{5(s)}$) (Alberty., 1998) was normalised using carbon to relate the thermodynamic data for the wood pellets ($C_4H_6O_{3(s)}$) used.
- Solid residues in the plasma reactor were regarded as solid carbon.

- With reference to Figure 4.11 and Table 4.2, lost mass was assumed to be $H_2O_{(g)}$ only for the analysis at 400 ^{0}C. This means that the amount of water in the experimental data was normalised to be similar to that of the theoretical water calculated at equilibrium.

Case 1- Total energy supplied to heat the wood pellets from 25 ^{0}C to reactor temperature is the same as the total heat removed when the product gases are cooled from reactor temperature to 25 ^{0}C. Also, heat is supplied to the plasma reactor by electricity at the respective process temperatures (400 ^{0}C, 600 ^{0}C, 800 ^{0}C and 1000 ^{0}C) and goes directly into the reaction heat losses. This case assumes a perfectly designed plasma where heat is perfectly integrated into the system without any losses.

The actual work required/supplied to the process for Case 1 is calculated using Eq. (4.13) and Eq. (4.14) respectively and is shown in Figure 4.14. The process temperature is represented by T which is equal to T_{Carnot} when the $\Delta G_{process}$ is equal to the minimum amount of work required for the process to occur and T = T_{bulk} when it represents the actual work supplied. T_o represents temperature at 25 ^{0}C.

$$W_{min\ required} = \Delta G_{(T_o)} = \Delta H_{(T_o)} \left(1 - \frac{T_o}{T_{Carnot}}\right) \quad \textbf{(4.13)}$$

$$W_{actual} = \Delta G_{(T)} = \Delta H_{(T)} \left(1 - \frac{T_o}{T_{bulk}}\right) \quad \textbf{(4.14)}$$

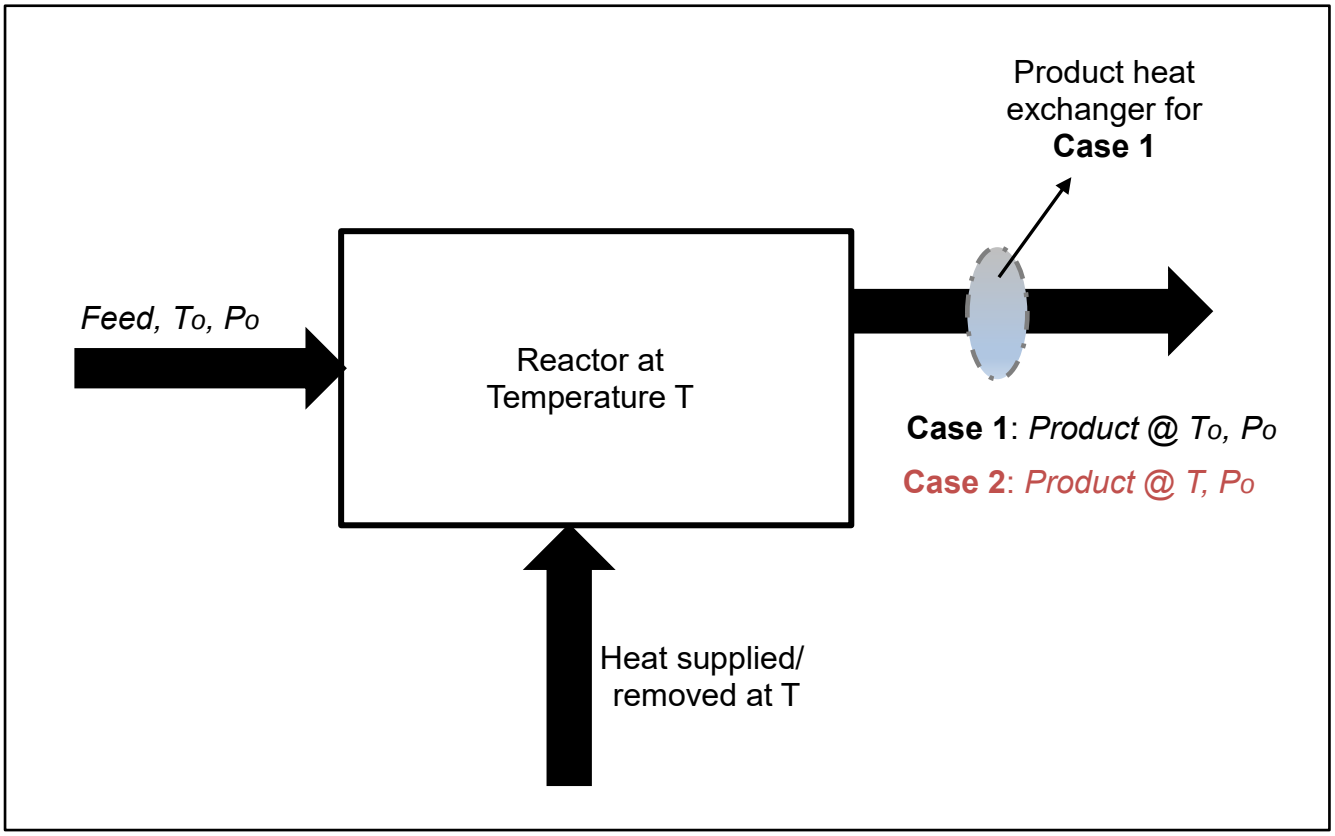

Figure 4.13: Simplified flow sheet for Case 1 and Case 2.

Case 2- The assumption in case one is relaxed. In this case, product gases are considered to leave at the temperature similar to the reactor temperature. This gives a more realistic analysis on what is happening with the plasma unit used. This scenario is shown in Figure 4.15 for exergy analysis.

In Case 2 the minimum work required is given by Eq. (4.15) and actual work supplied is given by Eq. (4.16)

$$W_{min\ required} = \Delta E(T) = \Delta H(T)\left(1 - \frac{T_o}{T_{Carnot}}\right) \quad \textbf{(4.15)}$$

$$W_{actual} = \Delta E(T) = \Delta H(T)\left(1 - \frac{T_o}{T_{bulk}}\right) \quad \textbf{(4.16)}$$

Case 1 and Case 2 are represented in a simplified flowsheet in Figure 4.13.

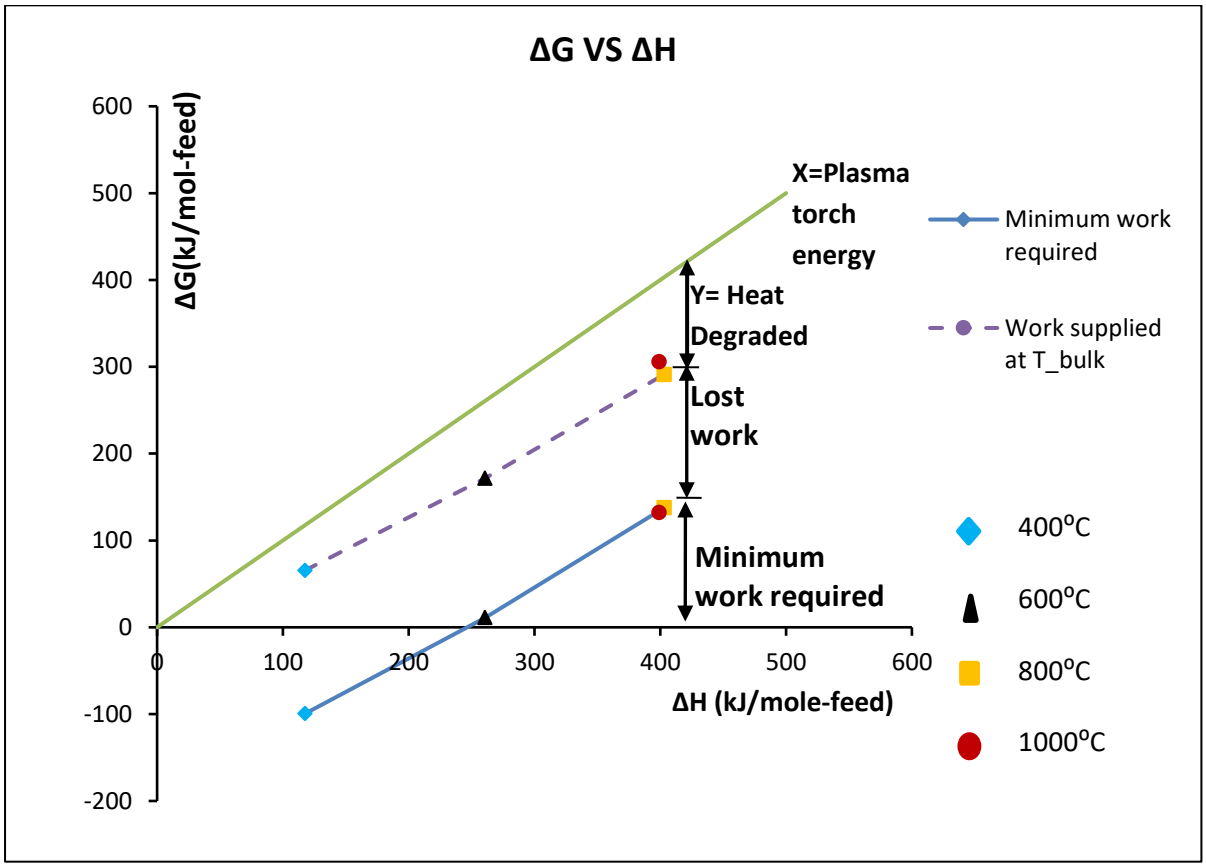

Figure 4.14: Work analysis for the pyrolysis process when all heat losses recovered, Case 1.

Figure 4.14 shows a plot of $\Delta H_{(T_o)}$ and $\Delta G_{(T_o)}$ explained in Case 1 while Figure 4.15 shows a plot of $\Delta H_{(T)}$ and $\Delta E_{(T)}$ explained in Case 2 and analysis is based on the Carnot temperature. The Carnot temperature denotes the temperature at which the minimum work can be supplied to a process to make it happen. In both cases, the temperatures at which we supply heat at to the process are greater than the Carnot temperatures. Thus, the processes are irreversible and will generate entropy. This means more work than required is being supplied via heat from electricity. Alternatively, the processes have potential to produce work. In the pyrolysis of wood pellets, work is not recovered. Hence, work is lost as irreversibility. The work lost is the difference between the Gibbs

Free Energy at the Carnot Temperature (minimum work required) and the work that is supplied to the process at temperature T. The data in Case 1 shows that the lost work averages about 150 kJ/mol for all temperatures studied while 200 kJ/mol of work is lost for Case 2.

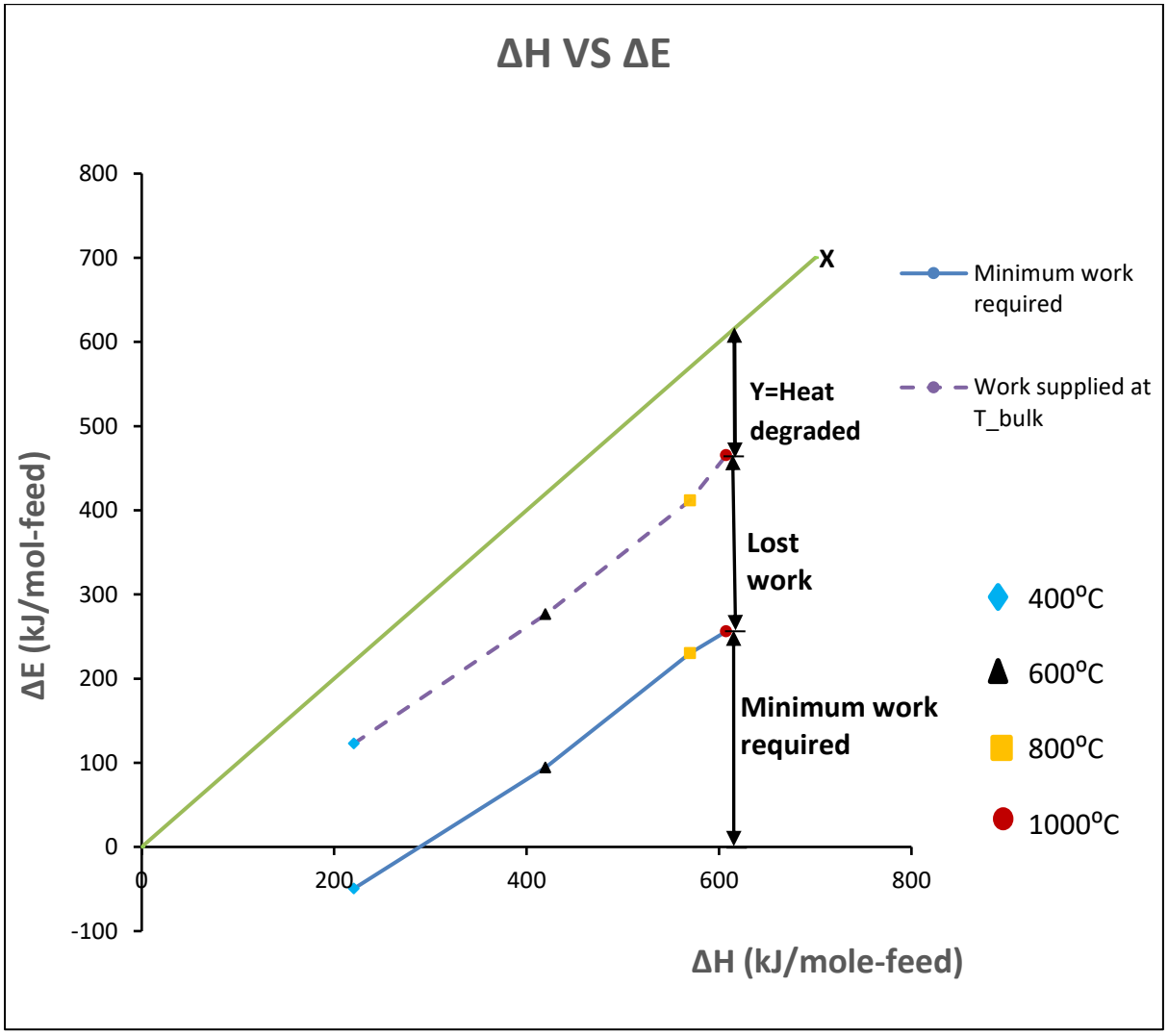

Figure 4.15: Exergy analysis for the pyrolysis process, Case 2.

The amount of lost work is shown in Figure 4.15 for the experiment at 1000 ^{0}C and similar comparison shows lost work for other temperatures. The work lost for the studied temperatures is very much similar to the lost work when an exergy analysis is considered. In all cases $\Delta G<\Delta H$ meaning that addition of minimum amount of heat at

the respective Carnot temperatures can supply the required work. However, the plot also shows that the amount of work lost decreases with increase in temperature. The work analysis in Figure 4.15 has shown that the plasma pyrolysis process is losing work. The work may be lost due to kinetics or when work (electricity) is converted to heat, hence reducing the quality of work via the irreversible process. Alternatively, work loss may be due to the direct running of the plasma at other temperatures other than the bulk temperatures observed. The plasma torch supplies pure work to the process, which is degraded into heat, making it irreversible. The work or energy supplied by the plasma is shown on the 45-degree line labelled X in Figure 4.14 and Figure 4.15 and the heat degraded is represented by Y in Figure 4.14.

It is also important to do a proper comparison of how much work is lost with changes in process temperature at the same time taking into account the amount of products formed. The magnitude of work required will be different due to the different resulting material balances. For a fair comparison of the process performance at different temperatures, it was opted to compare the ratio of the work lost to the minimum work requirement rather than to the magnitude of the work lost, which is highly influenced by the material balance. This analysis will also show us were the relative work loss is highest. Figure 4.16 shows us a plot of T vs $\frac{\text{Lost work}}{\text{Minimum work required}}$ for the scenario in Figure 4.15.

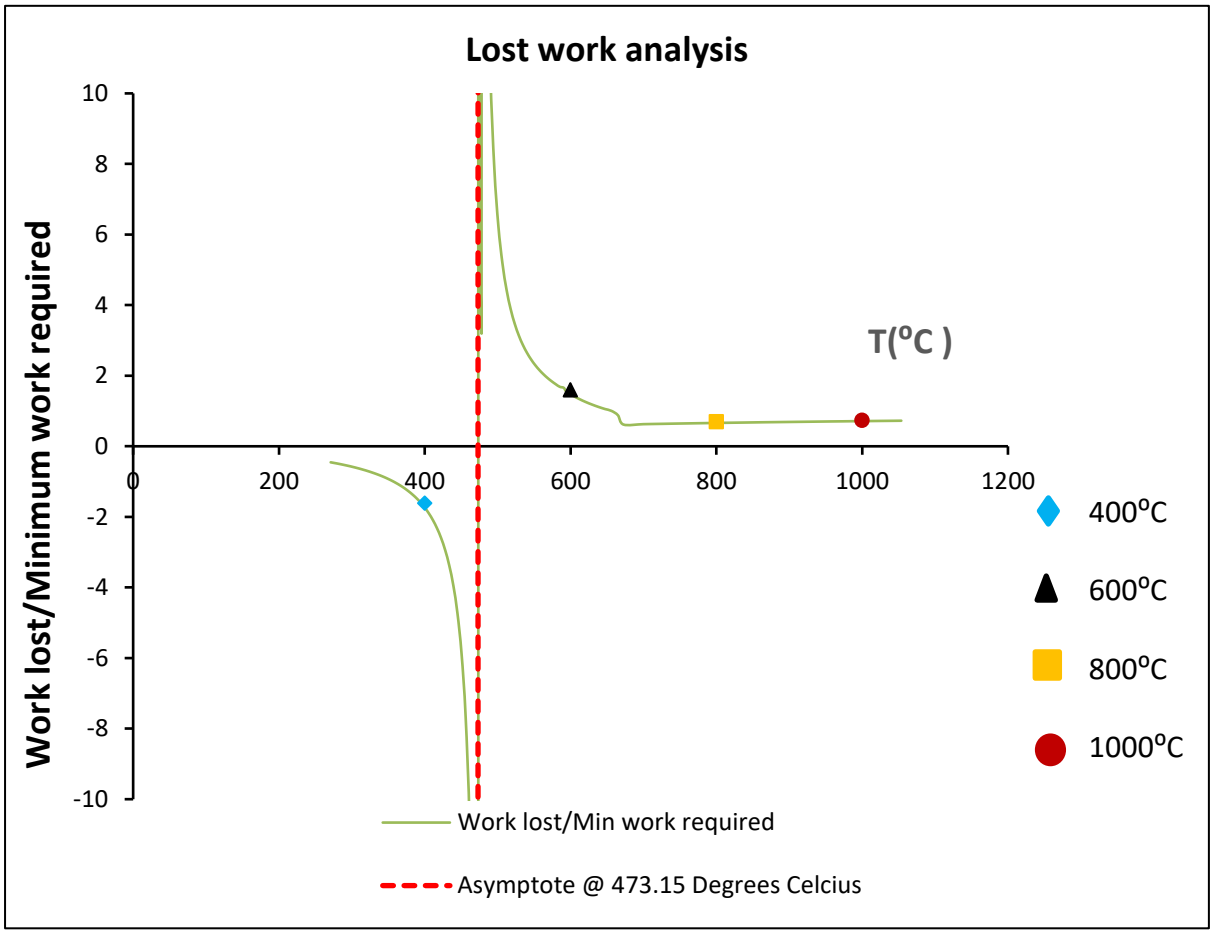

Figure 4.16: Relationship between lost work and minimum work required with temperature.

The ratio of the work lost with respect to the work required decreases as the process temperature increases from 600 ^{0}C to 1000 ^{0}C. As temperature increases, the ratio of the work lost to the minimum work required decreases compared to the work required. For the process at 400 ^{0}C as shown in Figure 4.14 and Figure 4.15, the process is capable of producing/recovering work when making products at the Carnot temperature, but the real process is losing work. This is shown in Figure 4.16, which shows the ratio of lost work to minimum work that could be recovered. At around 473 ^{0}C the ratio of lost work to minimum work required is infinity (asymptote on Figure 4.16). Hence running the process at this temperature will result in most work being lost. The lost work at all temperatures below 437 ^{0}C are large and using the plasma to

convert wood pellets at these regions is highly inefficient. This is because processes below 473 ^{0}C can actually produce work but is consuming work instead, while processes above this temperature cannot produce work.

4.4. Summary

The results show the production of syngas from plasma pyrolysis of wood pellets. The molar H_2/CO ratio for the product gas obtained for the temperatures 400 ^{0}C, 600 ^{0}C, 800 ^{0}C and 1000 ^{0}C was ~1:1. Temperature influences biomass conversion. The overall biomass conversion increased from 46 % at 400 ^{0}C to 82 % at 1000 ^{0}C. The mass conversion of carbon, hydrogen and oxygen in the feed to syngas also increased as temperature was increased. Small quantities of tars were observed in the pipelines and filtering section. For temperatures 400 ^{0}C and 600 ^{0}C, the products of plasma pyrolysis resulted in oil, char and syngas while for temperatures 800 ^{0}C and 1000 ^{0}C the products composed mainly of syngas and char. In this study, the nitrogen plasma process is able to simultaneously produce a high concentration of syngas and limit the production of tar from wood pellets at 800 ^{0}C and 1000 ^{0}C. Although high conversion of biomass is achieved for the studied conditions, the overall energy efficiency is about 20 %. This is due to the significant heat losses in the plasma torch and reactor chamber. This could be optimised in a better designed system. The work analysis shows that the amount of work lost with respect to the amount of work required by the process decreases with increase in temperature. The analysis shows the efficiencies of the reactions without considering the overall design of the reactor. The maximum amount of lost work for the process is observed to be at temperatures 473 ^{0}C and below because the processes are consuming work instead of producing work.

Referring to literature, plasma pyrolysis is considered as a better alternative to conventional methods due to its ability to reach high temperatures. While this has an advantage in producing cleaner gas, the work analysis has shown that it has a significantly low work efficiency. This could translate in higher CO_2 emissions and this is not good from an environmental point of view. In cases where energy efficiency is probably not important, the application of plasma pyrolysis might also be useful, for example in treating biomass waste, and other kinds of feeds like municipal waste that conventional technologies cannot handle. This will also reduce the amount of waste sent to landfills at the same time producing a valuable gas.

References

1. Agon N., Hrabovsky M., Chumak O., Hlina M., Kopecky V., Masˇlani A., Bosmans A., Helsen L., Skoblja S,Van Oost G., Vierendeels J., 2016. Plasma gasification of refuse derived fuel in a single-stage system using different gasifying agents. Waste Management, Vol. 47 pp. 246 –255.
2. Alberty Robert, A., 1998. Calculation of standard transformed Gibbs energies and standard transformed enthalpies of biochemical reactant. Archives of Biochemistry Biophysics, Vol. 353(1), pp. 116–130.
3. Doherty W., Reynolds A., Kennedy D., 2013. Aspen plus simulation of biomass gasification in a steam blown dual fluidised bed. Book Chapter: Materials and processes for energy: communicating current research and technological developments, A. Méndez-Vilas (Ed.), Formatex Research Centre.
4. Edbertho L., 2004. Plasma Processing of Municipal Solid Waste. Brazilian Journal of Physics, Vol. 34(4B).
5. Fabry F., Christophe R., Vandad J. R., Laurent F., 2013. Waste Gasification by Thermal Plasma: A Review. Waste and Biomass Valorization, Vol. 4 (3), pp. 421-439.
6. Fajri V., Adi S., Yulianto S. N., 2016. Thermodynamic Model for Updraft Gasifier with External Recirculation of Pyrolysis Gas. Journal of Combustion, Vol. Article ID 9243651, pp. 6.
7. Favas J., Monteiro E., Rouboa A., 2017. Hydrogen production using plasma gasification with steam injection. International Journal of Hydrogen Energy, Vol. 42 (16), pp. 10997–11005.
8. Gomeza E., Amutha R. D., Cheesemanb C. R., Deeganc D., Wisec M., Boccaccini A. R., 2009. Thermal plasma technology for the treatment of

wastes: a critical review. Journal of Hazardous Materials, Vol. 161, pp. 614–626.

9. Han J., Kim H., 2008. The reduction and control technology of tar during biomass gasification/pyrolysis: an overview. Renew and Sustainable Energy. Reviews, Vol. 12, pp. 397-416.
10. Higman C., Van der Burgt, M., 2008. Gasification, 2nd Ed; Elsevier Science (USA).
11. Hlina H., Hrabovsky M., Kavka T., Konrad M., 2014. Production of high quality syngas from argon/water plasma gasification of biomass and waste. Waste Management, Vol. 34, pp. 63–66.
12. Hrabovsky M., 2011. Thermal Plasma Gasification of Biomass, Progress in Biomass and Bioenergy Production, Dr. Shahid Shaukat (Ed.), ISBN: 978-953-307-491-7, InTech, Available from:http://www.intechopen.com/books/progress-in-biomass-and-bioenergy-production/thermal-plasma-gasificationof-biomass.
13. Hrabovsky M., Hlina M., Kavka T., Konrad M., Chumak O., Maslani A., 2009. Thermal plasma gasification of biomass for fuel gas production. High Temperature Material Processes: An International Quarterly of High-Technology Plasma Processes, Vol. 13:3–4, pp. 299–313.
14. Huang H., Tang L., 2007. Treatment of organic waste using thermal plasma pyrolysis technology. Energy Conversion and Management, Vol. 48, pp. 1331–1337.
15. Janajreh I., Raza S. S., Valmundsson A. S., 2013. Plasma gasification process: Modelling, simulations and comparison with conventional air gasification. Energy Conversion. Management, Vol. 65, pp. 801–809.

16. Je-Lueng S., Feng-Ju T., Kae-Long L., Ching-Yuan C., 2010. Bioenergy and products from thermal pyrolysis of rice straw using plasma torch. Bioresource Technology, Vol. 101, pp. 761–768.
17. Je-Lueng S., Ching-Yuan C., Wen-Kai T., Yu-Chieh Y, Jui-Ke L., Chin-Ching T., Heng-Yi L., Yuh-Jenq Y., Ching-Hui K., Lieh-Chih C., 2008. Major Products Obtained from Plasma Torch Pyrolysis of Sunflower-Oil Cake. Energy Fuels, Vol. 22 (1), pp. 75–82.
18. Lemmens B., Elslander H., Vanderreydt I., Peys K., Diels L., Oosterlinck M., Joos M., 2007. Assessment of plasma gasification of high caloric waste streams. Waste Management, Vol. 27 pp.1562–1569.
19. Lapuerta M., Hernández J., Pazo A., López J., 2008. Gasification and co-gasification of biomass wastes: effect of the biomass origin and the gasifier operating conditions. Fuel Process Technology. Vol 89, pp. 828–837.
20. Mikimasa I., Masatoyo S., 1998. Effect of arc current and electrode size on electrode erosion in ac plasma torches. Electrical Engineering in Japan, Vol. 124(4), pp. 10–17.
21. Mohan D., Pittman C. U. Jr., Steele P. H., 2006. Pyrolysis of Wood/Biomass for Bio-oil: A Critical Review. Energy & Fuels, Vol. 20, pp. 848–889.
22. Mountouris A., Voutsas E., Tassios D., 2006. Solid waste plasma gasification: equilibrium model development and exergy analysis. Energy Convers Manage. Vol. 47, pp. 1723–37.
23. Muvhiiwa R., Hildebrandt D, Matambo T., Ngubevana L., Chimwani N., 2017, The Impact and Challenges of Sustainable Biogas Implementation Towards a Bio-based Economy. 7: 20. doi:10.1186/s13705-017-0122-3;

24. Ngubevana L., Hildebrandt D., Glasser D., 2011. Introducing novel graphical techniques to assess gasification. Energy Conversion and Management. Vol. 52, pp. 547–563.
25. Ramzan N., Ashraf A., Naveed S., Malik A., 2011. Simulation of hybrid biomass gasification using Aspen plus: a comparative performance analysis for food, municipal solid and poultry waste. Biomass Bioenergy, Vol. 35(9), pp. 3962–3969.
26. Renew., 2004. Sustainable energy systems, definition of biomass. SES6-CT-2003-502705 WP2.1 /2.1.1 [Accessed 30 May 2017].
27. Schuster G., Loffler G., Weigl K., Hofbauer H., 2001. Biomass steam gasification - an extensive parametric modelling study. Bioresource Technology, Vol. 77, pp. 71–79.
28. Szente R. N., Munz R. J., Drouet M. G., 1992. Electrode erosion in plasma torches. Plasma Chemistry Plasma Processes, Vol. 12(3), pp. 372–343.
29. Vishal S. Vatsal N., 2016. Gasification – A Process for Energy Recovery and Disposal of Municipal Solid Waste. American Journal of Modern Energy. Vol 2(6), pp. 38–42.
30. Van Oost G., Hrabovsky M., Kopecky V., Konrad M., Hlina M., Kavka., 2009. Pyrolysis/gasification of biomass for synthetic fuel production using a hybrid gas–water stabilized plasma torch. Vacuum, Vol. 83, pp. 209–212.
31. Zhao Z., Huang H., Wu C., Chen Y., 2001. Biomass Pyrolysis in an Argon/Hydrogen Plasma Reactor. Engineering in Life Sciences, Vol. 1(5), pp. 197–199.

32. Zheyu L., Yitian F., Shuping D., Jiejie H., Jiantao Z., Zhonghu C., 2012. Simulation of Pressurized Ash Agglomerating Fluidized Bed Gasifier Using ASPEN PLUS. Energy & Fuels, Vol. 26 (2), pp. 1237–1245.

Chapter 5: Plasma gasification of wood pellets with oxygen using a nitrogen plasma torch: Analysis of material, heat and work balances.

Abstract

Energy in the form of a plasma is used to thermally decompose wood pellets in the presence of controlled amounts of oxygen. The resulting product gas mixture (syngas) consists of mainly carbon monoxide (CO) and hydrogen (H_2). Heat to sustain the endothermic gasification reactions is provided indirectly by (i) the electricity fed to the nitrogen plasma torch; and (ii) via the chemical potential of the oxygen fed to the reactor. Wood pellets, with an approximate molecular formula $C_4H_6O_{3(s)}$ and 6 % moisture content, were used as a feed. Experiments were carried out to investigate the syngas composition at 700 ^{0}C and 900 ^{0}C and a corresponding feed rate of wood pellets of 2 kg/h and 1 kg/hr respectively. The feed flow rate of oxygen to the process was varied from 0.15 kg/h- 0.6 kg/h. This was done to try and improve the carbon (C) efficiency observed during pyrolysis process where the major by- product constituted a high composition of solid C. An increase in the mole fraction of carbon dioxide (CO_2) in the product gas was observed as the oxygen (O_2) flow rate was increased at both temperatures. In addition, visible tars were observed at all gas flow rates for all the experiments at 700 ^{0}C but not for 900 ^{0}C. Although the maximum product gas yield reached an average of 86 % at 700 ^{0}C, the carbon and hydrogen efficiency were 64 % and 56 % respectively. Increasing the temperature to 900 ^{0}C increased the C and H efficiency to 75 % and 73 % respectively while the overall gas yield dropped to 82 %. The heat and work analysis show that less external heat energy is required by the process when O_2 feed is increased, because combustion supplements the heat supplied by the plasma torch. However, increasing the O_2 flow rate increases the lost

work and thus increases the irreversibility of the process. Although a clean (with no tars) synthesis gas is produced at a higher temperature, the product gas contains more CO_2 as compared to pyrolysis processes and the overall process is more irreversible.

5.1. Introduction

There has been increased interest in research towards supplementing heat energy requirements of gasification. In air or O_2 blown gasification processes, this energy is usually supplied by combustion of either the feed or product itself. This leads to an increase in the formation of CO_2 and an associated drop in the formation of CO, resulting in a syngas that has lower energy content. According to Worley and Yale (2012), O_2/ steam blown autothermal or direct gasifiers produces a gas with a higher heating value compared to air blown ones. This is due to the high quantity of N_2 and CO_2 in the product gas when air is used as a gasification agent.

It has been shown that allothermal gasification, where heat energy is supplied to the gasifier by an external source, is an efficient and economical technology (Gong et al., 2012). The heat can be supplied either by combusting a fossil fuel externally or via an electric heater. This is mainly done to prevent syngas dilution by either N_2 or CO_2. Application of a plasma torch reactor is a relatively new process that helps provide a constant supply of heat energy to the gasification process Hrabovsky (2011).

Generally, all biomass materials can be converted into syngas if they are brought in contact with a plasma flame due to its high-energy content, (Hlina et al., 2014). However, most biomass materials contain more C atoms compared to O atoms. Also

from Chapter 4 we have seen that there is insufficient oxygen to turn all the C onto CO, therefore C is one of the products that reduces C efficiency of the process. It is therefore necessary to add an oxidising medium(s) to ensure that there is a least a stoichiometric amount of oxygen atoms in the feed to the gasifier. This results in an increased yield of CO and reduced production of solid carbon from the surplus of C in treated biomass Hrabovsky (2009). The addition of O_2 or H_2O could remedy this. But in this investigation only O_2 was added to try and achieve the desired material balance.

The material balance in Eq. (5.1) defines the stoichiometric ratio (SR) of oxygen required to convert the wood pellets H_2 and CO (syngas). In this case SR is the amount of oxygen that needs to be added to the feed in order to produce H_2 and CO (syngas) in a molar ratio of 3:4. The water in the wood pellets is not taken into account in this calculation.

$$C_4H_6O_{3(s)} + 0.5O_{2(g)} \rightarrow 3H_{2(g)} + 4CO_{(g)} \quad \textbf{(5.1)}$$

If excess oxygen atoms are added in the feed, the excess oxygen will either combust with the carbon to form carbon dioxide or react with the hydrogen to form water. Gasification agents can be added in the form of a pure O_2, steam, air or even CO_2. Increasing the quantity of gasification agent added increases the carbon conversion, and this in turn influences the amount of CO produced. Gasification agents are also added to reduce the formation of tars, which usually occurs when carbon is heated with a limited amount of oxygen. The gasification process is effectively an incomplete oxidation of the carbon in biomass to produce CO, a scenario that occurs after a pyrolysis decomposition (Fabry et al., 2013).

Addition of O_2 also can provide energy to run the process and there is potential to reduce the energy requirement from plasma system. It is good to reduce plasma energy because it is high quality energy which is degraded by much when used for gasification as was shown in Chapter 4. By adding O_2 the process material balance is changed and therefore energy requirement can be reduced but at the expense of producing CO_2. So one would like to investigate the potential benefit of adding O_2 from an energy point of view.

Another important parameter in gasification processes is the ratio of O_2 fed to the reactor to the stoichiometric amount of O_2 needed for complete combustion of the wood pellets, which is defined as Equivalence Ratio (ER). This expresses how much O_2 is fed relative to the minimum required for combustion and is given by Eq. (5.2).

$$\text{Equivalence Ratio (ER)} = \frac{\text{Actual moles of oxygen gas fed to the process}}{\text{Moles of Oxygen required for complete combustion of fuel}} \quad \textbf{(5.2)}$$

According to Vineet et al., (2016); Thomas Reed and Ray Desrosiers (1979), an ER of about 0.25 gives an optimal product gas yield in gasification while this ratio can be as high as 0.3 for fluidised bed reactors. In his paper, Gungor (2009) mentions that all processes for biomass gasification have ERs that vary from 0.1 to 0.3. Ajay Kumar et al., 2009 and Narvaez et al., 1996 observed that a higher ER results in lower H_2 yield while at the same time increasing carbon conversion and reducing the tar content in a steam-air fluidised bed reactor. Zhang et al., 2012 varied ER from 0.08 to 0.12 in a plasma gasifier and the overall gas yield and energy efficiency increased while the Lower Heating Value (LHV) of syngas decreased. The LHV of a fuel is defined as the amount of heat released by combusting a specified amount of fuel. This assumes

latent heat of vaporisation of water in the reaction products is not recovered meaning water component of the combustion process is in vapour state at the end of combustion.

The thermodynamically favoured product is that which minimises the Gibbs Free Energy (G) of the system. It is predicted that CO and H_2 will be the major products at equilibrium when biomass is gasified. However, it is interesting to see whether the source of work and heat (plasma) to the gasifier will influence the equilibrium composition.

In this research, a plasma gasifier has been used and the amount of energy supplied to the process can be varied which allows the gasification temperature to be controlled. The main energy source for a plasma system is electricity, but the reactor is flexible enough that various oxidizing agents can be supplied, and these can also supply some of the energy for gasification by reacting with the feed. The addition of gasification agents in a plasma gasifier has an advantage compared to conventional gasification processes because the produced syngas can have a higher heating value as less CO_2 is formed Hrabovsky (2011). The ability to use energy from both electricity and combustion of feed to the reactor gives an extra degree of control to achieve high reaction temperatures. This can increase the amount of syngas produced per amount of feed as mentioned by Lapuerta et al., 2008.

In the previous work reported in Chapter 4, the process was carried out without a gasification agent in the plasma reactor; thus, the process occurring would be mainly pyrolysis. In this Chapter, the same analysis and procedure is being carried out but

with O_2 added as a gasification agent. Oxygen is added in increasing amounts to the process to find out firstly how the heat and work requirements of the process changes, and secondly to see the effect on the product composition and to compare the measured composition to that predicted by equilibrium. It is expected that addition of oxygen would also result in combustion of some of the biomass feed, hence supplementing the heat already provided by electricity supplied to the plasma system.

5.2. Experimental Procedure

Wood pellets, with molecular formula $C_4H_6O_{3(s)}$ and containing 6 % moisture by mass, were used as the feed to the plasma gasifier. The enthalpy of wood pellets was estimated from an Aspen simulation using the proximate and ultimate analysis of the wood pellets and the value was calculated as -5 177.8 kJ/kg. The calorific value of the wood pellets was calculated using the enthalpy and was found to be 18 648 kJ/kg. The method for determining the molecular formula and enthalpy is also described in Chapter 4.

The apparatus used in this analysis (Figure 5.1) is similar to the one described in Chapter 4 and the only difference is that O_2 is added to the process at the top of the plasma reactor chamber. The bulk reactor temperature was measured by using a type R thermocouple probe. The probe was placed away from the direct vicinity of the plasma flame and also the ceramic reactor wall lining. This was done to try and give us a good estimate of the reactor bulk temperature. The wood pellets entered the reactor at 25 ^{0}C and the product gas temperature of around 60 ^{0}C was measured after the quenching section using type-K thermocouple probes.

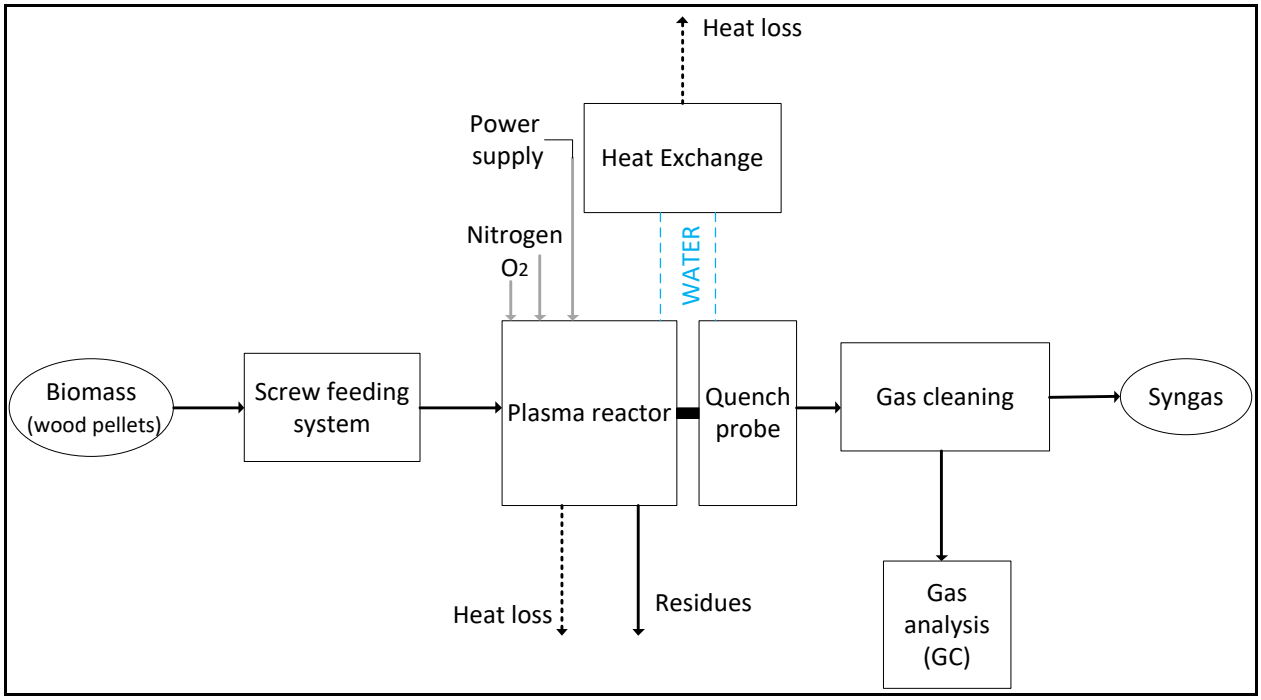

Figure 5.1: Simple flow diagram for the gasification process.

Wood pellets were gasified at temperatures of 700 ^{0}C and 900 ^{0}C with varying amounts of O_2. These two were the only temperatures studies because temperatures below 700 ^{0}C or higher than 900 ^{0}C could not be achieved due to operational and design limitations; temperatures below 700 ^{0}C could not be achieved because of combustion, when O_2 above SR was fed into the gasifier, increased the temperature to above 700 ^{0}C. Above 900 ^{0}C, the pressure of the reactor chamber increased to unsafe values. This pressure increase was caused by small particles being transported because of the higher product gas flows that occurred at higher temperatures and higher O_2 flow rates. As a result, the transported solid carbon particles settled in the horizontal piping section, blocking it and causing the pressure in the reactor to increase. At high outlet gas flow rates, solid particles of less than 300 µm would be carried out of the reactor and this would result in clogging of the gas line, increasing the pressure in the reactor.

The composition of the gas was measured after the gas-cleaning unit using an online Agilent 7890B Gas Chromatography (GC). It was assumed that the composition of the gas leaving the reactor is the same as that after the quench and cleaning unit. The measured composition was used for the material, energy and work analysis.

Table 5.1 shows the process parameters that were used for the gasification experiments. A feed rate of wood pellets of 1 kg/h was used for the experiments at 900 ^{0}C compared to the 2 kg/h at 700 ^{0}C. This is due to design limitations as the reactor temperature would fluctuate by more than +/- 75 ^{0}C when a feed of 2 kg/h was applied at 900 ^{0}C. However, for comparison and analysis sake, the results obtained for these two temperatures were normalised to 1 mole of wood pellets ($C_4H_6O_3$). Calculations of heat and work were also normalised for one mole of feed ($C_4H_6O_3$).

5.2.1. Gasification parameters

Table 5.1: Gasification parameters for the experiments at 700 ^{0}C and 900 ^{0}C. Note the feed rate of wood pellets was adjusted to keep the temperature at the required temperature.

Temperature	**700 ^{0}C**	**900 ^{0}C**
Wood pellets feed rate (kg/h)	Approx. 2	Approx. 1
Oxygen feed rate (kg/h)	0.15, 0.3, 0.45, 0.6	0.15, 0.3, 0.45
Equivalent Ratio ER	0.06, 0.12, 0.18, 0.24	0.12, 0.24, 0.36
Stoichiometric amount of Oxygen (kg/h)	0.314	0.15
Plasma power supply (kW/h)	11.3	12.05
Nitrogen flow (kg/h)	1.6	2

5.3. Results and discussion

The results of varying oxygen flow rate between 0.15 kg/h to 0.6 kg/h (i.e. below and above the stoichiometric requirement of the wood pellets feed flow rate) has been analysed in this study. The work analysis for this plasma system will be based on both experimental and theoretical simulations.

5.3.1. Material balance at 700 ^{0}C

The material balance for the process is shown in Table 5.2 and is calculated using the C, H and O atomic balances. The table was normalised to a feed of 1 mole of wood pellets ($C_4H_6O_3$). The desired material balance would produce CO and H_2 only, Eq. (5.1), while the real material balance from experimental data is given by Eq. (5.3) and produces CO_2 and H_2O as well. The individual material balance equation obtained for each experiment for the temperatures studied are given in Table 5.2 and Table 5.3.

$$C_4H_6O_{3(s)} + \boldsymbol{a}O_{2(g)} \rightarrow \boldsymbol{b}H_{2(g)} + \boldsymbol{c}CO_{(g)} + \boldsymbol{d}CO_{2(g)} + \boldsymbol{e}CH_{4(g)} + \boldsymbol{f}C_2H_{4(g)} + \boldsymbol{g}C_2H_{6(g)} + \mathbf{C_hH_iO_j}$$

(solid residue) + $\mathbf{C_kH_lO_m}$ (condensate + water vapour+ error) **(5.3)**

The amount of the gaseous products (b to g in Eq. 5.3) was measured from the gas phase analysis. The solid residue was collected and sent for elemental analysis allowing us to determine the moles of C, H and O remaining in the solid and hence calculate h, i and j in Eq. (5.3).

The difference between the left-hand side of equation and the values of b to j was used to determine the amount of condensate and water vapour and indeed any error in the measurements was also lumped into these values (values k, l and m).

Although it would have been beneficial to determine the C, H and O in the condensate collected, this was not possible due to lack of proper instruments (Inductively coupled plasma mass spectrometry (ICP-MS) and Atomic Absorption Spectroscopy (AAS) to do the analysis This resulted in the liquid sample to be kept for much longer making the samples prone to degradation which may affect the analysis.

It should be noted that the material balances in Table 5.2 were subject to some experimental error arising from inconsistent feeding of the screw feeder and to some extent, the composition of the wood pellets. Nonetheless, the experiments were conducted uniformly with the same degree of error assumed in the calculations.

Table 5.2: Material balance for the gasification process with different oxygen flow rates at 700 ^{0}C for a feed of 1 mol/h of wood pellets ($C_4H_6O_3$).

Oxygen Feed rate		**(x10^{-3} moles/h)**											
kg/ h	**x10^{-3} mole/ h**	**Gas products per mole of $C_4H_6O_{3(s)}$**						**Solid residue**			**Condensate, water vapour and error**		
	O_2	H_2	CO	CO_2	CH_4	C_2H_4	C_2H_6	C	H	O	C	H	O
	a	**b**	**c**	**d**	**e**	**f**	**g**	**h**	**i**	**j**	**k**	**l**	**m**
0.15	240	1896	2261	291	166	199	2	1059	377	120	0	359	277
0.3	478	1938	2126	510	179	132	2	993	269	108	0	599	226
0.45	717	1831	2090	648	240	112	2	815	274	154	0	646	180
0.60	957	1658	2026	801	327	127	4	818	253	129	0	615	205

The carbon has been accounted for in the gaseous phase as well as the solid and indeed there is a slight excess of carbon on the right-hand side of Eq. (5.3), at most 5 %, and this gives an indication on the accuracy of the experiments.

It can be seen from Table 5.2 that the material that is not accounted for is H and O, and this is what would be expected as the amount of water in the gas phase has not been measured. The ratio of H:O (l:m) varies from 1.3 to 3.6 and this is in line with what would be the case for the water vapour.

5.3.2. Increase in O_2 flow rate at a bulk temperature of 700 ^{0}C

The results in Figure 5.2 and Figure 5.3 show the variation in composition of syngas produced when 2 kg/h of wood pellets were subject to plasma gasification at 700 ^{0}C at different O_2 flow rates. The results show that the experimental analysis was close to steady state, considering the uniformity of the points at different times. The results show that increasing the O_2 feed rate results in a decrease in the H_2 and CO content and simultaneously increases CO_2 content. This ultimately reduces the overal syngas composition and in turn the LHV of the product gas. The molar ratio of H_2 to CO is about ~4:5. This is different to the 1:1 ratio achieved in the pyrolysis results in Chapter 4. It was not possible to measure the amount of H_2O in the gas phase and so this is not taken into account when calculating the mole composition in the gas phase.

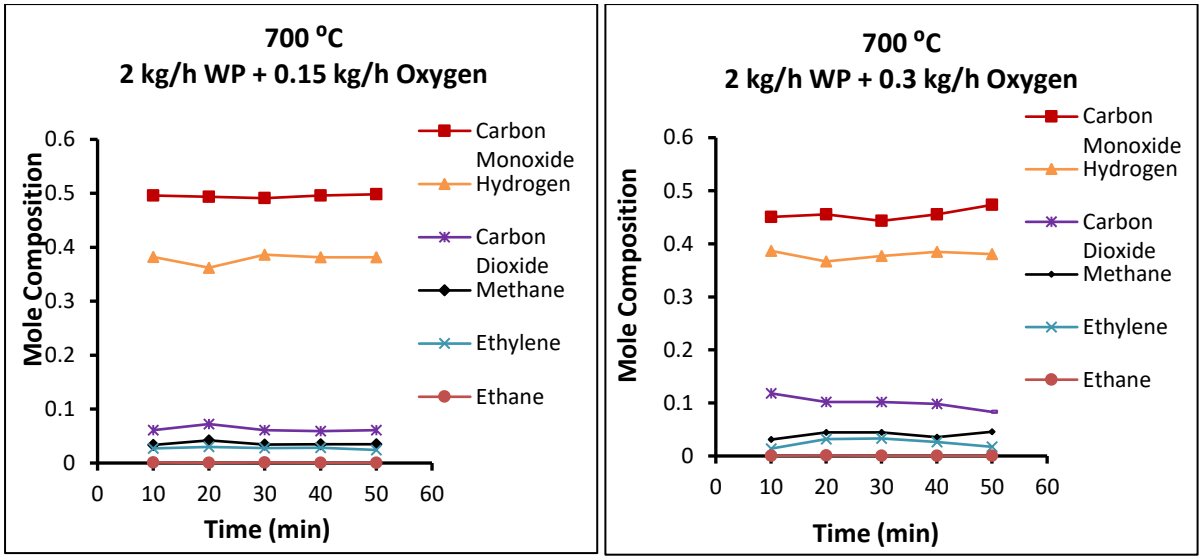

Figure 5.2: Changes in product gas composition with time measured in plasma outlet stream at a bulk temperature of 700 ^{0}C for a feed rate of 2 kg/h wood pellets on a water and nitrogen free basis for an oxygen feed of **a)** 150 g/h O_2**; b)** 300 g/h O_2.

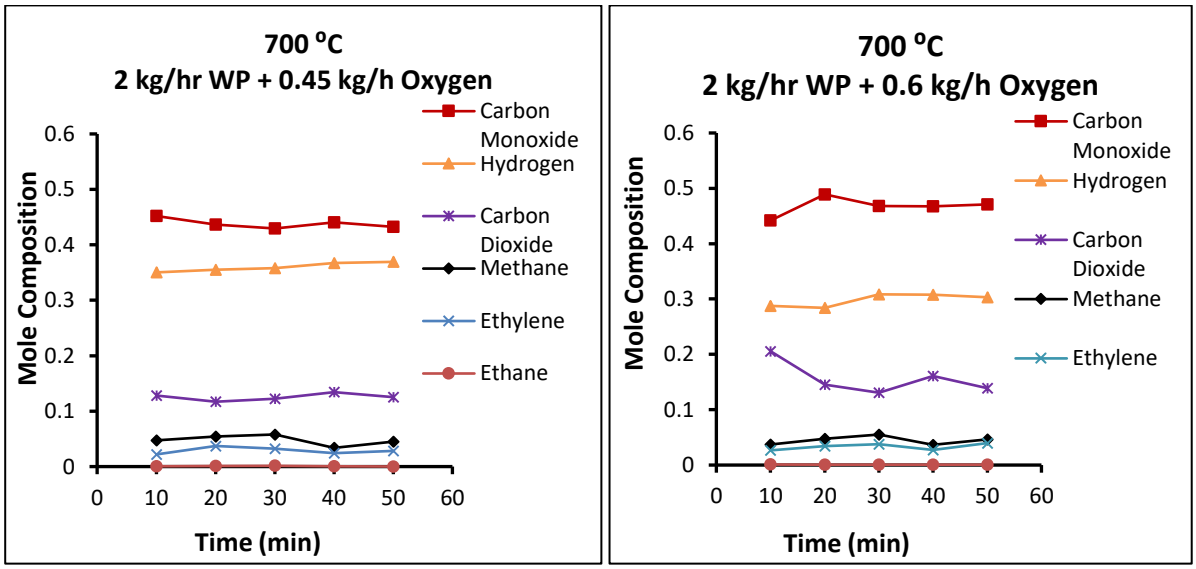

Figure 5.3: Changes in product gas composition with time detected in plasma outlet stream at a bulk temperature of 700 ^{0}C for a feed rate of 2 kg/h wood pellets on a water and nitrogen free basis for an oxygen feed of a) 450 g/h; b) 600 g/hr.

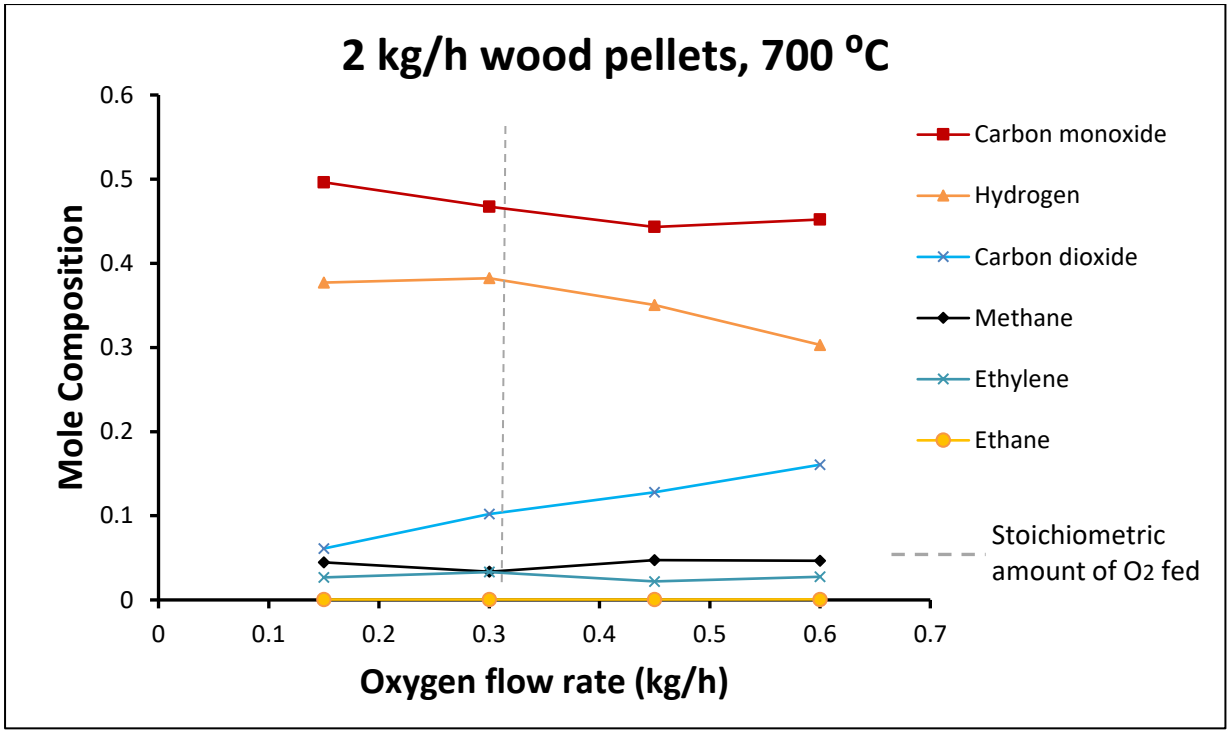

Figure 5.4: Change in the mole composition of the product gas with increase in oxygen flow rate at a bulk temperature of 700 ^{0}C on a nitrogen and water free basis. The dotted line corresponds to the SR of oxygen for making CO and H_2.

The stoichiometric amount of O_2 required to make CO and H_2 is about 0.314 kg/hr when 2 kg/hr of wood pellets are fed, as occurs for the experiments at 700 ^{0}C, and is shown by the grey dotted line in Figure 5.4. Above this amount, an excess amount of oxygen is fed, and this means that combustion has to occur where CO_2 and H_2O are formed. It can be seen in Figure 5.4 that the CO_2 composition increases fairly linearly with O_2 flow rate from 0.06 to 0.15 when the O_2 feed rate is increased from 0.15 kg/hr to 0.6 kg/hr respectively.

The slope of the CO_2 line in Figure 5.4 is approximately constant, while that of CO flattens out at high O_2 flow rates, suggesting that the excess O_2 reacts with the carbon in the solid feed, increasing the conversion. Although this is rather observed from mole fractions and not from actual moles, this can be explained further in terms of ER; more

CO_2 is produced when the equivalent ratio increases. Also, the actual moles in Table 5.2 shows that the moles of CO and H_2 are almost constant.

It must be noted that tars were also observed in the condensate in all the experiments at 700 ^{0}C. The tars were sticky and attached to the reactor and quench lining and could only be removed by wiping. This made difficult to collect and quantify the tars.

5.3.3. Mass conversion and efficiency

The mass efficiency of the plasma gasification process is measured in terms of biomass conversion as well as H and C efficiency. The mass efficiencies calculated do not include either the H_2O in the gas phase or the condensed phase. The "lost mass" is the missing mass between the known mass of feeds and the measured gas product, solid residues and mass of condensate. These efficiencies tells us how much solid has been converted to gas. The yield is defined in Eqs. (5.4, to 5.7) as

$$\text{H yield} = \frac{\text{H atoms in the product gas (excluding water)}}{\text{H atoms in feed}}, \quad \textbf{(5.4)}$$

$$\text{C yield} = \frac{\text{C atoms in the in product gas}}{\text{C atoms in feed}} \quad \textbf{(5.5)}$$

$$\text{O yield} = \frac{\text{O atoms in the product gas (excluding water)}}{\text{O atoms in feed including O2 feed}}, \quad \textbf{(5.6)}$$

$$\text{Gas yield} = \frac{\text{Total mass gas produced(excluding water)}}{\text{mass Biomass and O2 feed}} \quad \textbf{(5.7)}$$

Increasing the O_2 feed rate increases the C yield and slightly reduces that of H as shown in Figure 5.5.

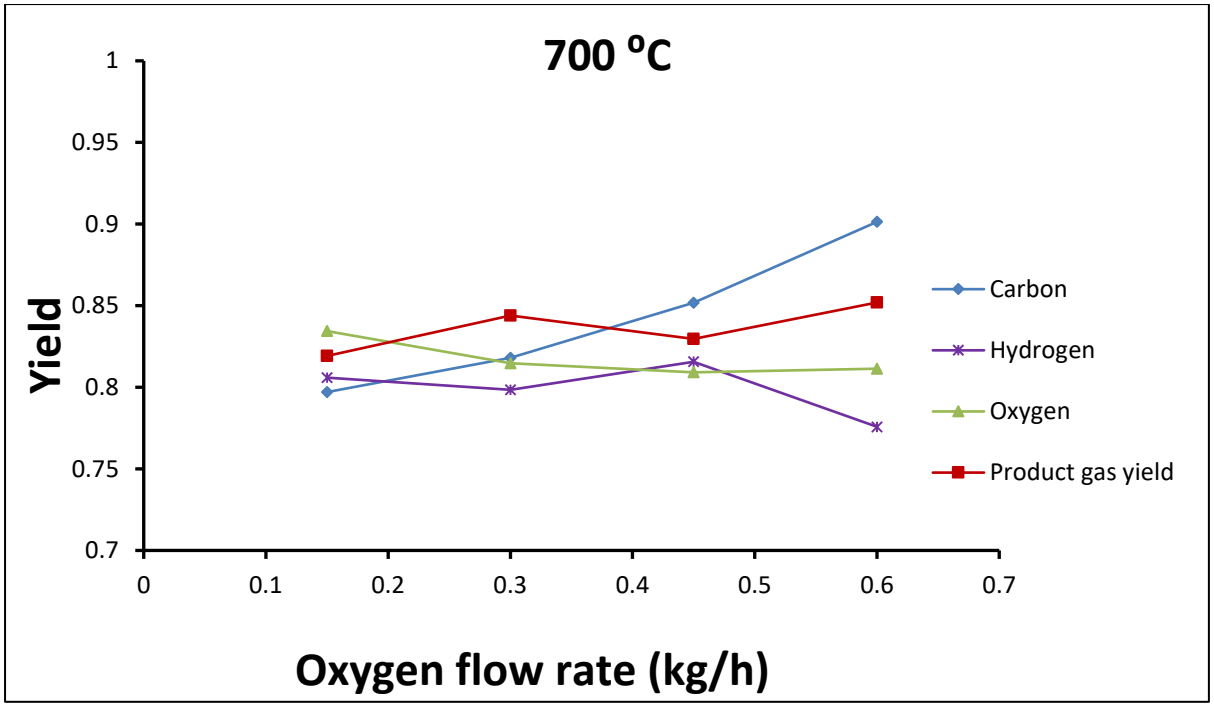

Figure 5.5: Changes in carbon, hydrogen, oxygen and product gas yield with increase in oxygen feed flow at 700 ^{0}C.

The H and C efficiencies are given by Eq. (5.8) and Eq. (5.9).

$$\text{H efficiency} = \frac{\text{H atoms in the H2 product}}{\text{H atoms in feed}}, \text{ C efficiency} = \frac{\text{C atoms in the in CO product}}{\text{C atoms in feed}} \quad \textbf{(5.8; 5.9)}$$

The H and C efficiencies are shown in Figure 5.6 and indicate that both the efficiencies decrease with an increase in O_2 feed to the process. Although the conversion of carbon increases as shown in Figure 5.5, the C efficiency initially increases, presumably as more carbon is gasified but then decreases as excess O_2 is supplied to the system due to combustion that produces CO_2. It is interesting that a high C efficiency also occurs at an O_2 flow rate higher than the SR, corresponding to an ER of 0.18. Vineet et al., (2016) suggested that at ER of 0.25 to 0.3 was optimal for gasification of biomass, and one could work with a slightly lower ER in the plasma system.

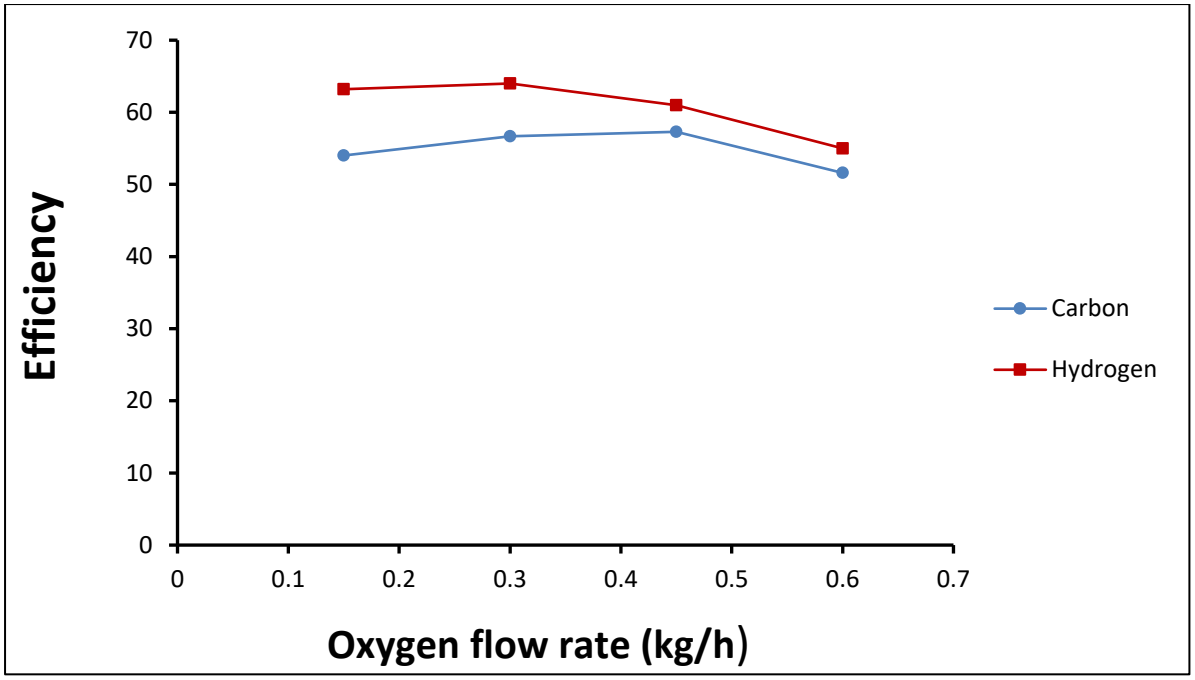

Figure 5.6: Hydrogen and carbon efficiency at different oxygen flow rates at 700 ^{0}C.

Figure 5.7 shows comparison of the molar amounts of products measured experimentally and those predicted from an Aspen equilibrium model using a Gibbs reactor for the given O_2 flow rates, assuming the system reaches equilibrium at 700 ^{0}C. The experimental results in Figure 5.7 are given by the dashed line and the Aspen simulations are denoted with solid lines. The amount of water in the gas phase is estimated from the values in Table 5.2. The experimental results at 700 ^{0}C do not follow the equilibrium thermodynamic trends predicted by Aspen. This, together with the gas composition results in Figure 5.4 suggests that the process occurring in the plasma reactor at 700 ^{0}C is both kinetically and thermodynamically limited. This is supported by the observation that the measured amount of C is greater than that predicted by thermodynamics, suggesting that more time is required to convert the solid. The CO_2 and CO approach equilibrium at higher O_2 flow rates, but more H_2 is predicted to form compared to that measured experimentally. Also, the C measured is more than the predicted equilibrium amount at higher O_2 flow rates (Note: The solid

carbon referred to as the measured carbon is the solid remains collected which included C, H and O elements. These were referred to as carbon because the solid residues constituted of mainly carbon as shown in Table 5.3.)

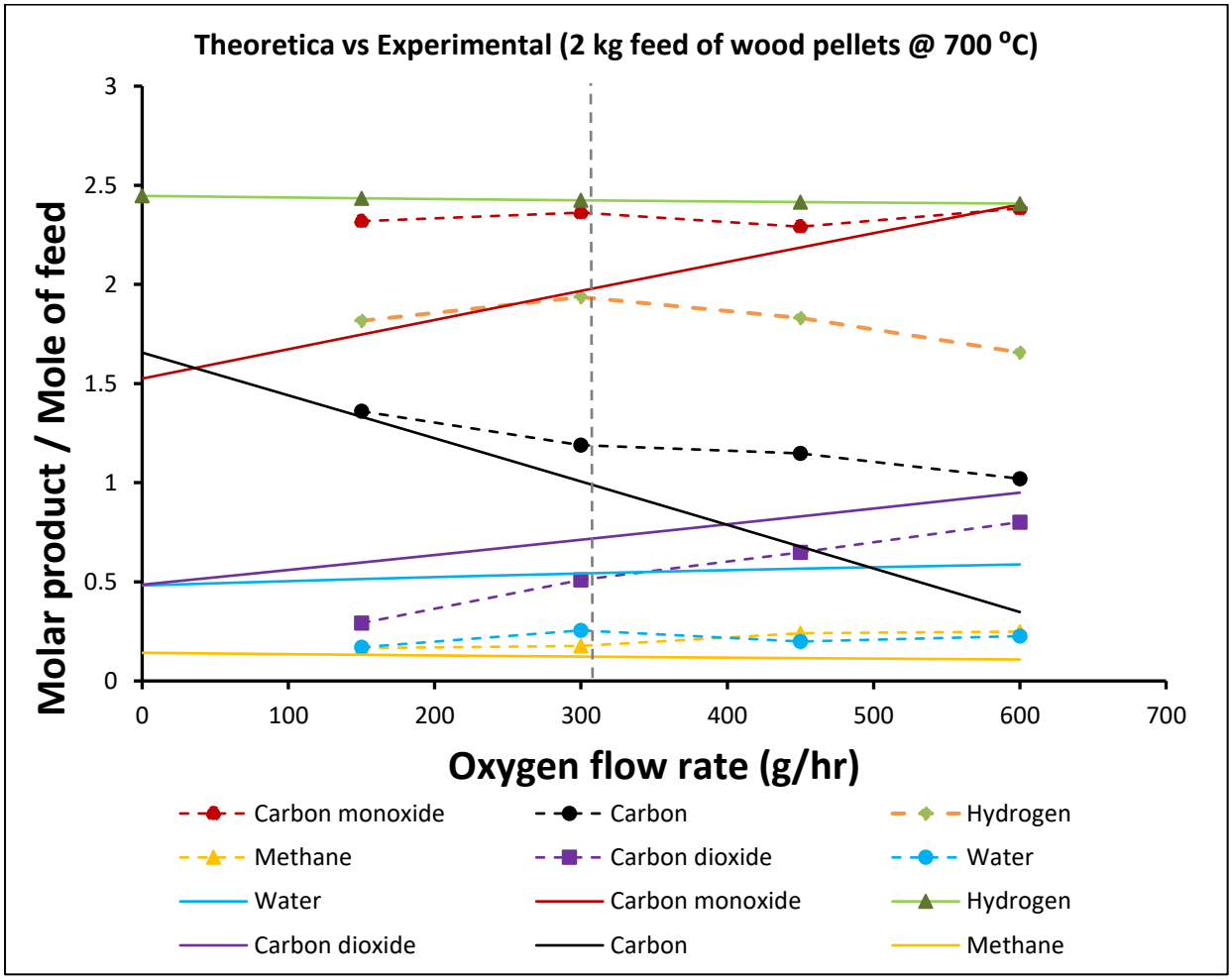

Figure 5.7: Comparison of experimental results and theoretical simulations using a Gibbs reactor for varying oxygen flow rates at 700 ^{0}C. The solid lines are the data predicted by equilibrium and the dotted lines join the experimentally measured data. The vertical dotted grey line indicates the SR of oxygen for making CO and H_2.

5.3.4. Material balance at 900 ^{0}C

Table 5.3 shows a summary of results for plasma gasification of wood pellets for various O_2 flow rates at 900 ^{0}C. The material balance in Table 5.3 clearly show that the formation of CO_2 increases with an increase in O_2 feed. The atomic balances show

that the moles not accounted for as condensate, water vapour and error. This lost mass includes the H_2O in the gas phase as this was not measured. The lost mass increases with O_2 flow rate, which would support the lost mass mainly being the water vapour which is a product of combustion.

Table 5.3: Material balance for the gasification process with different O_2 flow rates at 900 ^{0}C for a feed of 1 mole/h of wood pellets ($C_4H_6O_3$).

Oxygen Feed rate		**(x10^{-3} moles/h)**											
kg/h	**x10^{-3} moles/h**	**Gas products per mole of $C_4H_6O_{3(s)}$**						**Solid residue**			**Condensate, water vapour and error**		
		a	b	c	d	e	f	g	h	i	j	k	l
		H_2	CO	CO_2	CH_4	C_2H_4	C_2H_6	C	H	O	C	H	O
0.15	478	1994	2688	155	184	115	0	679	110	114	64	706	366
0.3	956	2174	2889	373	87	57	0	587	176	29	0	900	292
0.45	1435	2150	2756	754	86	61	0	259	187	24	23	925	147

5.3.5. Increase in O_2 flow rate at a bulk temperature of 900 ^{0}C

Figure 5.8 and Figure 5.9 show three experimental results obtained when wood pellets were gasified in a plasma reactor with different O_2 feed flows at 900 ^{0}C. Similar trends for gas composition observed for 700 ^{0}C were seen at 900 ^{0}C. It is observed that the amount of CO_2 increases with O_2 flow rate, while the amount of CO produced only decreases at the highest O_2 flow rate.

Figure 5.8a shows the molar composition when nitrogen gas is included while Figure 5.8b shows the results on a N_2 and H_2O free basis. This is just to show the composition of the actual output gas from the plasma system when the product gas is diluted with N_2 that was initially fed into the system as plasma gas. The plasma gasifier in its current configuration uses a lot of N_2, reducing the molar composition of the CO and H_2 and thereby the LHV. One of the recommendations from this work is that the design of the gasifier be modified to reduce the amount of N_2 used or to perhaps change the carrier gas to steam or CO_2, which might take part in the reactions, thereby improving the quality of the gas.

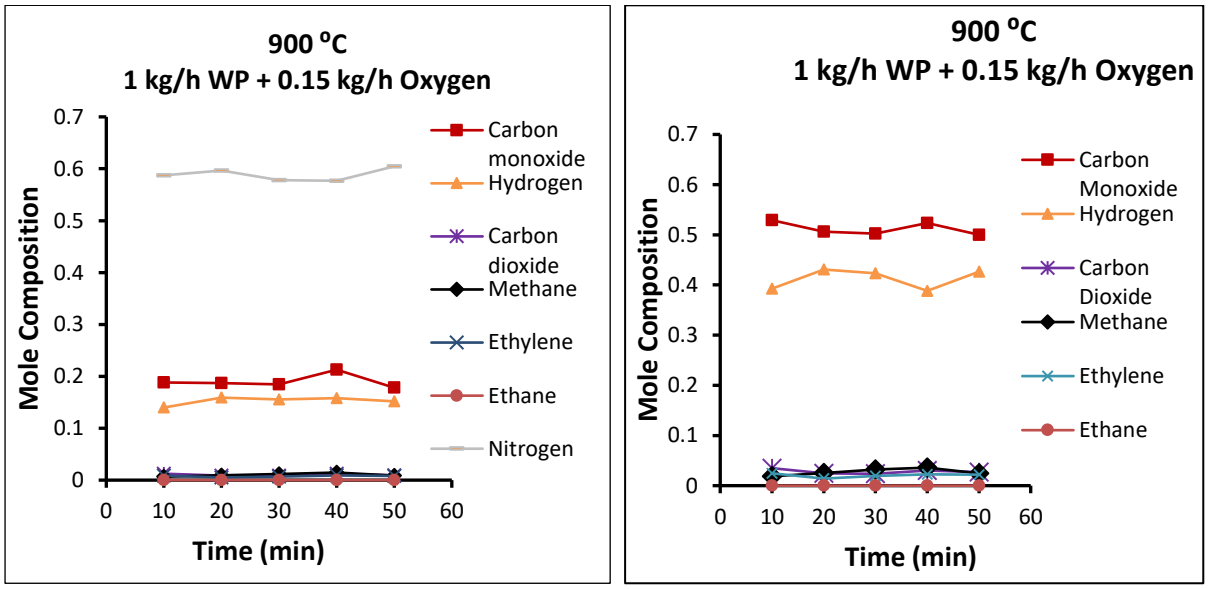

Figure 5.8: Changes in product mole composition with time detected in plasma outlet stream at 900 ^{0}C for a feed rate of 1 kg/h wood pellets and oxygen feed rate of 150 g/h; **a)** changes in gas composition on a water free basis, **b)** changes in gas composition on a nitrogen and water free basis.

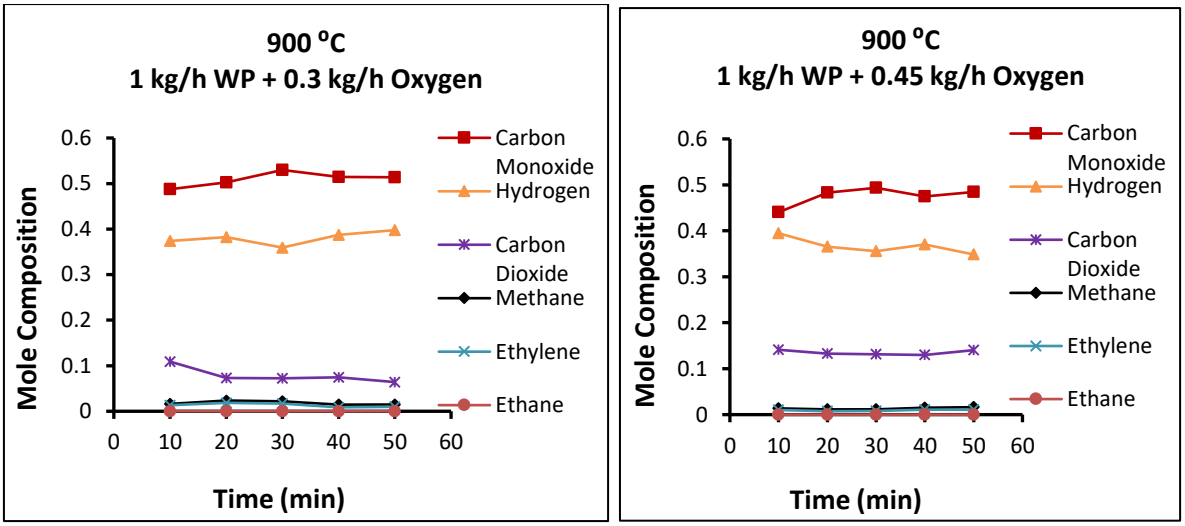

Figure 5.9: Changes in product gas composition with time detected in plasma outlet stream at 900 ^{0}C for a feed rate of 1 kg/h wood pellets on a nitrogen and water free basis and O_2 feed rate of **a)** 300 g/h; **b**) 450 g/h.

Figure 5.10 summarises how the composition of syngas changes with an increase in O_2 flow rate when the plasma gasification is operated at a bulk temperature of 900 ^{0}C. The data shows that the ratio of CO to H_2 is again approximately 4:5 and that the formation of CO_2 increases as the O_2 flow rate is increased, while the amount of H_2 formed decreases. The mole fraction of CO is not as sensitive to O_2 flow rate as that of H_2 is and does not change significantly with increased O_2 flow rate.

There were no visible tars observed for these three experiments carried out at 900 ^{0}C. In addition, no traces of ethane were found. This was different from the tars observed at 700 ^{0}C which were very much visible, sticky and could only be removed by wiping the affected areas (reactor and quench lining) and hence making it difficult to collect and quantify.

These results are compared to the results of G-H AR at 900 ^{0}C in Chapter 2A which shows in Figure 2.3A that CO and H_2 are preferred products at minimum G when ER

is zero. This explains the pyrolysis results in Chapter 4 where CO and H_2 gases were dominant at high temperatures. However, as ER increases three sets of material balance lie close to each other at the global minimum G as shown by the G-H AR in Figure 2.7A and Figure 2.11A. This shows that the range of products that may be expected from the plasma may include either of or all of the following species, H_2, H_2O, CO, CO_2 and C. This set of products is observed for an ER values of between 0.083 and 0.83.

In gasification two/ three material balances are close to minimum G hence it is difficult to predict which one will be favoured or what proportion of each will contribute to the favoured composition. In practice it is difficult to produce a syngas without making CO_2 gas and H_2O with solid C included otherwise factors such as kinetics, feed flow rate and mixing may play a role here. Looking further at Figure 2.15A, it shows that when the flow rate of O_2 is increased to an ER of 1.67, the expected products at minimum G are CO_2 and H_2O. This tells that thermodynamic does not have much influence in the product distribution at gasification temperatures but plays an important role in pyrolysis/AD and combustion processes. Simulation results and experimental data should tell us where we should be. And these are showing that a product mix of syngas, H_2O and CO_2 will be favoured at gasification temperatures studied.

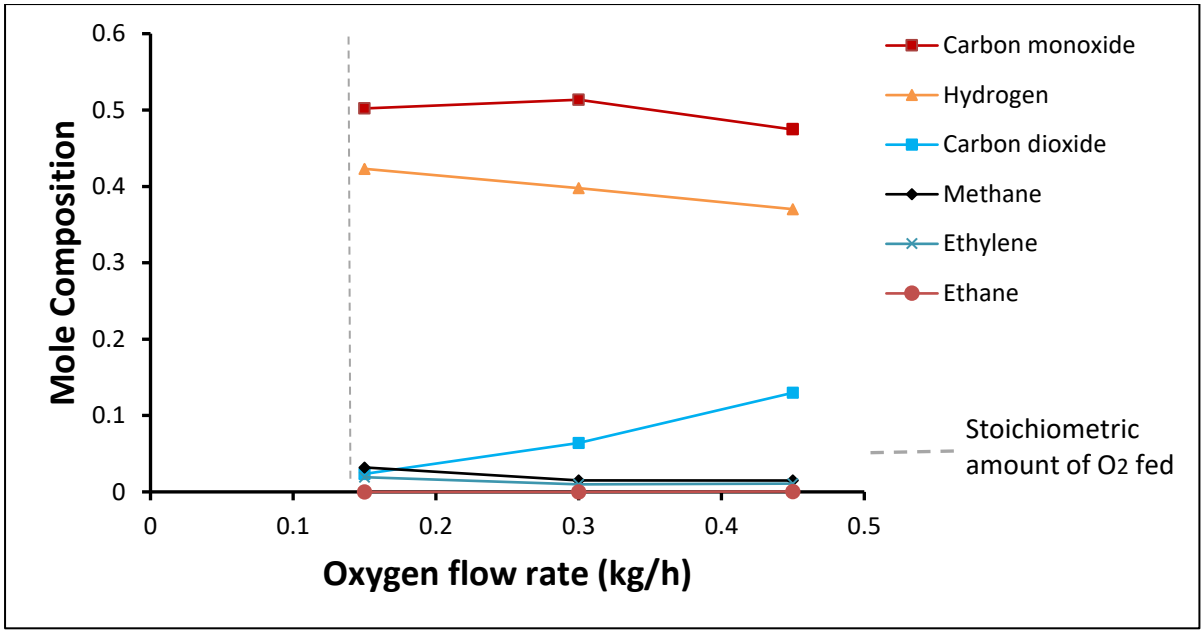

Figure 5.10: Change in the mole composition (on a nitrogen and water free basis) of the product gas with increase in O_2 flow rate at 900 ^{0}C. The vertical dashed line corresponds to the SR of oxygen for making CO and H_2.

The results in Figure 5.4 and Figure 5.10 show that there is not a significant change in the composition of CO, which supports that the increase in CO_2 is from C in the biomass combusting. This suggests that there is no trade-off between CO and CO_2. However, this is not what is usually observed as formation of CO_2 together with C in gasification processes is typically described by the Boudouard reaction. Also, Table 5.3 shows that the actual moles of CO are not significantly changing as compared to the formation of CO_2.

5.3.6. Mass conversion and efficiency

Figure 5.11 shows the atomic and product gas yield for gasification at 900 ^{0}C. Carbon yield increased from 82 % to 93 % when the O_2 flow rate was increased from 0.15 kg/h to 0.45 kg/h. Conversely, the H yield decreased with an increase in O_2 flow rate while the overall gas yield remains almost constant at 80 %. The highest gas yield is again

obtained at an SR greater than 1, in this case an ER of 0.24 which agrees with the literature values.

The H yield decreases, presumably due to hydrogen combusting to form water in the combustion process. The C yield increases however, meaning that more CO is formed, even if the CO_2 quantity is increasing as can be seen in Figure 5.10. The product gas yield at 900 ^{0}C is about 82 % and is lower than the 86 % obtained for gasification at 700 ^{0}C. It would be expected that gas yield at 900 ^{0}C is higher. The mass of residue solid was 0.32 kg, 0.27 kg 0.28 kg, and 0.24 kg for the respective O_2 flow rate at 700 ^{0}C compared to 0.12 kg, 0.08 kg and 0.08 kg for that at 900 ^{0}C, thus the conversion of solid was higher at the higher temperature as is expected. It is likely to be the fact that H_2O in the gaseous phases was not included in the definition of gaseous yield that causes the overall gas yield to be lower at higher temperature.

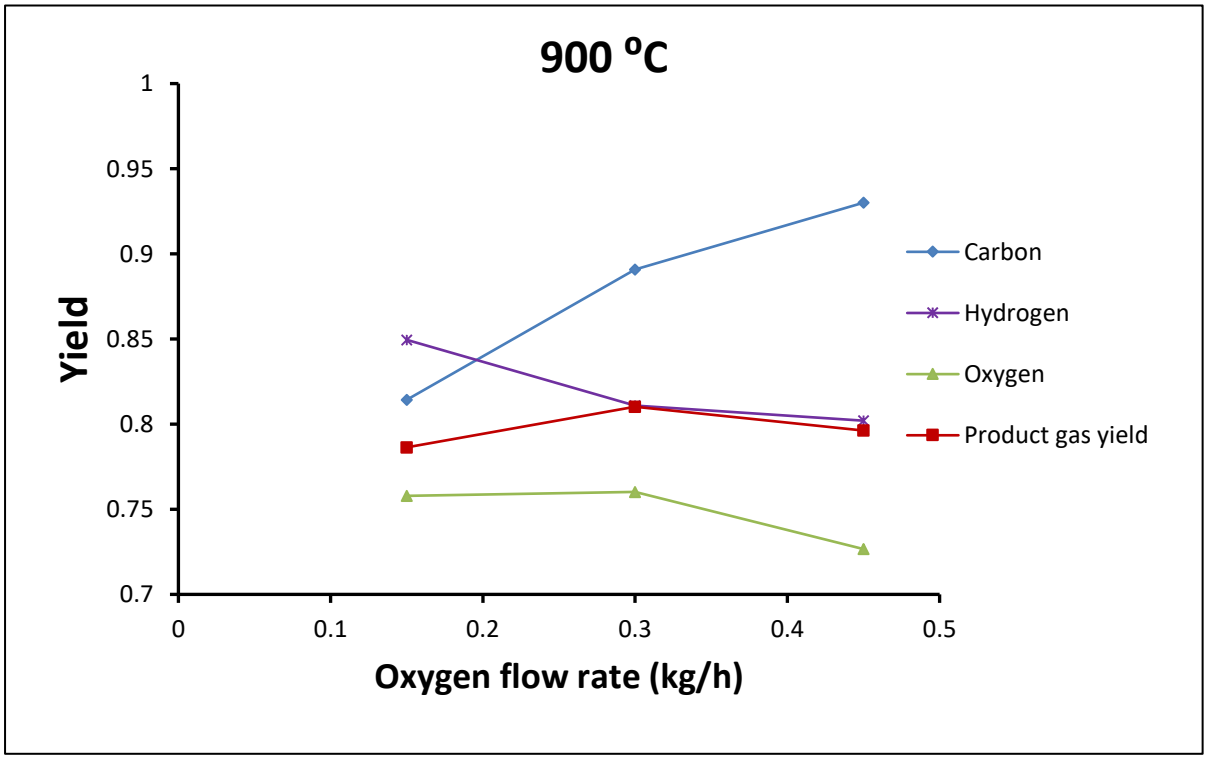

Figure 5.11: Changes in the yield of carbon, hydrogen, oxygen, product gases with increase in O_2 flow rate at 900 ^{0}C.

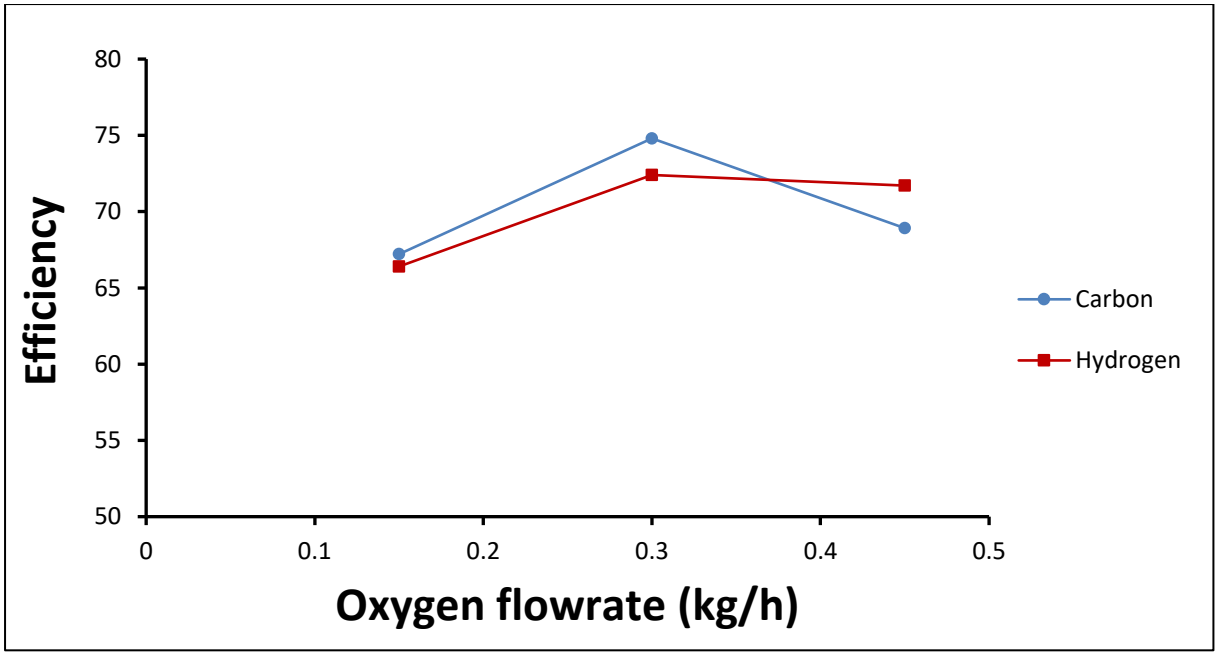

Figure 5.12: Carbon and Hydrogen efficiency as a function of O_2 flow rate at a bulk gasification temperature at 900 ^{0}C.

In Figure 5.12, the C and H efficiency initially increase with an increase in O_2 flow rate and then decrease due to the excess O_2 combusting rather than gasifying, forming CO_2 and H_2O.

The highest C efficiency is obtained when 0.3 kg /h of O_2 is fed together with 1 kg/h of wood pellets. The stoichiometric amount of oxygen for a feed of 1 kg/h wood pellets is 0.156 kg/h oxygen. One would expect to get the highest efficiency for carbon at around 0.15 kg/h O_2 if only the gasification reaction occurred; in this case is the highest efficiency was obtained at an ER of 0.12. This agrees with the literature where it is said Gungor (2009) that the best ER is between 0.1 and 0.3.

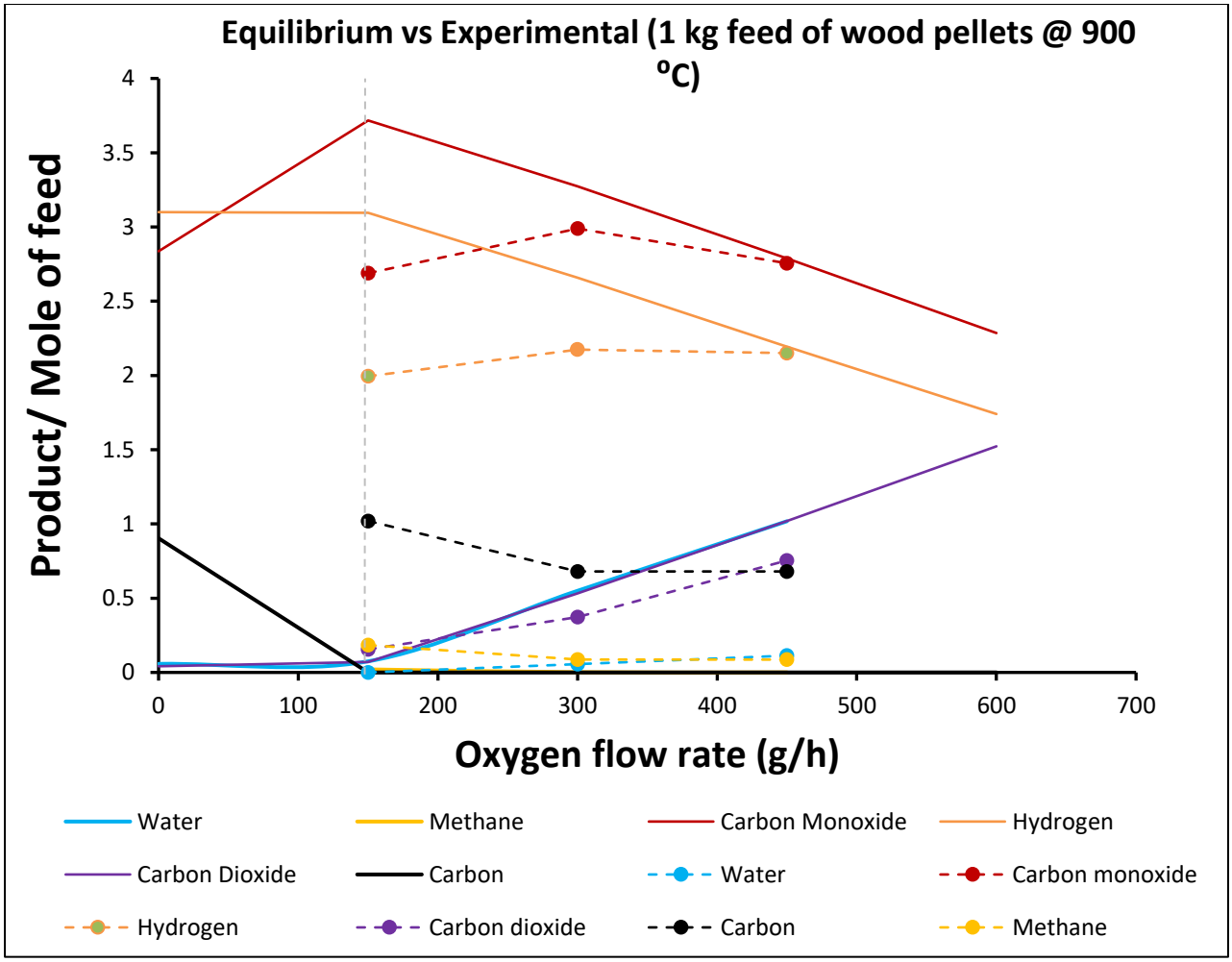

Figure 5.13: Comparison of experimental results and equilibrium simulations using a Gibbs reactor for varying oxygen flow rates at 900 ^{0}C. The solid lines are the data predicted by equilibrium and the dotted lines join the experimentally measured data. The vertical dotted grey line indicates the SR of oxygen for making CO and H_2.

The experimental results obtained for the three O_2 flow rates at 900 ^{0}C were compared to the predicted thermodynamic equilibrium predicted by Aspen simulations for a Gibbs reactor and the data is shown in Figure 5.13. The equilibrium simulation results show an increase in CO and a decrease in C as the amount of O_2 increased. CO reaches the maximum at SR of O_2 while C reaches zero suggesting that all the O_2 added formed CO by consuming C. This is also supported by the amount CO_2 which flat from the beginning until SR. It is also shown that beyond SR, O_2 is in excess consequently CO is consumed to make CO_2. H_2 seems unaffected until SR when it

starts decreasing also due to excess O_2 in the feed turning it into H_2O as indicated by its increasing amount after SR.

On the other hand, experimental results do not seem to corroborate the simulation findings suggesting that equilibrium was not reached. However there seems to be a similar trend as observed in the simulation; CO increases and goes through a maximum and starts decreasing as more O_2 while C decreases and goes through a minimum point and remain flat. This observation suggests that if the plasma reactor is designed and operated so as to reach equilibrium one would observe similar results as predicted by the simulation. This will make it possible to achieve the targeted material balance with almost 100 % C and H efficiency at SR as predicted by the simulation. This result was not observed at 700^0C, and thus temperature is a major factor in order to achieve the target at SR.

5.4. Plasma Gasification Energy Efficiency

The data on the energy content of the products are summarised in Table 5.4. The LHV of the wood pellets was 5.2 kWh/kg. As can be seen in Table 5.4, at 700 ^{0}C the LHV of the product gas increased with an increase in O_2 feed rate while at 900 ^{0}C the LHV decreased with O_2 flow rate. This may further strengthen the case that the CO_2 at 700 ^{0}C is being formed directly from carbon in biomass or other carbon containing compounds and not from CO. However, this is different for the case at 900 ^{0}C where there is a reduction in LHV when O_2 flow was increased. This may be as a result of either the increase in the formation rate of CO_2 or reduction in the quantity of hydrocarbons formed like CH_4. At 700 ^{0}C the CO and H_2 decrease but the CH_4 increases hence the LHV at 700^0C is increasing Figure 5.4. At 900 CO, H_2 and CH_4

decrease while CO_2 increases thus leading to decreasing LHV and this is shown in Figure 5.4. To some extent, three experimental points obtained at 900 ^{0}C are not enough to conclude this suggestion because at some point CO would start to form CO_2 when more O_2 is added.

The efficiency of the process was also measured in terms of the Mechanical Gas Efficiency (MGE) and Cold Gas Efficiency (CGE). The MGE is a comparison of the calorific value of the product gas to that of the wood pellets and is given by Eq. (5.10). The CGE considers the energy supplied to the process in addition to the mechanical gas efficiency and is given by Eq. (5.11).

$$\text{MGE} = \frac{\text{LHV of product gas}}{\text{LHV wood pellets}} \text{ x } 100, \qquad \textbf{(5.10)}$$

$$\text{CGE} = \frac{\text{Chemical energy content in product gas}}{\text{Chemical energy content in wood pellets + electric power supplied}} \text{ x } 100 \qquad \textbf{(5.11)}$$

The MGE and CGE for the various experiments are summarised for all the experiments in Table 5.4. The MGE and CGE for the experiments at 700 ^{0}C averages around 78 % and 35 % respectively; and that for 900 ^{0}C at about 80 % and 23 % respectively. There is no significant difference between the MGE at the two temperatures but the CGE is significantly lower at the higher gasification temperature. The CGE at both temperatures are low, meaning that only 20 to 30 % of the energy fed to the gasifier is stored in the product gas, the remained is lost, most likely by heat losses at the plasma torch and also as a result of system cooling. Smaller quantities of heat were also lost to the environment directly from the reactor wall through convection, but it was assumed that this was not the major heat loss. The CGE of the

plasma system used was slightly higher compared to that of 18 % simulated by Cohce et al., 2011 for biomass gasification to H_2 from palm oil shell.

Table 5.4: Summary of plasma gasification of wood pellets for 2 kg/h wood pellets at 700 ^{0}C and 1 kg/h wood pellets at 900 ^{0}C.

	Oxygen flow rate (kg/hr)	**0.15**	**0.3**	**0.45**	**0.6**
700 ^{0}C	**Solid; liquid residues(kg)**	0.32;0.06	0.28;0.09	0.27; 0.07	0.24; 0.08
	Biomass conversion %	82	84	83	85
	LHV(kWh/kg) product gas	3.89	4	4.05	4.26
	Mechanical Gas Efficiency (MGE)	75	77	78	82
	Cold Gas Efficiency (CGE)	34	35	35	37
900 ^{0}C	**Solid; liquid residues(kg/hr)**	0.12; 0	0.08;0.01	0.08; 0.02	-
	Biomass conversion %	79	81	80	-
	LHV(kWh/kg) product gas	4.22	4.13	3.96	-
	Mechanical Gas Efficiency (MGE)	81	80	76	-
	Cold Gas Efficiency (CGE)	23	23	22	-

Table 5.4 also shows that the amount of solid and liquid residues measured at the end of each experimental run. The quantity of liquid (condensate) measured increased with an increase in O_2 feed flow.

5.4.1. Heat and Work Analysis

Carrying out an analysis on heat and work requirements for a process is an important study in understanding process efficiency. It helps in understanding the sustainability of the process. This section does an Exergy (E_x) analysis on the experimental results

to determine the lost work, and therefore the degree of reversibility, for the plasma gasification process.

The energy input to the plasma gasifier is via electricity which is pure work and therefore has no entropy associated with it. This work is converted to high quality energy in the form of a plasma. Part of this energy in turn is degraded to heat at the bulk temperature in the gasifier.

In this analysis, the gaseous products are H_2O, H_2, CO_2, CH_4, CO. Char was assumed to be pure carbon, which as seen from Tables 5.2 and 5.3 is not a bad assumption in terms of the mass of the char. This assumption was made in order to be able to estimate the enthalpy and entropy of the char. The tars and condensate were neglected in the analysis as can be seen in Table 5.4 that there are only trace quantities formed. The measured gas composition (H_2, CO_2, CH_4, CO) was used to calculate the H and E_x of the product stream. The amount of H_2O in the gas phase was not detected by the GC and it was assumed that the WGS reaction was at equilibrium at 900 ^{0}C and this was used to infer the quantity of H_2O produced.

There are a number of ways of analysing the energy flows in the plasma gasifier. With reference to Figure 5.1, the feeds to the system are:

- Biomass (wood pellets)
- O_2 and
- N_2

These are all supplied at ambient temperature (measured to be around 25 ^{0}C) and ambient pressure (1bar).

The gas composition is measured after the quench. The product stream leaving the quench is between 40 ^{0}C and 60 ^{0}C at ambient pressure. The gas bulk temperature is measured in the reactor/ gasifier and it was assumed that the temperature of the gas stream leaving the gasifier and entering the quench is at this bulk temperature. The residues leave the gasifier at 25 ^{0}C.

An analysis of the energy efficiency of this system will or could include the irreversibility in the cooling of the torch, the quench and the heat losses of the reactor.

System 1

The system can be defined to include all the equipment and processes between the inlet to the gasifier and the exit from the quench. This can be simplified as illustrated in Figure 5.14.

The lost work from this system, (W_{lost}), would be defined by Eq. (5.12):

$$\sum\Delta G_{out}\,(T_o,P_o) - \sum\Delta G_{in}\,(T_o,P_o) = \sum\Delta E_{out}(T_o,P_o) - \sum\Delta E_{in}(T_o,P_o) = W_e - W_{lost} \qquad \textbf{(5.12)}$$

This W_{lost} would include the E_x of the heat lost via the plasma torch, the quench and the heat losses to the surroundings from the reactor as well as cleaning system.

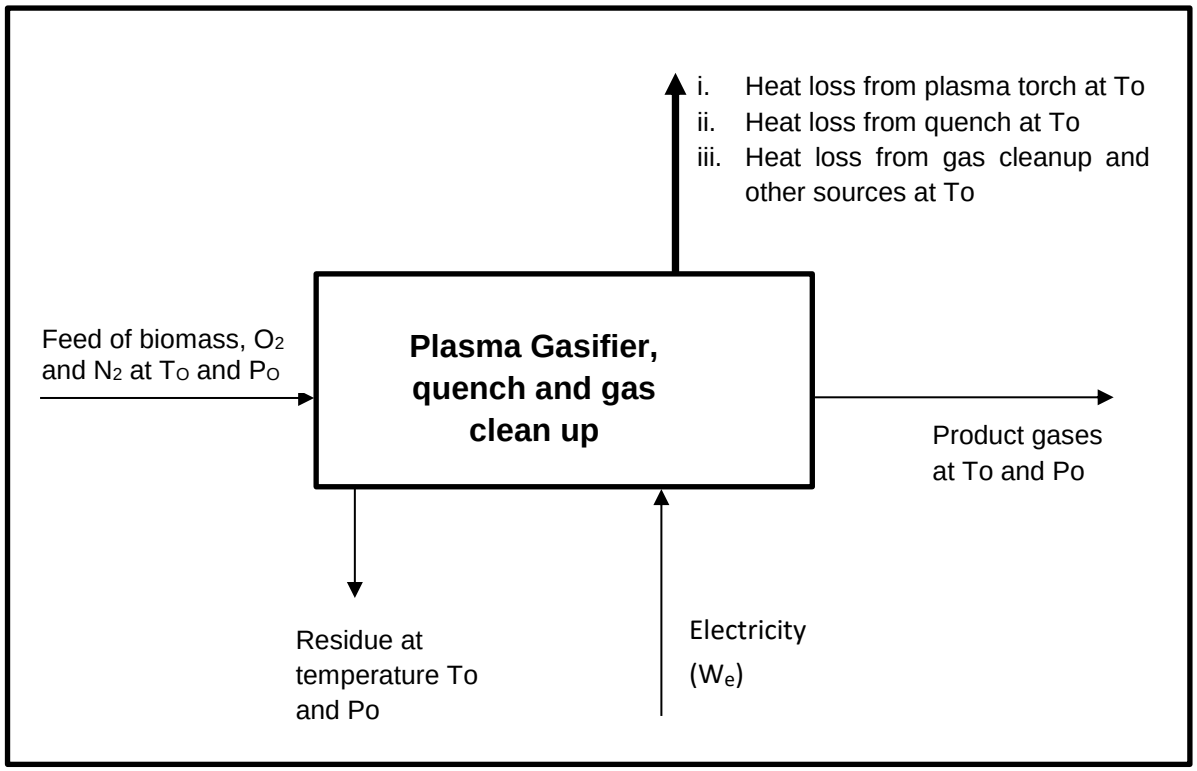

Figure 5.14: Simplified plasma system which includes heat loss from plasma torch, quench and gas clean up system.

System 2:

Assuming that the gas is quenched so fast that the composition of the gas leaving the plasma gasifier is frozen, then the composition of the gas stream leaving the quench would be the same as that leaving the gasifier. In this case, it can be assumed that the gas composition is as been measured and that temperature of the gas stream is at the bulk temperature of the gasifier.

This will allow for the lost work caused by the quench system to be ignored and give a better understanding of the irreversibility of the plasma gasifier on its own. The system that being considered here is shown in Figure 5.15:

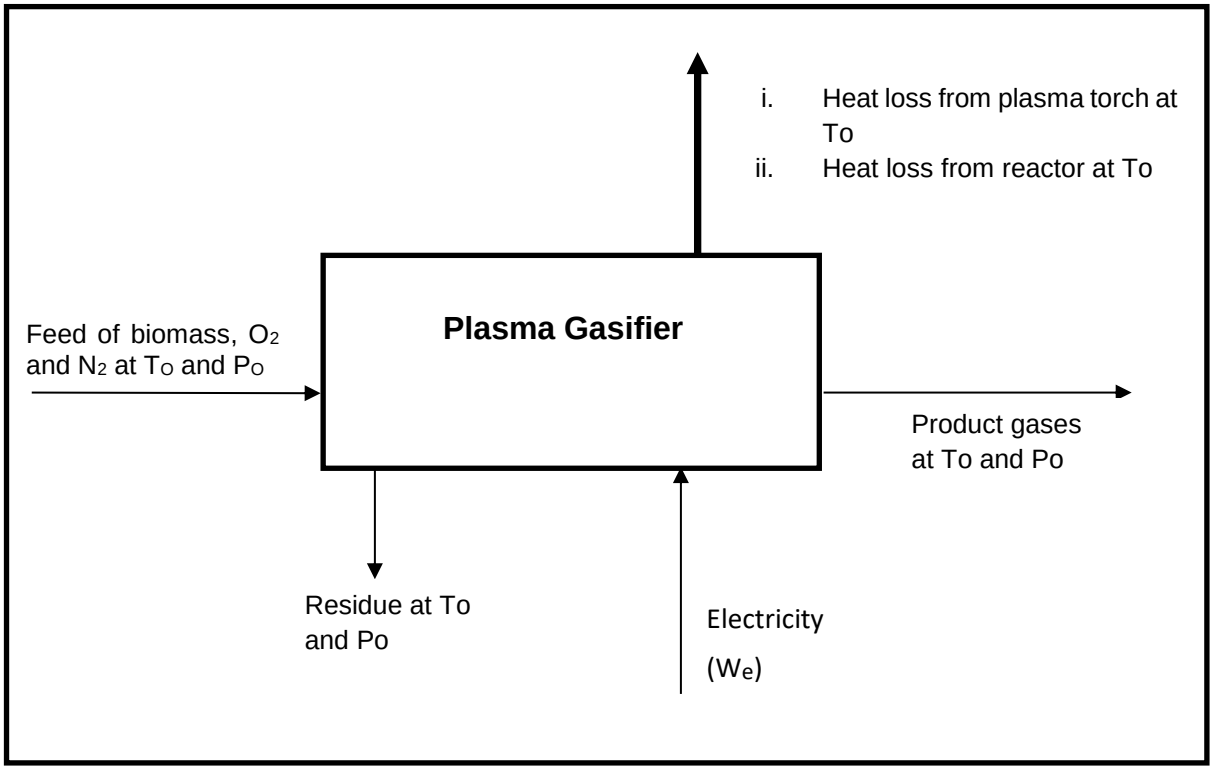

Figure 5.15: Plasma gasifier showing heat losses from the plasma torch and reactor walls.

The lost work from this system, W_{lost}, would be defined by Eq. (5.13) where this would include the E_x of the heat that is lost from the plasma torch as well as reactor walls.

$$\sum\Delta E_{out}(T, P_o) - \sum\Delta E_{in}(T_o, P_o) = W_e - W_{lost} \quad \textbf{(5.13)}$$

Where $\Delta E_{out}(T, P_o) = \Delta H_{out}(T, P_o) - T_o\Delta S_{out}(T, P_o)$ **(5.14)**

$$\Delta E_{in}(T_o, P_o) = \Delta H_{in}(T_o, P_o) - T_o\Delta S_{in}(T_o, P_o) \quad \textbf{(5.15)}$$

System 3

Looking at System 1 and 2, in the experimental set up it was not possible to quantify all the major heat losses around the reactor including heat loss from reactor walls, cleaning section and other sources. Thus, a proper work analysis on these systems

was not considered. However, focus can be put on the minimum energy requirement by looking at the material balance of the process. If An assumption is made that the material only sees the heat at the bulk temperature of the reactor one can then work out how much W (T_{bulk}) is supplied to the drive the reaction in comparison to how much W (T_{carnot}) is needed. In this way there is an idea of the system's performance based on the material balance only without worrying about the losses due to shortfalls in the reactor design.

To investigate the irreversibility of the chemical reactions themselves and the effect of the bulk temperature in the gasifier, then one could define a simplified system shown in Figure 5.16.

In this case, W_{lost} is only taking into account the irreversibility in the reaction as well as simplifying assumption that the heat for the reaction is added at a single temperature. This is rather different from the traditional approach used in modelling plasma gasifiers where it assumed that all the gas passes through the plasma and hence that the reactions all occur at the plasma temperature. System 3 constitute the bulk of the work analysis. The thermodynamic data for this analysis was based on the feed temperature of the wood pellets at 25 ^{0}C while that of the product gas was assumed to be similar to the reactor operating conditions (T= 700 ^{0}C/ 900 ^{0}C all at 1 bar).

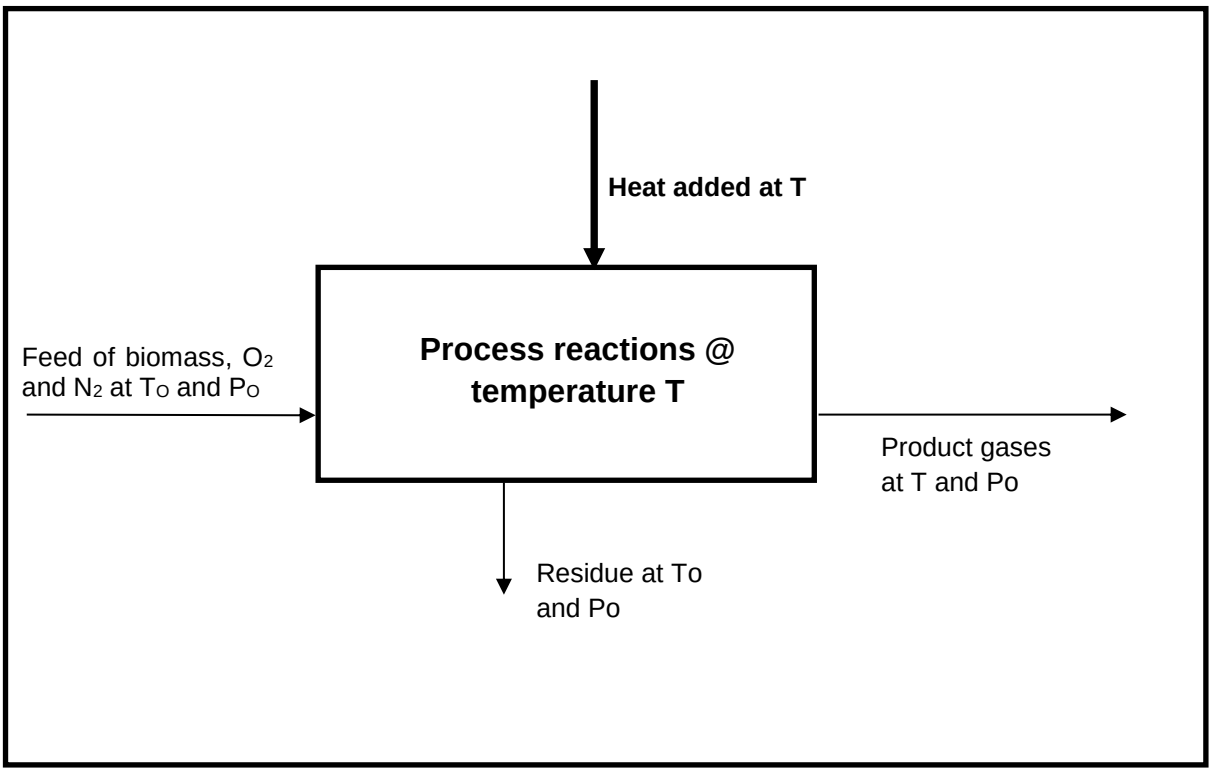

Figure 5.16: Heat and work loss from process reaction.

In this system the energy load for the process is defined by Q in Eq. (5.16).

$$Q = \Delta H_{out}(T, P_o) - \Delta H_{in}(T_o, P_o) \quad \textbf{(5.16)}$$

It is then the intention to find out how much of the supplied energy is actually used during the reaction for converting wood pellets to product gas. In order to determine this, an Exergy analysis is considered, and this will in turn help to find if there is any work that is lost. Firstly, the entropy balance given by Eq. (5.17) is combined with Eq. (5.14) and Eq. (5.15). A reversible process is assumed, and this results in $S_{generation}$ to be equal to zero thus leading to Eq. (5.18). The term W_{lost} represents the irreversibility in the reaction and can be obtained by defining the T in Eq. (5.18) as either Bulk Temperature of Carnot Temperature.

$$S_{generation} + \frac{Q}{T} = \Delta S \quad \textbf{(5.17)}$$

$$\Delta E_{in}\,(T_o, P_o) = \Delta E_{out}(T, P_o) - Q(1-T_o/T) + W_{lost} \quad \textbf{(5.18)}$$

The minimum amount of work required for a process to occur is supplied at a specific temperature called Carnot Temperature. If the heat is supplied at a temperature higher than the Carnot Temperature, then the process is supplied more work than required by virtue of the temperature of the heat (or quality of the heat); if the extra work/heat is not recovered for other uses then the process is irreversible, and the excess work is lost. Exergy calculations can be used when the temperature of the streams entering or leaving the process are not at ambient and gives us information on the work that is needed by the system and work that is actually put into the actual system. This information helps us to determine the reversibility of the process. To have a better understanding of the work flow, a 2-dimensional plot of E_x vs H is used. In order to achieve this, Eq. (5.18) is used where T is now defined as the Carnot Temperature to show minimum work required and/ or T to be the Bulk reactor temperature to show actual work supplied. The minimum work required by the system is given by Eq. (5.19) while the actual work supplied is given by Eq. (5.20) where T is the bulk reactor temperature. W_{lost} would mainly be the difference in work that is supplied to the process to the work that is actually used by the reaction to make products.

$$W_{min\ required} = \Delta E_{(T)} = \Delta H_{(T)}\left(1 - \frac{T_o}{T_{Carnot}}\right) \quad \textbf{(5.19)}$$

$$W_{actual} = \Delta E_{(T)} = \Delta H_{(T)}\left(1 - \frac{T_o}{T_{bulk}}\right) \quad \textbf{(5.20)}$$

The actual work required/supplied to the process for this case is calculated using Eq. (5.18) and Eq. (5.19) respectively. The process temperature is represented by T which is equal to T_{Carnot} when the $\Delta Ex_{process}$ is equal to the minimum amount of work required for the process to occur and T = T_{bulk} when it represents the actual work supplied. T_o represents temperature at 25 ^{0}C.

The heat and work analysis used experimental measured data and the calculations were compared to those obtained with the aid of Aspen Plus V8.6 where the process is the process is assumed to reach thermodynamic equilibrium. An R-Gibbs reactor in Aspen Plus is used to simulate equilibrium composition by using the G minimization method.

Figure 5.17 and Figure 5.18 shows the minimum work required by the gasification process and the actual work supplied to the system, based on the experimental work and the Aspen equilibrium calculation respectively. The difference between the minimum work required and the actual work supplied is the irreversible lost work. The heat and work flows were calculated based on conditions of the feed at 25 ^{0}C, 1 bar while the outlet/reactor temperature (T) was considered similar to that of the reactor. The analysis is based on a calculation of ΔH and change in ΔE_x between the feed at 25 ^{0}C and reactor temperature (T).

The work supplied by the plasma torch is given by the 45^0 line. As the O_2 flow increases, the work supplied line at the bulk temperature gets closer to the work supplied by the plasma torch as shown in Figure 5.17 to Figure 5.20. Ideally, this

means that there is less work being degraded/ lost from the actual work supplied by the plasma torch when the process is at equilibrium.

The results show that more heat energy is required for the process with the lowest O_2 flow rate at both temperatures studied. There is slightly more work that is lost when a high O_2 flow rate is fed to the system compared to lower flow O_2 feed flows. At a feed of 0.6 kg/h O_2 about 250 kJ/mol of excess work supplied is lost compared to the minimum work of 70 kJ/mol that is required for the process to occur. This is in comparison to about 200 kJ/mol that is lost when 0.15 kg/h of O_2 is fed. This can also be explained by the results in Figure 5.4 that clearly show that CO_2 production increases with an increase in O_2 feed flow. The combustion process is irreversible, so the system loses more work as excess O_2 is fed to the system. The reduction in lost work when O_2 flow is decreased can suggest that the difference in driving force between the desired products means that major product leaving the gasifier could be more influenced by kinetics, temperature gradients and might mean that stability of the system is not good. The product distribution would then depend more strongly on the design and operation of the plasma system. However, this irreversibility can also be attributed to the design of the plasma reactor because heat is lost at the plasma torch and also on reactor walls thus not taking part in the actual reaction.

The lost work shown in Figure 5.17 increase from about 200 kJ/mol when 0.15 kg/h of O_2 is fed to about 250 kJ/mol when O_2 feed flow is 0.6 kg/h. The amount of work that is supplied by the plasma torch is given by a 45-degree line marked x in Figure 5.17. Therefore, the difference between the work supplied by the plasma torch and the work that is actually supplied to the reaction by virtue of the bulk temperature of the reaction

is regarded as degraded heat. The degraded heat at the bulk temperature of the reactor is also work that is lost before it gets to the actual process reaction. This could be heat losses around the reactor that may be attributed to the mixing of the hot plasma flame with the cold gas and feed material entering the reactor. This means that the lost work could be heat at a different quality or different temperature that is degraded.

Theoretically, as shown in Figure 5.18, no work is required to the process assuming equilibrium is achieved when 0.6 kg/h of O_2 is fed to 2 kg/ h of wood pellets at 700 ^{0}C. The process actually has potential to produce work (~40 kJ/mol) when making the respective products in the material balance shown in Table 5.2 at 700 ^{0}C. This is shown by the negative value of the ΔE_x which means the process has potential to produce work. Nevertheless, the real process from experimental work shown in Figure 5.17 show that the process required close to 70 kJ/mol of work for the same feed rate of oxygen and wood pellets. The difference of 110 kJ/mol can be explained by the fact that a huge amount of energy is degraded when a plasma is used. This can suggest that the plasma reactor design may need to be improved or the kinetics need to be improved to enhance formation of the equilibrium predicted products.

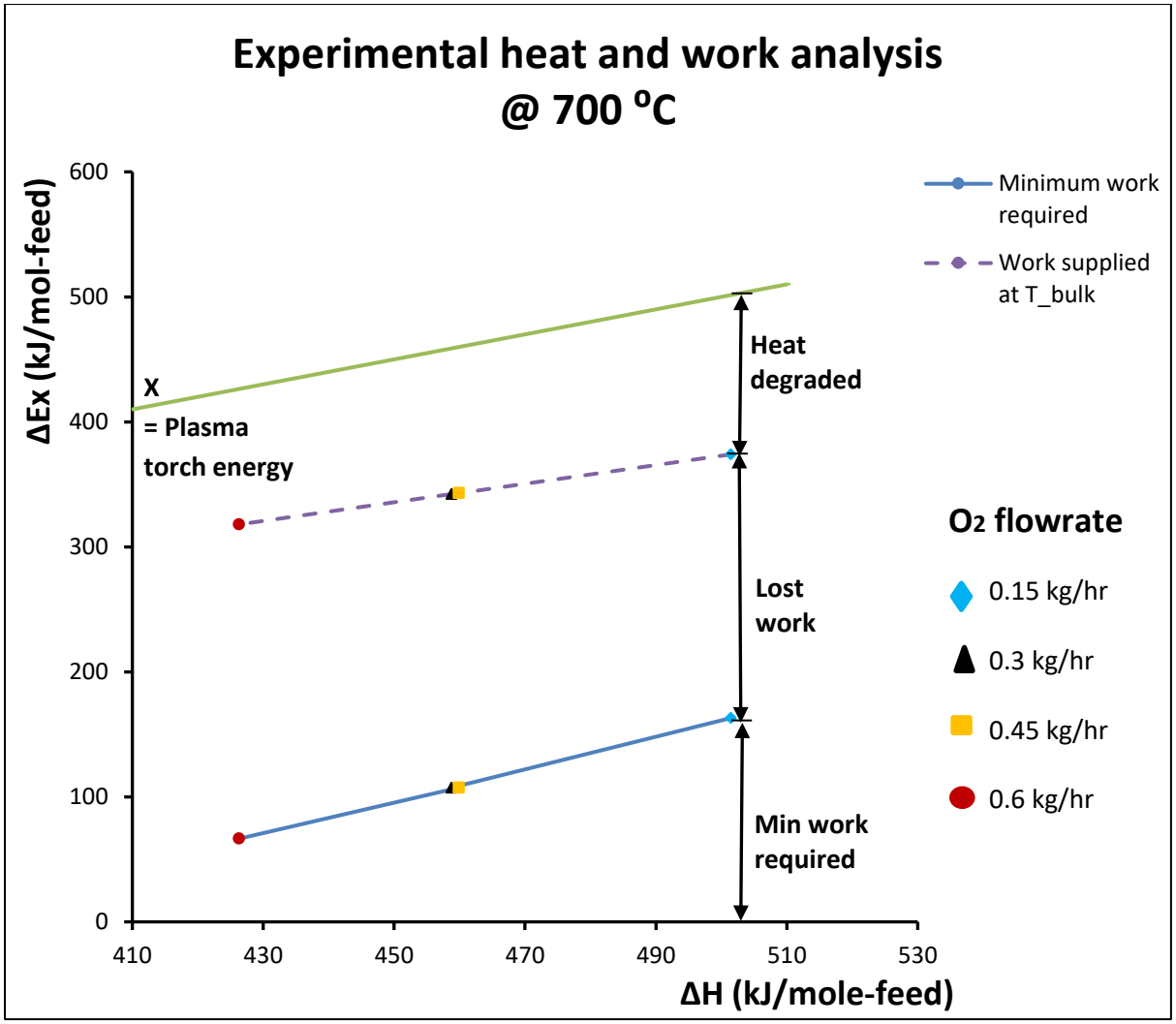

Figure 5.17: Heat and work analysis for the experimental data at 700 ^{0}C. The dotted line is the amount of work added, assuming that the work is added as heat supplied at 700^{o}C. The solid blue line is the minimum amount of work required if the work is supplied as heat only. The green line is the actual electricity consumed by the plasma torch per mole of feed material treated.

The heat and work analysis for the experimental and equilibrium simulations for converting wood pellets to syngas at 900 ^{0}C is shown in Figure 5.19 and Figure 5.20 respectively. The analysis is carried out when O_2 feed flow was increased from 0.15 kg/h to 0.45 kg/h for the experimental part and 0 kg/h to 0.6 kg/h for the theoretical equilibrium calculations.

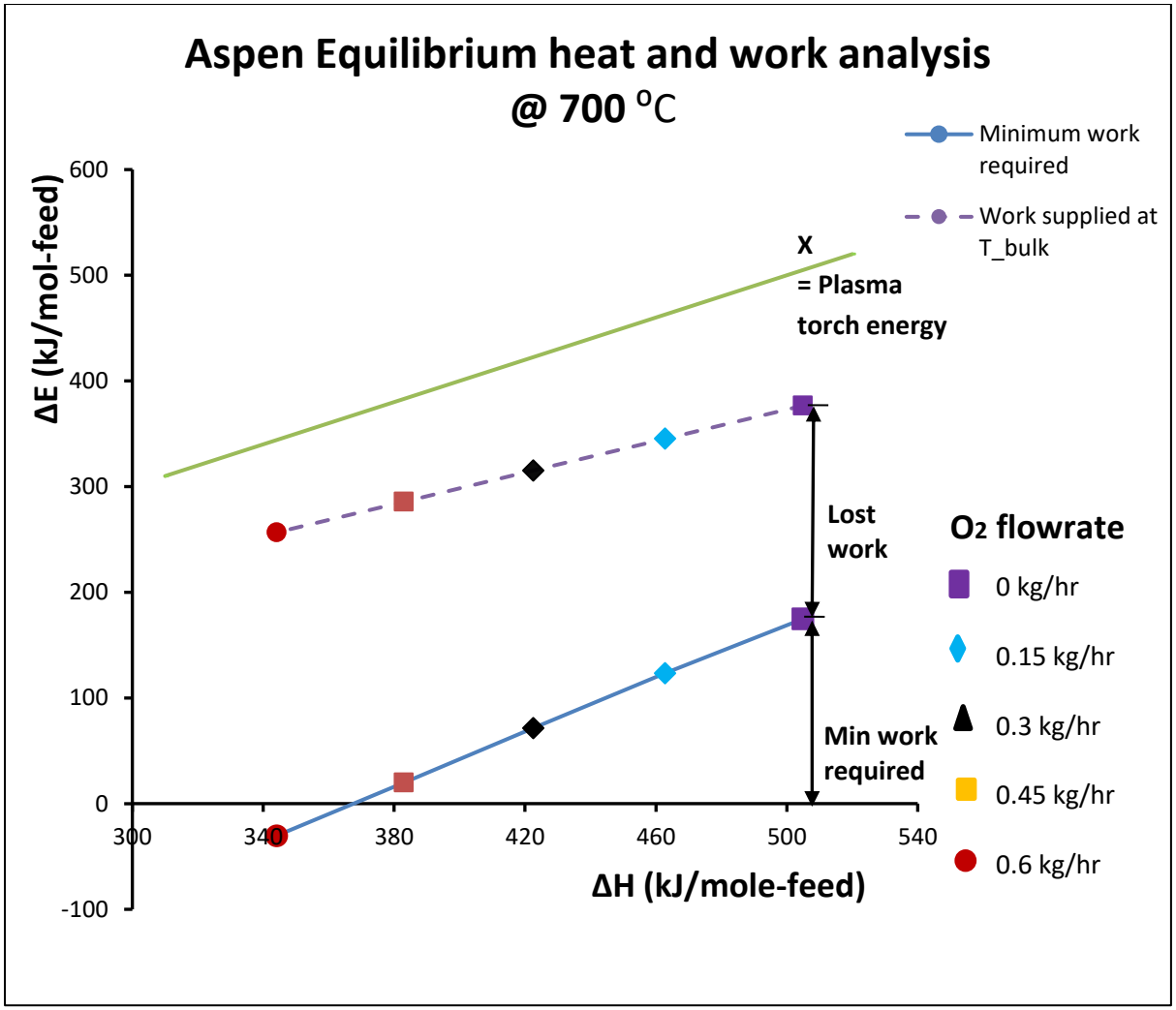

Figure 5.18: Heat and work analysis for the equilibrium data at 700 ^{0}C. The dotted line is the amount of work added, assuming that the work is added as heat supplied at 700^{o}C. The solid blue line is the minimum amount of work required if the work is supplied as heat only. The green line is the actual electricity consumed by the plasma torch per mole of feed material treated.

The analysis of experimental results based on Exergy shown in Figure 5.19 shows that about 80 kJ/mol is the minimum work required to make happen when 0.45 kg/h of O_2 is fed at 900 ^{0}C. However about 360 kJ/mol of work is supplied as heat. This means that about 280 kJ/mol of the excess work supplied is lost. This is also more than the 210 kJ/mol of excess work that is supplied when 0.15 kg/h of O_2 is fed to 1 kg/h of wood pellets. Note that there are three data points obtained from the experimental

work in Figure 5.19 and this is compared to five theoretical data point obtained from simulation Figure 5.20.

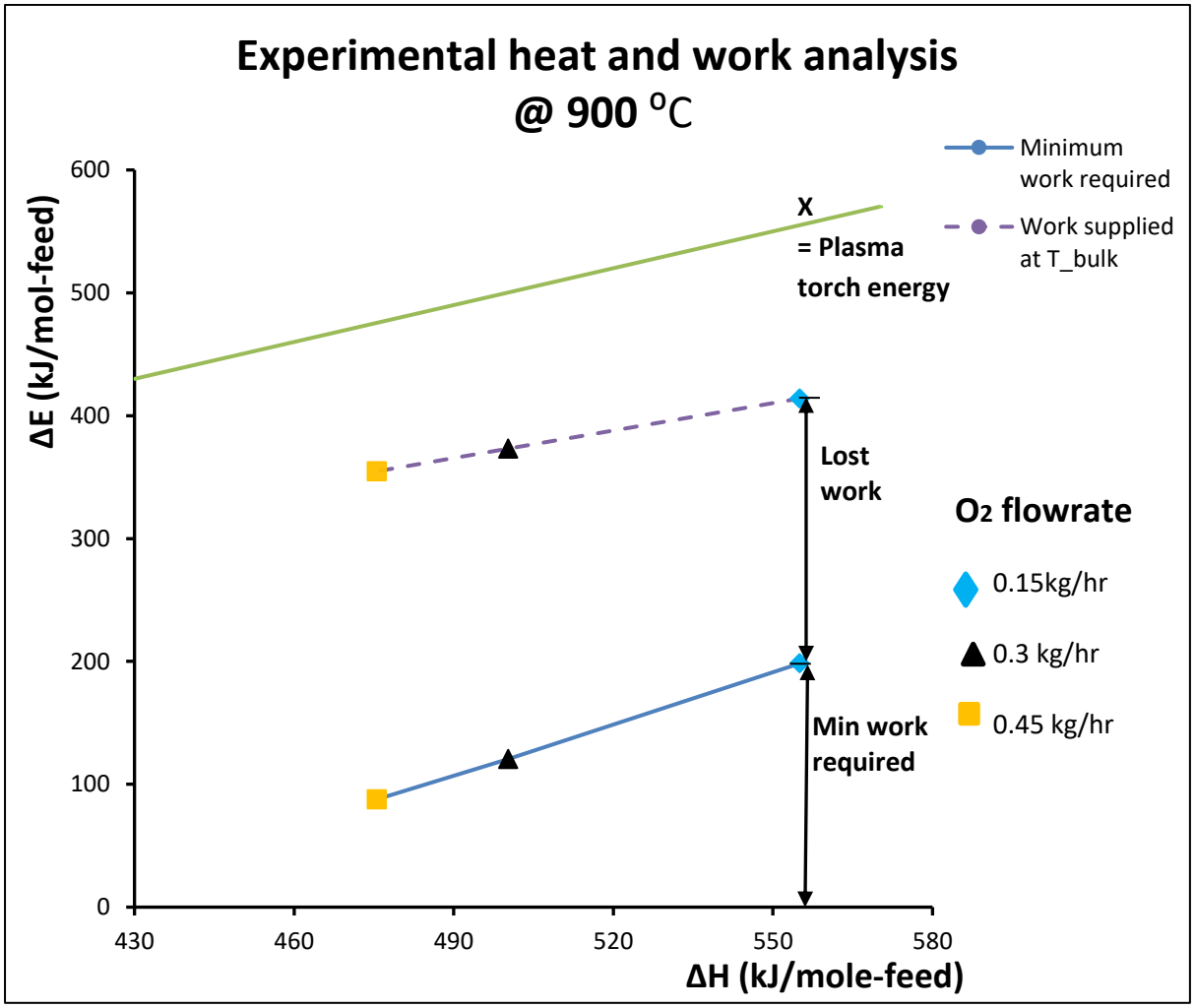

Figure 5.19: Heat and work analysis for the experimental data at 900 ^{0}C. The dotted line is the amount of work added, assuming that the work is added as heat supplied at 900^{o}C. The solid blue line is the minimum amount of work required if the work is supplied as heat only. The green line is the actual electricity consumed by the plasma torch per mole of feed material treated.

Figure 5.20 shows that when looking at the simulation data, there is no work required by the process when the O_2 flow rate is greater than 0.3 kg/h for a feed of 1 kg wood pellets in a plasma reactor. If a thermodynamic equilibrium can be reached, the process has potential to produce work when O_2 flow is increased above 0.3 kg/h as shown in Figure 5.20. This means that if equilibrium is reached, all the work supplied

to the process will be lost unless it is recovered as useful work. Nevertheless, the process still needs a supply of heat energy. To avoid work losses this heat must be supplied at temperatures below ambient which is not possible for a plasma reactor. Therefore, there must be a way of recovering the excess work being supplied to the process for it to be efficient. However, the lost work increases from about 210 kJ/mol when no O_2 is fed (pyrolysis) to about 350 kJ/mol when oxygen feed flow is 0.6 kg/h.

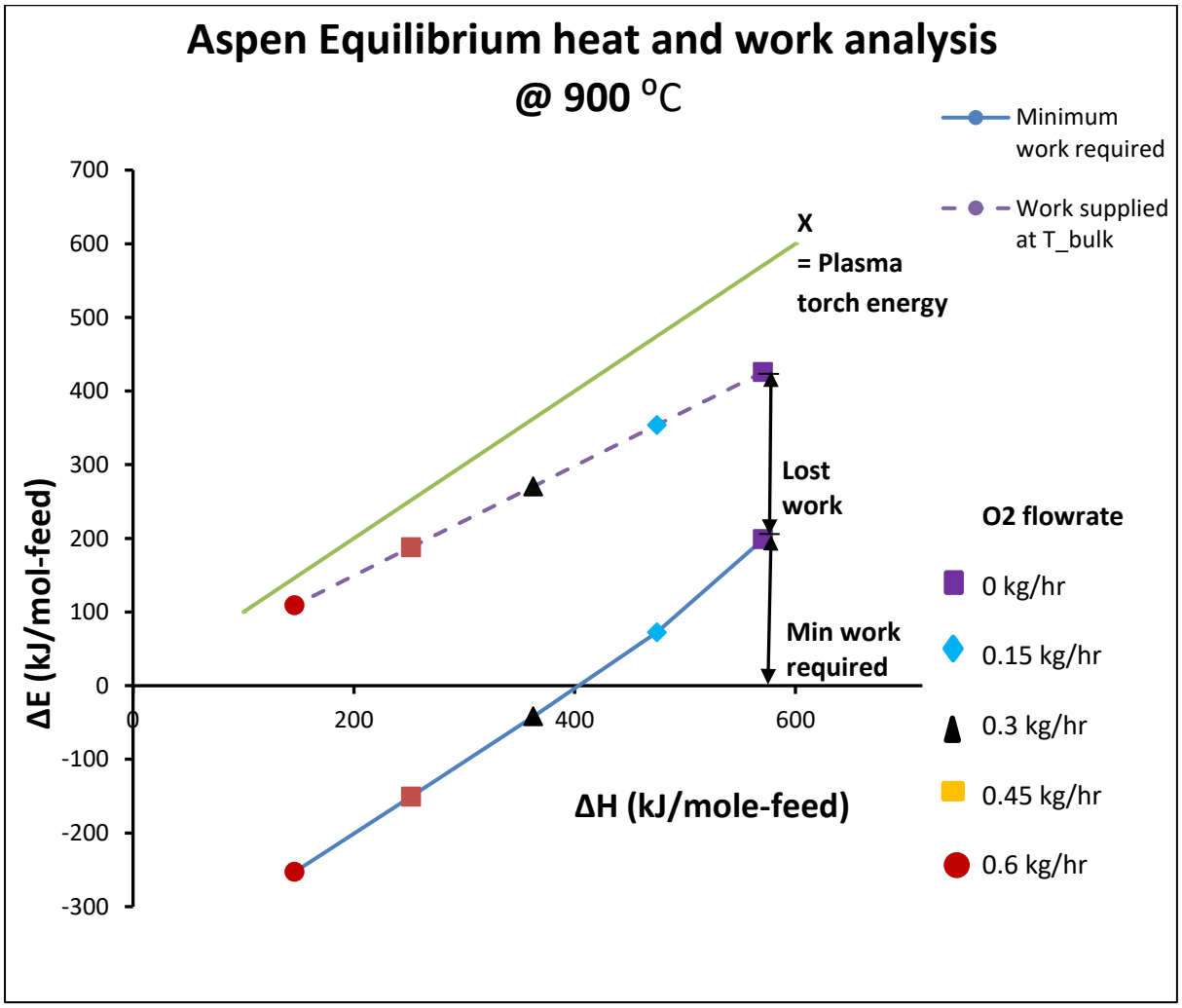

Figure 5.20: Heat and work analysis for the equilibrium data at 900 ^{0}C. The dotted line is the amount of work added, assuming that the work is added as heat supplied at 700^{o}C. The solid blue line is the minimum amount of work required if the work is supplied as heat only. The green line is the actual electricity consumed by the plasma torch per mole of feed material treated.

Comparing the work flow from simulations in Figure 5.18 and Figure 5.20, the heat and work at equilibrium exhibits the same trend but the magnitude of heat required for the process is different. At both temperatures, the more O_2 added to the process, thermodynamically, the more spontaneous the process is. The Exergy becomes more negative as more O_2 is added, meaning that the process does not require any work to happen. Considering the magnitude of the heat that is actually supplied to the process, this means that excess work is being added and is lost. This is because the process increasingly forms CO_2, which is irreversible when additional/ excess O_2 is fed above the stoichiometric requirement of the wood pellets to make syngas.

While the material balance shows the ability of producing a high-quality syngas from the plasma system, a cost benefit analysis of the overall process heat and work flow have to be considered. The composition of both H_2 and CO decrease with increase in O_2 feed. For both temperatures studied, the subsequent increase in O_2 flow results in increase in CO_2 formation. For all processes investigated, heat has to be added to the system because the ΔH is positive. If the work flow is considered, the overall process is not work efficient because more work than required is added to the system which ultimately becomes lost work. A combination of work degraded from the plasma torch and lost work associated with the reaction results in overall process work losses.

An ideal process would require no added work to happen or would produce work that can be recovered and used in other processes. This ideal region would lie where the ΔE_x is negative. From the experimental results that obtained, all processes require work addition to happen. In addition to this, more work is being supplied to the process and cannot be recovered hence, it is lost as irreversibility. For temperatures 700 ^{0}C

and 900 ^{0}C, less heat energy is required to the process when O_2 flow is increased. Because the combustion process is exothermic, it was also the intention to add O_2 to enhance this process and supply some heat energy to the system. This would reduce the amount of energy supplied from the plasma to the system. However, while this was achieved, work is lost, and CO_2 formation increase when more O_2 is added to the gasification process. The composition of syngas at 700 ^{0}C and 900 ^{0}C temperatures are almost similar. For both temperatures, work lost at the respective O_2 flow rates are almost similar while the heat requirements are more by about 20 kJ/mol at 900 ^{0}C. The work requirements at 700 ^{0}C are also slightly lower compared to that at 900 ^{0}C. With this information, one might suggest operating the process at 700 ^{0}C with no/ little amount of O_2 added to reduce on the workload. However, at 700 ^{0}C tar formation was observed while no tars were seen for experiments at 900 ^{0}C. The formation of tars can weigh heavily on process operation and maintenance costs and should also be considered in making a decision. Therefore, the information obtained in this study is important to designers and decision making on considering plasma gasification. It helps one to choose the process condition based on product quality, CO_2 production, heat and work requirements. Nevertheless, a different design of the plasma gasifier or improvement of the existing design may be required to see how the conditions obtained above can change.

5.5. Summary

Wood pellets were gasified in a plasma reactor with the aid of oxygen which was fed at different flow rates. The gas compositions were observed, and the heat and work analysis were analysed for temperatures 700 ^{0}C and 900 ^{0}C. The results show a decrease of the hydrogen yield with a simultaneous increase in carbon dioxide

composition when the oxygen feed flow was increased for a specific amount of wood pellets. As more oxygen is fed to the reactor, the combustion process also becomes increasingly dominant as observed in temperatures studied. Gasification at 700 ^{0}C resulted in tar formation while no visible tars were observed at 900 ^{0}C. This means that temperature has an effect on formation of tars. The mechanical gas efficiency averaged close to 80% for both temperatures while the cold gas efficiency was about 35 % and 23% for the experiments at 700 ^{0}C and 900 ^{0}C respectively. Although all processes still need a supply of heat energy, an increase in oxygen flow rate results in less energy being supplied by the plasma process. This is because some of the energy will be supplied by the combustion process as a result of excess oxygen being supplied to the process. The amount of work lost by the plasma gasification process increases with an increase in the oxygen flow rate. To conclude, adding excess oxygen to a nitrogen plasma reactor result in the combustion process. Although the combustion process is exothermic and supply heat energy to the process with the aim of reducing the energy supplied by the plasma power supply, this action produces carbon dioxide. This also produces heat that is not recovered and also result in the loss of work in form heat. It is therefore suggested to run the plasma reactor with minimum addition of oxygen when feeding in wood pellets. This produces a better-quality synthetic gas and results in reduced work losses.

References

1. Ajay K., Kent E., David D. J., Milford A. H., 2009. Steam-air fluidised bed gasification of distillers' grains. Effect of steam to biomass ratio, equivalent ratio and gasification temperature, Vol. 100 (6), pp. 2062–2068.
2. Arnaud L., Faïçal L., 2015. Allothermal Fluidized Bed Reactor for Steam Gasification of Biomass. Vol. 43(4), pp. 390-428.
3. Cohce M. K., Dincer I., Rosen M. A., 2011. Energy and exergy analyses of a biomass-based hydrogen production system. Bioresource Technology, Vol. 102, pp. 8466–8474.
4. Fabry F., Christophe R., Vandad J. R., Laurent F., 2013. Waste Gasification by Thermal Plasma: A Review. Waste and Biomass Valorization, Vol. 4 (3), pp. 421–439.
5. Gong C., Qian L., Fangjie Q., Bo X., Shiming L., Zhiquan H., Piwen H., 2012. Allothermal gasification of biomass using micron size biomass as external heat source. Bioresource Technology, Vol. 107, pp. 471–475.
6. Gungor A., 2009 Simulation of The Effects of The Equivalence Ratio on Hydrogen Production in Fluidized Bed Biomass Gasifiers .13th International Research/Expert Conference "Trends in the Development of Machinery and Associated Technology" TMT 2009, Hammamet, Tunisia, 16–21 October 2009.
7. Hlina M., Hrabovsky M., Kavka T., Konrad M., 2014. Production of high quality syngas from argon/water plasma gasification of biomass and waste. Waste Management, Vol. 34, pp. 63–66.
8. Hrabovsky M., Hlina M., Kavka T., Konrad M., Chumak O., Maslani A., 2009. Thermal plasma gasification of biomass for fuel gas production. High

Temperature Material Processes: An International Quarterly of High-Technology Plasma Processes, Vol. 13(3-4), pp. 299–313.

9. Lapuerta, M., Hernández, J., Pazo, A., López, J., 2008. Gasification and co-gasification of biomass wastes: effect of the biomass origin and the gasifier operating conditions. Fuel Process Technology, Vol 89, pp. 828–837.
10. Narvaez I., Orio A., Aznar M. P., Corella J., Biomass gasification with air in an atmospheric bubbling fluidised bed. Effect of six operational variables on the quality of the produced raw gas. Industrial Engineering and Chemistry Research, Vol. 35 (7), pp. 2110–2120.
11. Reed T., Desrosiers R., 1979. The Equivalence Ratio: The Key to Understanding Pyrolysis, Combustion and Gasification of Fuels. http://drtlud.com/BEF/EquivalenceRatioDiagram.pdf. [Accessed 12 Jan 2018]
12. Ozgur C., Feridun H., Ibrahim D., Yeong Y., 2010. Effect of gasification agent on the performance of solid oxide fuel cell and biomass gasification systems. International Journal of Hydrogen Energy. Vol. 35, pp. 5001–5009.
13. Vineet S., Ming Z., Peter C., Joseph Y., Xia Z., Mohammad Z M., Nilay S., Edward J. A., Paul S. F., 2016. An overview of advances in biomass gasification. Energy Environ. Sci, Vol. 9, pp. 2939–2977.
14. Worley M., Yale J., 2012. Biomass Gasification Technology Assessment. NREL. Harris Group Inc Atlanta, Georgia.
15. Zhang Q., Dor L., Fenigshtein D., Yng W., Blasiak W., 2012. Gasification of municipal solid waste in the plasma gasification and melting process. Applied Energy, Vol. 90(1), pp. 106–112.

Chapter 6: The Impact and Challenges of Sustainable Biogas Implementation: Moving Towards a Bio-Based Economy.

The results of this chapter have been published in the Journal of Energy, Sustainability and Society cited as **Ralph Muvhiiwa*,** Diane Hildebrandt, Ngonidzashe Chimwani, Lwazi Ngubevana and Tonderayi Matambo. *Energy, Sustainability and Society* 2017/ **7**:20 https://doi.org/10.1186/s13705-017-0122-3

I was the project leader and carried out the survey as well as writing the paper, the other authors are my supervisors and members of Engineers Without Borders-Unisa. The Muldersdrift community as well as Engineers Without Borders-Unisa also helped with putting up the structure that led to the survey results.

Abstract

Engineers face increasing pressure to manage and utilise waste (whether of animal, human or municipal origin) in a sustainable way. We suggest that a solution to the problem of organic waste in rural communities lies in their being able to convert it to biogas technology. This would offer smallholders and farmers a long-term, cheap and sustainable energy source that is independent of the national electricity grid. However, although the technology involved in making biogas from waste has already been fully developed, there are obstacles impeding its adoption. Firstly, there is a general ignorance about this source of energy among the very people who can most benefit from using it. Secondly, at present, South Africa has no regulatory framework to support the installation of biodigesters. The research focused on the current gap between knowledge and need. The two objectives were to raise general awareness of the many and varied benefits that biodigestion can offer, especially to rural communities; thus, demonstrating how it works. Using science events as a platform,

the team introduced the concept of biodigestion, its functioning and uses, to their audiences, and then invited informal responses, which were recorded. The second stage, the case study, entailed the setting-up of a small-scale ($10\,m^3$) household biodigester in the Muldersdrift community in Gauteng, South Africa. It was put into operation, using fresh cow dung as the feed. Members of the community were invited to watch every step of the process, and afterwards were asked to participate in a more formal survey, which sought their opinions on whether biodigestion offers a power source the individual farmer could (and would) use. The results presented in this paper were derived from a comparison of the 'before-and-after-installation' responses of the persons interviewed. We found that the members of the Muldersdrift community who had been involved in both phases of the case study (explanation followed by experience of a hands-on educational example) had become more willing to adopt the technology. The results justified our contention that, to ensure a greater adoption of biogas technology in South Africa, it is necessary to provide targeted communities with educational programmes and exposure to pilot plants.

6.1. Introduction

Although conversion of waste to biogas is an established technology, it has been under-used, probably because until recently, electricity was relatively affordable to most of the population in South Africa. However, the increase in both the demand for, and the cost of electricity, has prompted engineers to revive their interest in rolling out biogas technology in South Africa Musyani, (2013).

A salient reason for advocating biodigestion as an alternative source of energy is that electricity is not available in all parts of this country. Approximately 2.328 million

households, estimated by Triebel and Damm (2008) as representing 25–30% of South African families, meet their energy needs with traditional fuels such as firewood and charcoal Triebel and Damm (2008). Most of this group live in deprived circumstances in the urban slums and rural areas but have no knowledge of biogas technology.

The overarching purpose of this project was to test the hypothesis that if biogas can be fully exploited, it can supply a means of overcoming energy poverty in rural South Africa. It can also help reduce biomass waste that is sent to landfill and also reduce methane emissions.

The author reasoned that in order to introduce biogas to South Africans who lack access to a power supply, the first requirement must be to introduce them to the concept of biogas; the second being to teach them how the technology works. They started the process by identifying rural communities that did not have access to electricity, with a view to introducing them to the nature and functioning of biodigesters. A collaborative approach was applied throughout, and community members were asked for their views and queries about biodigestion; both before and after the pilot digester had been commissioned.

It is worth noting that our project was in alignment with South Africa's Development Plan (NDP) and bio-economy strategy, which aim to promote bio-innovations to achieve a sustainable economy based on biological resources, materials and processes. The production of biogas is also synchronous with the United Nations Sustainable Development Goals (SDG), especially goals number 1 and 7, which require that this technology can help reduce socio-economic poverty by providing

clean energy from renewable sources. South Africa is also signatory to the Kyoto protocol, which undertakes to cut back greenhouse gas emissions by 34 % by 2020 and 45 % by 2030 Munganga, (2013).

6.1.1. Biogas as an energy solution to rural South African communities

Due to the current energy shortages and cost of raising capital in South Africa, it is likely that the national power supply company (ESKOM) will be unable to continue expanding its network into the rural areas. This has given impetus to the search for alternative energy sources. Biogas offers a cheap, renewable and viable solution to the problem of providing energy to rural communities and farmers Tiepelt, (2015), and also has the merit of using waste that has been traditionally regarded as useless as the feedstock.

The technology involved in biogas production is fairly simple and can be implemented cheaply and efficiently by means of small-scale digester that are easy to use and maintain. These household biodigesters can offer benefits to all spheres of society but have a particular bearing on the needs of farmers in rural areas. They can use the gas produced for cooking and lighting, for charging batteries from running biogas generators and for fertilizing crops with the residual waste.

Another reason for identifying this group as most suitable for putting the biodigestion technology into practice is that small-scale farmers generally have free access to livestock waste, which provides feedstock for the digester. Normally, rural households use the raw manure obtained from their animals as a form of plant fertilizer, but this has a lower organic nitrogen content than the slurry created by the biogas digestion

process (Le., 1998; Johansson 2008; Nørgaard Anna Dorte and TybirkKnud (2014)), which is odourless, and makes a better fertiliser.

Also, the combustion of biogas provides a clean source of energy as it does not produce soot, like firewood. This helps reduce indoor air pollution, which in turn prevents respiratory infections and associated diseases Cassie, (2010). According to an evaluation by Pal 2002 in India, a biogas digester producing 2 cubic metres of biogas per day can replace approximately 270–300 kilograms of firewood per month, depending on the quality of the biogas. Studies of the domestic use of biogas carried out in rural areas in Zimbabwe and Kenya (Matsvange, (2016); KDBUS, (2014) also found that using biogas for cooking was more time-efficient than conventional fuels and this was a key factor in the willingness of people to adopt it. Although time is required to collect waste and feed the digester, it is a much shorter period than the equivalent required to gather firewood and charcoal.

Perhaps, the most important of its many advantages is that biogas can offer a decentralized energy solution to rural communities in South Africa.

6.1.2. The barriers to expansion and acceptance of biogas production in South Africa

There are currently around 700 biodigesters in South Africa Tiepelt, (2015). About 50% of these are small-scale domestic digesters, and only 10% are commercial installations Tiepelt, (2015). The remaining numbers, representing approximately 40%, are installed at wastewater treatment plants. There is still much room for further expansion but various difficulties, not connected with the technology as such, impede

it. The political and regulatory aspects of making access to biodigestion possible in South Africa are discussed briefly in a later section.

The focus of this article is on a key issue discussed during the National Biogas Conference, hosted by the Southern African Biogas Industry Association (SABIA) on 5 March 2015: the lack of awareness and understanding of biogas as a form of energy in the general public, which hinders the expansion of this technology in this country SABIA, (2015). It was this point on which the project was based.

Currently, most people who have the raw materials readily available, do not have any knowledge of biogas technology. It is therefore important to educate them by first explaining and then demonstrating this technology to rural communities. This would allow the team to deal with some misconceptions that smallholders and farmers might have about biogas, increase their understanding of the technology, and consequently enable them to realize the benefits it offers. Their acceptance of its usefulness is essential to their willingness to adopt biogas as a source of energy.

It is very difficult to devise a strategy with which to approach communities if the promoters have no understanding of the pre-perceptions and concerns of the farmers themselves. For similar reasons, the uptake of bio-digesters in other African countries is not high. In Kenya, biogas technology is not new, but the adoption process is still slow, owing to inadequate funds, poor infrastructure and a general ignorance of this technology among the people who might derive the greatest benefit from it KDBUS, (2014).

For all of the above reasons, the project designed by our team entailed two steps that would enable us to understand better how to increase the acceptance of biodigester technology within rural communities in South Africa. The first was to establish the level of knowledge about biogas technology in schools and rural areas. The second was to examine the differences in the views and responses of members of a rural community after the installation of a biodigester in their vicinity. A small-scale bag digester (approximately 10 cubic meters in volume was set up in the Muldersdrift community by a team from Engineers without Borders, based at the University of South Africa (EWB-Unisa). The feedstock for the biodigester was fresh cow dung. The performance of the bio-digester was rated according to the typical energy requirements of a household, such as gas cooking, lighting, and heating water.

6.2. Methods

6.2.1. Survey methodology

The first, informal survey followed a qualitative approach, because the team wanted to gather information on which they could base, and interpret, the quantitative approach used in the second survey (Jones., 1995; Newman., 1998; Bryman., 2012; Johnson and Christensen (2012)). The first was based on the spontaneous responses of participants in the science conferences to the concept Blankenship, (2010). (This type of approach allows the researcher to focus his or her efforts on gathering rich data from answers to the research questions). The second, more formal survey focused on the actual experience of smallholders and farmers witnessing the installation of the biodigester, the way it worked, and their assessment of its utility.

Step 1: Survey of perceptions concerning biogas technology

In order to understand the level of knowledge communities in South Africa have on biodigester technologies, the writers took part in four of the country's biggest science events, including "The Science Festival Africa" in Grahamstown and "The Sasol Expo" in Sasolburg, within a space of two years (2015–2016). The conferences were mainly held in small towns, located in predominantly rural and agricultural areas. The exception was Sasolburg, which is part of the so-called Vaal Triangle, which is highly industrialized, but is surrounded by agricultural land. Many people, largely comprising school pupils and members of the surrounding farms, attended these events. At all these events, a simple cardboard model of a biodigester (shown in Figure 1) was used to introduce those present to the nature and function of biogas and to invite their feedback. The purpose was to elicit what knowledge they had of biogas, their perceptions concerning it, and how safe they thought it was. There was no set questionnaire: it was an informal survey to determine people's responses to the idea of biogas. The researchers were particularly interested in finding out whether they were aware of biogas technology and its uses, and, if so, what level of understanding they had achieved. For those who had never come across the concept, they were questioned to gauge their reactions to it. Our central objective was to find out whether, or under what circumstances, they would embrace the idea of biodigestion. This approach is also very similar to the process synthesis approach used in chemical engineering to identify the most important factors in a complex system relatively quickly (Fox et al., 2013).

Figure 6.1: Simple display used by EWB-Unisa at the Science Expos to discuss biogas technology.

While step one involved ascertaining the knowledge of biogas technology in attendees at the science events, step two entailed a practical demonstration of how the technology works. The team did this by involving some members of the local farming community in the building and commissioning of a pilot biodigester.

Step 2: Case study –implementing biogas technology in a rural/farming South African community

6.2.2. Case study location

The researchers from the team had met a small-scale farmer in Mulderdrift when they were looking for manure for their laboratory experiments on anaerobic digestion to produce biogas. He had shown interest in what they were doing, as he had never heard of biogas before. Over time, he became familiar with the team and the work they

were doing and was very enthusiastic about seeing how a digester, built on his land, would work in practice.

A small-scale biodigester was built by the EWB team on a small farm in Muldersdrift, on the outskirts of Johannesburg. The area surrounding the location of the biogas plant comprises both agricultural allotments and farms It was from a catchment area within an approximately 3 km radius of the plot on which the digester was to be built that we recruited local people; mainly farmers and farm workers, who were willing to participate in our study. No specific criterion was used to pick those surveyed and the general answers we were given by the respondents were obtained through informal conversations/purposive sampling. These are shown in a later section of this research paper, when the “before” and after” stages of the surveys are compared.

6.2.3. The design and implementation of the biodigester

The biodigester chosen for the Muldersdrift experiment was of the biobag variety, because it is easier to maintain than a fixed dome brick digester. The design used a large biobag (made of durable reinforced and bacteria-resistant polyvinyl chloride (PVC) which can have a lifespan of more than 15 years). The biodigester is 8 metres long and has a diameter of 1 metre. Two manholes were constructed, using cement bricks to form the biodigester inlet and outlet. The digester (PVC) bag was then connected to the inlet and outlet using 25 cm diameter PVC piping. The biodigester bag was placed in a trench that slopes slightly downward from inlet to outlet, so that the inlet pipe was placed 20 cm higher than the outlet pipe. This was necessary for two reasons: the biodigester operates by means of gravity displacement; also, the difference in height forms a liquid seal preventing air from entering through the inlet

pipe into the biodigester. This system is simple to construct when compared with the conventional dome-shaped biodigester design. Another advantage of this type of biodigester is that the actual digester is made from light-weight PVC plastic and the only major construction effort required is digging the manholes.

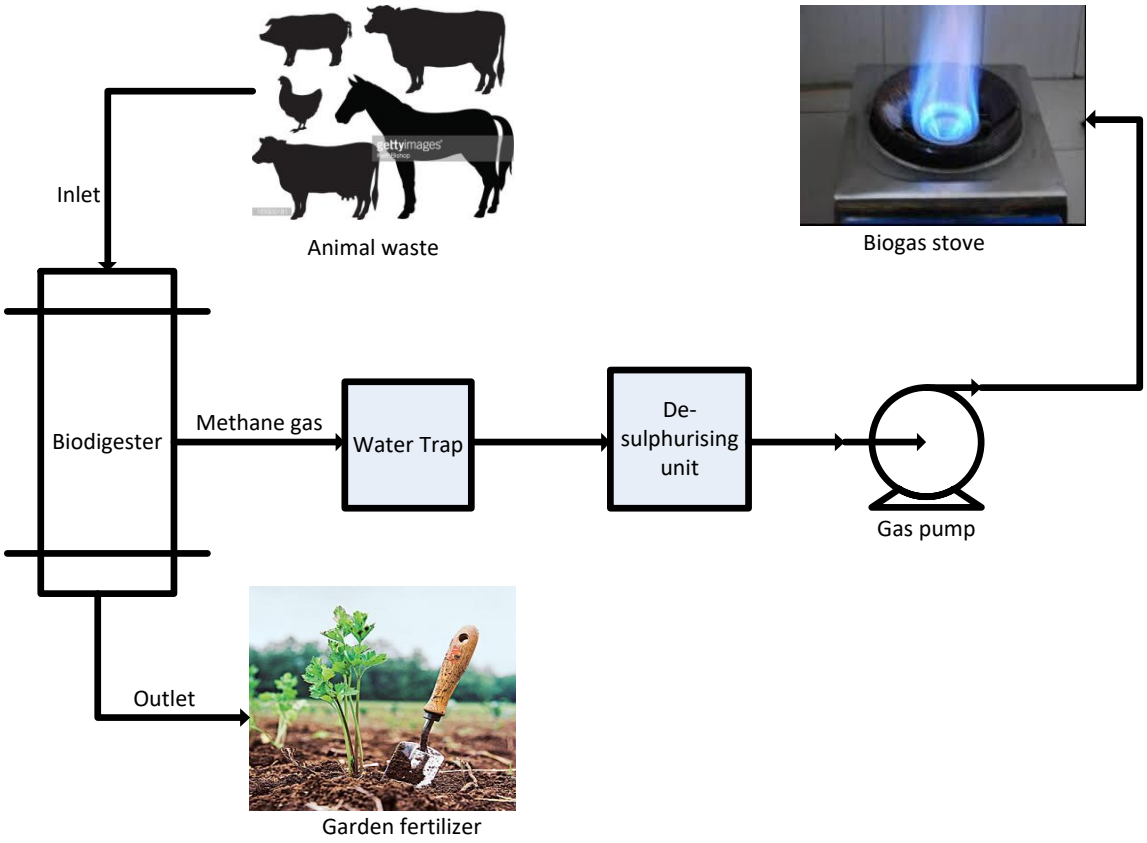

Figure 6.2: Typical small-scale biodigester system for rural operation (pictures from getty images).

Once a digester has been installed, fresh animal dung is collected and mixed with water in a ratio of at least 1:4 by volume to form slurry. The cow dung is collected from a cattle kraal where the animals sleep at night but graze on a free-range paddock during the day. (Incidentally, a drawback of the biogas process is that it requires a lot of water.) Twenty litres of slurry are fed every two days to the biodigester. The digestion retention time is around 20-40 days, during which time the waste material is broken down by a consortium of the bacteria that occur naturally in the manure, to

produce biogas (mainly methane and carbon dioxide) in the absence of oxygen. As the waste begins to digest, the biogas produced inflates the biobag and the gas is released through a valve to piping that is connected to the appliances in the farmhouse. The gas passes through a pressure pump (alternatively some weights, typically old tyres, are placed on the biobag to build up a pressure of 2.5 KPa, which is the minimum needed by the biogas stove or lamp). The gas pipeline also passes through a moisture trap and a desulfurising unit, which can be made by using a container filled with iron filings. All these small units are needed before the gas can be used and all are cheap to manufacture. The whole process is presented in Figure 6.2 and a picture of the inflated bag is shown in Figure 6.3.

The digester used was supplied by Biogas SA, and (as already noted) is simple to install and operate. The cost of a full kit imported biobag was about ZAR16 000 (USD $1120) in 2015/2016. Although this is a once-off cost, this amount is beyond the reach of many rural households. However, bricks can be moulded locally and if cement can be obtained, a cheaper type of digester can be built for a small household.

6.2.4. Performance of the biodigester

The biobag has a gas volume of about 4-5 cubic metres, and its output comprises around 53% of methane gas concentrate and the remaining 47% of carbon dioxide available for use per day in summer, when the temperatures average 25–30 ^{0}C. This gas can be used for a cooking for 2–3 hours a day and provides about 2 plus hours a day of lighting (using a gas lamp). The farmer can also use the gas to run a 700 W biogas generator for an hour per day (he can use this for battery charging) as well as to heat water for bathing in a 7 l/min gas geyser. The amount of water heated was

sufficient for the use of three adults. The digester is fed with a 20-litre amount of fresh waste slurry every second day, which is enough to supply the gas requirements of the household. The use of biogas saves the farmer about 1 hour per day, as he no longer has to spend time fetching and preparing firewood.

In winter, when temperatures are low (~15^{0}C), the range of usage becomes more limited, as the digester produces only enough gas for cooking. No gas is produced when there is frost (<10^{0}C) because the activity of the methanogen (mesophiles) bacteria reduces with a drop in temperature and becomes completely inactive at temperatures lower than 10 ^{0}C (Teodorita Al Seadi et al., 2008). The waste that is fed into the biobag during the coldest months can take up to 30 days to digest and produce gas, so that the waste that the farmer feeds in today will produce usable gas only in about a month's time.

Figure 6.3: Typical operational biodigester at the small-scale farm in Muldersdrift, Johannesburg, South Africa.

6.2.5. Community survey after exposure to biogas technology

Throughout the step-by-step construction and operation of the digester, we explained to the community members how the production of the biogas gas takes place, and the different ways in which it can be used. We made clear that although bacterial activity helped to produce the gas during the decomposition of waste materials, the resultant gas did not contain dangerous bacteria. After this two-phase introduction had been completed, most of the participants indicated that they would adopt the technology if it would save them more time and money than relying on traditional sources of energy.

The post-installation survey took the form of a qualitative, cross-sectional study with purposive sampling. The research data were obtained from about 25 people and took the form of a questionnaire that aimed to assess whether they had a basic knowledge of science, what they knew about biodigesters, and their attitude towards biodigester technology and science in general. None of the respondents to this survey had visited any of the Science Expos. The demographics concerning race, age and their rating according to the Living Standards Measure (LSM), which is commonly used in South Africa were looked at. Some of the questions concerned the energy sources currently used by each respondent and the problems connected with employing them. One of the key questions asked concerned the respondent's access to feed, water and the transportation of biodigester feed. It was also important to establish the main income-generating activities of each participant, as well as his or her ability to maintain the digester. Other questions involved the capability of the participant to adhere to the safety regulations for biogas use, and his or her keenness to learn more about the technology.

6.3. Results

6.3.1. Results of Surveys from Science Expos

The survey conducted at the science events, revealed that less than 10% of the high school pupils interviewed had any knowledge of biogas technology. What was also very surprising was their resistance to the concept. Most students said that the technology was not possible, and also not "ethical". These students were concerned about the source of the biogas. They thought that since it is made from manure (or

worse, sewage) it could be contaminated and use of the biogas could cause illness. The local farmers surveyed also appeared to have little knowledge of the biogas technology but, in contrast, they were very willing to learn and implement it if it offered any benefit to them. An important aspect for the farmers was their wish to see a working biodigester unit and also to have a clear understanding of the economics concerned before they implemented the technology. At the science event in Sasolburg 2016, students from 7 out of 46 schools' survey had knowledge of biogas. Although Sasolburg is industrialized, and the community in the area seemed to have some awareness of biogas, they still lacked information about it and had had no exposure to this technology.

6.3.2. Results of the Muldersdrift case study

Initially, 64% of the respondents - including the owner of the farm on which the biodigester was located, had no knowledge about the nature and application of biogas while the balance knew about biogas. The remainder had seen programmes on the subject on television, while others had read about it.

It was clear from the data that there is also lack of proper structures that can help to inform people about the advantages of using biogas, because the majority of respondents to the first survey had no knowledge of this technology. This is especially true in rural areas where people have access to the required waste materials.

Also, information on biogas is mostly available only to researchers, not the potential users of this technology. This poses the need for us to bridge the process of turning the technology and research into practice in South Africa. The opinion expressed by

SABIA on this issue is that in order to boost the public's awareness and understanding of the biogas technology in South Africa, a great deal of financial support will be required SABIA, (2015). This has not so far been forthcoming.

The case study found that after the educational process, most community participants indicated that they would adopt the technology if it would save them more time and money than the sources of energy currently available to them. Our analysis of the case study results showed that there were a number of key themes that emerged from the answers of most of the respondents.

6.3.3. Community survey pre-installation

6.3.3. Key themes

These themes (below), are discussed individually and are based on pre- and post-implementation responses.

6.3.3.a. Feedstock availability

It was clear from the survey data that there was a pervasive perception that biogas technology works only for people who have sufficient animal and agricultural waste available to them to obtain a reasonable quantity of gas for energy. This perception is definitely not unfounded. However, crop production and animal husbandry are predominant in the rural areas and farms, so this section of the population can find ways to tap into this supply of material. About 68% of respondents, many of them farm labourers or workers in the area, mentioned that although they did not own livestock, they were willing to travel to collect animal waste from neighbouring farms.

6.3.3.b. Hygiene-related concerns

Many of those surveyed expressed concern that biodigestion is unhygienic, as one uses smelly and bacteria-infested waste to produce energy. Although the pre-implementation data was not quantitatively recorded, more than 50% of the people surveyed after the science events expressed worry and doubt that biogas was hygienically acceptable. They feared that they would be exposed to contact with the (dangerous) bacteria in the waste material; for example, while preparing the slurry feed for the digester or during cooking. Such exposure, they believed, would be harmful to their health.

However, after the installation, most of the people who had seen how the technology worked had accepted that it posed no health risk. Figure 6.4 show that 88% of the respondents do not have any concerns about the hygiene of using biogas technology for cooking purposes. Although these data do not allow an accurate comparison of pre- and post-perceptions of the risks of changing to biogas, the researchers were confident that they had seen a positive change in mindset.

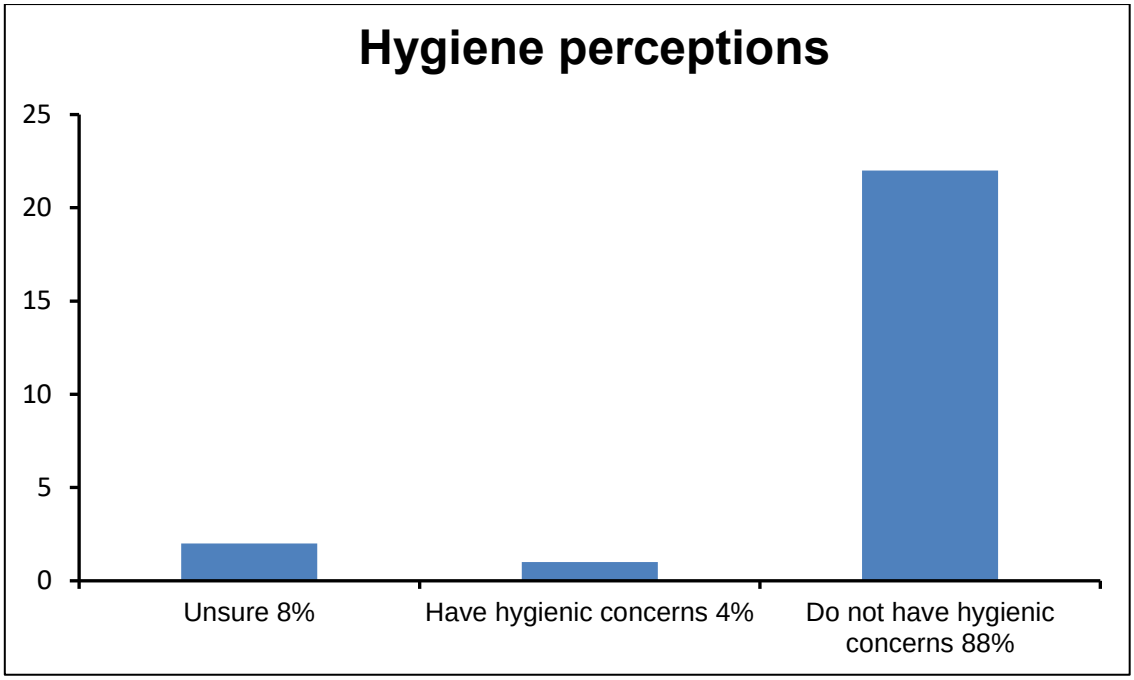

Figure 6.4: Post implementation, hygienic perceptions about the use of biogas post implementation.

6.3.3.c. Access to energy

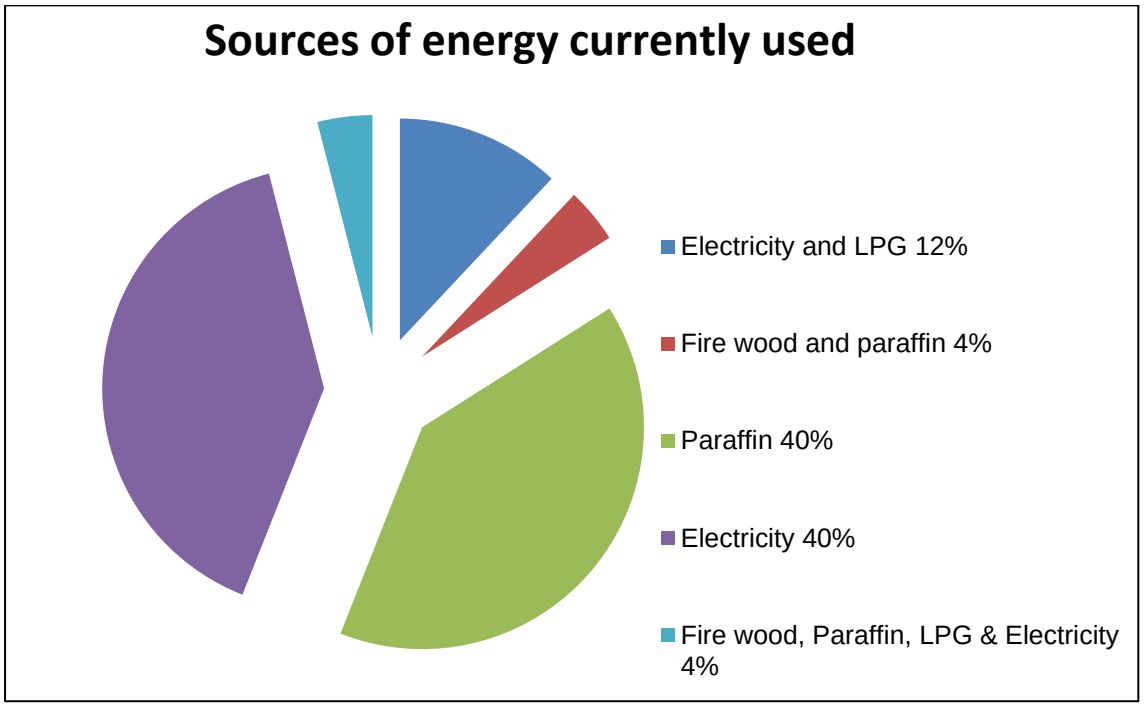

Figure 6.5: Post implementation, sources of energy currently used.

Another prevalent theme raised in the pre-implementation survey was that community members are accustomed to using traditional energy sources like coal, paraffin and firewood. Consequently, they see no reason why they should shift to biogas.

The survey, as presented in Figure 6.5, shows that 80% of the people in the community use electricity and paraffin as a source of energy. The owner of the farm where the digester was installed had used firewood, electricity, paraffin and LPG interchangeably for cooking. Currently, after the installation of the biodigester at the farm, 100% of the farmer's energy supply for cooking comes from biogas, except in winter when gas production is low. Post implementation, after seeing how the technology works, 92% of the respondents indicated that they would be willing to change from their traditional sources of energy to biogas for cooking (Figure 6.6). Only one person indicated a refusal to change to biogas, preferring to continue using his current source.

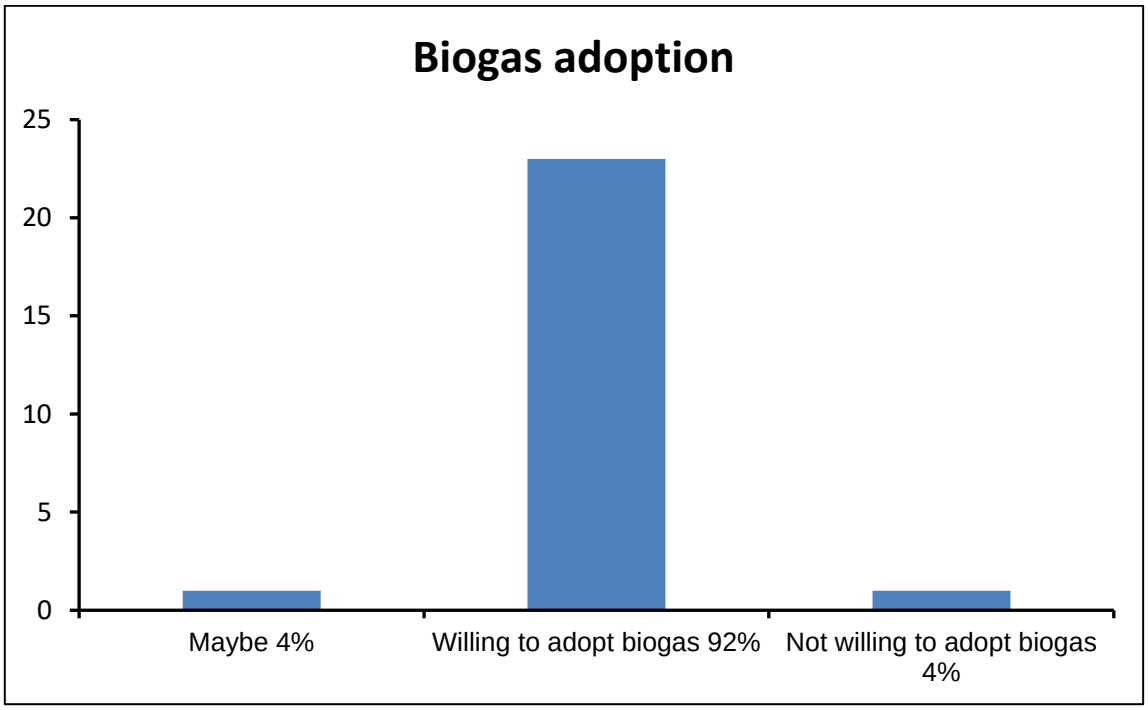

Figure 6.6: Post implementation, biogas adoption in relation to performance of technology.

6.3.3.d. Cost

A matter raised by most of the interviewees was that, while some of them see this technology as not practical, others are constrained from trying it only by a lack of the necessary building materials and knowledge of how to implement the technology. Most particularly though, by lacking the means of meeting the capital costs of building such a structure.

The capital cost involved in purchasing and installing a biodigester presented a major challenge to the interviewees, although 92% of the respondents to the formal survey indicated that they were willing to adopt this technology. One respondent expressed a willingness to provide 50% of the capital cost, while another could raise only about 7.5% of the amount needed. None of them envisaged that the cost of maintaining the digester would present a problem.

6.3.3.e. Safety and emissions

Although the nature of biogas technology raises the possibility that a biodigester represents an explosion risk, generally biogas is a safe technology. The concentration of methane ranges from 40%–70%, which is low compared to the concentration in LPG gas (90% ≥). The biogas inside a biodigester is usually at an operating pressure of around 2.5 kPa, low enough to avoid an explosion. If the biogas leaks from a small biodigester, the gas can become relatively diluted by the ambient air, as the biodigester is typically constructed in the open. The building/kitchen where the biogas is used needs to be well ventilated so that in the event of a leak, the gas is diluted. It is also assumed that if the user is able to follow the safety measures for using LPG

gas, then he or she should be able to adopt and use biogas. The process is anaerobic, meaning that it occurs in the absence of oxygen; thus, as long as the pressure in the digester is higher than atmospheric pressure, the chances of an explosion are reduced as oxygen is required for combustion. In general biogas is lighter than air, and hence escapes into the atmosphere in the event of any leaks; whereas, even small leaks of LPG gas, which is heavier than air, can lead to an explosion. After practical demonstration through the building of the biodigester, 84% of the respondents to the survey perceived the handling and use of biogas technology as easy and safe. The relevant appraisals are summarized in Figure 6.7.

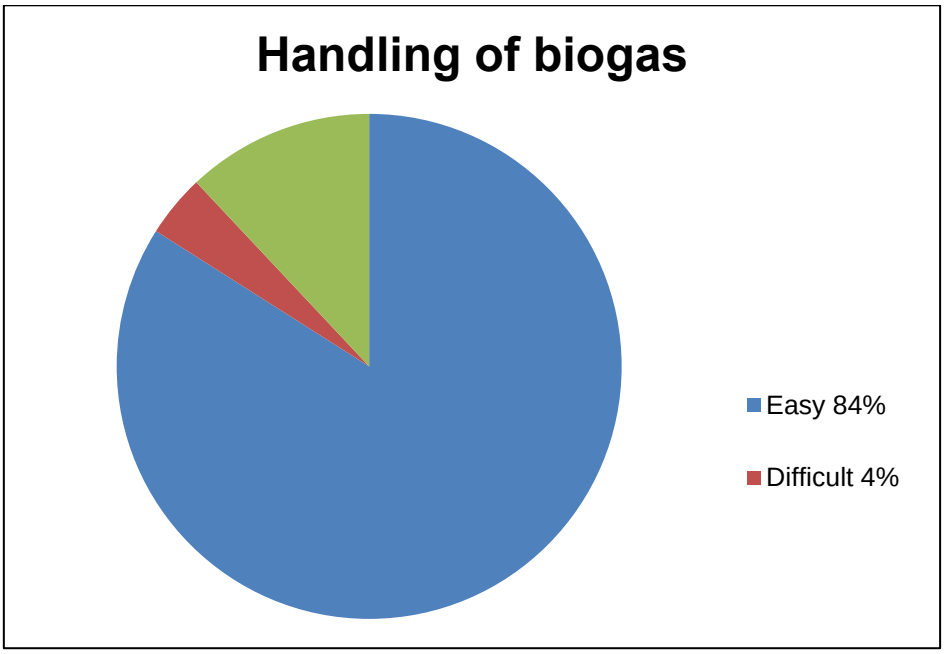

Figure 6.7: Post implementation, handling of biogas after exposure.

In addition, communities need to be educated regarding the fact that 99% of the pathogens and bacteria in the feed are destroyed in the digester under anaerobic conditions, making it safe to handle the bio-slurry (also referred to as bio-fertilizer), which can be used for vegetable farming. Furthermore, the biogas is effectively bacteria-free and is thus safe to use. The smell that may come from the gas comes

from sulphur-containing compounds and can be controlled by passing the gas through iron filings, leaving an odour-free, clean-burning fuel. However, in the pilot demonstration the farmer reported that there was neither odour from the manure nor any operational problems connected with the entire process.

6.3.3.f. Age group and profession survey

Figure 6.8a and Figure 6.8b compares the different ages of the people surveyed, and the nature of the work they do in the community. Sixty percent are workers in jobs ranging from self-employed, farm or lodge employees, or people doing piece jobs. Twenty percent are farm owners while the remaining 20% are unemployed. Thirty-one percent of the respondents were aged between 31-40 years whereas 50% were above 40 years old.

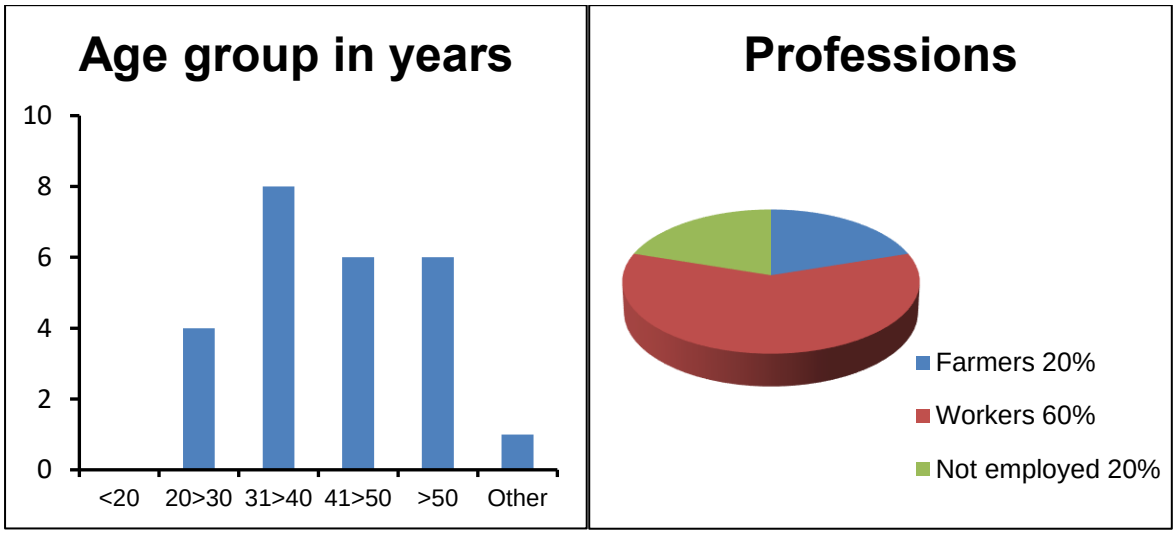

Figure 6.8: Post Implementation **(a):** Age grouping of the respondents, and **(b)** general occupations of the respondents.

6.3.4. Summary of results

Overall, the survey indicated that two issues remained problematic.

- **Feedstock availability**: Many respondents felt that only those with access to fairly large numbers of feedstock, whose numbers remain consistent, can benefit from this technology. Consequently, biodigestion was seen to be most suitable for farmers or farm workers.
- **Cost**: The majority continued to believe that the capital costs of installing a biodigester are too high. This may be a challenge that needs to be addressed by government and entrepreneurs. For example, if bio-bag biodigesters could be manufactured in South Africa, that might drive down the cost to more affordable levels.

These responses were similar to those found by Matsvange (2016), who carried out research on changing to biodigestion at different locations in Zimbabwe. The findings were that people are willing to adopt the technology if the questions of availability of feedstock and cost were addressed.

6.4. Discussion

Based on surveys and the answers of the respondents, our research team has elicited that education and 'hands-on' exposure to biodigestion have a positive effect on the adoption process. A clearer understanding of biogas technology will impart greater confidence in potential users, which will increase the likelihood that the technology will be adopted. This in turn will be supported by noticeable benefits, as suggested by many other researchers. These include less time spent on gathering energy sources for cooking, thereby freeing up time for other activities; reduction in deforestation, a cleaner cooking process.

The benefits of lighting, cooking and time efficiency mentioned in the literature were actually demonstrated in our research by the reports of the recipient of the biodigester. Although research has also shown that the initial (and most important) barrier to adoption of biogas technology is lack of knowledge, other constraints emerged once that knowledge had been imparted.

The barrier of capital costs is formidable: researchers and government need to work together to make cheaper digesters available and to supply financial support to enable households or communities to build biodigesters. The energy consumed by the two-plate stove at Muldersdrift farm was rated at 2 000 Watts. It was used on average for 2 hours per day for 30 days a month. The price of electricity, as set out in the electricity tariffs for the 2014/15 Mogale City Local Municipality was ZAR 1.5423/kW.hr. The total amount saved by changing to biogas per year is ZAR2 220.91 (approximately USD$155, using an exchange rate of 1USD: 14.34 ZAR- December 2016). To extrapolate, after 15 years, an amount of ZAR33.313.68 (USD $2325) can be saved, using as a template, the cost of cooking by electricity. More savings can be achieved if the calculations include power for lighting and geyser and generator usage. Although the capital cost of the imported bio-bag kit is a once-off amount of ZAR16 000 (USD $1120) and the construction costs are around ZAR 5000 (USD $350), the use of biogas has a long-term cost benefit, as the analysis of cost saved shows. This cost benefit will be enhanced if the bag can be produced more cheaply locally, or if less profit is made on the sale. The results of this case study show that if biogas use was adopted on a large scale, a sustainable bio-based economy is attainable.

Although this study was carried out in one location, which may limit its general applicability, it was clear from the post-implementation survey in the Muldersdrift community that there had been a complete shift in attitude after the local farmers had seen a biodigester constructed and put to work. This then suggests there is a need to roll out more digesters in similar rural societies.

However, this initiative faces barriers other than acceptance of biogas digestion by the targeted communities. The introduction of a new technology requires policy support from South Africa's government, which itself needs to understand how biodigestion works and what potential it has to improve the lives of ordinary Africans. To date, there is little or no information available on how much the country's decision-makers and even average South Africans know about biogas, or biogas technology. Unless provision is made to educate both the authorities and the public on the advantages of changing to biogas and to demonstrate that biogas technologies are safe and secure, there can be little hope that the necessary policy framework and start-up financing will be provided by the government. This would probably involve training a number of facilitators who can help the public to become aware of and assimilate the working and nature of biogas production.

At present, despite intensive planning and the efforts made by the Department of Trade and Industry (DTI) and other stakeholders, we continue to lack an adequate regulatory structure to support a large-scale launch of biogas technology SABIA, (2015). According to the Department of Energy, the owner of a biogas project is required to register with the National Energy Regulator of South Africa (NERSA), which requires that the owner conform with multiple environmental regulations. These

in turn have resulted in complex zoning legislation that must be complied with before any waste-to-energy biogas projects can be initiated Ruffini, (2013). At present, South Africa has no legal or policy guidelines to facilitate registration with NERSA, or to simplify compliance with zoning regulations. Another obstacle is the intricate administrative processes currently needed for project development and authorisation, especially at municipal level.

In order to tackle these issues, various stakeholders, including the Department of Energy (DEO), have begun to draft a policy framework for the installation of biodigesters in remote regions of South Africa and identifying rural households that would be able to use one. Accordingly, the framers of the policy should aim to take into account the availability of suitable feed, water and finance in the case of each recipient, as the biodigester should be sustainable in terms of cost. The last is of vital importance. At present, South Africa's government does not make any provision to fund, or create, dedicated financial mechanisms, incentives and grants to assist the adoption of biogas. The most serious obstacle to supplying digesters to the rural poor is the capital outlay required to buy and install them.

Some progress has been made. Currently, a committee is being set up to consult on legal issues relating to the registration, certification and licensing of rural biodigesters. Yet, despite the advances made in policy in recent years, there remains a gap that needs to be filled.

6.5. Summary

This research has shown that education and exposure are the key tools required to help increase the adoption of biogas in rural and small-scale farming areas. The judicious use of these tools (education and exposure) could help unlock the enormous promise that we can build a bio-based economy, in by these means alleviate poverty in rural South Africa, both as far as energy provision and a better standard of living are concerned. The findings also show that a successful collaboration between research and community engagement can generate knowledge and skills that can be transferred to help a community to adopt biogas as a form of renewable energy. It is also recommended that government should play a role in disseminating biogas technology as a renewable source of power in rural areas. This would help to promote greater awareness of the technology, which in turn would expand its adoption. The construction of pilot digesters in rural communities will also expose the members of that community to the practical advantages of this technology, thus helping them to enjoy its benefits.

It is important that policy makers should note that education is the driving force, because it can erase misconceptions. There is, therefore, a need for the government to provide platforms for learning and demonstration of biogas technology in order to support and expand the application of this sustainable form of energy. Also, while some researchers prefer to encourage and concentrate on high temperature processes like gasification and pyrolysis because they flag out biological processes as slow and inefficient. The results of this project have shown that despite the process of making biogas being slow, this technology can be welcomed and be used sustainably by different communities.

References

1. Blankenship D. C., 2010. Applied Research and Evaluation Methods in Recreation. United States of America: Library of Congress Cataloging-in-Publication Data.
2. Bryman A., 2012. Social Research Methods (4th ed.). United States: Oxford University Press.
3. Cassie B., DiLeo M., Lee J., 2010. Methane Creation from Anaerobic Digestion. In R. Thompson (Ed.), Worcester Polytechnic Institute. pp. 59
4. Fox J. A., Hildebrandt D., Glasser D., Patel B., 2013. A graphical approach to process synthesis and its application to steam reforming. AIChE Journal, Vol. 59(10), pp. 3714-3729.
5. Johansson K., 2008. Biogas residues as fertilizers effects on plant growth and soil microbiology. Report, Dept. of Microbiology, SLU, Uppsala.
6. Johnson B., Christensen L., 2012. Educational Research: Quantitative, Qualitative and Mixed Methods (4th ed.). California: SAGE Publications Inc.
7. Jones R., 1995. Why do qualitative research? It should begin to close the gap between the sciences of discovery and implementation. British Medical Journal, Vol. 311(2).
8. Kenya Domestic Biogas User Survey (KDBUS)., 2014. http://www.snv.org/public/cms/sites/default/files/explore/download/biogas users kpt survey-kenya final report oct 2014.pdf.
9. Le Ha C., 1998. Biodigester effluent versus manure from pigs or cattle as fertilizer for production of cassava foliage (*Manihotesculenta*) Livestock Research for Rural Development. Vol. 10(3)

http://www.fao.org/ag/aga/agap/frg/lrrd/lrrd10/3/chau1.htm. [Accessed 15 Oct 2015].

10. Matsvange D., Sagonda R., Kaundikiza M., Zaba P., 2016. Biogas technology diffusion and adoption mechanisms in Zimbabwe. Africa Insight, Vol. 45(4), pp. 148-166.
11. Mogale City., 2014. http://www.mogalecity.gov.za/content/pdfs/tariffs/2014/final tariffs1415 electricity.pdf. [Accessed 11 Nov 2015].
12. Munganga G., 2013. Overview of Biogas Market in South Africa. http://www.energy.gov.za/files/biogas/presentations/2013-NBC/2013-Overview-of-biogas-market-in-South-Africa.pdf. [Accessed November 2016].
13. Musyani G. C., 2013. The emerging biogas industry in South Africa – What opportunities? Integrated Sustainability services (ISS), February 15, 2013.http://iss-za.net/page2col.php?page=24&section=76. [Accessed 8 Nov 2015].
14. Newman I., 1998. Qualitative-quantitative research methodology: Exploring the interactive continuum: SIU Press. pp. 2.
15. Nørgaard A. D., Tybirk K., 2014. Scandinavian Biogas Handbook: Aspects of planning a biogas plant. Agro Business Park, Denmark.
16. Pal S., 2002. Evaluation study on National Project on Biogas Development (NPBD), Renewable energy, Domestic biogas, Monitoring & evaluation, New Delhi, India, pp.1–105.
17. Ruffini A., (2013), SA not using its biogas potential. Africa Powers Journal http://www.esi-africa.com/sa-not-using-its-biogas-potential/. [Accessed 15 Oct 2015].

18. South African Biogas Industry Association (SABIA)., 2015 National Biogas Conference, Standards and Regulations 5 March 2015. http://www.energy.gov.za/files/biogas/2015-Biogas-Conference/Day-1/SABIA-Standards-and-Regulations-25 March2015.pdf. [Accessed 15 Oct 2015].
19. Teodorita A. S., Dominik R., Heinz P., Michael K., Tobias F., Silke V., Rainer J., 2008. Biogas Handbook. Esbjerg, Denmark, pp. 23-25.
20. Tiepelt M., 2015. South African International Renewable Energy Conference. http://www.sairec.org.za/wp-content/uploads/2015/10/M-Tiepelt-SAIREC-Conference.pdf. [Accessed November 2016].
21. Triebel R., Damm O., 2008. A Synthesis Report on Biomass Energy Consumption and Availability in South Africa. A report prepared for ProBEC. http://www.ecoguinea.org/uploads/5/4/1/5/5415260/biomassenergy consumption availability sa.pdf. [Accessed 11 Nov 2015].

Chapter 7: Conclusions

There is an urgency to find ways of reducing CO_2 emissions to reduce the impact of Global Warming on the climate. However, at the same time, there is a need to find ways to supply energy to people who have had limited access to energy in order to help with economic development and improvement of their quality of life.

Waste biomass is renewable and is widely available in rural areas. Thus, utilisation of this waste and converting it to more useable forms of energy could have the potential to help meet the energy needs of people in rural areas. The question then arises: what stops the adoption of this technology? Anaerobic Digestion (AD) is an old technology and yet it is not widely used in Africa. Is this because of technical issues, difficulty in operating, social resistance, costs, or any other factor? Part of the research in this thesis looks to begin identifying the possible barriers to the technology. Among the issues considered is the limits of performance of these systems and how stable the production of the desired product would be in terms of thermodynamic driving forces.

Waste materials such as plastic and tyres, are not strictly renewable but ways of utilising these materials, so that they do not end up in landfills, or even worse in our oceans or polluting the landscape, is becoming urgent. Recycling of plastics is a route that is used in many developed economies, but in developing countries recycling plastic has not been widely implemented. Indeed, waste plastic bags, caught on fences and waving in the wind have been referred to as the "flower of Africa" (Lacey. 2005; Goko., 2017) and the increasing quantities of plastic waste is a major concern for many African governments. Converting this waste, as well as other carbon containing wastes such as biomass, to energy offers both a feed stock that is in

plentiful supply as well as route of converting this waste to a more useful product, namely energy. A different technology must be adopted to convert this material to a gas (typically referred to as syngas) that can be used for energy generation, and we look at high temperature processing routes to again understand the limits of performance and how this depends on operating parameters.

7.1. The Attainable Region (AR) approach to targeting

The AR is broadly defined as the set of all possible outputs for a given feed and set of processes. The AR is a region in the space of variables chosen to describe the system. Once the AR has been found, the region can be searched using a given objective function in order to find the maximum value of this function. This allows us to then determine the target, or limit of performance for the system of interest. The performance of real systems can then be compared to this target in order to see if there is room for improvement in the system performance.

Two different AR's were used in this thesis, a material balance limited AR and the AR in the Gibbs Free Energy – Enthalpy Space. These will be discussed below.

7.1.1. The Material Balance Limited AR (MB AR)

This is the set of all possible material balances for a given feed and defined possible species in the products. The AR lies in the space that describes the material balances for the process. It depends only on feeds, and possible products considered do not depend on temperature, pressure etcetera. Extreme points on boundary of the region represent points where certain species are zero. These extreme points can be

described by a material balance that describes how feed can be converted to the non-zero products.

7.1.2. The AR in Gibbs Free Energy – Enthalpy Space (G-H AR)

The G-H AR was used to find the thermodynamic limits for converting biomass into valuable gaseous products. The G and H of the outputs from all material balance (that is the points in or on the boundary of the MB AR) are calculated. Calculating G and H is effectively a linear transformation of composition, The G-H AR depends on temperature and pressure and the effect of these variables on G-H AR can be seen which gives understanding as to how the thermodynamically favoured products change with operating conditions.

There are various insights that can be seen from the G-H AR. Among these are that:

- Compositions represented by points that lie in the G>0 region are not spontaneous. Thus, these points would not be achievable in either an anaerobic process or a process where no eternal work was added.
- Points that lie in the G<0 region are spontaneous. Thus, these points are in principal achievable. The more negative G, the greater the driving force or the more work that could be recovered from the process.
- The composition corresponding to the point at minimum G is that which would be thermodynamically favoured.

By tracking this point of minimum G and how it changes with temperature allows us to see how the thermodynamically favoured product would change with operating conditions.

7.1.2.1. The GH AR without oxygen

It was considered that the GH AR for a feed of 1 moles of glucose (which was used as a surrogate compound to biomass) and constructed the G-H AR for temperatures between 25 ^{0}C and 1500 ^{0}C. The possible products considered were CH_4, H_2, CO_2, water and CO. O_2 was not considered to be either a product or feed. This region would describe process occurring without the addition of O_2, such as AD and pyrolysis.

The G-H-AR at 25 ^{0}C is a region that would describe the possible products from AD. The analysis shows that CH_4 and CO_2 gases are favoured products at minimum G for temperatures up to about 700 ^{0}C. The production of the favoured product at these conditions would be exothermic.

- What was concluded is that AD, or biogas production, is a form of low temperature gasification. CO_2 and CH_4 would be the preferred product in terms of having the largest chemical potential driving force. This could be interpreted that if there was a consortium of bacteria that were cooperating or competing in the digestion process, the bacteria that produced the thermodynamically favoured product, namely CO_2 and CH_4, would release the most possible available work by converting the feed into the most thermodynamically favoured product. This available work could then be used to reproduce more bacteria, meaning that the bacteria consortium would be enriched in that type of bacteria. Alternatively, the

available work could be translated into the biggest driving force for the reaction and hence the largest rate of reaction.

- Making H_2 as the preferred product would possible be difficult as the difference in G between the feed and H_2 product is much smaller than that for the thermodynamically favoured product of CH_4. This smaller driving force could translate into lower rates of reaction and lower growth rates of the bacteria. Conversely, according to reaction path for AD H_2 is one of the intermediate products although in small quantity, which is consistent with positive G (small equilibrium conversion). This probably happens at the beginning of the reaction process because it is fast but does not go far because of positive G, and also disappear as it is being used in other reactions. This could also explain why other experimental results show the presence of H_2, in that if it is removed fast enough from the reaction mixture after being formed it can remain in gaseous phase for a long time. Thus, explaining why H_2 would mostly not happen in AD using kinetics may not be correct.
- Changing the temperatures between 20 ^{0}C to 100 ^{0}C does not significantly affect the theoretical results.

CO and H_2 are preferred products from about 800 ^{0}C to 1 500 ^{0}C and the processes become endothermic. This shows that the range of products changes from CH_4 and CO_2 (biogas) at lower temperatures to H_2 and CO (syngas) at higher temperatures. Thus, in pyrolysis process, one might expect that at temperatures around 800 ^{0}C or higher that CO and H_2 are the dominant product.

7.1.2.2. The G-H AR with oxygen

However, in contrast, when small amounts O_2 less than the Stoichiometric Ratio (SR) for combustion is included as a feed and/or product in the thermodynamic calculations, at temperatures below 700 ^{0}C, H_2O and C are preferred products at minimum G. Above 800 ^{0}C H_2 and CO would be preferred. Thus, this analysis would predict similarly, when a continuous supply/ excess of oxygen is added to the process at high temperatures, the thermodynamic AR shows that CO_2 and H_2O (products of combustion) are produced exothermically.

7.2. Experimental Results

Although the products where G< 0 in the G-H AR are thermodynamically feasible, they may not be technologically feasible. Hence, a comparison of the thermodynamic and experimental data is needed to give reasonable conclusions and possible optimisation techniques.

7.2.1. Experiments on biological Anaerobic Digestion

A product ratio of CO_2: CH_4 was also approximately 1:1 and these ratios are in line with the material balance. A comparison of the AR with experimental results from a batch process of AD at 30 ^{0}C shows that the products of digesting dog faeces, cow dung and glucose lie in the region where G is minimum on the thermodynamic AR. The relationship of the theoretical and experimental analysis is fundamental as it is a step forward into finding out how living organisms work in relation to the laws of thermodynamics. It tells us that bacterial action in digestion of glucose, cow dung and

dog faeces is possibly limited by a thermodynamic driving force in terms of the products that are achieved.

7.2.2. Experimental results for anaerobic conversion of biomass (pyrolysis) at temperatures greater than 400 ^{0}C using a nitrogen plasma gasifier

Wood pellets ($C_4H_6O_3$) were processed in a plasma gasifier and the product distribution was measured. No O_2 was fed to the system; that is the system operated under anaerobic conditions. The bulk temperature was varied between 400 ^{0}C and 1000 ^{0}C and the flow rate of wood pellets was also varied. The temperatures in the plasma section however were believed to exceed 2000 ^{0}C, and so there are big temperature gradients in the gasifier and the gas passing through the reactor could see very different temperature profiles, depending on the path that the gas follows. The results were normalised to one mole of wood pellets feed for comparison.

The effect of temperature on pyrolysis gasification was analysed using the MB AR and G-H AR. A molar ratio of 1:1 for H_2 and CO in the product gas was observed at all temperatures. In addition, H_2 and CO constituted about 86 mole % on a water and nitrogen free basis. The remainder of the gas was comprised of CO_2, CH_4 and traces of ethene. The G-H AR predicts that

- At temperature below 600 ^{0}C, CO_2 and CH_4 are the thermodynamically preferred products.
- At temperatures above 800 ^{0}C, CO and H_2 are the thermodynamically preferred products.

- At temperatures between 600 ^{0}C and 750 ^{0}C, the thermodynamically preferred products are CO_2 and H_2.

It would seem that because of the temperature gradients in the reactor, most of the reactions are occurring at a temperature higher than the measured bulk temperature as the product that is measured experimentally is thermodynamically favoured at temperatures higher than 900 ^{0}C. Furthermore, there could be some of the material reacting at temperatures lower than the bulk temperature as CO_2 and CH_4 would typically be the preferred product at temperatures below 500 ^{0}C and traces of this are found at higher operating temperatures.

The efficiency of the process was measured in terms of the carbon conversion to all product gases which increased from 43 % to 77 %, at temperatures ranging from 400 ^{0}C to 1000 ^{0}C respectively. The overall biomass conversion increased from 46 % at 400 ^{0}C to 82 % at 1000 ^{0}C. Tars were observed for experiments at 400^{0}C and 600^{0}C only. Although high conversion of biomass is achieved for the studied conditions for pyrolysis and gasification, the overall energy efficiency based on the Cold Gas Efficiency (CGE) was low. The CGE averaged about 25 % for temperatures 400 ^{0}C and 1000 ^{0}C and about 40 % for temperatures 600 ^{0}C and 800 ^{0}C. By operating at higher temperatures, one can produce quality syngas and no tars at the expense of extra energy to the process.

Considering the heat and work analysis for both processes, some equilibrium results obtained from Aspen thermodynamic simulations using the Gibbs Reactor were compared to the experimental data. For pyrolysis and gasification, two cases were

considered; one where a perfectly designed plasma reactor without any heat losses and another which looks at a realistic analysis on what is happening in the reactor and includes heat losses. Thus, an exergy analysis was considered for the second case. The results from both cases show that work is lost from the process. The material balance was normalised to one mole of feed for the different temperatures studied. Hence, the ratio of the work lost to the amount of work required for the process to happen was considered for analysis. The data in the perfectly designed plasma gasifier shows that the lost work averages about 150 kJ/mol for all temperatures studied while 200 kJ/mol of work is lost for the real experiment. The results show that the maximum amount of lost work for the process is observed to be around 473 ^{0}C for the real process.

7.2.3. Experimental results for aerobic conversion of biomass (gasification) at temperatures greater than 400 ^{0}C using a nitrogen plasma gasifier

In the second set of experiments, oxygen was introduced at ER's between 0.06 and 0.36. The flow rate of wood pellets was varied, and the experiments were run at bulk temperatures of 700 ^{0}C and 900 ^{0}C. At lower temperatures, carbon was formed which block the exits pipes and caused the system pressure to increase. The formation of carbon at lower temperatures is supported by the G-H AR shown in Figure 2.2A where C and H_2O are the favoured products at lower temperatures.

An approximate molar ratio of 4: 5 of hydrogen to carbon monoxide was observed at both temperatures; this would seem to indicate that the oxygen reacts preferentially with the H_2 rather than CO. Tars were observed at 700 ^{0}C while no visible tars were seen at 900 ^{0}C. The mass conversion of the biomass to product gas averages about

85% at 700 ^{0}C and 80 % at 900 ^{0}C, which is an average over all the oxygen flow rates. This would indicate that the conversion of the biomass has kinetic limits due to reactor, and that at the higher temperature, when the gas volumetric flow rate is higher resulting in a lower residence, the biomass has less time to react and thus has a lower conversion. The high volumetric flow rate is due to increased carbon dioxide production from combustion of an increased oxygen feed. This is also attributed to the increased plasma gas (nitrogen) that was used to increase the temperature to 900 ^{0}C

The Cold Gas Efficiency averaged about was 35 % and 23 % for the temperatures 700 ^{0}C and 900 ^{0}C respectively. This efficiency was lower than the ones obtained for the pyrolysis experiments.

Although O_2 was added, the experiments show that an addition of heat was necessary to achieve products. An increase in the oxygen flow rate resulted in less energy being required by the thermodynamic process to produce syngas. This is because some of the energy is provided via the combustion process because of oxygen being supplied to the process. The amount of work lost by the plasma gasification process increases with an increase in the oxygen flow rate. A possible explanation for this is that more work is being added into the process via combustion and is not all used directly in the reaction, some of it is lost due to heat losses. Another explanation could be that combustion itself is highly irreversible and leads to work losses; thus, by adding more oxygen, more combustion happens leading to more work losses. This impacts heavily to the overall efficiency of the process.

A limitation on the AR exists and arises from a complex calculation resulting from the number of degrees of freedom. This is based on the possible products which can be formed with the material balances as well as the atomic species present. Thus, the experimental results obtained from the plasma process did not show a reasonable relationship with the AR. However, there is a coherence of the gases produced in the experimental data with those predicted by the AR at minimum G

7.3. Final thoughts and recommendations

Technically converting biomass to a gas has large thermodynamic driving forces and the product gases are useful source of energy or feeds for other processes. Thus, these processes, whether low temperature or high temperature conversion should be relatively easy to run.

The low temperature anaerobic route to gasifying biomass waste, using microbes as catalysts, has a very simple G-H AR, and the preferred products are CH_4 and CO_2. The exact ratio of CO_2:CH_4 will be determined by the material balance but will be roughly 50:50, depending on the exact C:H:O in the feed material. These units should be relatively stable to operate as none of the other products have G's that are as negative as that of the desired product. Although this is not part of the scope of this thesis, small scale anaerobic digesters have been installed in the community and these do run easily and stably with little intervention from the operator which seems to support our conclusion.

One however could ask, why then have simple technologies, such an AD, not been widely adopted in Africa? On the surface, it should not be a technology barrier as the

G-H AR shows a process with good driving forces and a very well defined overall thermodynamically favoured product.

To this end the author has worked with communities and spoke to people about their knowledge about the technology, their concerns and their possible interest in using new approaches to supply energy for cooking and lighting. It found that people were not aware of the technology but would be very interested in adopting a technology that supplied energy cheaply. To our surprise however, the major concern was around hygiene and safety, in that if the gas was made from “poo” how could the gas be clean and would cooking with it not contaminate the food and make people sick? This in hindsight is a very reasonable concern, although it had never occurred to the researchers that this would be a perception.

The author thinks that what this study highlighted is that the technology side of new processes is in some sense relatively straight forward and easy. However, when technologies are to be used by the public, then the concerns, needs and expectations of the public have to be addressed and this is probably a bigger challenge than the technological issues.

To this end, the team of researchers on anaerobic digesters has expanded to include social scientists, phycologists and economists. This in turn is an interesting problem as getting students and researchers from the various disciplines to communicate amongst themselves and with the public is quite challenging and discussion on this challenge is beyond the scope of this research.

This thesis shows a theoretical and experimental analysis of converting biomass to a combustible gas. Being able to determine what the global minimum G in the G-H AR plot is, and what material balance this corresponds to is useful in understanding what the thermodynamic target is in terms of favoured product. It is shown that the product achieved at both low and high temperatures is mostly determined by the thermodynamically favoured product. It is also useful to see what other products (material balances) lie in or close to the boundary of the G-H AR, at minimum G. If the difference in G between these products and that at the overall minimum G is fairly small, then the likelihood of co-producing these products is high these as the differences in thermodynamic driving force are small. This could indicate how stable the operation is in terms of producing a product with a well-defined composition (material balance) and how dependant getting the desired product is on operation and design of the equipment.

What is found is that anaerobic process such as digestion and pyrolysis seem to have a simpler and more clearly defined product at minimum G on the G-H AR. This could lead to expect that the operation of these processes is simpler and more stable in that the desired product has a very large thermodynamic driving force compared to other possible products on the boundary of the G-H AR. It is indeed found this experimentally. Processes where oxygen is included, such as gasification, can have a more complicated boundary of the AR at minimum G with various reactions/ material balances having similar G's. Thus, the exact relationship between the CO_2: CO and H_2 ratios could be quite dependent on operation and design in the way the process approaches global thermodynamic equilibrium. The implications of this is that any equipment or process that is designed to utilise this gas must be flexible in being able

to handle a wide range of CO:H_2 ratios, especially if looking to design a simple, relatively small scale, cheap, high temperature biomass to energy plants that are operated by relatively non-skilled operators.

References

1. Lacey M., 2005. Flower of Africa: A Curse That's Blowing in the Wind. The Ney York Times, 7 April. https://www.nytimes.com/2005/04/07/world/africa/flower-of-africa-a-curse-thats-blowing-in-the-wind.html
2. Goko C., 2017. Plastic bags: a hard habit to break. Financial mail, 10 August. https://www.businesslive.co.za/fm/fm-fox/2017-08-10-plastic-bags-a-hard-habit-to-break/

Appendices

A.1. Thermodynamic data

Table A1.1: Enthalpy and Gibbs Free energy data.

Component	ΔH kJ/mol	ΔG kJ/mol	A	B	C	D	Cp(kJ/mol-K)
Methane (g)	-74.52	-50.49	1.702	0.009081	-0.000002164	0	0.03531
Water (l)	-285.83	-237.15	75.29		-	-	0.07529
Carbon dioxide (g)	-393.51	-394.37	5.457	0.001045	-	-115700	0.03711
Glucose (s)	-1262.1	-915.9	-	-	-	-	0.115
CO(s)	-110.53	-137.2	3.376	0.000557	-	-3100	0.0292
Water(g)	-241.83	-228.6	3.47	0.00145	-	-12100	0.03358
Ethane(g)	-83.85	-31.95	-	-	-	-	-
Ethylene(g)	52.51	68.43	-	-	-	-	-
Cellulose	-955	-659	(Allberty et al., 1998)				
Wood pellets	-636.67	-439.33	Normalised from cellulose($C_6H_{10}O_5$) values from $C_4H_6O_3$				
Hydrogen(g)	0	0	3.249	0.000422	-	8300	0.02882

Table A1.2: Lower and upper explosive limits for H_2 and CO (www.mathesongas.com).

	LEL (vol %)	UEL (vol %)
H_2	4	75
CO	12.5	74.5

A.2. Attainable Region

Matlab Script MuPAD

```
k:=[{b+d+e<=1,a<=0.5,a+3*b-c+3*d>=0,-2*a+c-
3*d+6*e>=0,b>=0,c>=0,d>=0,e>=0},a+b+c+d+e]:linopt::corners(k,[a,b,c,d,e])
```

Table A1.3 to A1.6 shows the vertices/ extents obtained for the various flows of oxygen when 1 mole of glucose is fed to a gasification process. The material balance does not change when temperature is increased by the change in H and G changes hence resulting in a shifted AR.

Table A1.3: Extents of reactions obtained when 1 mole of glucose is fed together with 0.000001 moles of oxygen at 25 ^{0}C.

Point	ε 1	ε 2	ε 3	ε 4	ε 5	ΔH(kJ/mol)	ΔG(kJ/mol)
1	-3	0	0	1	0	1038.09	763.5
2	-3	1	0	0	0	1262.19	915.9
3	-1.5	0	0	1	0	706.515	351.993
4	0	0	0	0	0	0	0
5	0	0	0	0	1	-188.718	-455.532
6	0	1	0	0	0	599.04	92.886
7	0	0	3	1	0	-142.437	-419.577
8	0	1	3	0	0	81.663	-267.177
9	0	0	0	0.33333	0.6666666	-0.833	-323.525

Table A1.4: Extents of reactions obtained when 1 mole of glucose is fed together with 0.5 moles of oxygen at 25 ^{0}C.

Point	ε 1	ε2	ε 3	ε 4	ε 5	ΔH (kJ/mol)	ΔG (kJ/mol)
1	-3	0	0	1	0	1038.09	763.5
2	-3	1	0	0	0	1262.19	915.9
3	-1.5	0	0	1	0	706.515	351.993
4	0	0	0	0	0	0	0
5	0	0	0	0	1	-188.718	-455.532
6	0	1	0	0	0	599.04	92.886
7	0	0	3	1	0	-142.437	-419.577
8	0.5	0	0	0	1	-299.243	-592.701
9	0.5	1	1	0	0	316.056	-164.304
10	0.5	0	0.5	0	1	-385.473	-652.712
11	0.5	0	0	0	0.16666	-141.978	-213.091
12	0.5	0.16666	1	0	0.16666	-214.597	-317.631
13	0.5	1	3.5	0	0	-115.092	-464.357
14	0.5	0	0.5	0	0.08333	-212.481	-235.141
15	0.5	0.83333	0	0	0.16666	357.222	-135.686
16	0.5	0	0	0.55555	0.44444	13.90033	-372.691
17	0.5	0.16666	3.5	0.83333	0	-301.842	-591.357
18	0.5	0	3.25	0.91666	0.08333	-343.048	-619.753

Table A1.5: Extents of reactions obtained when 1 mole of glucose is fed together with 5 moles of oxygen at 25 ^{0}C.

Point	ε 1	ε 2	ε 3	ε 4	ε 5	ΔH (kJ/mol)	ΔG (kJ/mol)
1	-3	0	0	1	0	1038.09	763.5
2	-3	1	0	0	0	1262.19	915.9
3	-1.5	0	0	1	0	706.515	351.993
4	0	0	0	0	0	0	0
5	0	0	0	0	1	-188.718	-455.532
6	0	1	0	0	0	599.04	92.886
7	0	0	3	1	0	-142.437	-419.577
8	3	0	0	0	1	-851.868	-1278.55
9	3	1	6	0	0	-1098.86	-1450.25
10	5	0	4	0	1	-1983.8	-2307.31
11	5	0	5	0	1	-2156.26	-2427.33
12	5	0.333333	6	0	0.666666	-2066.14	-2364.54

Table A1.6: Extents of reactions obtained when 1 mole of glucose is fed together with 10 moles of oxygen at 25 ^{0}C.

Point	ε1	ε 2	ε 3	ε 4	ε 5	ΔH (kJ/mol)	ΔG (kJ/mol)
1	-3	0	0	1	0	1038.09	763.5
2	-3	1	0	0	0	1262.19	915.9
3	-1.5	0	0	1	0	706.515	351.993
4	0	0	0	0	0	0	0
5	0	0	0	0	1	-188.718	-455.532
6	0	1	0	0	0	599.04	92.886
7	0	0	3	1	0	-142.437	-419.577
8	3	0	0	0	1	-851.868	-1278.55
9	3	1	6	0	0	-1098.86	-1450.25
10	6	0	6	0	1	-2549.77	-2821.69

Calculation of Gibbs Free Energy for Cellulose

Table A1.7: Calculation of G for Cellulose

		Enthalpy [kJ/mol]	**Gibbs** [kJ/mol]
Monosaccharides	Glucose	-1262.19	-915.9
	Fructose	-1259.38	-915.51
		-1260.79	**-915.705**
Disaccharides	Sucrose	-2199.87	-1564.7
	Lactose	-2233.08	-1567.33
		-2216.48	**-1566.02**
	Water	-285.83	-237.19
	Dehydration	19.265	28.205
Polysaccharide		**-955.69**	**-650.31**

Method from	Perks and Liebman "Estimation of the Enthalpies of Formation of Some Common, Solid-Phase Compounds of Considerable Theoretical Importance" Journal Structural Chemistry, Vol. 11, No. 5, 2000
Data from	Allberty "Calculation of Standard Transformed Gibbs Energies and Standard Transformed Enthalpies of Biochemical Reactants" Archives of biochemistry and biophysics Vol. 353, No. 1, May 1, pp. 116–130, 1998.

A.3. Raw data for digestion

Figure A2.1 below shows concentration changes obtained from anaerobic digestion of cow dung and dog faeces. However, the data used in Table 3.1 excluded nitrogen and results were only obtained at day 82.

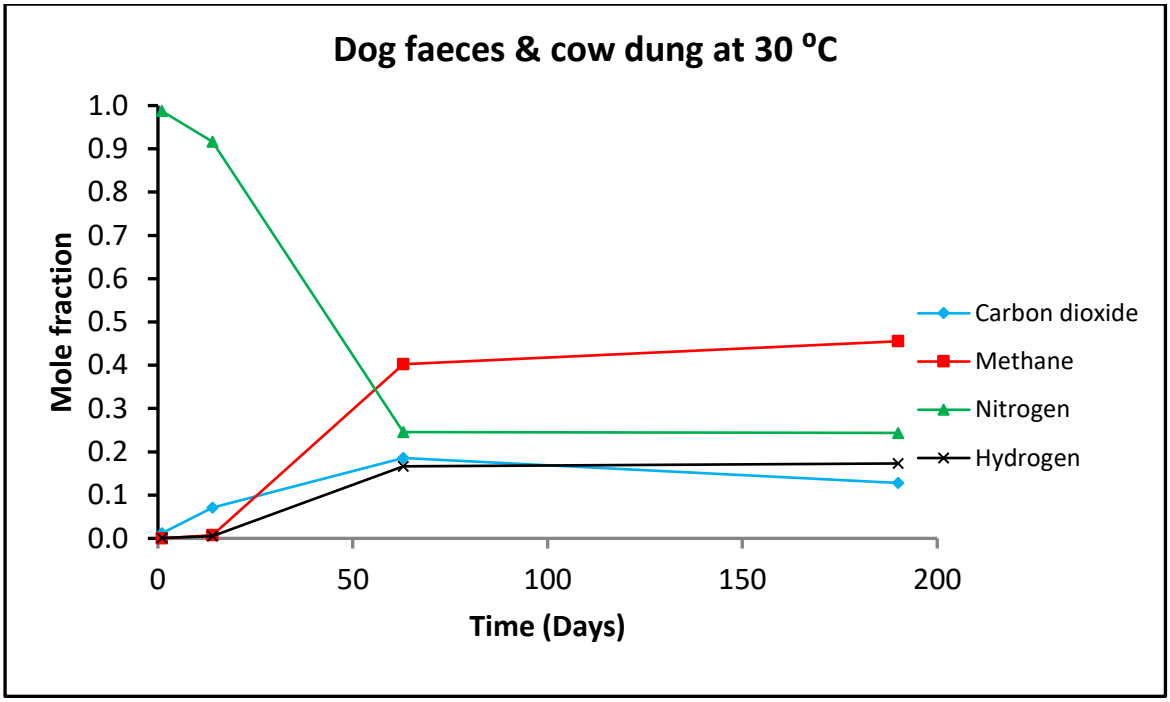

Figure A2.1: Graph showing changes in gas concentration in the sample containing dog faeces and cow dung at 30 ^{0}C (Muvhiiwa et al., 2016).

A.4. Plasma system for Pyrolysis

Table A3.1: Material balance for the experimental results shown in Chapter 4, Figure 4.8 and Table 4.2.

Temperature (^{0}C)	Experimental material balance
400	$26.5C_4H_6O_{3(s)} \rightarrow 26.7H_{2(g)} + 29.1CO_{(g)} + 4.9CO_{2(g)} + 4.7CH_{4(g)} + 3.1C_2H_{4(g)} + 0.2C_2H_{6(g)} + \sim 9.8C_{5.8}H_3O_{1.7(s)}$ *and (120g) liquid products*.
600	$25C_4H_6O_{3(s)} \rightarrow 42H_{2(g)} + 46CO_{(g)} + 5.9CO_{2(g)} + 5.2CH_{4(g)} + 5.4C_2H_{4(g)} + 0.2C_2H_{6(g)} + (5.2C_7H_{2.5}O_{0.8(s)}$ *and (200g) liquid products*
800	$20.1C_4H_6O_{3(s)} \rightarrow 39.8H_{2(g)} + 42.7CO_{(g)} + 4CO_{2(g)} + 4.2CH_{4(g)} + 4.9C_2H_{4(g)} + 0.1C_2H_{6(g)} + 2.6C_{7.25}H_2O_{0.7(s)}$.
1000	$9.8C_4H_6O_{3(s)} \rightarrow 18.2H_{2(g)} + 21.2CO_{(g)} + 2CO_{2(g)} + 1.8CH_{4(g)} + 2.6C_2H_{4(g)} + 1.4C_{7.25}H_{1.25}O_{0.7(s)}$.

Table A3.2: Typical raw data for Pyrolysis Gasification.

	Experiment #	Reactor T (^{0}C)	[CO]	[H2]	[CO2]	[CH4]	[C2H4]	[C2H6]
~ 400^{0}C 2.7kg/hr	1	418	0.453	0.363	0.074	0.052	0.056	0.0021
	2	395	0.425	0.39	0.072	0.0687	0.045	0.0024
	3	400	0.405	0.392	0.093	0.0677	0.042	0.0021
	4	400	0.391	0.434	0.082	0.057	0.036	0.0013
	5	411	0.409	0.445	0.065	0.0497	0.031	0.0011
~600^{0}C 2.55kg/hr	1	606	0.457	0.427	0.037	0.0323	0.044	0.0013
	2	616	0.456	0.405	0.049	0.0414	0.048	0.0018
	3	597	0.447	0.398	0.059	0.045	0.049	0.002
	4	599	0.449	0.385	0.06	0.0522	0.052	0.0023
	5	607	0.44	0.403	0.055	0.0493	0.051	0.002
~800^{0}C 2.05kg/hr	1	783	0.448	0.428	0.039	0.0383	0.046	0.0011
	2	814	0.445	0.43	0.042	0.0382	0.043	0.0012
	3	796	0.447	0.43	0.038	0.0374	0.046	0.001
	4	810	0.445	0.414	0.044	0.0456	0.05	0.0013
	5	816	0.446	0.416	0.042	0.0436	0.051	0.0012
~ 1000^{0}C 1.0kg/hr	1	989	0.452	0.482	0.019	0.0174	0.029	0
	2	1017	0.453	0.464	0.023	0.0239	0.036	0
	3	1002	0.443	0.417	0.042	0.0475	0.05	0
	4	990	0.446	0.471	0.062	0.0213	1E-05	0
	5	998	0.47	0.434	0.06	0.0357	1E-05	0

Effect of Nitrogen on Equilibrium

The results in Figure A3.1 and A3.2 satisfied our assumption that nitrogen does not affect equilibrium.

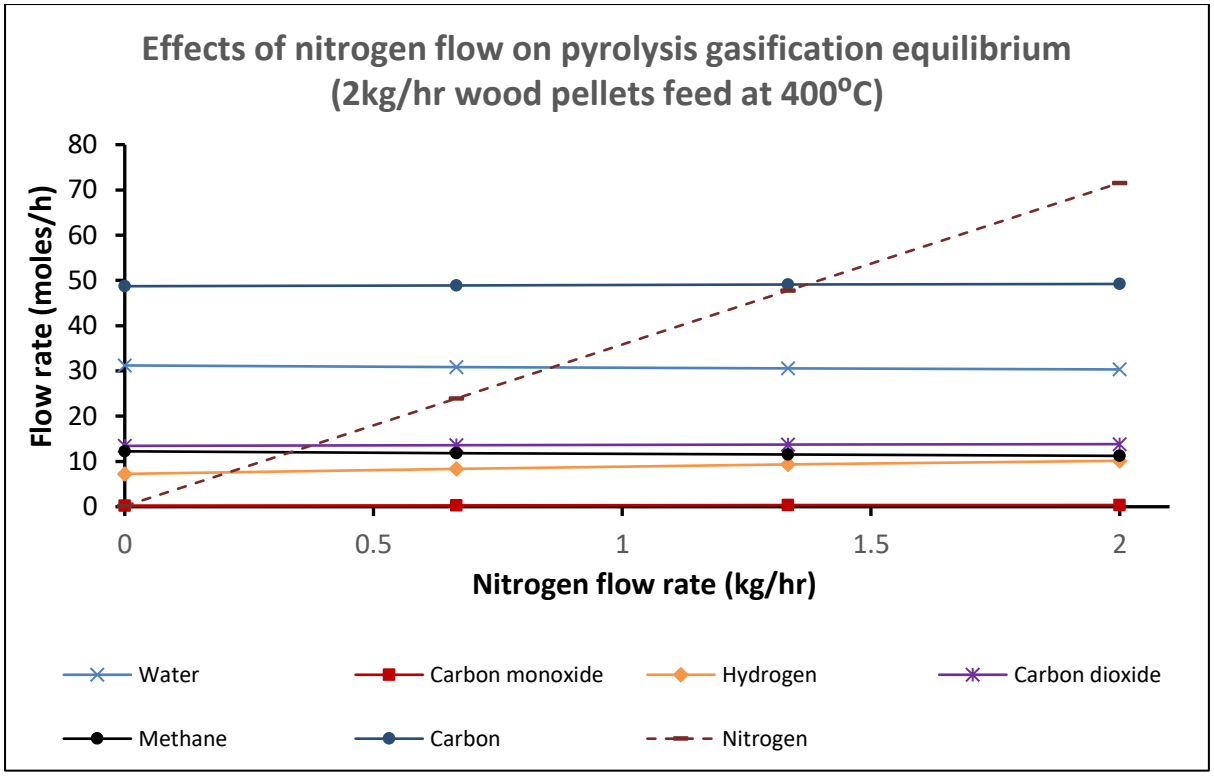

Figure A3.1: Effects of nitrogen flow on equilibrium for the pyrolysis gasification of wood pellets at 400 ^{0}C.

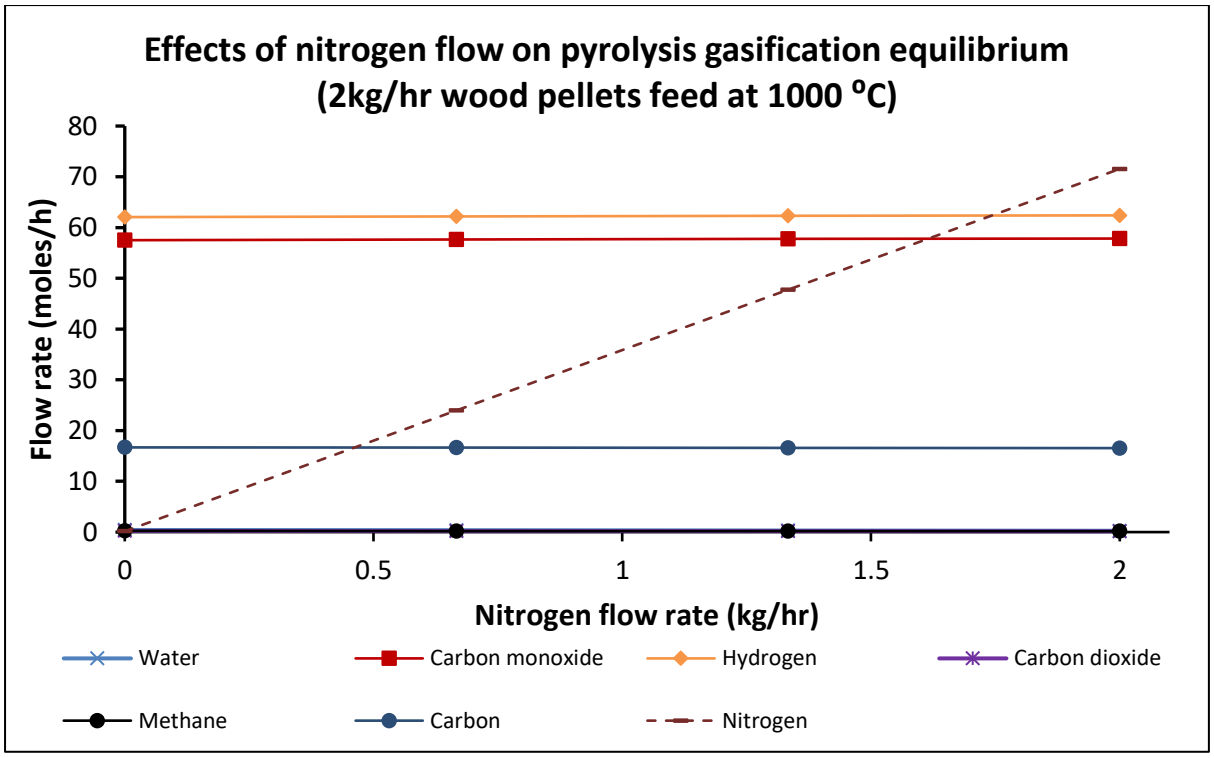

Figure A3.2: Effects of nitrogen flow on equilibrium for the pyrolysis gasification of wood pellets at 1000 ^{0}C.

Work requirements

Table A3.3: Summary of Exergy calculation.

Temperature/ ^{0}C	Wood pellets feed/ moles	Water feed/ moles	H Products kJ/mol	E Products kJ/mol
400	24.91	9.01	-15943.3	-14897.58
600	23.5	8.8	-6736.36	-9706.03
800	18.9	6.8	-2355	-5054.5
1000	9.2	3.3	-727.26	-2172.78

The war recorded as feed in Table A3.3 is the 6 % moisture content of the feed wood pellets. The work was calculated using the Equations below.

$$W_{min\ required} = \Delta E_{(T)} = \Delta H_{(T)} \left(1 - \frac{T_o}{T_{Carnot}}\right)$$

$$W_{actual} = \Delta E_{(T)} = \Delta H_{(T)} \left(1 - \frac{T_o}{T_{bulk}}\right)$$

Table A3.3: Summary of work calculation.

ΔH kJ/hr	ΔE kJ/hr	Tcarnot/ K	Work/ kJ/mol
84.10	-76.03	156.58	46.85
440.57	111.91	399.67	290.13
599.07	254.14	517.83	432.63
644.36	285.15	534.84	493.46

A4: Aspen Simulations

Figure A4.1 shows the Aspen simulation flowsheet used to calculate heat energy for wood pellets and respective equilibrium compositions at various feed and temperatures. The feeds used were 2.7 kg, 2.55 kg, 2.05 kg and1 kg for pyrolysis and 2 kg and 1 kg for gasification. The respective temperatures were 400 ^{0}C, 600 ^{0}C, 800

^{0}C and 1000 ^{0}C for pyrolysis and 700 ^{0}C and 900 ^{0}C for gasification. The two reactors used were the RYield and RGibbs where the feed was considered as non-conventional. The ideal gas property model was used. The proximate and ultimate analysis in Table 4.1 were used as inputs into the RYield reactor and subsequently into the RGibbs reactor to find the equilibrium products from the respective quantities of wood pellets and oxygen fed. The calorific value in Table 4.1 was obtained using a model in Aspen called HCOALGEN which is the General Coal Enthalpy Model in the Aspen Physical Property System (Aspen Plus V8.6)

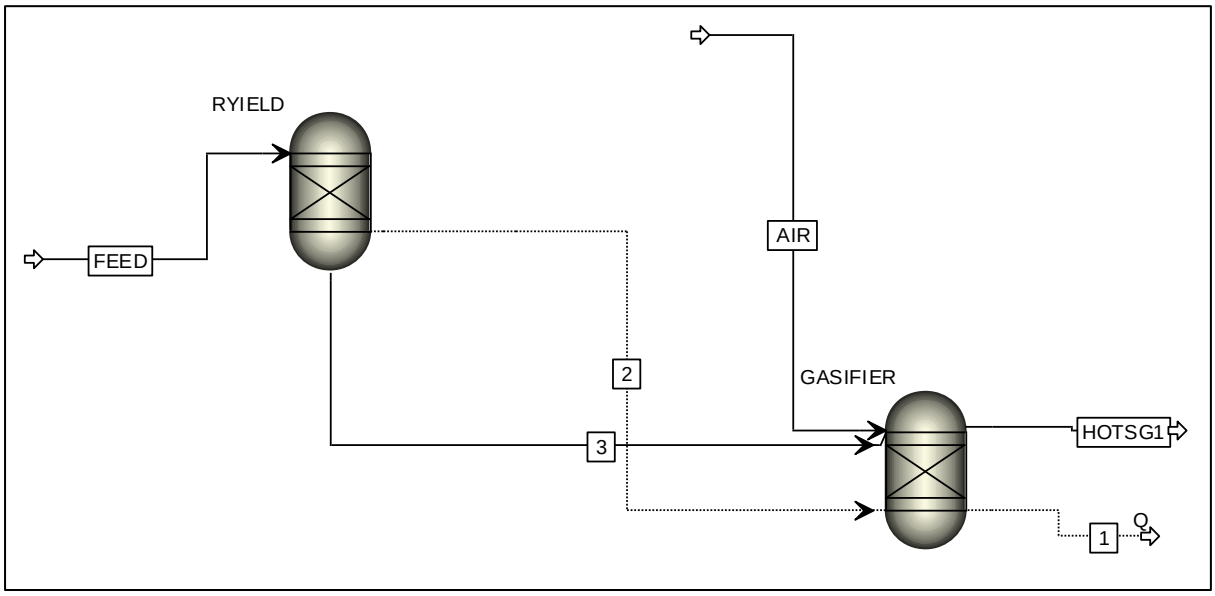

Figure A4.1: Aspen simulation flowsheet used to calculate heat energy for wood pellets and respective equilibrium compositions at various feed and temperatures.